MEASURING AND MODELING OF AIR POLLUTANT DISPERSIONS FROM CEMENT PLANTS

KANYANEE SEANGKIATIYUTH

A THESIS SUBMITTED IN PARTIAL FULFILLMENT
OF THE REQUIREMENT FOR THE DEGREE OF
DOCTOR OF ENGINEERING IN CHEMICAL ENGINEERING
FACULTY OF ENGINEERING
KING MONGKUT'S INSTITUTE OF TECHNOLOGY LADKRABANG
2011

KMITL-2011-EN-D-228-069

หัวข้อวิทยานิพนธ์	การวัดและการจำลองการกระจายตัวของมลพิษทางอากาศจากโรงงานผลิตปูนซีเมนต์
นักศึกษา	นางสาวกัญญาณี แสงเกียรติยุทธ
รหัสนักศึกษา	49061703
ปริญญา	วิศวกรรมศาสตรดุษฎีบัณฑิต
สาขาวิชา	วิศวกรรมเคมี
พ.ศ.	2554
อาจารย์ที่ปรึกษาวิทยานิพนธ์	รศ. ดร. อัญชลีพร วาริทสวัสดิ์ หล่อทองคำ
อาจารย์ที่ปรึกษาวิทยานิพนธ์ร่วม	ดร. วนิสา สุรพิพิธ

บทคัดย่อ

งานวิจัยนี้ศึกษาการกระจายตัวของฝุ่นรวม (Total suspended particulate matter: TSP) ฝุ่นขนาดเล็กกว่า 10 ไมครอน (Particulate matter with diameter less than 10 μm: PM_{10}) ความเข้มข้นเฉลี่ยรายชั่วโมงของแก๊สไนโตรเจนไดออกไซด์ และแก๊สซัลเฟอร์ไดออกไซด์ที่ถูกปล่อยจากโรงงานผลิตปูนซีเมนต์ 4 แห่งในเขตอำเภอแก่งคอย จังหวัดสระบุรี ในรัศมี 25 กิโลเมตรจากตำแหน่งอ้างอิงคือโรงงานผลิตปูนซีเมนต์ของบริษัท ปูนซีเมนต์นครหลวง จำกัด (มหาชน) โดยการตรวจวัดและการทำนายด้วยแบบจำลองทางคณิตศาสตร์ คือ American Meteorological Society-Environmental Protection Agency Regulatory Model (AERMOD) ซึ่งใช้สมการคณิตศาสตร์เกาเซียนพลูม และ California Puff Dispersion Model (CALPUFF) ซึ่งใช้สมการคณิตศาสตร์เกาเซียนพัฟ สำหรับความเข้มข้นของฝุ่นรวมสามารถอนุมานได้ด้วยความเข้มข้นของ PM_{10} เพราะที่ปล่องของเตาเผาปูนซีเมนต์ติดตั้งเครื่องดักจับอนุภาคด้วยไฟฟ้าสถิต จากแบบจำลองทั้งสองพบว่าความเข้มข้นเฉลี่ยราย 24 ชั่วโมงสูงสุดของ PM_{10} และค่าความเข้มข้นเฉลี่ยรายชั่วโมงสูงสุดของ NO_2 และ SO_2 ที่ 12 จุดตรวจวัด และที่สถานีตรวจวัดของกรมควบคุมมลพิษ 2 แห่ง มีค่าไม่เกินระดับความเข้มข้นตามมาตรฐานคุณภาพอากาศในบรรยากาศของประเทศไทย ในขณะที่ความเข้มข้นเฉลี่ยรายชั่วโมงสูงสุดของ NO_2 ที่อยู่นอกช่วงเวลาของการตรวจวัดเพื่อประเมินผลกระทบด้านสิ่งแวดล้อมของโรงงานมีค่าเกินมาตรฐาน

การประเมินสมรรถนะของ AERMOD และ CALPUFF โดยการพล็อต Quantile-Quantile ของความเข้มข้นเฉลี่ยรายชั่วโมงของ NO_2 ในช่วงฤดูแล้งและฤดูฝน พบว่าค่าความเข้มข้นเฉลี่ยรายชั่วโมงของ NO_2 ในฤดูแล้งใกล้เคียงกับเส้นแกนกลาง (ค่าตรวจวัด = ค่าทำนาย) มากกว่าในฤดูฝน แสดงว่าการทำนายผลในฤดูแล้งด้วยแบบจำลองมีความใกล้เคียงกับค่าวัดมากกว่า ทั้งนี้ความ

คลาดเคลื่อนเกิดจากปฏิกิริยาการตกสะสมเปียก (Wet deposition) ของกรดไนทริกจากแก๊สไนโตรเจนไดออกไซด์ในบรรยากาศที่มีความชื้นสูง อย่างไรก็ตามการประเมินสมรรถนะของ AERMOD และ CALPUFF ยังคงไม่ชัดเจน เพราะข้อมูลจากการตรวจวัด 1 สัปดาห์ ที่ใช้ในการทำนายผลสั้นเกินไป ดังนั้นเพื่อยืนยันผลการประเมินสมรรถนะของแบบจำลองได้วิเคราะห์หาเส้นทางการแพร่กระจายตัวของความเข้มข้นเฉลี่ยรายชั่วโมงของ NO_2 ด้วยแบบจำลอง CALPUFF ผลการจำลองพบว่าในฤดูแล้งเส้นทางการแพร่กระจายจะไปยังทิศเหนือ และ/หรือ เฉียงไปทางตะวันตก และ/หรือ เฉียงไปทางตะวันออกของพื้นที่ศึกษา แต่ในฤดูฝนจะเปลี่ยนทิศไปทางทิศตะวันตกของพื้นที่ศึกษาซึ่งเป็นบริเวณพื้นที่หน้าพระลานและเขาน้อย ผลการศึกษานี้แสดงให้เห็นว่าการไหลของอากาศและการกระจายตัวของ NO_2 ในพื้นที่แก่งคอยไม่ได้ถูกควบคุมด้วยลมประจำถิ่นและลมประจำฤดูกาลเท่านั้น แต่ยังขึ้นกับความซับซ้อนของสภาพภูมิประเทศ นอกจากนี้จาก CALPUFF ยังพบว่าพลูมของ NO_2 ในทั้งสองฤดูมักไม่เคลื่อนตัวพาดผ่านพื้นที่ของจุดตรวจวัดทั้ง 12 แห่ง ดังนั้นจำเป็นต้องพิจารณาตำแหน่งของจุดตรวจวัดที่เหมาะสมกว่านี้ต่อไป

Thesis Title	Measuring and Modeling of Air Pollutant Dispersions from Cement Plants
Student	Ms. Kanyanee Seangkiatiyuth
Student ID.	49061703
Degree	Doctor of Engineering
Program	Chemical Engineering
Year	2011
Thesis Advisor	Assoc. Prof. Dr. Anchaleeporn W. Lothongkum
Thesis Co-advisor	Dr. Vanisa Surapipith

Abstract

This research examined the dispersion of total suspended particulate matter (TSP), particulate matter with a diameter less than 10 μm (PM_{10}), hourly averaged concentrations of nitrogen dioxide (NO_2) and sulfur dioxide (SO_2) from 4 cement manufacturers in Kaeng Khoi, Saraburi, Thailand. The dispersion was considered within a 25-km distance from the Siam City Cement Public Company Limited (SCCC), a reference point, by both measurement and modeling using the American Meteorological Society-Environmental Protection Agency Regulatory Model (AERMOD), a Gaussian plume model, and the California Puff Dispersion Model (CALPUFF), a Gaussian-puff model. For a cement plant with an electrostatic precipitator at the cement stack, the concentration of TSP can be reported in terms of PM10 concentration. From the AERMOD and CALPUFF simulations, the 24-hour averaged concentration of PM_{10}, the maximum 1-hour averaged concentrations of NO_2 and SO_2 at 12 receptors and 2 semi-permanent monitoring stations of the Pollution Control Department (PCD) stayed within the National Ambient Air Quality Standards (NAAQSs) of Thailand, while the maximum 1-hour averaged concentration of NO_2, which was not measured during 7 days for the EIA, exceeded the NAAQS.

The performances of the AERMOD and CALPUFF were validated by the Quantile-Quantile plots of 1-hour averaged NO_2 concentrations in dry and wet seasons. The 1-hour averaged NO_2 concentrations in dry season were mostly fitted to the middle line (measured = simulated) compared to those in wet season indicating that the model prediction in dry season was closer to the measurement due to high NO_2 deposition reactions in wet

environment. However, the performances of both the AERMOD and CALPUFF were still inconclusive because the measurement data from the EIA reports using in the simulation were obtained in a short period of 1 week. Therefore, the real-time hourly concentrations of NO_2 were analyzed to confirm the prediction by the model. By using the CALPUFF, it was found that the trajectories or plumes of NO_2 concentrations in dry season dispersed to the north of the domain, sometimes switched to the west and/or the east of the domain, whereas in wet season, the trajectories of NO_2 concentrations moved to the west of the domain to Na Phra Laan and Kao Noi areas. This study shows that the air circulation and NO_2 dispersion in Kaeng Khoi are not controlled only by local and seasonal winds but also the complex topography of the study areas. Furthermore, by the CALPUFF it was observed that the locations of 12 receptors were not always hit by the NO_2 trajectories in both seasons. As a result, suitable locations of the receptors should be considered. As a result, suitable locations of the receptors should be considered.

Acknowledgements

The author would like to express her gratitude to Assoc. Prof. Dr. Anchaleeporn W. Lothongkum (Thesis advisor) and Dr. Vanisa Surapipith (Thesis co-advisor) for their support and fruitful advice to complete this work. The assistance and the licensed ISC-AERMOD View version 4.6.2 from the Siam City Cement Public Company Limited are also acknowledged.

Research grant IUG50K0021 from the Royal Golden Jubilee (RGJ), Thailand Research Fund (TRF) is highly appreciated.

Sincere thanks go to Mr. Thanit Pulivekin, Executive Consultant, the Siam City Cement Public Company Limited, for his contribution, encouragement and helpful suggestions.

The author would like to thank Assist. Prof. Dr. Kraichat Tantrakarnapa, the Department of Environmental Health Sciences, Faculty of Public Health, Mahidol University for his suggestions and providing the licensed ISC AERMOD View version 5.4.

The author is very grateful to Prof. Dr. C. Jerry Lin, the Department of Civil Engineering, Lamar University, Beaumont, Texas for his kind contribution and helpful suggestions during her stay at Lamar University for 6 months.

Deep appreciations also go to the Air Quality and Noise Management Bureau, Pollution Control Department, the Ministry of Natural Resources and Environment for providing monitored air quality and meteorological data, particularly allowing Dr. Vanisa Surapipith to serve as the co-advisor; the Thai Meteorological Department for providing meteorological data; and Faculty of Engineering, King Mongkut's Institute of Technology Ladkrabang for providing facilities.

Last but not least, the author would like to acknowledge her family for their love and unlimited support.

Kanyanee Seangkiatiyuth

Contents

Contents (cont.)

Contents (cont.)

List of Tables

List of Tables (cont.)

List of Tables (cont.)

Tables **Page**

List of Tables (cont.)

Tables **Page**

List of Figures

List of Figures (cont.)

Figures **Page**

List of Figures (cont.)

List of Figures (cont.)

Figures **Page**

List of Figures (cont.)

List of Figures (cont.)

List of Figures (cont.)

List of Figures (cont.)

Chapter 1

Introduction

1.1 Rational

Saraburi, a province located about 100 km north-east of Bangkok, is one of an important industrial areas in Thailand. There are 1,420 industrial sites distributed in 13 districts such as mining, stone crushing, cement and concrete manufacturers, automobile parts industry, agriculture, etc. Most of the industry sites, of about 335, 217 and 206, are located in Nong Kae, Kaeng Khoi and Chaloem Phra Kiat districts, respectively [1]. More details of the industries in Saraburi are shown in Appendix A.

Large area of Nah Phra Laan (NPL), a sub-district of Chaloem Phra Kiat, has been confronted the emission of particulate matter (PM) and covered by smog from the mineral and crushing industries for years. As a result, many projects from academic and government sectors concerning the PM impacts on this area were operated [2-7]. For a sustainable control of PM emissions, Nah Phra Laan was thereby announced as the pollution control zone by the Pollution Control Department (PCD), the Ministry of Natural Resources and Environment in 2006 [8]. Currently, many public activities concerning the reduction of PM throughout the year such as cleaning days, the competition and campaign of PM emission control, etc have been launched. However, high PM concentrations in the atmosphere over the National Ambient Air Quality Standards (NAAQSs) of 120 $\mu g/m^3$ are found randomly at times [9].

Although there are big 4 cement manufacturers (the Siam Cement Public Company Limited: SCG, Siam City Cement Public Company Limited: SCCC, TPI Polene Public Company Limited: TPIPL, and Thai Pride Cement Company Limited: TPCC) located in Kaeng Khoi district, a few projects on air pollution by academic and government sectors have been studied in Kaeng Khoi. Some projects are available in the connecting areas (Nah Phra Laan in Chaloem Phra Kiat district). However, such studies are not enough to provide the strategies for pollution prevention and control in Saraburi. In general, each cement company is requested to report the potential air pollution on the communities nearby the company in the Environmental Impact Assessment (EIA) report, at least twice a year and otherwise case-by-case reports. Even the activities in Kaeng Khoi district are not similar to those in Nah Phra Laan, there are possible emission impacts on public health. In fact, the cement manufacturers are known as the major source of air pollutions, i.e., PM, nitrogen oxides (NO_x), sulfur dioxide (SO_2), carbon dioxide (CO_2), volatile organic compounds (VOCs), dioxins, heavy metals, etc. In addition, the cement production is a substantial source of the emission of CO_2 (a green house gas: GHG) which causes the global warming and climate change. Managing of CO_2 emissions by cement manufacturers in Thailand are reviewed elsewhere. The Holcim (U.S.) Inc. reported that PM, which is emitted from all steps of cement production, is the major emission from the cement manufacturers. Table 1.1 shows that the kiln is the main source of the emissions of PM_{10}, NO_x and SO_2 in cement production.

Table 1.1 Air pollutant emissions from cement production units reported by the Holcim (U.S.) Inc. [10].

Units	Emitted pollutants (tons/year)		
	PM_{10}	NO_x	SO_2
Convey-screen	15.89	Nil	Nil
Primary crusher/screen	10.96	Nil	Nil
Raw material silos	19.52	Nil	Nil
Coal/coke unload	7.88	Nil	Nil
Coal and coke, crush, store, (un) load & grinding	33.1	Nil	Nil
Coal outside storage piles	0.28	Nil	Nil
Coke outside storage piles	0.28	Nil	Nil
Coal silo loading and unloading	3.00	Nil	Nil
Coke silo loading and unloading	1.13	Nil	Nil
Kiln	163.6	6,868	543.1
Clinker cooler	75.09	Nil	Nil
Inside clinker from cooler	5.26	Nil	Nil
Cement kiln dust silo load	2.25	Nil	Nil
Cement kiln dust silo unload	16.92	Nil	Nil
Emergency clinker bins loading	4.13	Nil	Nil
Emergency clinker storage silos	0.09	Nil	Nil
Clinker mill	17.72	Nil	Nil
Cement load/unload at silos	20.12	Nil	Nil
Bulk cement railcar load outs	1.80	Nil	Nil
Bulk cement rail load out	0.00	Nil	Nil

Note: Nil means that emission of this pollutant from this emitting unit is un-quantifiably small and deserves no further consideration.

Because the air pollution from the cement production is a crucial issue, therefore, this research examines the dispersion of total suspended particulate matter (TSP), particulate matter with a diameter less than 10 μm (PM_{10}), hourly averaged concentrations of nitrogen dioxide (NO_2) and sulfur dioxide (SO_2) from 14 stacks of 4 cement manufacturers in Kaeng Khoi, so-called the cement complex. Their locations are shown in Figure 1.1. The total production capacities of 4 cement manufacturers in 2008 are approximately 23.6 Mt/year, which is about 79% of the total cement production capacity in the country [11]. The air pollutant dispersion is studied by both modeling and measurement because (i) there is no permanent air monitoring station in Kaeng Khoi and (ii) the routine measurement of air pollutants according to the EIA requirements cannot represent air quality of the study areas. To resolve these limitations, the American Meteorological Society-Environmental Protection Agency Regulatory Model (AERMOD), a Gaussian plume model, and the California Puff Dispersion Model (CALPUFF), a Gaussian puff model, are used. The AERMOD and CALPUFF are air dispersion models recommended by the U.S. EPA [12-14]. They have been using by a number of Thai environmental consultants as assessment tools for EIA evaluations. Both software programs can apply for such a case in mountain areas identifying as the complex terrain. For these reasons, the AERMOD and CALPUFF are used in this work to evaluate the emissions from the cement complex. The results in this work are expected being primary guidelines for the cement industry to establish the strategy of air pollution control.

1.2 Study areas

Saraburi is a province in the central plain of Thailand as shown in Figure 1.1. There are 13 districts on the total area of 3,576.4 km^2 with a population density of 111 persons/km^2. The 4 cement manufacturers in Kaeng Khoi district, about 108 km north-east of Bangkok, are within 25 km apart from each other and located in the limestone mountains beside the highway. One cement manufacturer in the center of the complex was designated as the reference point (the cement stack No.1 of the SCCC) for the receptor distances. The study areas are in the center of heavy transportation. The area of surrounding communities is about 801.1 km^2 with a population density of 79 persons/km^2 [15]. Most of the population is farmers. The east side of the study areas is high plains and plateaus next to the Khao Yai National Park, which consists of complex mountains of high peaks about 800 to 1,351 meters above sea level. The regional climate is dominated by northeast and southwest monsoons with different rainfall and temperature characteristics. The northeast monsoon brings relatively cool and dry air from the central of the Asia continent around the middle of October to March. The southwest monsoon from the Indian Ocean is characterized by periods of intense rain from April to October with some thunderstorms. The average rain fall in the study areas is about 1,600 mm, which is 80% during the rainy season. The average temperatures in the summer and winter range from 13-36 $^{\circ}$C and in the rainy season from 19-37 $^{\circ}$C. Due to the mountains in the study areas, the meteorological conditions are affected by the valley breezes and mountain breezes. Both breezes relate to wind directions at day and night. The valley breezes occur during the daytime when the sun heats the valleys and the slopes of mountains. The air near the mountain surface is heated, expanded and risen up the mountain sides. On the other hand, the mountain breezes occur during the nighttime when the valleys are cooled rapidly with out-going long-wave radiation at the night, the air nearby the cooler surface flows down the slopes to the valleys due to higher density [16].

1.3 Research objectives

The main objective of this study is to use the AERMOD and CALPUFF as the tools to simulate the dispersion of air pollutants from 4 cement manufacturers in Kaeng Khoi, Saraburi. The concrete objectives are as follows:

1.3.1 To set up the emission inventory for the Kaeng Khoi and its vicinity

1.3.2 To investigate the complex terrain that induces local air circulations in Kaeng Khoi by the California Meteorological Model (CALMET)

1.3.3 To simulate the dispersion of air pollutants from 4 cement manufacturers by the AERMOD and CALPUFF and validate the model performances

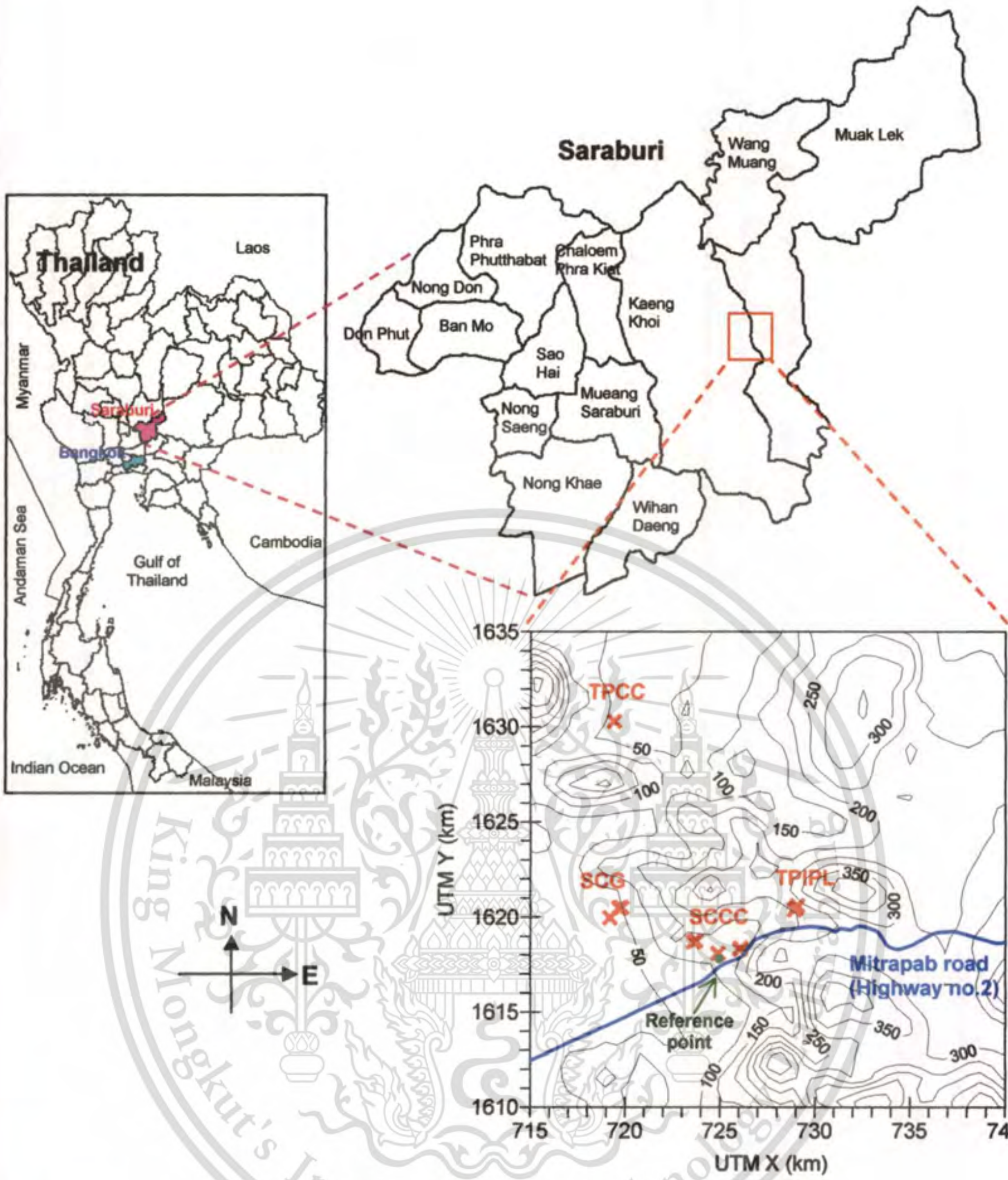

Figure 1.1 Locations of the cement manufacturers in Kaeng Khoi, Saraburi.

1.4 Scope of the study

1.4.1 Collect the observed meteorological factors and concentrations of pollutants at the monitoring stations in Kaeng Khoi

1.4.2 Analyze air pollutants and their relationship to meteorological factors

1.4.3 Collect and compile the emission inventory based on the data of the Pollution Control Department, EIA reports and other sources

1.4.4 Simulate local meteorological conditions by the CALMET

1.4.5 Simulate the dispersion of air pollutants by the AERMOD and CALPUFF

1.4.6 Verify the simulation results with the measurement data

This study shows the impacts of emissions from the cement manufacturers in Kaeng Khoi district by integrating the monitoring measurement and the simulation by software programs (the AERMOD and CALPUFF) which are recommended by the United States Environmental Protection Agency (U.S.EPA). Figure 1.2 illustrates the structures of 5 chapters. **Chapter 1** presents the study areas and a brief overview of this study. **Chapter 2** reviews background theories and relevant literature for a comprehensive understanding of how to evaluate and encounter the air pollution problems. The methodology relating to the emission inventory, measurement and modeling are presented in **Chapter 3**. Accordingly, in **Chapter 4** the results are discussed. Finally, **Chapter 5** is the conclusions and recommendations.

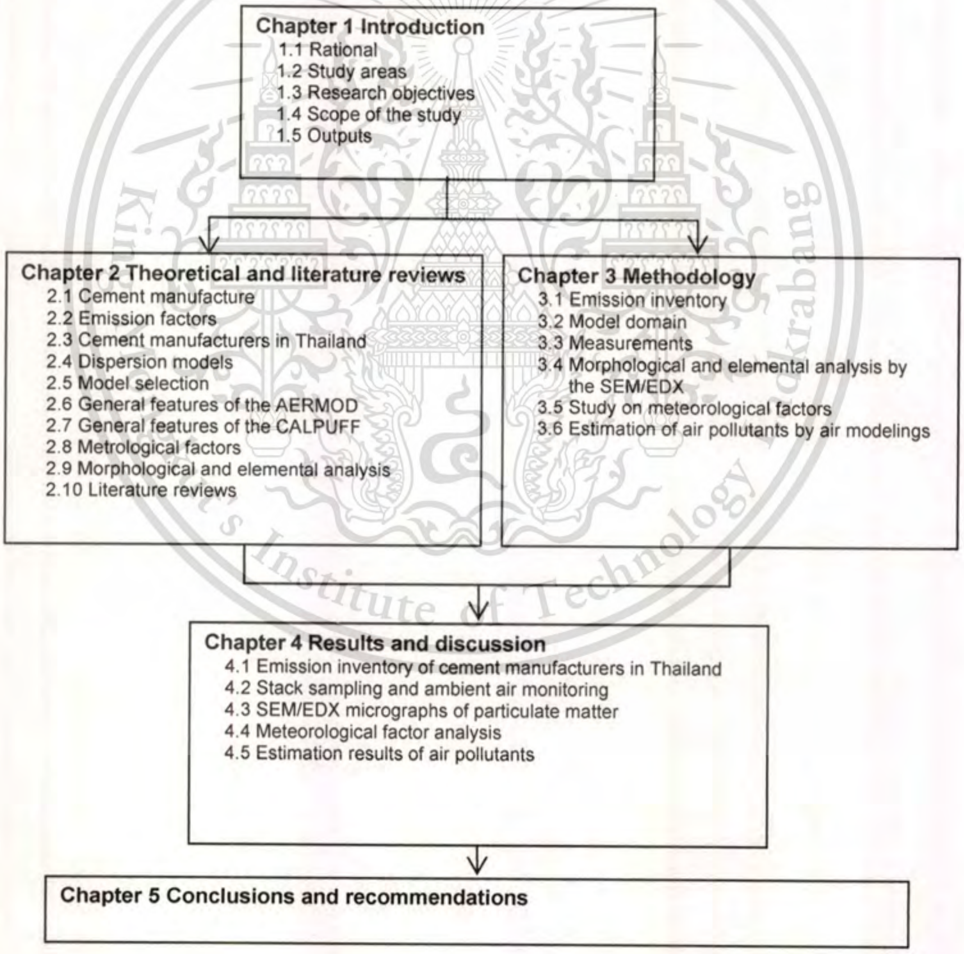

Figure 1.2 The structures of this study.

1.5 Outputs

1.5.1 Information about pollutant impacts on the communities nearby the cement complex in the study areas by the simulation and measurement

1.5.2 Guidelines on air pollution control and air quality management for the cement manufacturers

Chapter 2

Theoretical and literature reviews

In this chapter, air pollutants from the cement manufacture and their emissions, the cement companies in Thailand and the ambient air quality standards are described. General descriptions of the dispersion models for air quality management and meteorological factors are discussed. In the end, the literature showing the applications of the AERMOD and CALPUFF in the cement plants is reviewed.

2.1 Cement manufacture

Generally, the cement production begins at the quarry. Most of raw materials are combined with high and low grades of shale and limestone ($CaCO_3$) from the quarry. The compositions of these shale and limestone are the oxides of aluminium, calcium, silicon and iron. Limestone rock and other raw materials are blasted and loaded into the trucks and transported to the crushers or to stockpiles. The raw materials are conveyed from the primary crusher to the storage bins then to the ball mills where they are ground, and finally sent to the storage silos. The homogenized raw materials or homogenized ground raw meals are preheated in the cyclones to initiate the dissociation of calcium carbonate ($CaCO_3$) to calcium oxide (CaO) and CO_2. To keep the temperature sufficiently high, the primary fuels, i.e., fuel oils, natural gas, coals, petroleum coke, and the secondary fuels, e.g., ground tires, chopped plastics, paper wastes, etc., are fed into the preheating system. The preheated ground raw meals then proceed to the kiln for calcination. The kiln temperature is up to 1,450 $^{\circ}C$. The coals used as the primary fuel are fed to keep the temperature high enough in the burning zone for the chemical reactions taking place. When the clinker leaves the kiln, it is cooled, then transported to the finishing mill feed bins or other storages. From the finishing mill feed bins, the clinker, gypsum and other additives are transported to the finishing ball mills, where they are ground to product. The final cement product is conveyed to the storage silos where it is loaded into railroad cars or bulk trucks [17-18]. The cement production process is summarized in Figure 2.1.

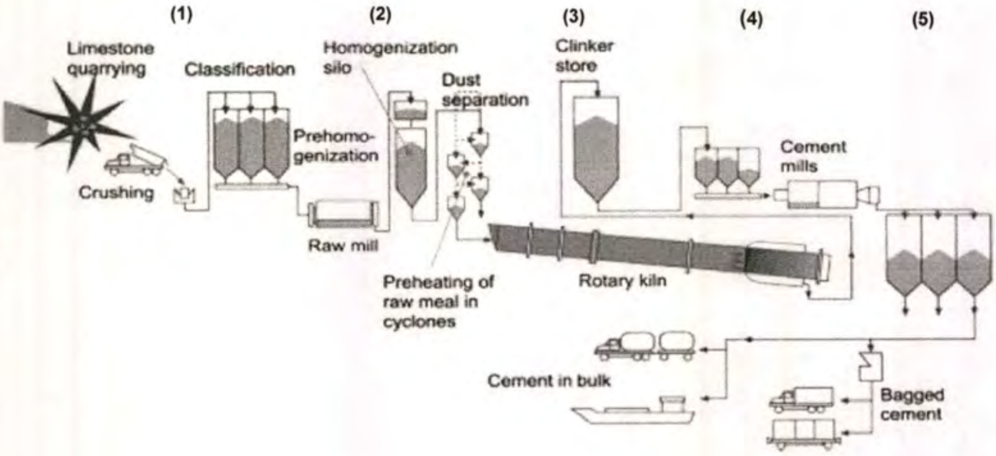

Figure 2.1 Flow chart of cement production: (1) Crushing and proportioning, (2) Raw milling and blending, Pyro processing, (3) Burning and cooling, (4) Cement milling, and (5) Storage and packing [17-18].

Two kinds of typical cement productions are wet and dry processes. The wet process requires simple process control and instrumentation and less manpower than the dry process but it consumes a large amount of energy to dry the slurry of 2.4 GJ/ton or 20% of total energy consumption [17-18]. The energy consumption for wet and dry processes is summarized in Table 2.1

Table 2.1 Average energy of dry and wet processes (GJ/ton) [17].

Heat requirements	Dry process	Wet process
Chemical reactions	1.76	1.76
Evaporation of water	0	2.4
Heat loss	1.4	1.7
Total	**3.16**	**5.86**

2.1.1 Air pollution from cement manufacture

According to Figure 2.1, the cement production process includes (1) quarrying and crushing, (2) raw material storage, (3) grinding and blending (the dry process only), (4) clinker production, (5) grinding and (6) packaging and loading [17-18]. The PM has been considered as a major emission. It is emitted from all steps of the cement production. Other gases, e.g., NO_x, sulfur oxides (SO_x), CO_2, etc., are emitted during the combustion process from the cement kiln. A wide range of pollutants can be emitted if the combustion reactions do not reach completion.

Incomplete combustion can lead to emissions of specific hazardous organic air pollutants, although these pollutants are generally emitted at substantially low levels. These emissions, for example, VOCs, ammonia, hydrogen chloride and heavy metals depend on types of fuels [19].

Even though there are various emissions from cement manufacturers, the most commonly selected air quality indicators for urban and industrial air pollution are criteria air pollutants such as PM_{10}, NO_2, SO_2 and CO while the secondary air pollutants such as $PM_{2.5}$, aerosols and O_3, are increasingly concerned. Other air pollutant indicators of potential impacts are, for example, polycyclic aromatic hydrocarbons (PAHs), benzene, toluene, ethylbenzene and xylenes (BTEX), chlorinated compounds, polychlorinated dibenzodioxins (PCDDs) and Polychlorinated dibenzofurans (PCDFs), VOCs and other heavy metals such as arsenic (As), cadmium (Cd), copper (Cu), lead (Pb), mercury (Hg) and nickel (Ni). Some of these indicators are related to air pollution standards, the permit emissions and air quality guideline values. These indicators give the ideas to assess health impacts. Two legislation standards in Thailand are as follows:

- National Ambient Air Quality Standards (NAAQSs) written in terms of concentration ($\mu g/m^3$ or ppm (parts per million)), and

- National Source Performance Standards (NSPSs) written in terms of mass emission per unit of time or unit of production (g/min or kg of pollutant per ton of production produced) [20-25].

Both standards are established to protect the public health. The Thai government has set up the NAAQSs to consider acute and chronic effects of the principal pollutants, i.e., TSP, PM_{10}, $PM_{2.5}$, Pb, NO_2, SO_2, CO and O_3. The NAAQSs along with the guidelines on air quality of the World Health Organization (WHO) as shown in Table 2.2 are higher than the WHO's guidelines because their impacts on socioeconomic and the implementation of the control measures are also taken into account. In case of the NSPSs, they have been established according to the industrial types. For example, the allowable emissions from cement kilns in Thailand are listed in Table 2.3. The emissions of TSP, NO_x and SO_2 are mainly permitted under the differential limitation depending on their toxicity to the public. Moreover, the new cement kilns are forced to reduce their emissions by cutting their allowable emissions. Lately, many countries have launched policies to control air pollution in their countries. For example, the U.S. EPA has issued the policy to protect Americans' health in January 2010 by reducing the allowance emissions of air pollution from the country-wide cement kilns [24]. According to the U.S. EPA, by 2013 the cement manufacturers are expected to reduce annual emissions from present as follows:

- Hg 7,470 kg (92%),
- total hydrocarbons 10,600 tons (83%),
- PM 11,500 tons (92 %),
- acid gases measured as hydrochloric acid 5,800 tons (97%), and
- SO_2 110,000 tons (78%).

Table 2.2 National ambient air quality standards in Thailand and WHO's guidelines [21-22].

Pollutants	**Average in period of time**	**Standard values, µg/m³ (ppm)**	
		Thailand	**WHO's guidelines**
$PM_{2.5}$	24 h	≤50	≤25
	Annual	≤25	≤10
PM_{10}	24 h	≤120	≤50
	Annual	≤50	≤20
TSP	24 h	≤330	-
	Annual	≤100	-
NO_2	1 h	≤320 (0.17)	≤200 (0.11)
	Annual	≤57 (0.03)	≤40 (0.02)
SO_2	10 minutes	-	≤500 (0.19)
	1 h	≤780 (0.30)	-
	24 h	≤300 (0.12)	≤20 (0.008)
	Annual	≤100 (0.04)	-
O_3	1 h	≤200 (0.10)	-
	8 h	≤140 (0.07)	≤100 (0.05)
	Annual	≤100 (0.04)	-
CO	1 h	≤34,200 (3)	-
	8 h	≤10,260 (9)	-
Lead (Pb)	1 month	≤1.5	-

- is not available

Table 2.3 Emitting standards for the cement kilns in Thailand [23].

Kilns of cement types	**Emissions, mg/m³ (ppm)**		
	TSP	**NO_x**	**SO_2**
Existing kiln (built before 19th January 2004)			
Grey cement	≤300	≤1,129 (600)	≤131 (50)
White cement	≤300	≤1,129 (600)	≤1,571 (600)
New kiln (built after 19th January 2004)			
Grey cement	≤120	≤941 (500)	≤131 (50)
White cement	≤120	≤941 (500)	≤1,309 (500)

Note: All emissions were reported under dry condition with excess oxygen 7% at 25 °C and 760 mmHg.

The emissions from industrial and other activities give impact not only to the local area but also to the regional, continental and global scales. The small particle pollutants such as fine PM, CFCs, HCFCs and GHGs can be transported globally as shown in Figure 2.2. Furthermore, various complex physical and chemical processes may involve during their transportation [25].

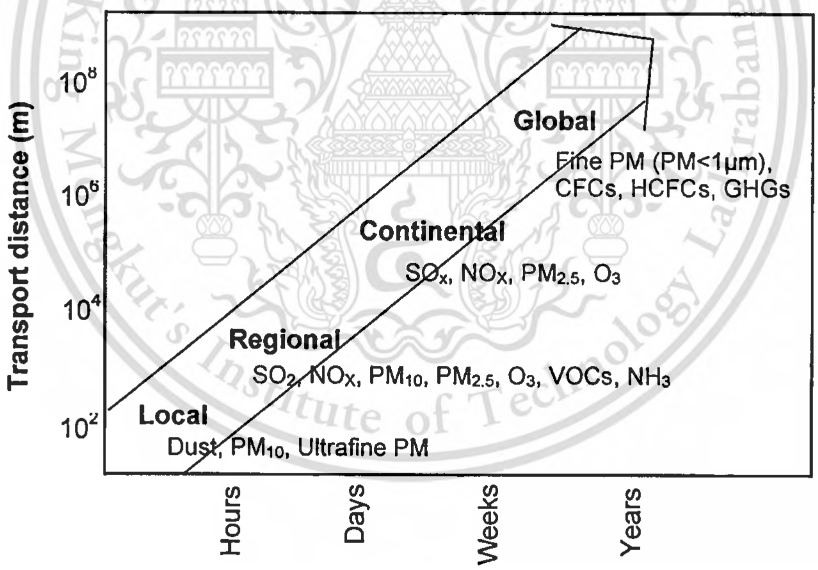

Figure 2.2 Transport scales of the pollutants [25].

The pollutants emitted from the burning process of the cement kiln are described in brief.

(1) PM

The PM emitted from the cement kiln is solid, fine-grained and high alkaline component. It can be removed from the exhaustible gas of the cement kiln by the control devices such as cyclone, bag filter, electrostatic precipitator, etc [20]. A large amount of PM can be sent back to the cement production process as secondary raw materials. Practically, some PM can be reused directly, while some require a treating process before sending back. The PM, which is not returned to the production process, is typically disposed in land-based disposal units, i.e., landfills, waste piles, or surface impoundments. But some of the emitted PM is sold for beneficial reuse. Generally, the PM emitted from the cement kiln ranges in size with diameters from 0.12-100 μm [26]. In Thailand, TSP, PM_{10} and $PM_{2.5}$ have been considered and limited their concentrations in atmosphere to protect public health. Actually, the TSP is used as an indicator for PM because TSP emissions include the components of PM_{10} and $PM_{2.5}$. The U.S. EPA classifies the size of PM according to the potential to cause health problems. Two particle pollution categories are:

- coarse particles: 2.5-10 μm in diameter, and
- fine particles: smaller than 2.5 μm in diameter.

The U.S. EPA is practically concerned the particles of their diameters 10 μm or smaller, particularly, less than 2.5 μm because they can pass through the nose and throat to the lungs [27-28].

(2) NO_x

The NO_x is typically referred to a mixture of such compounds as nitric oxide (NO) and NO_2. Normally, the NO_2 is harmful to respiratory system, and its ambient concentration is set in accordance with the NAAQSs. The NO and NO_2 are involved in photochemical reactions and rapidly exchange. Therefore, the NO_x emission standards in ambient air have been considered in terms of NO_2. In the cement production process, NO_x is generated in burning zones of the cement kiln and the precalcination vessel. Virtually, all thermal NO_x is generated in the region of the flame at the highest temperature, approximately from 1,650 °C to 1,980 °C. The amount of generated NO_x depends on types of fuels [17, 29]. As shown in Table 2.4, coal generates the largest amount of NO_x and gives the lowest heating value comparing to those of fuel oil and natural gas. However, due to dramatic increase of fuel oil price, most cement plants have changed their burning systems to match up with the combination of coal and waste fuels. So far, it is still unclear about the air pollution impact as no existing reports on this issue. For example, the SCCC's kilns operate at a temperature of 1,800 °C and can burn all types of fuels including the municipal wastes.

Table 2.4 Emission factors for nitrogen oxides [17, 30-32].

Sources	Averaged NO_x emissions (kg/ton of burned fuels)	Heating values (MJ/kg)
Coal	9.1	26-30
Fuel oil	8.7	42-43
Natural gas	4.7	46-47

(3) SO_x

Sulfur oxides from the combustion processes includes lower sulfur oxides (S_nO, S_7O_2 and S_6O_2), sulfur monoxide (SO), sulfur dioxide (SO_2), sulfur trioxide (SO_3) and higher sulfur oxides (SO_{3+x} where $0 < x \leq 1$). SO_2 is the predominant pollutant species in combustion products from the burning zone of cement kiln at high temperature and is used as a precursor for SO_x concentration. SO_2 is a colorless gas with sharp odor and extremely corrosive in the presence of water. It is a very aggressive pollutant and can damage vegetation and the respiratory systems of human beings and animals. Sulfur is generally found in the cement kiln from fuels and other raw materials such as shale, limestone, etc. Therefore, the potential emissions of SO_x depend basically on sulfur cycles (from lower sulfur oxides, SO, SO_2, SO_3 to higher sulfur oxides), which are influenced by sulfur contents in fuels and raw materials, and the production process (wet or dry process). It is possible to reduce SO_x emissions from the combustion by the following methods:

- pre-treatment by removal or reduction of sulfur in the fuels, and
- post-treatment by applying alkaline scrubbers to remove SO_x from the combustion gases. Normally, the SO_2 can react with CaO in raw materials to form calcium sulfite ($CaO + SO_2 \longrightarrow CaSO_3$) during calcination and combustion processes in the cement kiln [29].

(5) CO_2

The CO_2 is a typical GHG causing global warming and climate change. It shares 77% of all GHGs in the world. The amount of CO_2 in the atmosphere has increased from 280 ppm to 380 ppm since the beginning of the industrial age of 1800 C.E. [33-35]. The CO_2 emissions mainly come from thermal and power generating industries (35%), cement industry (22%) and road transport (18%). Other sources of CO_2 emission are non-road transport, refinery and energy-related industries, etc [33, 36]. Of all the CO_2 emission of 22% from cement industry, 60% comes from calcination and 40% comes from combustion [37-38]. The calcination process thermally decomposes $CaCO_3$ to CaO and CO_2. It should be noted that substantial quantities of CO_2 emissions are generated from the calcination of limestone or other calcareous materials [37].

(6) Dioxins

Dioxins are carcinogen. Apart from many other adverse health effects, tumor development, birth defects, reproductive disorders, immune system disorders and skin disorders are caused by exposure to dioxins. They are generated from precursor molecules from incomplete combustion at high temperatures and later react further in the lower temperature region of the combustion chamber. Dioxin is claimed to form at a temperature of 250-450 $^{\circ}C$. With either lower or higher temperature inhibits dioxin formation. In common cement production, dioxins are rarely generated because of very high temperature combustion. This critical temperature of 250-450 $^{\circ}C$ occurs when the combustion gases are cooled in flue ducts, heat exchangers, air pollution control equipment or the stack. Hence, the reduction of flue gas temperature in the pollution control device below 250 $^{\circ}C$ can substantially control dioxin formation in cement kilns [39-40].

Many cement manufacturers have been using waste tires and other wastes containing chlorine compounds as the secondary fuels to save the energy cost, however, burning wastes and primary fuels (mostly coal) results in incomplete combustion and enhances dioxin formation. According to a case study of "Holcim's Trident Kiln", it was found that burning waste tires increased dioxin emissions by 60%. Other studies by the U.S.EPA also revealed that using waste tires significantly increased the emissions of cancer-precursor dioxins [10].

(7) VOCs

The VOCs are aliphatic or aromatic hydrocarbons with low molecular weight of alcohols, ketones, esters and aldehydes. The emissions of VOCs to the atmosphere can cause the following problems.

- irritation of mucous membranes of the respiratory systems
- photochemical smog
- reduction of the ozone layer

Even the VOCs are minor contaminants in combustion process but some VOCs such as styrene (C_8H_8) and limonene ($C_{10}H_{16}$) can react with NO_x or O_3 to produce new oxidation products and secondary aerosols which can cause sensory irritation symptoms. Unspecified VOCs are important in smog generation. In cement manufacture, it is possible to find VOCs in exhaust gases of the rotary kiln from a low temperature pyrolysis of organic matters in raw materials. It is necessary to emphasize that VOCs emissions cannot be controlled without modifications of the combustion process, for example, by post-treatment techniques, e.g., thermal oxidation and/or catalytic oxidation [29].

(8) Heavy metals

Heavy metals in fuels and raw materials are found in cement clinker and solid wastes, e.g., ash, PM from cement plants. The emissions of metal compounds from cement kilns can be classified into three groups as follows:

- volatile metals, i.e., mercury (Hg) and thallium (Tl),
- semi-volatile metals, i.e., antimony (Sb), cadmium (Cd), lead (Pb), potassium (K), selenium (Se), zinc (Zn) and sodium (Na), and
- nonvolatile metals (refractory metals), i.e., arsenic (As), barium (Ba), chromium (Cr), copper (Cu), manganese (Mn), nickel (Ni), vanadium (V) and silver (Ag).

Although the partitioning of metal groups is affected by kiln operating conditions. The nonvolatile metals are mostly found in the clinker, while the volatile and semi-volatile metals are discharged to the primary exhaust stack and the bypass stack, respectively. Among the above metals, mercury is seriously concerned because it can enter an aquatic system and accumulate in the food chain [29, 41].

2.2 Emission factors

The volumes of emissions can be estimated by the emission factors (EFs) which are basically a ratio of mass of a pollutant emitted to a measured level of source activity. The EFs relate the quantity of a pollutant released to the atmosphere with an activity associated with the release of that pollutant, e.g., pounds of particulate emitted per ton of oils or coals, kilograms of particulate emitted per megagram (Mg) of oils or coals. The EFs facilitate the estimation of the emissions from various sources of air pollution. In most cases, these factors are simply averaged from all available data (e.g., activities and pollutants from cement plants using oil or coal based on the standards of each location) and generally assumed to represent the long-term averages of all equipment and facilities which are used in the source category [42].

The general equation to calculate the typical emissions is:

$$E = A \times EF \tag{2.1}$$

where:

E = Emissions (e.g., lb or kg of each pollutant/year)

A = Activity or production rate (e.g., ton or megagram of oils or coals/year)

EF = Emission factor (e.g., lb of each pollutant/ton of oils or coals)

The EFs are the database for the emission inventories (EIs) which report all of the emissions from industrial activities and transportation. The EIs are published on papers and websites such as Emission Database for Global Atmospheric Research (EDGAR) [43], Global Emissions Inventory Activity (GEIA) [44], Transport and Chemical Evolution over the Pacific (TRACE-P) [45], Regional Emission Inventory in Asia (REAS) [46], U.S. EPA, European Environment Agency (EEA), Intergovernmental Panel on Climate Change (IPCC), etc.

Although EIs to estimate the emissions from several sources are available but no database of any cases in Thailand exist. Thus, it is necessary to select the most suitable EIs (case-by-case basis) for the industries in Thailand. In this work, the potential emissions from the cement manufacture are estimated in accordance with the European Monitoring and Evaluation Program (EMEP)/EEA air pollutant emission inventory guidebook-2009 [42].

2.3 Cement manufacturers in Thailand

In Thailand, the primary cement product is called grey or portland cement. Grey cement is a fine powder consisting of a mixture of four basic materials: lime, silica, alumina and iron compounds. The most common cement production system in Thailand is dry process using the rotary kiln since it consumes less energy than wet process [11]. Only the Thai Sathapana Co., Ltd., which is the smallest cement manufacturer, still operates the semi-wet process with the shaft kiln. Coals and gases, which may be supplemented by waste-derived fuels such as waste tires, waste oils, solvents and other similar materials, are used as fuels by almost cement manufacturers [10, 17].

There are 9 grey cement companies of which the cement plants are distributed throughout Thailand. The total annual clinker and cement production capacities of all cement companies are about 46.8 and 56.5 Megaton (Mton), respectively [11]. However, the actual cement production is 30 Megaton which is about 53% of full capacity. From Table 2.5 and Figure 2.3, the SCG Group is the biggest cement manufacturer in Thailand. There are 5 cement plants under the cooperation of the mother company, namely SCG Cement Company Limited. One of all is located in Kaeng Khoi, Saraburi where the natural resources of limestone and shale are. In Kaeng Khoi, the SCCC is the largest cement manufacturer followed by the TPIPL and SCG.

Table 2.5 Cement companies in Thailand [11, 47].

Cement companies	Founded	Production capacities (Mton/year)	Foreign partnership (Country)	Stock holdings (%)
SCG Cement Company Limited	1998	23.2	-	-
Siam City Cement Public Company Limited	1968	14.8	Holcim group (Switzerland)	32
TPI Polene Public Company Limited	1987	9.1	-	-
Asia Cement Public Company Limited (ACC)	1989	5.0	Italcementi group (Italy)	25
Jalaprathan Cement Public Company Limited (JCC)	1956	2.3	Italcementi group (Italy)	37
Cemex (Thailand) Company Limited (CMEX)	1990	0.8	Cemex group (Mexico)	99
Thai Pride Cement Company Limited	2005	1.0	Italian Thai Development Public Company Limited (ITD) (Thailand and Italy)	99
Thai Sathapana Company Limited	No data	0.2	No data	No data
Samukkee Cement Limited	1991	0.1	-	-
Total		**56.5**		

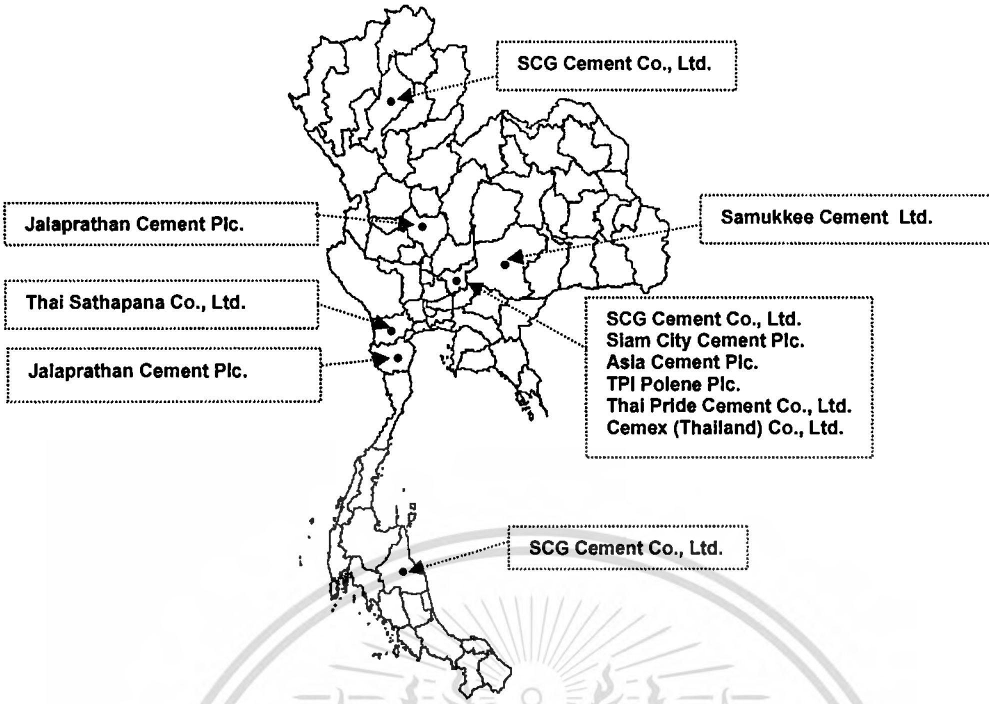

Figure 2.3 Locations of the cement plants of each company in Thailand [11].

After the economic recession in Thailand in 1997, some cement companies were forged alliances with foreign companies. The joint venture companies are Holcim Group, Italcementi Group, Cemex Group, and Italian Thai Development Public Company Limited (ITD). Details of the cement companies in Thailand are shown in Table 2.5. At present, the internal market of cement manufacturers in Thailand focuses on grey and mixed cements while the export market concentrates on clinkers and grey cement. Refer to the market share in Thailand in Figure 2.4, the SCG shares the largest internal market of 38% followed by SCCC (27%), TPIPL (18%), ACC (9%) and JCC (4%) and others-Cemex (Thailand) Co., Ltd., TPCC, Thai Sathapana Co., Ltd., and Samukkee Cement Ltd (4%).

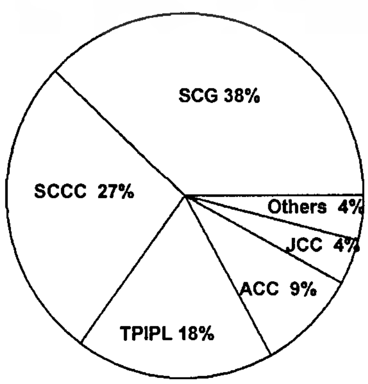

Figure 2.4 Market share of cement manufacturers in Thailand [47].

2.4 Dispersion models

2.4.1 General descriptions of dispersion models

Dispersion model is a tool to predict the potential impacts of the pollutants from the existing sources for air quality management. Actually, the models are mathematical equations operating through the computer simulations [20, 48-50]. Various computer software programs to simulate the dispersion of pollutants are used. The simulation results depend on the selected mathematical equations for types of the dispersions, i.e., types of pollutants (PM, NO_x, SO_x, etc.) or plume/puff dispersion. These mathematical equations simulate the transport, diffusion, chemical transformation, physical interactions and removal of pollutants in the atmosphere with the typical solutions being expressed as the concentrations at receptor locations at the simulation time. To calculate the emission concentration of each pollutant, usually the selected air dispersion model requires the following typical input data, i.e.,

- meteorological conditions, i.e., wind speed and direction, the amount of atmospheric turbulence or stability class and the ambient air temperature
- characteristics of the emission sources, i.e., source location and height, location and diameter of vent stack, pollutant emission rate and exit velocity
- the topographies of source and receptor locations
- location, height and width of any obstructions (such as buildings or other structures) in the trajectories of the emitted pollutants.

To date, several air dispersion models are accepted worldwide. Many of them are developed and accepted by the U.S. EPA. All approved regulatory models are listed in the Guideline on Air Quality Models [12].

2.4.2 Gaussian models

The Gaussian models are widely used for estimating the concentration of the pollutant at a point downwind from one or more emission sources. Various software programs in the Gaussian model are developed based on the Gaussian equations. Equation 2.1 is the basic equation of the Gaussian model. It has been developed for more effective simulation of the pollutant dispersion. The widely used models are Gaussian plume and Gaussian puff [49-50].

$$C(x,y,z,t) = \frac{Q}{(2\pi)^{3/2}\sigma_x\sigma_y\sigma_z}\exp\left\{-\frac{1}{2}\left[\left(\frac{x-\bar{u}t}{\sigma_x}\right)^2+\left(\frac{y}{\sigma_y}\right)^2+\left(\frac{z}{\sigma_z}\right)^2\right]\right\} \tag{2.1}$$

where

$C(x,y,z,t)$	=	downwind concentration at a point (x,y,z,t) (g/m^3)
Q	=	emission rate of pollutant (g/s)
$\sigma_x, \sigma_y, \sigma_z$	=	dispersion coefficients along x, y, z directions (m)
u	=	mean wind speed at x direction (m/s)
y	=	lateral distance (m)
z	=	vertical distance (m)

(1) Gaussian plume model

Gaussian plume model have been using in the U.S. since mid-1960s. It is considered as a well-understood, easy-to-apply and internationally-approved computational approach to calculate the concentration of a pollutant at a certain time and location [51]. It is a steady-state dispersion model consisting of a group of the formulas based on the steady-state condition. The formulas of the Gaussian plume model do not depend on time, although they do represent an ensemble time average. The meteorological conditions are assumed to remain constant during the instantaneous dispersion from source to a receptor. The pollutant emissions and meteorological conditions vary hourly but the model calculations in each hour are independent. In principle, the plume characteristics of the model depend on emissions and meteorological conditions and do not change over time. The steady-state models calculate the hourly-averaged concentration in the ambient from source data and meteorological conditions that are uniform across the modeling domain. The Gaussian plume equation is shown in Equation 2.2.

Figure 2.5 shows the Gaussian distribution of pollutant concentrations in the horizontal and vertical directions with the maximum concentration at the center of the plume. This model basically describes the transport and mixing of the pollutants by assuming that the dispersion of pollutants by plume spread results from molecular diffusion. The pollutant concentrations in horizontal and vertical plume dimensions are distributed normally in bell shape curve [50-54].

$$C(x,y,z) = \frac{Q}{2\pi\sigma_y\sigma_z u}\exp\left[-\frac{(y-y_0)^2}{2\sigma_y^2}\right]\exp\left[-\frac{(z-z_0)^2}{2\sigma_z^2}\right] \tag{2.2}$$

where

C (x,y,z)	=	downwind concentration at a point x,y,z (g/m^3)
Q	=	emission rate of pollutant (g/s)
σ_y, σ_z	=	plume dispersion coefficients at lateral and vertical distances, respectively (m)
u	=	mean wind speed along the downwind of x direction (m/s)
y	=	lateral distance (m)
z	=	vertical distance (m)

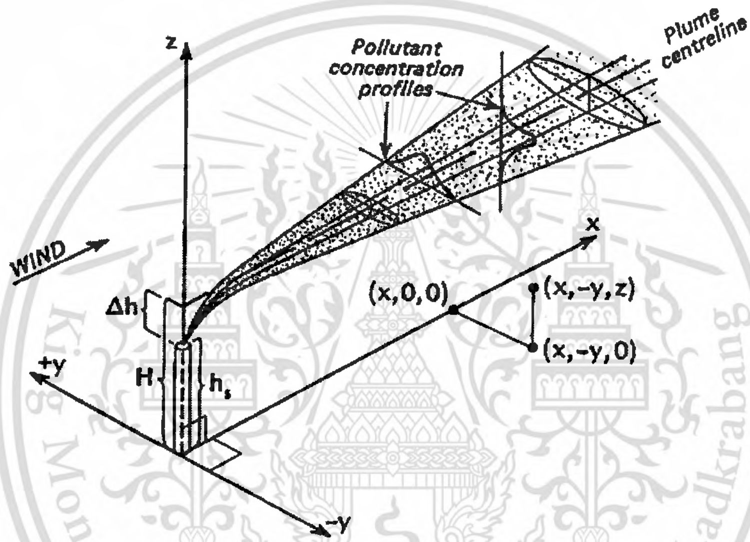

Figure 2.5 Typical Gaussian plume dispersion of pollutants from an elevated source [53].

(2) Gaussian puff model

Even though Gaussian plume models are used commonly in the U.S. and other countries worldwide for regulatory impact assessments, the efforts have been made to increase computational efficiency of pollutant dispersion. The Gaussian puff model in Equation 2.3 has been developed to remedy the limitations attributing to steady-state models. The Gaussian puff model simulates a release of puff series in the space at time by varying wind field and assuming a continuous emitting plume or instantaneous cloud of pollutants. The puffs are assumed to have Gaussian or bell-shaped concentration profiles in their vertical and horizontal planes. The puffs are represented by interlocking circles that become larger further away from the releasing point, as shown in Figure 2.6. This enables the model to account for a variety of effects such as spatial variability of meteorological conditions, causality effects, dry deposition and dispersion over different land surfaces, plume fumigation, low wind-speed dispersion, transformation of pollutant and wet removal [49, 54].

$$C = \frac{Q}{2\pi\sigma_x\sigma_y} g\left\{\exp\left[-\frac{1}{2}\right]\left[\frac{d_a}{\sigma_x}\right]^2 \exp\left[-\frac{1}{2}\right]\left[\frac{d_c}{\sigma_y}\right]^2\right\} \quad (2.3)$$

$$g = \frac{2}{\sqrt{2\pi}\sigma_z} \sum_{n=-\alpha}^{\alpha} \exp\left[-\frac{1}{2}\frac{\left(H_e + 2nh\right)^2}{\sigma_z^2(S)}\right]$$

where

C	=	ground-level concentration (g/m^3)
Q	=	mass of pollutants in the puff (g)
d_a	=	distance from the puff center to the receptor in along-wind direction (m)
d_c	=	distance from the puff center to the receptor in cross-wind direction (m)
g	=	vertical term of the Gaussian equation (m)
H_e	=	effective height of the puff center (m)
n	=	multiple reflections of puff
h	=	mixed-layer height (m)
σ_x	=	standard deviation in along-wind direction (m)
σ_y	=	standard deviation in cross-wind direction (m)
σ_z	=	vertical standard deviation (m)
S	=	distance travel by the puff (m)

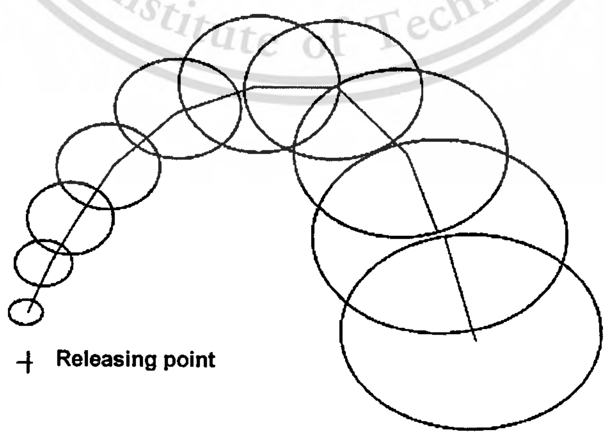

Figure 2.6 Graphical representation of puff modeling approach [54].

2.5 Model selection

At present, a variety of air dispersion models are available for users. Each air dispersion model is suitable for the evaluation of a certain source impact. The selection of a model to fit the characteristics of the releasing source is an important concern. Key factors to choose the most appropriate model are for example [49, 54-56]:

- downwash issue
- availability of resources, e.g., meteorological data, topographic data and source characteristics
- land-sea interface
- detail and accuracy of the database, e.g., air quality and meteorological data
- accuracy for analysis and level of detail, e.g., domain size
- technical competency of model users
- meteorological and topographical complexities of the area such as characteristics of wind flows and elevation of the study area.

The selection of suitable air dispersion models in this current work, i.e., the American Meteorological Society-Environmental Protection Agency Regulatory Model (AERMOD) and the California Puff Dispersion Model (CALPUFF), is based on the regulatory and recommendation by the U.S. EPA.

2.6 General features of the AERMOD

AERMOD is the steady-state plume model developed as a next-generation model to ISCST3. The basic equation of this model is Gaussian plume equation. It can incorporate more complexity algorithms and concepts such as planetary boundary layer theory and advanced methods to cope with complex terrain. The AERMOD is used to evaluate the dispersion at a distance not over 50 km from the emission source [12-13]. Generally, the AERMOD is composed of three parts: the AERMOD Terrain Preprocessor (AERMAP), the AERMOD Meteorological Preprocessor (AERMET) and the AERMOD dispersion module. The AERMAP processes the terrain data in conjunction with a layout of receptor and sources for the AERMOD control files. The AERMET formats the meteorological data for the AERMOD. Currently, there are various sources of the AERMOD models, e.g., the U.S.EPA, Lakes Environmental Software, Scientific Software Group (SSG), etc. It is claimed that all commercial versions of the AERMOD are based on the mathematical model similar to the version of the U.S.EPA [57-59].

This work, the ISC-AERMOD View, which is a commercial AERMOD by the Lakes Environmental Software, is selected because it is an easy-to-operate software and requires the simple format input data. The ISC-AERMOD View is a user-friendly interface for four U.S. EPA air dispersion models, i.e., ISCST3 model, ISC-PRIME model, AERMOD model and AERMOD-PRIME model. Similar to the AERMOD version of the U.S.EPA, the commercial AERMOD consists of the AERMAP, a preprocessing unit, and the AERMET, a meteorological unit. The POST View and WRPLOT View are postprocessing units which are used to view the output of the AERMOD and AERMET. These additional units are available in the commercial version. Some graphical programs, however, can be applied to view the outputs of the AERMOD program. Examples of graphical programs are such as Surfer, ArcGIS, etc. The AERMOD modeling system is summarized in Figure 2.7.

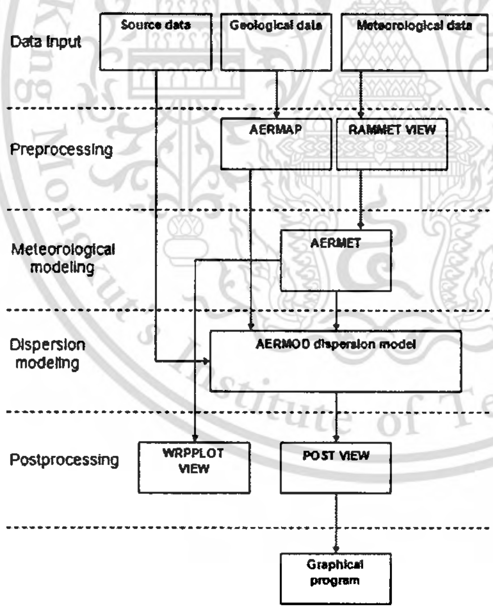

Figure 2.7 AERMOD modeling system.

The 3 main parts of the AERMOD are as follows:

(1) AERMOD

The AERMOD is a dispersion model itself with the main function of calculating outputs.

(2) AERMAP

In case of the applications to elevated terrain, the user must input a hill height scale along with the receptor elevation. The U.S. EPA AERMAP terrain-preprocessing program can be used to generate hill height scales as well as terrain elevations for all receptor locations. Two types of intermediate result files are used for debugging purposes. One contains information related to the model results and the other contains grid profiles of meteorological variables.

(3) AERMET

The AERMET meteorological preprocessor will format meteorological variables/data for the deposition algorithms in the AERMOD. The additional variables include the precipitation code, precipitation rate, relative humidity, surface pressure and cloud cover. These additional variables are automatically included after the standard variables for each hour and do not require any additional inputs. The precipitation data are required for wet deposition calculations in the AERMOD and can be obtained from the SAMSON, HUSWO or ISHD (TD-3505) formats which are supported by the AERMET. The meteorological data file for new deposition algorithms is read as a free format file. Each field on a record is separated from adjacent fields by a comma or by one or more spaces. The input meteorological data file consists of a header record that includes the latitude and longitude, surface station name, upper air station name, the on-site station name and the AERMET version date [13, 56-61].

Each subsequent record is composed of the surface data and upper air data.

- Surface data are meteorological data measuring near the earth's surface directly by instrumentation, i.e., wind speed (WS), wind direction (WD), relative humidity (H), ambient air temperature (T), dew point (DP), precipitation, ceiling height (CH), cloud cover (CC) and global radiation. The surface data are formatted in the National Climatic Data Center (NCDC) CD-144 format or the Solar and Meteorological Surface Observational Network (SAMSON) format.

- Upper air data are meteorological data measuring in the vertical layers of the atmosphere. The upper air data are in formatted of the standard NCDC TD-6201 data format or the NCDC, CD-ROM Forecast Systems Laboratory (FSL) rawinsonde data format before using as the input of the AERMET.

2.7 General features of the CALPUFF

CALPUFF is a multi-layer, multi-species non-steady-state puff dispersion modeling system that simulates the effects of time-varying and space-varying meteorological conditions on pollution transport, transformation and removal. It can be applied on scales of tens to hundreds of kilometers. The CALPUFF is designed specifications for the modeling system including the capability to treat time-varying point and area sources, inert and chemical pollutants, rough or complex terrain situations and long range transport.

The CALPUFF model was originally developed by the Sigma Research Corporation (SRC) in late 1980s under the contract with the California Air Resources Board (CARB) and was first issued in 1990. The SRC subsequently became part of the Earth Tech, Inc. Since the CALPUFF has been designating as a preferable air quality model by the U.S. EPA, the Earth Tech, Inc. is selected as the model-designated distributor. The ownership to distribute and maintain the model has switched from the Earth Tech, Inc. to the TRC Environmental Corporation since April 2006 [62-64].

To date, the CALPUFF has been used in a wide variety of applications by registered users worldwide in more than 105 countries [63]. In Thailand, the CALPUFF is not popular for the Environmental Impact Assessment (EIA) because it operates with meteorological input data from at least 3 meteorological stations and its operating system is rather complex. Since the domain in this work is on the mountain area classifying as the complex terrain, the CALPUFF is one of suitable programs for such area. The CALPUFF modeling system includes three main components, i.e., CALMET, CALPUFF and CALPOST. More details about these components are described below.

(1) CALMET

CALMET is a meteorological model which includes a diagnostic wind field generator containing objective analysis and parameterized treatments of slope flows, kinematic terrain effects, terrain blocking effects, a divergence minimization procedure, a micro-meteorological model for overland and overwater boundary layers. The CALMET model obtains the necessary control information and input meteorological data from a number of different input files. The control file (CALMET.INP) contains the data that define a particular model run such as starting date and time, horizontal and vertical grid data and model option flags. Geophysical data including terrain elevations, land use and surface characteristics are read from a formatted data file so-called GEO.DAT. The meteorological input to CALMET can be obtained from either actual observations or other meso-scale meteorological models such as MM5 (the Fifth-Generation National Center Atmospheric Research (NCAR)/Pennsylvania State University (Penn State) Mesoscale Model) or Weather Research and Forecasting (WRF) or a combination of both. For actual observations, the minimum requirements, e.g., wind speed, wind direction, relative humidity, pressure, temperature, cloud cover and ceiling height are observed from at least 3 surface stations. In addition to the aforementioned parameters, the upper air profiles from radiosondes launching twice a day (or higher frequency of data from wind and temperature profilers) are required. The outputs of the CALMET can be expressed by the PRTMET, a postprocessing program. The PRTMET can display user-selected portions of the meteorological data file produced by the CALMET meteorological model [63-64].

(2) CALPUFF

CALPUFF is the air dispersion module that simulates the transport and dispersion of pollutants emitted from model sources as puffs by using the temperature and wind field generated by the CALMET. The simulation is based on the Gaussian Puff formulation with options to select various dispersion coefficients for the growth of each puff from emission sources at time (hourly or less). Parameters and effects such as pollutant species, type of source, receptor location, plume rise effect, land use effect and terrain effect are required to set in the program. The primary output files from the CALPUFF contain either hourly concentrations or hourly deposition fluxes which are evaluated at selected receptor locations. The outputs are in the forms of CONC.DAT, DFLX.DAT or WFLX.DAT depending on the sort of output user obtaining from the CALPUFF.

(3) CALPOST

CALPOST same as PRTMET is the postprocessing program for processing the outputs from the CALPUFF like PRTMET. The outputs of the CALPOST are shown in terms of grid values (x,y,z) data files which can be converted into a picture by a graphical program illustrating the dispersion and differential concentrations of the pollutants from model sources. Without using other graphical programs, therefore, the outputs from the CALPOST are numerical values and rather difficult to analyze.

There are different sources of the CALPUFF modeling system, for example, the Earth Tech, Inc., Lakes Environmental Software, Scientific Software Group, etc. In this work, a free-of-charge CALPUFF PROfessional Beta 5.2.0 by the Earth Tech, Inc. is selected. This software is designed for estimating the impacts of the pollutants in mountain area and can be downloaded from www.src.com. The CALPUFF modeling system is summarized in Figure 2.8.

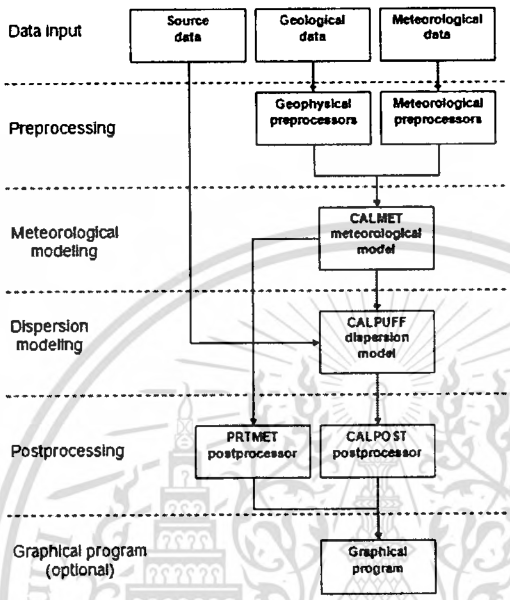

Figure 2.8 CALPUFF modeling system.

2.8 Meteorological factors

2.8.1 Wind

Wind speed and direction are two important measurements. The wind speeds and directions at the surface and aloft can help to predict the transportation of pollutants. The wind speed is generally recorded in knots or meters per second (m/s). In contrast to the oceanography, wind directions in meteorology discipline are not given in reference to the direction in which they are blowing, but rather the direction from which they are blowing. The westerly wind blows from west to east, whereas the northerly wind blows from north to south. The wind direction is generally measured in degrees due north but in the AERMOD modeling format it is in ten of degrees. The simplest way to measure the wind speed and direction at the earth's surface is by using wind cups and vanes, respectively.

Similarly, windrose (a graphical plot of wind speed and direction) is used to view how the wind is distributed at a particular location. Windrose contains each spoke in color-coded bands that show wind speed ranges. The windroses typically use 16 cardinal directions such as north (N), north northeast (NNE), northeast (NE), etc. and may be subdivided into as many as 32 directions. In terms of angle measurement in degrees, north corresponds to 0° to 360°, east to 90°, south to 180° and west to 270° [65-66]. The wind directions are classified in Table 2.6.

Table 2.6 Classification of wind directions [66].

Abbreviation	Wind direction	Degrees
N	north	0°
NNE	north northeast	22.5°
NE	northeast	45°
ENE	east northeast	67.5°
E	east	90°
ESE	east southeast	112.5°
SE	southeast	135°
SSE	south southeast	157.5°
S	south	180°
SSW	south southwest	202.5°
SW	southwest	225°
WSW	west southwest	247.5°
W	west	270°
WNW	west northwest	292.5°
NW	northwest	315°
NNW	north northwest	337.5°

2.8.2 Relative humidity

The relative humidity (RH) is a term most frequently used to express the amount of moisture in the air. It is a weight ratio between actual water vapor and water vapor at saturation and is usually expressed in percentage. The value can change by adding or removing moisture, and by increasing or decreasing temperature [65].

$$\text{Relative humidity} = \frac{\text{mass of water vapor}}{\text{mass of water vapor at saturation}} \times 100 \quad (2.4)$$

2.8.3 Pressure

Air pressure is the force exerted by air molecules on a particular surface. The pressure at the surface is measured by a barometer. Among many types of barometers, the most common barometer for meteorological purposes is the mercury barometer. Air pressure is commonly expressed in millibars (mbar) or inches of mercury (in Hg). The sea level pressure is typically 1,013 mbar or about 30 in Hg [65].

2.8.4 Temperature

Ambient air temperature is a parameter that affects plume rise, atmospheric conditions, direction of the local winds such as in-land and sea breezes showing the effects of hills and valleys. The decrease in temperature with height is called lapse rate, which indicates an index of the dispersion capacity of the atmosphere. Three conditions of lapse rates are as follows:

- neutral condition: actual lapse rate = adiabatic lapse rate
- unstable condition or superadiabatic: actual lapse rate < adiabatic lapse rate
- stable condition or subadiabatic: actual lapse rate > adiabatic lapse rate [50-53].

2.8.5 Precipitation

Precipitation is the quantity of water or snow falling to the earth at a specific place within a period of time. In Thailand, the precipitation is, normally, rain reported in millimeter (mm). Air pollution can be removed by wet deposition because of the precipitation [65].

2.8.6 Ceiling height

Ceiling height or cloud layer height is the distance between the ground level to the cloud base. The ceiling height is determined by several methods but estimation is the most frequent method. It is acceptable to determine the ceiling heights of low scattered cloud layers or higher cloud layers. More accurate methods such as launching a balloon are required when the cloud layer forms a ceiling, especially if the layer height is below 3,000 feet because the balloon moves up very fast [65].

2.8.7 Cloud cover

The amount of cloud cover and the duration of its presence determine the amount of sunshine reaching the ground, and thereby, determine the ground heat flux contributing to the turbulence kinetic energy which controls the mixing of air pollution. The cloud cover is reported in 0-10. The lowest number, 0, indicates clear sky, 1-5 is scattered or is partly cloudy (10-50 % of the sky is covered by clouds), 6-8 is mostly cloudy, 9 is overcast and 10 is obscured [49].

2.8.8 Global radiation

Global radiation is the total short-wave radiation from the sky falling onto a horizontal surface on the ground. It includes direct solar radiation and diffuse radiation resulting from reflected or scattered sunlight [65].

2.9 Morphological and elemental analysis

The scanning electron microscope (SEM) shows the image sample surface by scanning it with a high-energy beam of electrons in a raster scan pattern. The SEM provides a highly detailed topographical view of a material at high magnifications. A wide range of magnifications from about 10 times is possible. The magnified image can be captured for further evaluation. The SEM can be coupled with the Energy Dispersive X-ray (EDX) to analyze the elemental chemical composition of the samples. The SEM/EDX is commonly used in such a field, e.g., metallurgy, failure analysis, composite manufacturing, geology, corrosion, material characterization, etc.

Some examples of SEM/EDX in environmental applications are shown below.

The SEM/EDX can be used to analyze the PM in the atmosphere to investigate its possible impact to the human's health. According to the image in Figure 2.9, the SEM was applied to analyze the morphological properties of the graphitized pollen grain contaminant particle. The image of the pollen was magnified and then the EDX was applied to find its element. The results of EDX showed that the pollen grain contained mainly carbon with small amounts of oxygen and sulfur [67].

The Pollution Control Department, Thailand applied the SEM/EDX to analyze the yellow PM in Bang Saphan district, Prachuap Khiri Khan [68]. The images of yellow PM were magnified between 65× and 400× to study their morphological properties and elemental compositions. It was found that the yellow PM was irregular shape. Some morphological images were similar to those of palm and sunflower pollens, as shown in Figures 2.10-2.11. The results of the EDX showed that main elemental compositions of the yellow PM were C and O and small amount of Ca, as shown in Table 2.7. From the images by the SEM and the elemental composition by the EDX, it can be concluded that the yellow PM was the pollen of flowers from the surrounding of the study area. The chemical property of the yellow pollen PM was analyzed by the pH test of the rain fall collected in the study area for 1 year. The pH of the rain fall was normal indicating that the yellow PM had no impact to human's health because the compositions of the yellow PM were mainly carbon and oxygen without any toxic element.

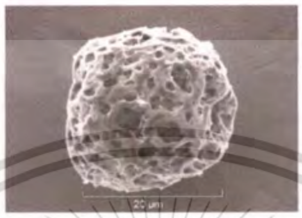

Figure 2.9 The SEM image of a graphitized pollen grain contaminant particle [67].

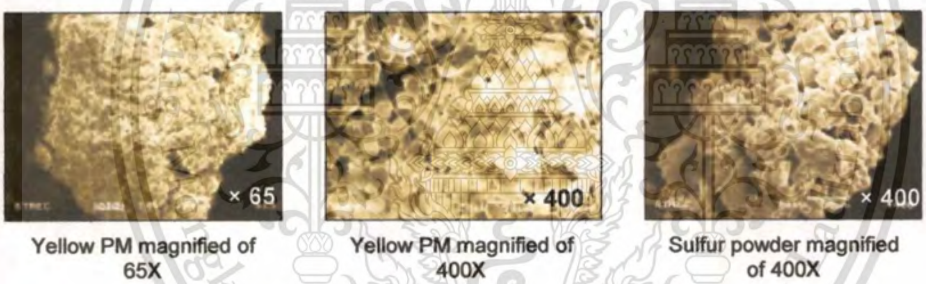

Figure 2.10 Yellow particulate matter and sulfur powder [68].

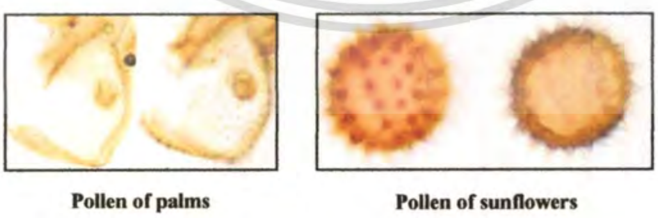

Figure 2.11 Morphological images of palm and sunflower pollens [68].

Table 2.7 Elemental compositions in yellow particulate matter [68].

Elements	Sampling date/Amount of element (%)	
	11[st]- 13[th] June 2008	7[th]- 9[th] August 2008
Carbon (C)	49.00 – 68.63	57.85 – 68.43
Oxygen (O)	28.72 – 37.86	28.85 – 35.13
Calcium (Ca)	0.56 – 2.48	0.42 – 3.88

2.10 Literature reviews

2.10.1 Air pollution in Saraburi

As mentioned in Chapter 1, Saraburi has suffered from air pollution impact for more than 10 years, particularly the area in Nah Phra Laan with existing mining, stoning and cement industries. The following works by academic and government sectors showed their concern to the problems and seek proper solutions to control the pollutant impacts in Nah Phra Laan.

Phajon-Aripai K. [2] studied PM_{10} dispersion from stone-crushing plants in Nah Phra Laan by the Industrial Sources Complex Short Term model (ISCST). Most of the simulation results were under the observations. Underestimation by the model was attributed to the calculation without significant emission sources from transportations because the Nah Phra Laan was located near the complex terrain of mountain chains. The ISCST model is known to suit the flat terrain not the mountain area. Therefore, it is possible to obtain errors from the program.

Moondee et al. [3] reported the effects of TSP and PM_{10} on the students' health in Nah Phra Laan. The TSP and PM_{10} in the ambient air were collected from the schools located near and far from quarry and stone-crushing industries. The health data were revealed that the prevalence of all respiratory symptoms of the students in Nah Phra Laan was statistically significant higher than those of the students outside Nah Phra Laan.

During 2005-2006, the PCD employed the SECOT Company Limited, an environmental, safety and monitoring company to establish the emission inventory (EI) for the investigation of PM impact around the industrial areas in Nah Phra Laan [7]. It was reported that most PM_{10} came from the transportations, stone-crushing industries, cement industries, mineral industries and residential activities of 43.25%, 36.00%, 20.06%, 0.67%, and 0.02%, respectively. In 2008, Pimonsree [6] updated the EI of the PCD and applied the Hybrid Particle and Concentration Transport model (HYPACT) with Lagrangian option and the Regional Atmospheric Modeling

System (RAMS) to evaluate the PM_{10} dispersion in Nah Phra Laan. The model results showed that high PM_{10} concentrations were in the industrial areas, particularly at downwind direction.

Above research works showed the awareness of PM impact and the efforts to reduce PM concentrations in the atmosphere at Nah Phra Laan. However, there are a few research projects on air pollution in Kaeng Khoi district, the adjacent area to the east of Nah Phra Laan, where 4 major cement plants are located.

Hung [69] studied the impacts of the emissions from the selected cement kiln of the SCCC using secondary fuels such as activated carbon, papers, plastics, rags and fabrics. The measurement results showed the concentrations of TSP and benzene at 7 receptors of 191-220 g/m^3 and 1.9-5.2 g/m^3. Polychlorinated biphenyls (PCBs) congeners were 9.6-13.7 mg/m^3. All emissions of HCl, CO, NO_x and SO_x were in the permitted values of the cement kilns in Thailand. In 2008, Prakitcharoensuk [70] applied the Industrial Sources Complex Short Term model (ISCST3) to study the impact of the PCBs emissions from the selected cement kiln. It was reported that the highest PCB concentration was observed at the east of the domain. The geography of Kaeng Khoi is identified the complex area as it is plateau consisting of mountain chains and the surrounding areas near the Kao Yai Natural Park. As a result, the ISCST3 was not proper to estimate the impacts of the PCBs emissions in this area. Thereby, the AERMOD and CALPUFF were recommended.

2.10.2 The applications of Gaussian dispersion models in air pollution

Justification to use a simple or complex atmospheric dispersion model depends on types of pollutants, numbers of releasing sources, domain size and locations (near the sea or mountain area), etc. In this current work, the AERMOD and CALPUFF Gaussian models are reviewed.

The following examples show the applications of AERMOD.

Sax and Isakov [71] estimated variability and uncertainty in predicted hexavalent chromium concentrations generated by welding operations at a shipbuilding and repair facility in California, USA by the ISCST3 and AERMOD. From a practical perspective uncertainty is most important at receptors with highest predicted concentrations. In this case study, emissions were the primary source of uncertainty. They found that both models were sensitive to the location of emission sources, meteorological and model parameters. Simplified modeling approaches may lead to errors in pollutant concentration estimates, especially in close proximity to the emission sources where predicted concentrations are highest.

Caputo et al. [72] compared the results from 3 models: Gaussian plume model (AERMOD and Hybrid Plume Dispersion Model (HPDM)), segmented Gaussian plume model (PC Code System from Maria (PCCOSYMA)) and Lagrangian model (Hybrid Single-particle Lagrangian Integrated Trajectory (HYSPLIT)). The meteorological data were generated by the RAMS. It was reported that the main differences of the outputs from 3 models were originated in the sensible heat flux and friction velocity computation, whose values impact directly on the Monin–Obukov length and mixing height calculation. These differences and the strong dependence of the results on them indicated that more development to improve the algorithms for the calculations of meteorological variables (mainly during stable conditions) should be done.

Venkatram et al. [73] estimated the sulfur hexafluoride (SF_6) tracers which were sampled at several receptors within 20 m from the emission source by the Industrial Source Complex - Plume RIse Model Enhancements (ISC-PRIME) dispersion model and AERMOD/Plume RIse Model Enhancements (PRIME). The evaluation by both models indicated that the highest concentrations were overestimated but the lower range of the concentrations was underestimated.

Bhardwaj [74] reported that the predicted results by the AERMOD were very close to the observed values when the AERMET was run with the twelve sectors' land use parameter values around three kilometers at the meteorological site. Furthermore, the AERMOD was highly sensitive to the input data for 1-hour and 3-hour averaged periods. Less impact in the variation in predicted concentrations for annual averaged period and 24-hour averaged period with respect to data specification of the study areas was observed.

Orloff et al. [75] applied the ISCST3 and AERMOD to predict hydrogen cyanide (HCN) concentration in the atmosphere around the gold heap leach field. They reported that the major sources of uncertainty in the model predictions were the complex terrain of the area and the uncertainty in the emission rates of HCN from the leach field.

Stein et al. [76] combined 3 models of the Community Multi-scale Air Quality (CMAQ), HYbrid Single-Particle Lagrangian Integrated Trajectory (HYSPLIT) and AERMOD in a hybrid modeling applications. Each model was subjected to (i) the CMAQ was applied to provide the regional background concentrations and urban-scale photochemistry, (ii) the HYSPLIT was applied to provide the spatially resolved concentrations of the selective sources, and (iii) the AERMOD was applied to simulate mobile emissions from the selected major roads. It was found that the hybrid modeling approach showed a somewhat better statistical performance than the high resolution nested Eulerian model. However, the differences were evident between modeling methods and available monitoring site data.

Kesarkara et al. [77] applied the AERMOD coupling with Weather Research and Forecasting (WRF) to predict the impact of PM_{10} in Pune, India. The comparison of observed and simulated concentrations showed that the model generally underestimated the concentrations over the city. It might because the data from this case study were not sufficient to conclude the suitability of regionally averaged meteorological parameters for running the AERMOD. The additional simulations with different WRF parameterizations along with an improved pollutant source data must be added for enhancing the reliability of the AERMOD/ WRF modeling system.

Isakov et al. [78] applied the AERMOD to simulate observed tracer concentrations from a tracer field study conducted in Wilmington, California, USA using four different sources of inputs (i) onsite measurements, (ii) National Weather Service measurements from a nearby airport, (iii) readily available forecast model outputs from the Eta Model, and (iv) readily available and more spatially resolved forecast model outputs from the Fifth-Generation National Center Atmospheric Research (NCAR)/Pennsylvania State University (Penn State) Mesoscale Model, known as MM5, prognostic model. The results indicated that comprehensive models such as MM5 and Eta have the potential of providing adequate meteorological inputs for currently used short-range dispersion models such as the AERMOD.

Mazur et al. [79] applied the AERMOD to predict hourly ground-level concentrations of total gaseous mercury (TGM) emissions from the coal-fired power plants located on the Lake Wabamun area at Genesee and Meadows sites in Alberta, Canada under normal operating conditions. The Genesee site but not Meadows site was directly affected by the coal-fired power plants and SO_2 with the occurrence of the north-west winds. The AERMOD modeling predicted that TGM emissions from the coal-fired power plants under normal operating conditions could influence their relevant hourly ground-level concentrations in ambient air.

Venkatram et al. [80] used the AERMOD to estimate the contribution of traffic-generated emissions of the selected VOCs such as benzene, 1,3-butadiene and toluene to ambient air concentrations at downwind receptors ranging from 10 m to 100 m from the edge of a major highway in Raleigh, North Carolina, USA. The results demonstrated the suitability of the formulation in AERMOD to estimate the concentrations of mobile source emissions near roadways.

Zou et al. [81] studied the effectiveness of the AERMOD at different time scales in estimating of SO_2 concentrations in Dallas and Ellis counties, Texas, USA. They reported that the 8-hour, daily, monthly, and annually averaged SO_2 concentrations by the simulation matched their respective observed concentrations much better compared with the simulated 1-hour and 3-hour averaged SO_2 concentrations. The AERMOD performed better in simulating SO_2 concentrations when combined point and mobile emission sources were used as model inputs rather than using point or mobile emission sources alone. Furthermore, the AERMOD performed much better in simulating the high end of the spectrum of SO_2 concentrations in the study area compared to the results of 1-hour, 3-hour, 8-hour and 24-hour scales.

Worldwide applications of the CALPUFF are reviewed as follows:

Doolgindachbaporn [82] applied the CALPUFF to simulate 1-hour and 24-hour averaged concentrations of SO_2 from the Mae Moh thermal power plant, Lampang, Thailand. It was reported that no impact was observed from new units (12 and 13) which operated under 95% efficiency of the desulfurization. About 5,000 g/s of SO_2 emitted in the morning and 10,000 g/s in the afternoon.

Godfrey and Clarkson [83] applied the CALPUFF/CALMET in a complex orographic and very stable polar environment to confirm the measurement of plume trajectories under worst case conditions from Scott Base, Ross Island, Antarctica. CALMET was used to predict the meteorological fields of two characteristic low dispersion days and CALPUFF was used to predict the pollutant footprint and trajectory for each event. The model output is shown to be realistic by the trajectories of constant density balloons.

Barna and Gimson [84] examined the inter-suburb dispersion of PM in Christchurch, New Zealand during a wintertime particulate pollution episode. The dispersion was simulated by the CALPUFF/CALMET/RAMS/ modeling system using the data from a detailed emission inventory of home heating, motor vehicles and industry. It was found that the peak concentrations of PM occurred at night when particulate emissions from wood- and coal-burning domestic heating appliances were at a maximum and emitted to a stable boundary layer.

Levy et al. [85] applied the CALPUFF dispersion model with meteorological data derived from the National Oceanic and Atmospheric Administration's (NOAA) to evaluate primary and secondary PM from nine power plants in Illinois, USA. The simulated results indicated that the public health was affected significantly by long-range transport and the emissions from the power plants.

Surapipith [86] used the CALMET/CALPUFF to analyze the pollution and meteorology over the European Black Triangle, Krusne Hory (Czech) or Erzgebirge (German) mountain area. The large brown coal fired power plants in the valley, adjacent to the Krusne Hory, were considered as key sources of NO_x, SO_2 and PM. It was reported that the transport of air pollutants was very sensitive to wind direction under the right stable conditions. In addition, increasing flue-gas temperature or stack height could increase SO_2 concentration in some parts of the mountain plateau.

Jiang et al. [87] applied a photochemical Eulerian grid modeling system, consisting of MM5/CALMET/California Photochemical Grid Model (CALGRID) to evaluate ozone in the Puget Sound region of Washington State. Within the receptor grid, the process analysis showed that ozone concentrations increased during the day as chemical production exceeded the net effects of deposition and vertical diffusion. Concentrations decreased after mid-afternoon when horizontal advection began to dominate the other processes. When applied along the air mass transport path, process analysis showed that during most of the day, chemical production was larger than the other processes and caused the air mass ozone concentration to steadily increased during transport downwind of the urban core. The simulated results indicated that the ozone concentration depended on VOC/NO_x ratio in the atmosphere.

Elbir [88] used CALMET/CALPUFF to predict SO_2 emissions from industrial and domestic heating sources in Izmir, the third biggest province in Turkey. Statistical analyses were carried out to evaluate the model performance by comparing the predicted and measured time series of sulfur dioxide concentrations at four monitoring stations. It was reported that the overall model performance for four monitoring stations was acceptable with an accuracy of 68%. The agreement of model predictions and measurements was better for two urban monitoring stations compared with the other urban stations.

Kanokkarnjana [89] applied the CALPUFF/CALMET and the ISCST3 to evaluate NO_x, SO_2 and PM_{10} dispersions in the Laem Chabang Industrial Estate, Chonburi, Thailand. Two different case studies were investigated by the CALPUFF (i) fresh water and (ii) seawater. The fresh water case, with no effect function in the coastal area, was used to inspect the performances of CALPUFF and ISCST3. The 1-hour maximum concentrations of NO_x, SO_2 and PM_{10} outputs from the ISCST3 were 2065, 2132 and 165 $\mu g/m^3$, respectively. In case of fresh water, the 1-hour maximum concentrations of NO_x, SO_2 and PM_{10} by the CALPUFF were 611, 1437 and 243 $\mu g/m^3$. The corresponding values of the seawater case were 603, 1198 and 203 $\mu g/m^3$, respectively. Both models indicated that these maximum concentrations occurred at the western part of Laem Chabang during the modeling period.

Song et al. [90] applied the CALPUFF to evaluate PM_{10} in Beijing, China. They reported that cold air from the northwest or north intruded over Beijing for 4 days in winter accompanied by high wind speeds. The PM_{10} was, in addition, swept out of Beijing after the cold fronts and accumulated again once the winds stopped until the next cold air intrusion.

Wang et al. [91] applied the CALPUFF and ISCST3 to predict downwind odor concentrations and back-calculating area source odor emission rates. The comparison between the predicted and field sampled downwind concentrations indicated that the CALPUFF model could fairly well predict average downwind odor concentrations. However, the ISCST3 tended to underpredict downwind odor concentrations when compared to the measured concentrations. Both the CALPUFF and ISCST3 models failed to predict peak odor concentrations using the constant average emission rate. The odor emission rates obtained by back-calculating fluxes using the CALPUFF and ISCST3 models with the same field measurements of downwind odor concentrations were significantly different.

Yang et al. [92] used a coupled regional air quality modeling system to investigate the time spatial variations in airborne particulate matter, the influences of complex terrain and meteorological conditions upon boundary layer structure and PM_{10} concentration distributions. Analysis of model results illustrated that the pollutants emitted from Mentougou, China could be transported to Beijing municipal area along certain transport pathways. The PM_{10} concentration distributions showed heterogeneity characteristics. Contributions of the Mentougou sources to the PM_{10} concentrations in Beijing municipal area were up to 0.1–15 $\mu g/m^3$.

Indumati et al. [93] used CALMET/CALPUFF modeling to study atmospheric dispersion of SO_2 pollutant over land–water–land interface. They reported that the default scheme to handle inhomogeneous surfaces by the CALMET/CALPUFF could not manipulate the different turbulence characteristics over such surfaces. An alternative method was suggested to incorporate different turbulent characteristics over inhomogeneous surfaces by using the appropriate atmospheric stability category over different surfaces. It was also shown that the effect of water body on the ground level concentration decreased as the distance from the water body increased.

MacIntosh et al. [94] compared the deposition of cadmium (Cd), lead (Pb) and zinc (Zn) predicted by the CALPUFF. The results demonstrated that the CALPUFF could provide reasonably accurate predictions of the patterns of long-term air pollutant deposition in the near-field associated with emissions from a discrete source in complex terrain.

The following works are examples of using Gaussian dispersion model to evaluate the pollutants from cement manufacture.

Goyal et al. [95] applied two different air quality models, IITST, a combination of the Gaussian plume and Gaussian puff models, and ISI (ASME), a Gaussian plume model, to predict monthly averaged TSP concentrations over the industrialized cities of India. They reported that the IITST model was more appropriate to estimate particulates than the ISI.

Baroutian et al. [96] studied the dispersion of PM_{10} from continuous sources of the Kerman Cement Plant, and the dispersion conditions by using the Gaussian plume model that incorporated source related factors and meteorological factors. The result showed that the concentrations of PM_{10} in the ambient air (590-1,370 m from the stacks) were higher than the annual averaged concentration of PM_{10} by the WHO's guidelines.

Silvester et al. [97] used the computational fluid dynamics (CFD) to investigate the dispersion and deposition of fugitive mineral dust particles generated during rock blasting operations. The results indicated that the retention of the particles in ambient depended on wind direction under neutral conditions. In addition, the retention was highest at the longest distance from the blast location to the downwind pit boundary in the study.

Chapter 3

Methodology

This chapter describes 3 consecutive steps to study the impacts of pollutants from 4 cement manufacturers of the cement complex on the communities nearby Kaeng Khoi, Saraburi. Firstly, the potential emissions from the cement manufacturers in the study areas were estimated by preparing the input data for the AERMOD and CALPUFF in 1-year period. The hourly releasing rates of TSP, PM_{10}, NO_x and SO_2 from the stacks of each cement manufacturer were simulated. Secondly, meteorological data and the concentrations of pollutants in the ambient were analyzed. The morphological properties and elements of the TSP and PM_{10} collected at the selected receptors were characterized by the SEM/EDX. Finally, the meteorological fields were simulated by the CALMET to generate wind fields in the areas. The concentrations of pollutants were simulated by the AERMOD and CALPUFF to understand their dispersion during typical episodes. The simulated and measured concentrations were compared to verify the model performance. Details of these steps are summarized in the flow chart as shown in Figure 3.1.

3.1 Emission inventory

3.1.1 Estimation of the emissions from cement manufacturers by emission factors

As mentioned in Chapter 2, types and volumes of the emitted pollutants from cement production depend on cement or clinker production. The pollutant emissions could be estimated by using the emission factors (EFs). In this work, the emissions were estimated according to the European Monitoring and Evaluation Program (EMEP)/EEA air pollutant emission inventory guidebook-2009 which is widely used by the national level of European Union (EU) [42]. The emissions from the production of clinker and grey cement were considered by Equation 3.1. Annual production of clinker and cement of the cement manufacturers in Thailand are shown in Table 3.1.

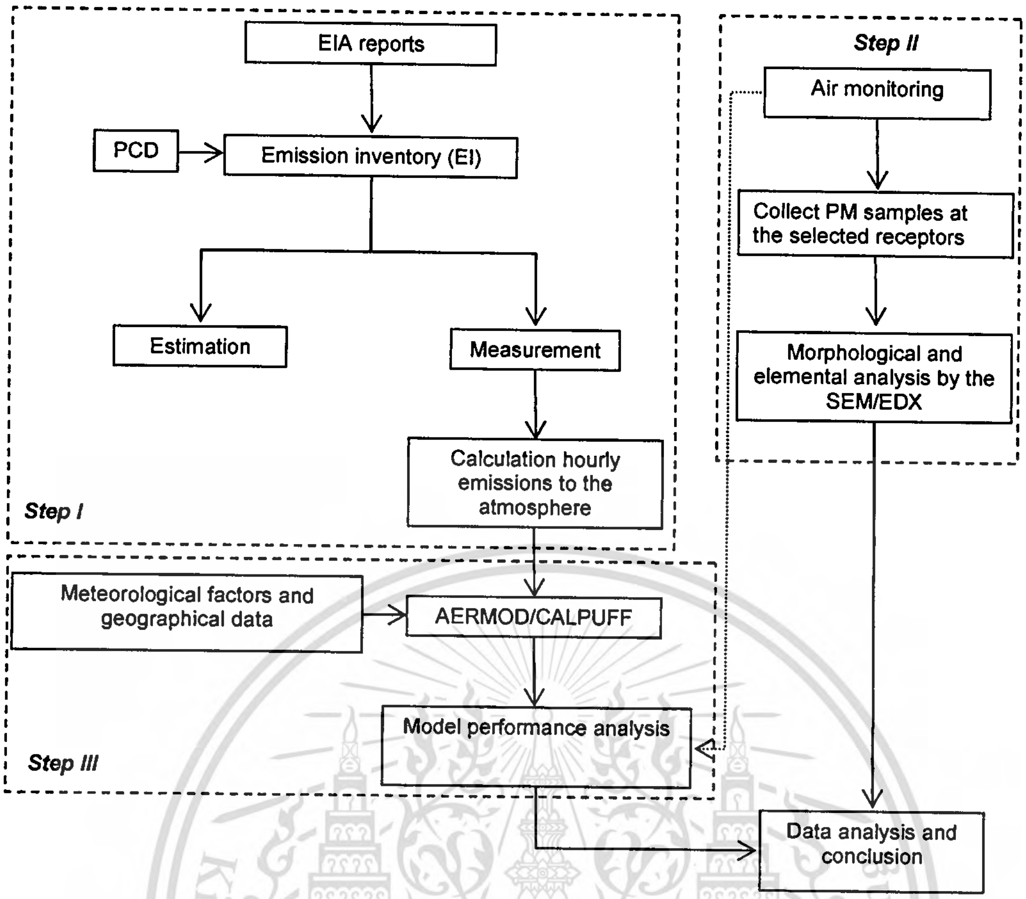

Figure 3.1 Procedures of research methodology.

$$E_{pollutant} = AR_{production} \times EF_{pollutant} \tag{3.1}$$

where

$E_{pollutant}$ = the emission of a pollutant in a year (kg/annum)

$AR_{production}$ = the annual production of clinker or cement (in ton)

$EF_{pollutant}$ = the emission factor of the pollutant (kg pollutant/ton clinker or ton cement), Appendix B

Table 3.1 Clinker and cement from cement manufacturers in Thailand [1, 11].

No	Cement company	Type of process	Location	Production (Megatons/year)	
				Clinker	Cement
1	Jalaprathan Cement Public Company Limited	Dry process with rotary kiln	Cha-am, Phetchaburi	1.13	1.19
2	Jalaprathan Cement Public Company Limited	Dry process with rotary kiln	Takhli, Nakhon Sawan	1.10	1.15
3	Cemex (Thailand) Company Limited	Dry process with rotary kiln	Chaloem Phra Kiat, Saraburi	0.80	0.84
4	TPI Polene Public Company Limited	Dry process with rotary kiln	Kaeng Khoi, Saraburi	8.58	9.07
7	Thai Sathapana Company Limited	Semi-wet process with the shaft kiln	Pak Tho, Ratchaburi	0.09	No data
8	Siam Cement (Thung Song) Company Limited	Dry process with rotary kiln	Thung Song, Nakhon Si Thammarat	6.57	6.91
9	Siam Cement (Kaeng Khoi) Company Limited	Dry process with rotary kiln	Kaeng Khoi, Saraburi	6.94	7.30
10	Siam Cement (Tha Luang) Company Limited	Dry process with rotary kiln	Ban Mo, Saraburi	2.92	3.07
11	Siam Cement (Kao Wong) Company Limited	Dry process with rotary kiln	Phra Phutthabat, Saraburi	3.65	3.84
12	Siam Cement (Lumpang) Company Limited	Dry process with rotary kiln	Chae Hom, Lampang	2.01	2.11
13	Siam City Cement Public Company Limited	Dry process with rotary kiln	Kaeng Khoi, Saraburi	14.05	14.78
15	Asia Cement Public Company Limited	Dry process with rotary kiln	Phra Phutthabat, Saraburi	4.75	4.99
16	Thai Pride Cement Company Limited	Dry process with rotary kiln	Kaeng Khoi, Saraburi	0.91	0.96
17	Samukkee Cement Limited*	Dry process with rotary kiln	Pak Chong, Nakhon Ratchasima	0	0.12
			Total	53.49	56.35

*Samukkee Cement Limited has not operated the kiln since the plants were started up. It operates only grinding clinker units.

3.2 Model domain

Figure 3.2 and Table 3.2 show model domains in this study. All of the domains covered the areas nearby the cement manufacturers in Kaeng Khoi. The ISC-AERMOD View has been developing for years and version 7.0 is the latest version [57]. In this work, the ISC-AERMOD View Version 4.6.2 and 5.4 (Lakes Environmental Software, Waterloo, Ontario, Canada) were used. The ISC-AERMOD View version 4.6.2 is for the domain size of 39.5 km × 39.5 km while the CALPUFF is for the domain size of 50 km × 50 km. The ISC-AERMOD View version 5.4 is modified to cover a larger domain in a long-distance area of 64.5 km × 64.5 km. In this work, we applied the ISC-AERMOD View version 5.4 to Nah Phra Laan. In case of the CALPUFF we used the CALPUFF PROfessional Beta 5.2.0 though the latest version is 6.4 [62].

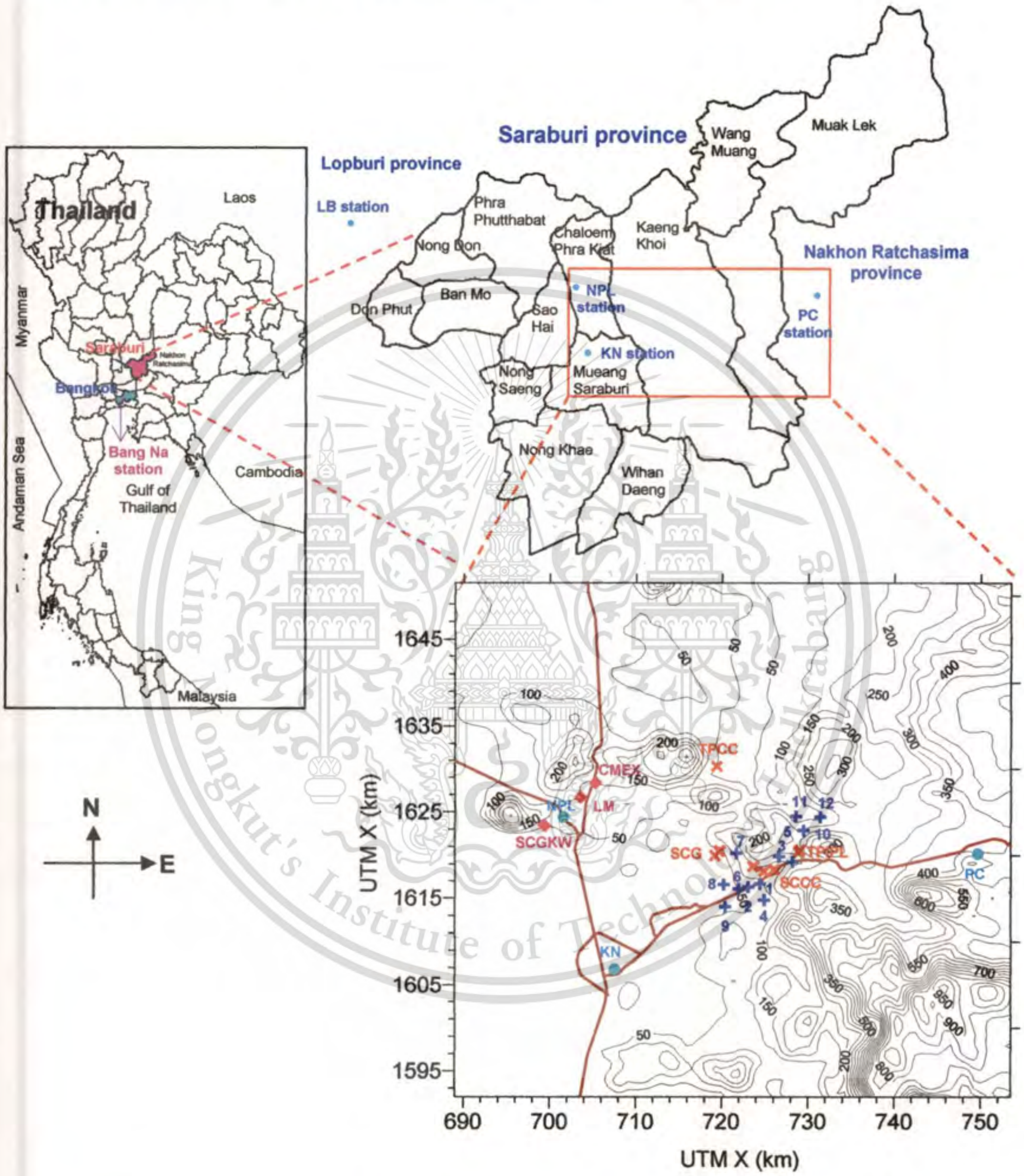

Figure 3.2 Model domains in Saraburi: (●) meteorological stations, (+) receptors, (×) stacks of cement plants in Kaeng Khoi and (♦) stacks of cement plants in NPL.

Table 3.2 Model domains in this study.

Domain No.	Model domain, UTM (X, Y) (km)	Cement manufacturer in domain	Meteorological station in domain	Software model
1	(701.0,1602.0) to (740.5,1641.5)	SCCC, TPIPL, SCG, TPCC	NPL, KN	ISC-AERMOD View Version 4.6.2, 5.4
2	(701.0,1593.0) to (751.0,1643.0)	SCCC, TPIPL, SCG, TPCC	NPL, KN, PC	CALPUFF PROfessional Beta 5.2.0
3	(689.0,1592.0) to (753.5, 1656.5)	SCCC, TPIPL, SCG, TPCC, SCGKW, LM, CMEX	NPL, KN, PC	ISC-AERMOD View Version 5.4

Note: KN (Kao Noi), PC (Pak Chong), LM (Limemaster Co., Ltd.)

3.3 Measurements

In general, the stack sampling was inspected every month by the staff of the cement companies. High stack is built to reduce the ground-level concentration from a point source. The emission levels were limited by the emission control equipment which were installed at the stacks. Twice a year, it is compulsory that the cement company employs a third party (a consulting company) to collect the emissions and monitor the concentrations of pollutants from the stacks for the EIA report. For our convenience, the emissions from 14 stacks of 4 cement manufacturers (6 stacks of SCCC, 4 stacks of SCG, 3 stacks of TPIPL and 1 stack of TPCC) were obtained from their EIA reports. The emissions of PM_{10}, NO_2 and SO_2 were simulated by the AERMOD and CALPUFF. In evaluation of the PM emissions, the TSP emitted from the stacks was used as PM_{10} input data for the AERMOD. By setting up the electrostatic precipitator with high efficiency of 99.99% at the stack, it could be assumed that the TSP emissions from the stacks were PM_{10}, and considered the released TSP as PM_{10} [20, 48]. The geometry of 14 stacks of 4 cement manufacturers in Kaeng Khoi is shown in Table 3.3.

However, the pollutants from the similar sources of cement manufacturers from the connecting areas, i.e., Nah Phra Laan are possible to impact Kaeng Khoi area. To evaluate the effect of the emissions from Nah Phra Laan, the emissions from 9 stacks of 3 cement manufacturers in Nah Phra Laan were additionally used as the input data for the AERMOD.

These emissions were obtained from the emission report investigated by the Pollution Control Department [7]. The geometry of 9 stacks of 3 cement manufacturers is shown in Table 3.4.

- 3 stacks of SCG (SCGKW): at Siam White Cement Co., Ltd. (2 stacks) and at Siam Cement (Ta Luang) Co., Ltd. (1 stack)
- 2 stacks of Cemex (Thailand) Company Limited (CMEX)
- 4 stacks of Limemaster Co., Ltd. (LM)

Table 3.3 The geometry of the stacks of 4 cement manufacturers in Kaeng Khoi.

No.	Name	Diameter (m)	Stack height (m)	Coordinate (UTM X, Y) (km)
1	SCCC 1	3.60	95.0	724.88, 1618.08
2	SCCC 2	4.00	95.0	724.90, 1618.08
3	SCCC 3	4.00	102.0	726.08, 1618.37
4	SCCC 4	4.00	102.0	726.04, 1618.27
5	SCCC 5	5.20	120.0	723.72, 1618.76
6	SCCC 6	5.20	120.0	723.58, 1618.70
7	SCG 3	3.00	105.0	719.64, 1620.46
8	SCG 4	3.20	105.0	719.71, 1620.46
9	SCG 5	3.96	97.0	719.80, 1620.49
10	SCG 6	4.20	102.0	719.18, 1619.95
11	TPIPL 1	5.00	125.0	728.98, 1620.46
12	TPIPL 2	5.00	125.0	729.06, 1620.58
13	TPIPL 3	5.00	125.0	728.91, 1620.38
14	TPCC	3.00	95.0	719.40, 1630.28

Table 3.4 The geometry of the stacks of 3 cement manufacturers in Nah Phra Laan.

No.	Name	Diameter (m)	Stack height (m)	Coordinate (UTM X, Y) (km)
1	SCGKW1	3.82	120.8	699.46, 1623.38
2	SCGKW2	2.10	60.2	699.30, 1623.46
3	SCGKW3	2.10	60.2	699.28, 1623.46
4	CMEX1	2.50	60.0	705.30, 1628.35
5	CMEX2	2.50	60.0	705.31, 1628.42
6	LM 1	0.60	37.0	703.58, 1626.67
7	LM 2	0.60	37.0	703.59,1626.68
8	LM 3	0.60	37.0	703.53, 1626.70
9	LM 4	0.60	37.0	703.54, 1626.68

3.3.1 Stack sampling

The TSP, PM_{10}, NO_2 as NO_x and SO_2 emissions from the stacks of 4 cement plants in Kaeng Khoi were collected by 'stack sampling' in accordance with the Code of Federal Regulations, 40 CFR Part 60 in Appendix A [98] as summarized in Table 3.5. The volumetric flow rate of the effluent gas from the stack was measured by a pitot tube at several points of the duct. The stack sampling was implemented at stable cement production. The emission concentration was reported at actual oxygen or excess oxygen of 7%. However, to compare with the emission standard value, the measured emission was corrected at 7% excess oxygen by Equation 3.2. In this work, 14 stack samplings were obtained from the EIA reports.

$$\text{Concentration of pollutant (excess } O_2 \text{ 7\%)} = \frac{\text{measured concentration} \times (20.9 - 7)}{20.9 - \%\, O_2 \text{ of measured concentration}} \quad (3.2)$$

Table 3.5 Summary of stack sampling methods [98].

Measured pollutants	Reference methods
TSP	U.S. EPA method 5
PM_{10}	U.S. EPA method 5
NO_2 as NO_x	U.S. EPA method 7
SO_2	U.S. EPA method 6

3.3.2 Ambient air monitoring

The monitoring data were analyzed in order to understand the impact of air pollution in Kaeng Khoi. The details of 2 types of air monitoring stations, semi-permanent and non-permanent, are described below.

(1) Semi-permanent monitoring station

Two semi-permanent air monitoring stations of the Pollution Control Department (Nah Phra Laan and Kao Noi stations) are in Saraburi province. The concentrations of the pollutants (PM_{10}, NO_2, SO_2, CO and O_3) were detected continuously and reported in hourly averaged concentrations. The standard or equivalent methods applied in monitoring the concentrations of pollutants are summarized in Table 3.6. The additional duties of the Nah Phra Laan and Kao Noi stations are measuring the meteorological parameters which relate to pollutant emissions.

(a) Nah Phra Laan station

(b) Kao Noi station

Figure 3.3 Semi-permanent monitoring and meteorological stations of the Pollution Control Department in Saraburi.

Table 3.6 Sampling methods at monitoring stations.

Pollutants	Monitoring stations		
	NPL	KN	12 receptors of SCCC
TSP	not measured	not measured	Gravimetric method
PM_{10}	Equivalent method: Tapered element oscillating microbalance (TEOM)	Equivalent method: Beta ray attenuation (BAM)	Gravimetric method: High volume
NO_2	Chemiluminescence	Chemiluminescence	Chemiluminescence
SO_2	UV Fluorescence method	UV Fluorescence method	UV Fluorescence method
CO	Non-dispersive infrared detection	Non-dispersive infrared detection	not measured
O_3	UV absorption photometry	UV absorption photometry	not measured

(2) Non-permanent monitoring station

Due to no permanent or semi-permanent air monitoring stations in Kaeng Khoi, the concentrations of pollutants were based on 7-day continuous monitoring data from the SCCC's EIA report twice a year according to the monitoring methods in Table 3.6. The 12 receptors were located near the residential areas expecting to receive the emissions from the cement manufacturers. TSP and PM_{10} were collected by the samplers as shown in Figure 3.4. The finest temporal resolutions concentrations of TSP and PM_{10} in the EIA were 24-hour averages. The NO_2 and SO_2 were reported by 1-hour averages. The coordinates of the 12 receptors are shown in Table 3.7.

(a) TSP sampler

(b) PM10 sampler

Figure 3.4 TSP and PM_{10} samplers.

Table 3.7 The 12 receptor sites of SCCC.

No.	Receptor names in EIA reports of SCCC	Coordinate (UTM X, Y) (km)
1	Tubkwang Electrical Substation	724.40, 1616.64
2	Tubkwang Nursery School	723.05, 1616.27
3	Ban Pha Sadet	726.62, 1619.86
4	Chumchon Nikom Tubkwang Songkror 1	724.92, 1614.77
5	Subbon Temple	728.18, 1619.23
6	Tubkwang Temple	721.94, 1616.07
7	Tubkwang Animal Conservation Station	721.68, 1620.24
8	Pa Phai Temple School	720.20, 1616.56
9	Warukaram Temple	720.38, 1613.99
10	Hin Lub Temple	729.48, 1622.86
11	Baan Tha Sao Temple	728.58, 1624.48
12	Subpradoo Temple	731.41, 1624.42

3.4 Morphological and elemental analysis by the SEM/EDX

The TSP and PM_{10} in ambient air at the selected receptor (2-m above ground level with a flow rate of gas stream of 10 L/min) were collected continuously for 24 hours. After 24 hours, the glass fiber filters of the sampler were removed and dried. The TSP- and PM_{10}-attached fiber filters were cut into small pieces and mounted on an aluminum SEM stub using conducting tap then coated with gold for a higher quality electron image of morphological and elemental studies by the SEM/EDX: JSM-6400 scanning microscope, JEOL. Accelerating voltage of 21 keV was used during the analysis.

3.5 Study of meteorological factors

Large-scale meteorological systems in Thailand are nominated by seasonal winds from northeast and southwest directions and several parts of the area in the east of the study domain were covered by mountains. Hence, the study areas were influenced by two types of winds (i) the large-scale meteorological systems by NE and SW seasonal winds and (ii) the mesoscale meteorological systems by mountain-valley breezes.

Wind speed and direction in the study domain were plotted in terms of windroses to examine the dominant winds over the study area. The 10-m surface meteorological parameters above ground level were obtained from Nah Phra Laan (NPL), Kao Noi (KN), Pak Chong (PC) and Lopburi (LB) stations.

The PC and LB are meteorological stations belong to the Thai Meteorological Department (TMD). Three-hour averaged data were the finest temporal resolution data obtained at these stations. The surface data such as wind speed and direction, relative humidity, pressure, rain fall, ceiling height and cloud cover were measured. The NPL and KN belong to the Pollution Control Department are both meteorological and monitoring stations without the observation of ceiling height and cloud cover. The cloud cover and ceiling height were obtained from PC meteorological station. The measurement data at the NPL and KN stations are reported on 1-hour averaged basis.

The wind field was analyzed by the California Meteorological Model (CALMET), a meteorological model of the CALPUFF. The surface data were obtained from NPL, KN, PC and LB stations, whereas the upper air data were obtained from Bang Na meteorological station. All of the surface and upper air data were formatted according to the guidelines of the CALMET [64]. The photographs of NPL, KN, PC and LB stations are shown in Figures 3.3 and 3.5. The locations and details are shown in Table 3.8. Since the CALMET needs 1-hour averaged data to operate, therefore, the finest 3-hour averaged data from PC station, e.g., wind speed and direction, etc were used for the 2 hours lacking the measured data. For example, the 1st, 2nd and 3rd hours used the first 3-hour averaged data, and the 4th, 5th and 6th hours used the second 3-hour averaged data and so on. In case a sensitive parameter like the temperature, each increment of the average value of the first 3-hour and the second 3-hour averaged data was consecutively used for the 2nd and 3rd hours lacking the measured data.

Generally, the upper air data are measured twice a day at 00 and 12Z (Greenwich Time) by radiosonde or rawindsonde in the vertical layers of the atmosphere. In Thailand, the upper air data are reported by the Thai Meteorological Department and can be downloaded from the website of University of Wyoming (http://weather.uwyo.edu/upperair/sounding.html) or http://raob.fsl.noaa.gov/. In this work, we used the upper air data at Bang Na meteorological station which record the data once a day at 7.00 a.m. (local time) for the 00 universal time (UT, Greenwich Time). To run the CALMET, the upper air data were formatted into the Forecast Systems Laboratory (FSL) format, see details in Appendix C.

(a) Pak Chong station (b) Lopburi station

Figure 3.5 Meteorological stations of the Thai Meteorological Department.

Table 3.8 Locations and details of the meteorological stations.

Meteorological stations	Collected data by	Meteorological parameters	Distance from the reference point (km)	UTM (X,Y) (km)	Direction to the the reference point
NPL	PCD	surface air data: G, P_I, RH, T 10 m: WD, WS_1 (hourly basis data)	24	707.5, 1606.8	WNW
KN	PCD	surface air data: G, P_I, RH, T 10 m: WD, WS_1 (hourly basis data)	21	701.6, 1624.4	SW

Table 3.8 Locations and details of the meteorological stations (cont.).

Meteorological stations	Collected data by	Meteorological parameters	Distance from the reference point (km)	UTM (X,Y) (km)	Direction to the the reference point
PC	TMD	surface air data: P_2, RH, T 10 m: WD, WS_2 CH, CV (3-h basis data)	25	749.7, 1620.2	E
LB	TMD	surface air data: P_2, RH, T 10 m: WD, WS_2 CH, CV (3-h basis data)	52	675.3, 1636.6	NW
Bang Na	TMD	surface air data: P_2, RH, T 10 m: WD, WS_2 CH, CV (3-h basis data) upper air data: DWPT, H, P2, RH, T, WD, WS_2 (once a day)	120	673.6, 1511.7	SSW

Notes: the reference point (the cement stack No.1 of the SCCC) is in center of cement complex

CH = ceiling height (feet)

CV = cloud cover (tenths)

DWPT = dew point temperature (°C)

G = global radiation (W/m^2)

H = height above sea level (m)

P_1 = pressure (mmHg)

P_2 = pressure (hPa)

RH = relative humidity (%)

T = dry bulb temperature (°C)

WD = wind direction (degree from the north)

WS_1 = wind speed (m/s)

WS_2 = wind speed (knot)

3.6 Estimation of air pollutants by air modelings

3.6.1 Estimation by the AERMOD

The AERMOD model was run with commercial interfaces. The ISC-AERMOD View Version 4.6.2 and 5.4 (Lakes Environmental Software, Waterloo, Ontario, Canada) were developed specially for Microsoft Windows. Figure 3.6 shows the data flow of the AERMOD modeling system composing of AERMAP, AERMET and AERMOD. The necessary input data in the system are shown.

- The **AERMAP** requires the digital terrain data for the AERMOD. Generally, the ISC-AERMOD View supports a wide variety of digital elevation terrain data formats, e.g., USGS DEM, GTOPO30 DEM, U.K. DTM, U.K. NTF, xyz Files, CDED 1-degree and AutoCAD DXF, etc. In this work, the GTOPO30 DEM (~900 m, 30 arc-sec) was downloaded free of charge from http://www.src.com. The GTOPO30 was transformed in xyz files by the Global Mapper program before using in the AERMOD.

- The **AERMET** requires two types of meteorological data files: surface data (a file containing surface scalar parameters) and upper air data (a file containing vertical profiles).

The surface data are formatted in the SAMSON format which contains all of the necessary meteorological parameters (e.g. dry and wet particle deposition and wet vapor deposition) for estimation of pollutant concentration. The requirements of the SAMSON format are explained in Appendix D. Similar to the CALMET, the AERMET requires the formatted upper air data in the FSL.

The input data for the AERMAP, AERMET and AERMOD and the AERMOD setting are summarized in Tables 3.9-3.10.

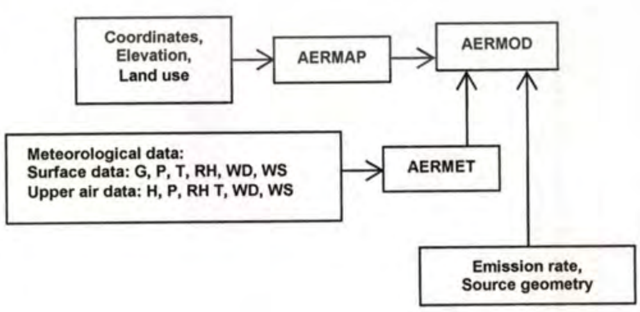

Figure 3.6 Data flow of the AERMOD modeling system (abbreviation see notes in Table 3.8).

Table 3.9 Input data for the AERMOD modeling system.

Model	Input data
AERMAP	**Geophysical data:** terrain height (m)
AERMET	**Geophysical data:** land use data **Surface data:** wind speed (m/s), wind direction (degrees), ceiling height (hundreds of feet), cloud cover (tenths), air temperature (K), relative humidity (%), pressure (mbar) **Upper air data:** pressure (mbar), height of balloon above sea level (m), temperature (K), wind speed (m/s), wind direction (degrees)
AERMOD	**Emission:** stack elevation (m), emission rate (g/s), stack height (m), stack exit temperature (K), stack diameter (m), stack exit velocity (m/s) geophysical file (from AERMAP) meteorological file (from AERMET)
POST View	dispersion data (from **AERMOD**)

Three sensitivity tests of the model in ISC-AERMOD View version 4.6.2 were studied.

1. Sensitivity of period averaged meteorological data to the prediction of AERMOD: use domain number 1 in Table 3.2.

2. Sensitivity of precipitation to the prediction of AERMOD: use domain number 1 in Table 3.2.

3. Sensitivity of upper air data to the prediction of AERMOD: use domain number 1 in Table 3.2.

The ISC-AERMOD View versions 4.6.2 and 5.4 were applied to estimate the dispersion of PM_{10}, NO_2 and SO_2 in the vicinity of the cement complex in Kaeng Khoi which covered 39.5 km×39.5 km. In case the dispersion of PM_{10} in Kaeng Khoi and Nah Phra Laan are estimated by the ISC-AERMOD View version 5.4 using domain number 3 in Table 3.2 (64.5 km×64.5 km). Both versions were run with grid spacing of 0.5 km.

3.6.2 Estimation by the CALPUFF

In this work, free CALPUFF PROfessional Beta 5.2.0 downloaded from the website of the Earth Tech, Inc. (http://www.src.com) was used. The model domain covered 50 km × 50 km on UTM 47P coordinated between 701E to 751E and 1593N to 1643N according to domain number 2 in Table 3.2. Both discrete and grid modes (grid spacing 0.5 km × 0.5 km) were selected to observe ground-level pollutant concentrations at 12 receptors and the impact areas. The input data for CALPUFF including CALMET and CALPOST were prepared in separate files according to Figure 3.7. The input data, details in Appendix D, and model setting of the CALPUFF are summarized in Tables 3.11-3.12.

Table 3.10 Summary of the AERMOD model setting.

Source type		Point source
	Units	stack height (m)
		stack diameter (m)
		stack exit temperature (K)
		stack exit velocity (m/s)
		emission rate (g/s)
	Pollutants	PM_{10}
		NO_2
		SO_2
	Dispersion model	urban
	Terrain	elevated (m)
	Dispersion averaged	1-h, 24-h, 1-yr
	Building downwash	No
	Chemical reaction	No
	Wet deposition	Yes (input precipitation data)
		No (not input precipitation data)
	Dry deposition	No
	Emission factors	No
	Number of stacks	PM_{10} – 14
		PM_{10} – 23
		NO_2 – 14
		SO_2 – 14
Grid size		0.5 km^2
Receptor type		Uniform Cartesian Grid
Domain		see Table 3.2
	Elevation terrain	Yes
	Receptor height	No
Receptor type		discrete receptor tool
Details of the discrete receptors		see Table 3.7

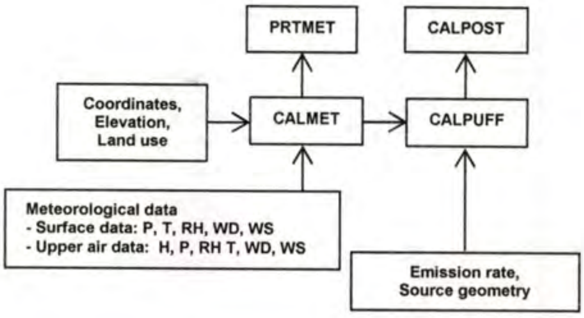

Figure 3.7 Data flow of the CALPUFF modeling system.

The meteorological data at each grid point for CALPUFF input data were generated by the **CALMET**. The surface data provided by CALMET were obtained from 3 surface stations and 1 upper air station. In this work, the sensitivity tests of the outputs of the CALPUFF were studied as follows:

- Case 1: no chemically reactive module, no wet deposition and no ozone background

- Case 2: no chemically reactive module, no ozone background, but include wet deposition module

- Case 3: RIVAD/ARM3 with wet deposition module and default ozone background

- Case 4: RIVAD/ARM3 with wet deposition module and hourly ozone background

- Case 5: MESOPUFF with wet deposition module and hourly ozone background

The meteorological input data for all cases were the same. The surface data were obtained from NPL, KN and PC stations whereas the upper air data were obtained from Bang Na meteorological station. The layer cell faces in the CALMET was set vertically to 11 layers from 0, 20, 50, 100, 200, 300, 600, 900, 1200, 1500, 1800 and 2100 m. The terrain was read from the GTOPO30 DEM by the Global Mapper program. The land use and coordinates of pollutant emitting sources and receptors were identified from an aerial photography orthographical image (scale 1:25,000), which was purchased from the Land Development Department, Ministry of Agriculture and Cooperatives. The data of land use were formatted manually before using in the CALMET.

The **CALPOST** is used to manage the primary data obtaining from the CALPUFF. In this study, the CALPOST was used to arrange 1-hour and 24-hour averaged maximum pollutant concentrations at grid and discrete receptors. The output data were written in grid format then plotted in the contours by a graphical software program (Surfer version 8) to identify the maximum concentration and compare with the AERMOD outputs.

Table 3.11 Input data for the CALPUFF modeling system.

Model	Input data
CALMET	**Geophysical data:** land use data, terrain height **Surface data:** wind speed (m/s), wind direction (degrees), ceiling height (hundreds of feet), cloud cover (tenths), air temperature (K), relative humidity (%), pressure (mbar) **Upper air data:** pressure (mbar), height above sea level (m), temperature (K), wind speed (m/s), wind direction (degrees)
CALPUFF	**Emission:** stack elevation (m), emission rate (g/s), stack height (m), stack exit temperature (K), stack diameter (m), stack exit velocity (m/s) meteorological file (from CALMET)
CALPOST	dispersion data (from CALPUFF)

Table 3.12 Summary of the CALPUFF model setting.

CALPUFF	
Map projection	UTM: Universal Transverse Mercator
	datum: WGS-G
	UTM zone: 47 N WGS-G: WGS-84, global coverage
	grid origin: 701, 1593 (x, y km)
	grid spacing: 0.5 km
	number of cells: 50×50×11 (NX, NY, NZ)
	cell face heights: 0, 20, 50, 100, 200, 300, 600, 900, 1200, 1500, 1800, 2100 m
Species	PM_{10}
	NO_2
	SO_2
Chemical transformation method	- not modeled
	- RIVAD/ARM3
	- MESOPUFF
Dry deposition	Yes
Meteorological data format	CALMET binary file (CALMET.DAT)
Ozone background	- No
	- Yes
Wind speed profile	ISC URBAN-1/ RURAL
Transitional plume rise	Yes
Stack tip downwash	Yes
Vertical wind shear above the top stack	No
Partial plume penetration	Yes

Table 3.12 Summary of the CALPUFF model setting (cont.).

CALPUFF	
Plume element modeled as	puff
Dispersion option	Pasquill-Gifford coef. (rural, ISC curves) and McElroy-Pooler coef. (urban)
Terrain adjustment method applied to grid and discrete receptors	partial plume path adjustment
Discrete receptors	see Table 3.7
Number of stacks	PM_{10} – 14
	NO_2 – 14
	SO_2 – 14
Output units	$\mu g/m^3$

3.6.3 Model output analysis

The outputs of the AERMOD, CALMET and CALPUFF in the study area were analyzed consecutively as follows:

(1) CALMET performance for surface meteorology was checked by the scatter plots of the measured and simulated meteorological parameters, i.e., temperature, wind speed and wind direction. In addition, the wind speeds and directions from the CALMET were plotted to check the wind fields.

(2) The maximum concentration of each pollutant was simulated by each case to consider the impacts of the pollutants in the study areas.

(3) The impact areas, where the simulated pollution concentrations were higher than the values in NAAQSs, were calculated by the ARC GIS 9.3.

(4) The populations in the impact areas were calculated by the following Equation.

$$\text{People (persons)} = \text{Impact area (km}^2\text{)} \times \text{Population density (persons/km}^2\text{)} \quad (3.3)$$

The population density of Kaeng Khoi was 79 persons/km^2 [15].

(5) The concentration-time series were plotted to compare the hourly of pollutant concentrations of the monitoring pollutants and the simulation results from the AERMOD and CALPUFF.

(6) The Quantile-Quantile plots (Q-Q plots) between the monitoring data and the simulation results from AERMOD and CALPUFF were used to verify the model performance. The Q-Q plots were created by ranking the hourly measured and simulated concentrations, then

pairing them by rank. The ranked vectors were subsequently plotted as a conventional scatter diagram. The middle line of the Q-Q plot with a unit slope showed equal concentration of the measurement and the simulation. The other two lines (below and above the middle line) marked half levels and double levels of the measurement and the simulation show half-under and double-over predictions, respectively [99]. Good agreement between the measured and simulated concentrations was indicated by all data were in line with the middle line. Possible model transport problems were designated by the lowest and highest model concentrations deviated from the middle line. The offsets of the median values showed a more serious problem where atmospheric reactions or deposition mechanisms might not be included in the simulation model.

(7) The simulated plumes of 1-h averaged concentration of NO_2 by the CALPUFF in the study area were plotted to indicate the area of high impact.

Chapter 4

Results and discussion

In this chapter, the ambient air quality, particularly in the areas nearby 4 cement manufactures in Kaeng Khoi, Saraburi were analyzed by measurement and compared with the simulation results from the AERMOD and CALPUFF software models. The measured and simulated concentrations of pollutants in ambient air were finally compared with the permit values by the National Ambient Air Quality Standards to evaluate the air pollutant impact on the study areas.

4.1 Emission inventory of the cement manufacturers in Thailand

The emission inventory of cement manufacturers in Thailand were based on the kiln capacities as detailed in Table 3.1. The estimation was calculated according to the European Monitoring and Evaluation Program (EMEP)/EEA Air Pollutant Emission Inventory Guidebook-2009. The calculation of the pollutant emissions by Equation (3.1) provided the average amount of pollutants releasing to the atmosphere. These fundamental results facilitate the cement manufacturers and the government to establish proper strategies for pollution prevention and control.

PM is mainly air pollutant from cement production. Without electrostatic precipitator (ESP), the cement manufacturers in Thailand emitted TSP, PM_{10} and $PM_{2.5}$ with enormous volume of 12,397,458; 5,635,208; and 6,198,729 tons/year, respectively. About 78% of the PM emissions from the cement manufactures in Thailand were from Saraburi and 60% of that came from Kaeng Khoi where 4 cement manufacturers were located [11]. The SCCC released the highest total volume of the PM followed by TPIPL, SCG and TPCC. The calculated PM emissions are shown in Tables 4.1 and 4.2.

Table 4.1 PM emissions from cement manufacturers.

Pollutants	Kaeng Khoi (tons/year)	Saraburi (tons/year)	Thailand (tons/year)
TSP	7,065,080.0	9,869,816.0	12,397,457.6
PM_{10}	3,211,400.0	4,486,280.0	5,635,208.0
$PM_{2.5}$	3,532,540.0	4,934,908.0	6,198,728.8

Table 4.2 PM emissions from cement manufacturers in Kaeng Khoi.

Cement plants	Emissions (tons/year)		
	TSP	PM_{10}	$PM_{2.5}$
SCCC	3,252,480.0	1,478,400.0	1,626,240.0
TPIPL	1,996,280.0	907,400.0	998,140.0
SCG	1,605,120.0	729,600.0	802,560.0
TPCC	211,200.0	96,000.0	105,600.0
Total	**7,065,080.0**	**3,211,400.0**	**3,532,540.0**

From the methodology in section 3.1, other pollutants emitted during the cement production were NO_x, SO_x, CO and non-methane volatile organic compounds (NMVOCs), heavy metals and dioxins. The total emissions of NO_x, SO_x, CO and NMVOCs from cement manufacturers in Thailand were 82,905; 20,004; 106,974 and 5,349 tons/year, respectively. The calculated emissions of NO_x, SO_x and CO are shown in Tables 4.3 and 4.4.

Normally, heavy metals, typical As, Cd, Cr, Cu, Hg, Ni, Pb, Se and Zn, cannot be eliminated by burning at high temperature. In cement production, heavy metals are released from cement kiln with solid wastes [17, 29]. A few of them might come along with PM emitted from the stacks. The emissions containing heavy metals posed a significant health risk. All of them are estimated based on the cement productivity, following the methodology in section 3.1. The calculated results are shown in Tables 4.5 and 4.6.

Burning process in cement production is at high temperature up to 1,400 ^{o}C. It is possible that dioxins , e.g., Benzo (a) pyrene, Benzo (b) fluoranthene, Benzo (k) fluoranthene, HCB, Indeno (1,2,3-cd) pyrene, PCB and PCDD/F are formed during the process. The calculated dioxins are shown in Tables 4.7-4.8.

Table 4.3 Emissions of NO_x, SO_x, CO and NMVOCs from cement manufacturers.

Pollutants	Emissions (tons/year)		
	Kaeng Khoi	Saraburi	Thailand
NO_x	47,240.1	66,023.0	82,905.0
SO_x	11,398.6	15,930.7	20,004.2
CO	60,955.0	85,191.0	106,974.2
NMVOCs	3,047.8	4,259.6	5,348.7

Table 4.4 Emissions of NO_x, SO_x, CO and NMVOCs from cement manufacturers in Kaeng Khoi.

Pollutants	Emissions (tons/year)			
	NO_x	SO_x	CO	NMVOCs
SCCC	21,781.4	5,255.6	28,105.0	1,405.3
SCG	10,749.3	2,593.7	13,870.0	693.5
TPIPL	13,295.1	3,208.0	17,155.0	857.8
TPCC	1,414.4	341.3	1,825.0	91.3

Table 4.5 Emissions of heavy metals from cement manufacturers.

Pollutants	Emissions (tons/year)		
	Kaeng Khoi	Saraburi	Thailand
As	0.808	1.13	1.42
Cd	0.244	0.341	0.428
Cr	1.25	1.75	2.19
Cu	1.97	2.76	3.46
Hg	3.35	4.69	5.88
Ni	1.49	2.09	2.62
Pb	2.99	4.17	5.24
Se	0.771	1.08	1.35
Zn	12.9	18.1	22.7

Table 4.6 Emissions of heavy metals from cement manufacturers in Kaeng Khoi.

Pollutants	Emissions (tons/year)			
	SCCC	SCG	TPIPL	TPCC
As	0.372	0.184	0.227	0.0242
Cd	0.112	0.0555	0.0686	0.0073
Cr	0.576	0.284	0.352	0.0374
Cu	0.909	0.449	0.555	0.0590
Hg	1.55	0.763	0.944	0.1
Ni	0.689	0.340	0.42	0.0447
Pb	1.38	0.680	0.841	0.0894
Se	0.356	0.175	0.217	0.0231
Zn	5.96	2.94	3.64	0.387

Table 4.7 Emissions of dioxins from cement manufacturers.

Pollutants	Emissions (tons/year)		
	Kaeng Khoi	Saraburi	Thailand
Benzo (a) pyrene	0.00198	0.00277	0.00348
Benzo (b) fluoranthene	0.00853	0.0119	0.015
Benzo (k) fluoranthene	0.00235	0.00328	0.00412
HCB	0.335	0.469	0.588
Indeno (1,2,3-cd) pyrene	0.00131	0.00183	0.0023
PCB	0.0305	0.0426	0.0535
PCDD/F	0.00152	0.00213	0.00267

Table 4.8 Emissions of dioxins from cement manufacturers in Kaeng Khoi.

Pollutants	Emissions (tons/year)			
	SCCC	SCG	TPIPL	TPCC
Benzo (a) pyrene	9.13×10^{-4}	4.51×10^{-4}	5.58×10^{-4}	5.93×10^{-5}
Benzo (b) fluoranthene	3.93×10^{-3}	1.94×10^{-3}	2.40×10^{-3}	2.56×10^{-4}
Benzo (k) fluoranthene	1.08×10^{-3}	5.34×10^{-4}	6.60×10^{-4}	7.03×10^{-5}
HCB	1.55×10^{-1}	7.63×10^{-2}	9.44×10^{-2}	1.00×10^{-2}
Indeno (1,2,3-cd) pyrene	6.04×10^{-4}	2.98×10^{-4}	3.69×10^{-4}	3.92×10^{-5}
PCB	1.41×10^{-2}	6.94×10^{-3}	8.58×10^{-3}	9.13×10^{-4}
PCDD/F	7.03×10^{-4}	3.47×10^{-4}	4.29×10^{-4}	4.56×10^{-5}

Pham Thi Bich Thao [100] calculated the emissions of PM_{10}, NO_x, SO_2, CO, submicron black carbon (BC), ammonia (NH_3), non-methane volatile organic compounds (NMVOCs), and submicron organic carbon (OC) from energy-consumed industries by using the document guide, namely Compilations of Air Pollutants Emission Factors, known as AP-42 EFs and IPCC. The central regional, where the cement complex is located, showed the largest total emissions, followed by the eastern region as shown in Table 4.9. The calculated results implied that cement manufacturers consumed high energy and released high emissions. However, we cannot compare the results from this work with ours because of different emission factor database. Their estimations did not classify specific types of industries. They used emission factors from several sources (the AP-42 EFs, IPCC and EIA reports) without measurement data from the emission sources, while this work applied the EMEP/EEA Air Pollutant Emission Inventory Guidebook-2009. From this point, Thailand should provide the EFs databases of each industry for being able to control air pollution for less pollutant impact and high air quality.

Table 4.9 Annual emissions due to energy consumption in industrial facilities by region in Thailand [100].

Region	Emissions (tons/year)							
	PM_{10}	NO_x (as NO_2)	SO_2	CO	BC	NH_3	NMVOCs	OC
Central	135,300	74,600	301,400	118,100	5,200	1,000	21,300	5,600
Eastern	58,300	20,200	119,300	21,600	1,300	300	5,600	1,300
Northern	9,400	6,000	19,200	16,600	400	100	2,800	400
Northeastern	14,800	5,900	18,200	26,500	700	100	3,300	700
Southern	13,800	4,600	18,800	10,300	500	100	500	500
Total	**231,600**	**111,300**	**476,900**	**193,100**	**8,100**	**1,600**	**33,500**	**8,500**

4.2 Stack sampling and ambient air monitoring

In this part, the concentrations of the pollutants sampled at the stacks and in ambient air were reported and discussed. The measurements at the stacks were formally known as 'stack sampling' whereas in the ambient were 'ambient air monitoring or monitoring'. To evaluate the impact of pollutant emissions from cement manufacturers, both stack sampling and ambient air monitoring were measured. The emitting and monitoring results were compared to find the emission impacts on the communities.

4.2.1 Stack sampling

According to the EIA reports, the stack samplings of TSP as PM_{10}, NO_2 and SO_2 from cement manufacturers in Kaeng Khoi in terms of mass of each pollutant/volume were converted to mass of pollutant/time in tons/year and g/s. Their annual emissions were shown in Table 4.10. With the electrostatic precipitators of 99.99% efficiency at the stacks, TSP released from the stacks can be considered as PM_{10} [20, 48]. From Table 4.10, the SCG emitted the highest PM_{10} in Kaeng Khoi, whereas, the SCCC with high temperature combustion emitted the highest NO_2. From the EIA reports of 4 cement manufacturers, they released SO_2 much lower than NO_2, TSP and PM_{10} because SO_2 in flue gas reacted with $CaCO_3$ in raw materials during cement combustion. The total emission rate of SO_2 in 2007 was about 315 tons/year or 10 g/s or in terms of concentration 1-12 mg/m^3, which was lower than the permit of the Department of Industrial Works, Ministry of Industry of 131 mg/m^3. From Table 4.10, TPCC, the smallest cement manufacturer in this area, emitted very low emissions of TSP as PM_{10}, NO_2 and SO_2.

Table 4.10 Annual emissions from stack samplings of the 4 cement manufacturers in Kaeng Khoi [101-104].

Cement manufacturers	Emission rates, tons/year (g/s)		
	TSP (as PM_{10})	**NO_2 (as NO_x)**	**SO_2**
SCCC	1,037.0 (32.9)	25,897.1 (821.2)	147.7 (4.7)
TPIPL	1,161.0 (36.8)	9,857.0 (312.6)	146.9 (4.7)
SCG	2,012.4 (63.8)	7,022.2 (222.7)	16.7 (0.53)
TPCC	75.4 (2.4)	462.0 (14.6)	3.6 (0.1)
Total	**4,285.8** **(1,35.9)**	**43,238.3** **(1,371.1)**	**314.9** **(10.0)**

4.2.2 Ambient air monitoring

In this section we discuss the monitoring concentrations of PM_{10}, NO_2, SO_2, CO and O_3 from 2 semi-permanent monitoring stations for the connecting areas of Kaeng Khoi, and the monitoring concentrations of TSP, PM_{10}, NO_2 and SO_2 from 12 non-permanent monitoring stations in the vicinity of the cement manufacturers.

(1) Semi-permanent monitoring station

The PM_{10}, NO_2, SO_2, CO and O_3 in ambient air were monitored continuously by 2 semi-permanent monitoring stations of the Pollution Control Department (Nah Phra Laan: NPL and Kao Noi: KN stations). As stated in section 3.3.2, these stations are both meteorological and monitoring stations, but their main purpose is monitoring air pollutants. Both NPL and KN stations are located near the residential areas within 25-km radius from the cement stack No.1 of the SCCC (the reference point) as shown in Figure 4.1.

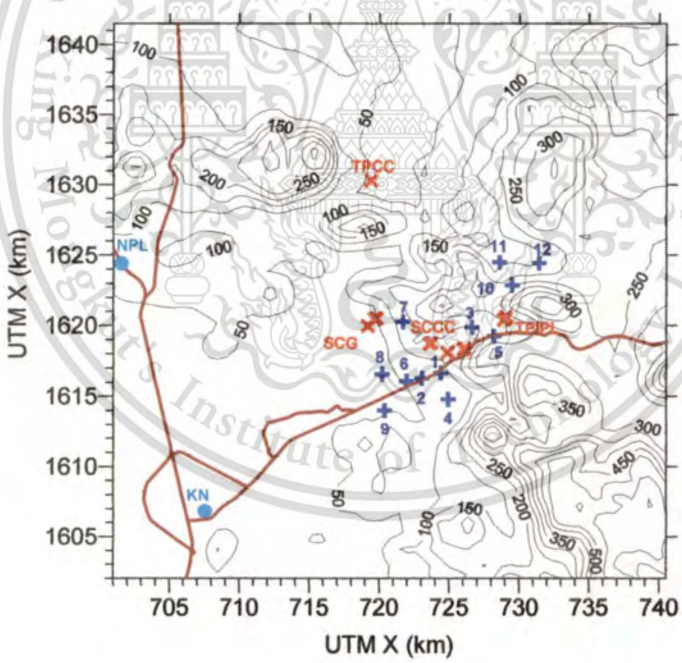

Figure 4.1 Locations of the Nah Phra Laan and Kao Noi stations and cement manufacturers in Kaeng Khoi: (●) monitoring stations, (+) receptors and (×) stacks of cement plants.

The hourly averaged concentrations of PM_{10}, NO_2, SO_2, CO and O_3 were monitored from 2 stations during 2005-2007. Figure 4.2 shows the box plots of each pollutant's trend and dispersion.

PM_{10} accounts for the emissions from cement manufacturers, mineral industries and transportations in the area. From Figure 4.2, it can be seen that the monitoring results of PM_{10} agree with the surrounding circumstances of NPL station. The average concentrations of PM_{10} in 2005, 2006 and 2007 of 108, 125 and 103, $\mu g/m^3$ were much higher than 50 $\mu g/m^3$ by the National Ambient Air Quality Standard (NAAQS, Thailand) and 20 $\mu g/m^3$ by the WHO's Guidelines. Although PM_{10} emissions from each industry nearby NPL station was in control and not higher than the permit but the total emission of PM_{10} was significant and could impact the communities. Compared to the respective permits by the Pollution Control Department, almost no impacts from NO_2, SO_2, CO and O_3 were observed. The annual CO in the ambient air was higher than PM_{10}, NO_2, SO_2 and O_3 but its concentration was much lower than 1-hour and 8-hour averaged values of 34,200 and 10,260 $\mu g/m^3$ by the NAAQS.

At KN station, the concentrations of PM_{10}, NO_2, SO_2, CO and O_3 did not violate the NAAQS limits. From 2005-2007, the 1-year averaged values of PM_{10} of 31, 33, and 42 $\mu g/m^3$ were within the NAAQS limit but higher than the WHO's Guidelines. One-year averaged PM_{10} in this area was much lower than that nearby NPL station. It is possible that road traffics attribute to major pollutant emission source because KN station is in the middle of the town near the intersection of Mitrapab Road to the central of Saraburi, Nakhon Ratchasima and Lopburi.

In summary, the NPL area has been facing high PM concentrations, although various campaigns against the PM emissions have been set up. Less air pollution was observed in KN area.

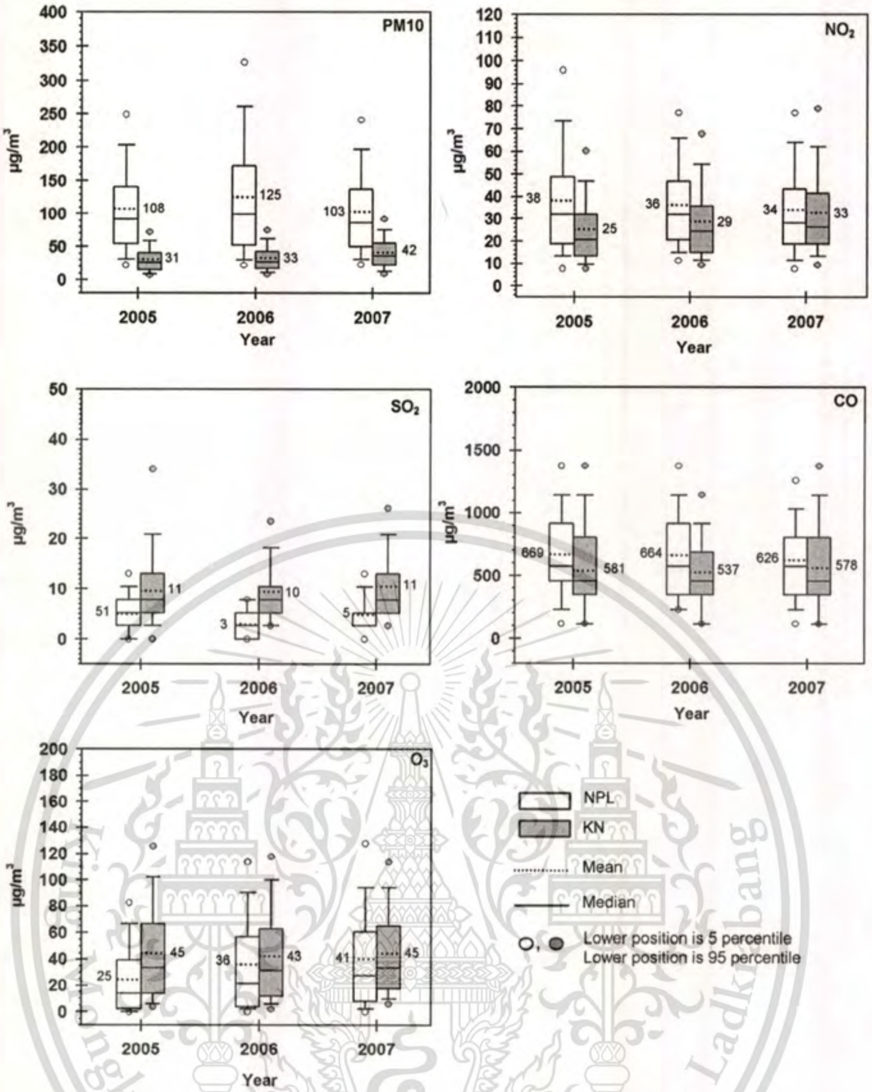

Figure 4.2 Box plots of hourly averaged concentrations of PM_{10}, NO_2, SO_2, CO and O_3 monitored at Nah Phra Laand and Kao Noi stations during 2005-2007.

Apart from showing pollution trends by the box plots, the relations between air pollutants and the wind at the monitoring stations were analyzed and shown by the scatter plots of pollutants and the windroses in dry and wet seasons, see Figures 4.3 - 4.6.

In fact, the climate in Thailand is divided into 3 seasons under the influences of 2 seasonal winds: northeast and southwest monsoons. Three seasons are winter (Nov.-Feb.), summer (Mar.-Jun.) and rainy season (Jul.-Oct.). The dry and wet seasons in this work are classified according to different rainfall (no rain and intense rain) and the monitoring period in the EIA reports of the SCCC. The monitoring to consider the pollutant dispersions is supposed to be in the period of the northeast and southwest monsoons. Therefore, dry season is under the influence of northeasterly monsoon from January to April and November to December. The wet season is under the influence of southwesterly monsoon from May to October.

Figures 4.3-4.6 show the 1-hour averaged concentrations of PM_{10}, NO_2, SO_2, CO and O_3 monitored at NPL and KN stations against wind direction to observe the dispersion of pollutants under the influences of seasonal monsoons in dry and wet seasons. The rain fall in the study areas in dry season was 90-240 mm and 700-1,100 mm in wet season. The average temperature in dry and wet seasons was 13-36 °C and 19-37 °C, respectively.

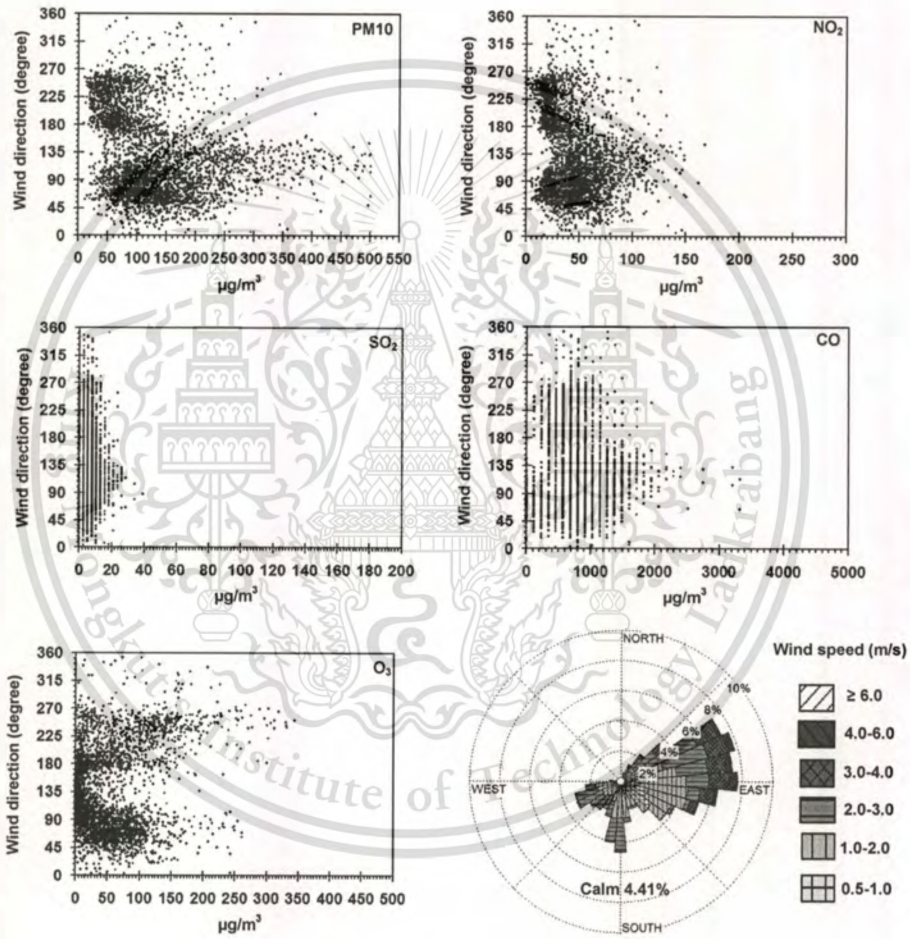

Figure 4.3 Wind direction against hourly averaged concentrations of PM_{10}, NO_2, SO_2, CO and O_3 monitored at Nah Phra Laan station in dry season.

In dry season, the windroses in Figure 4.3 shows that the wind regimes at NPL station were clearly dominated by easterly and northeasterly winds with southerly and southwesterly winds. The strongest wind speed was not higher than 6 m/s, coming from the east and northeast directions. According to the scatter plots of the pollutants and windroses in Figure 4.3 together with Table 2.6 in chapter 2, we can see that most pollutants dispersed at 45, 90, 225 and 180 degrees corresponding to the northeasterly, easterly, southwesterly and southerly winds. However, in wet season as shown by the windroses in Figure 4.4, the direction of the dominant wind at NPL station changed to westerly, southwesterly and southerly winds. The scatter plots show that most pollutants dispersed at 225, 180 and 270 degrees corresponding to the southwesterly, southerly and westerly winds.

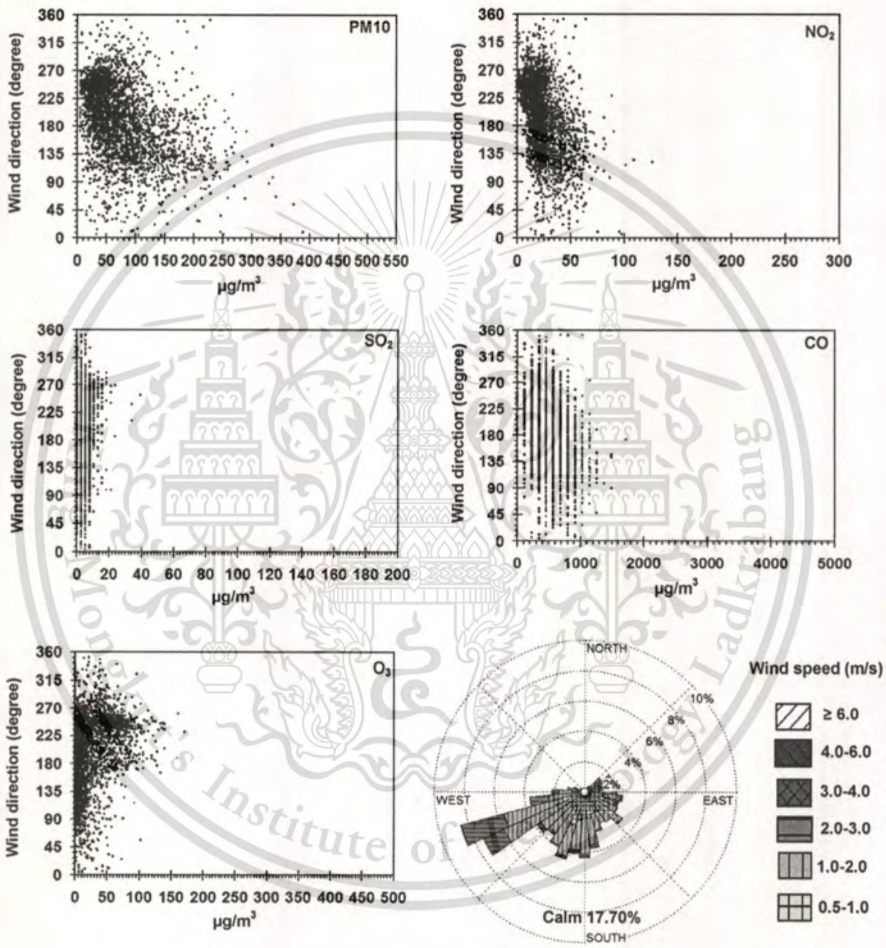

Figure 4.4 Wind direction against hourly averaged concentrations of PM_{10}, NO_2, SO_2, CO and O_3 monitored at Nah Phra Laan station in wet season.

In case of KN station, the winds in dry season were dominated by the easterly, southerly, southwesterly and westerly winds as shown in Figure 4.5. Most pollutants dispersed at 90, 180, 225 and 270 degrees corresponding to the easterly, southerly, southwesterly and westerly winds. In wet season, the southeasterly, southerly and northwesterly winds were outstanding, as shown in

Figure 4.6. All pollutants dispersed at 135, 180, and 315 degrees corresponding to the southeasterly, southerly and northwesterly winds.

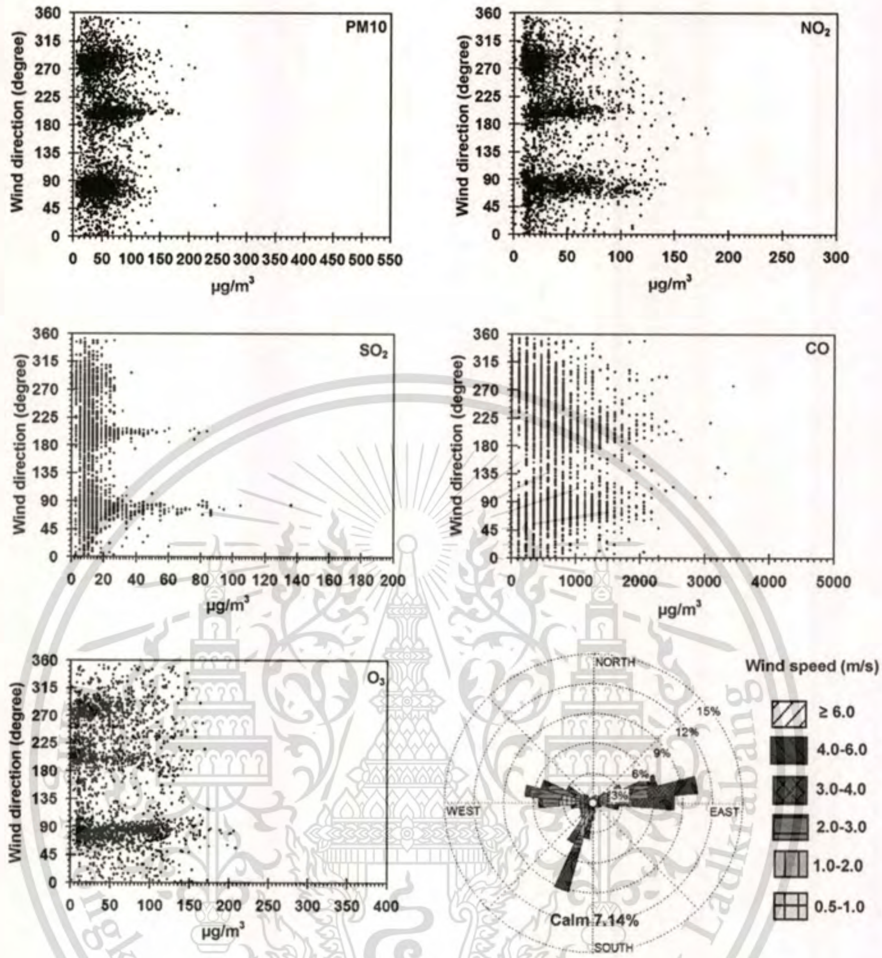

Figure 4.5 Wind direction against hourly averaged concentrations of PM_{10}, NO_2, SO_2, CO and O_3 monitored at Kao Noi station in dry season.

From the scatter plots of pollutants and the windroses, most wind directions in dry and wet seasons are likely different from the directions of seasonal monsoons. This phenomenon can attribute to the effects of valley breezes and the local channeling effect of the station. The concentrations of pollutants at NPL and KN stations in dry season were higher than in wet season due to less wet scavenging and less pollutant deposition [105].

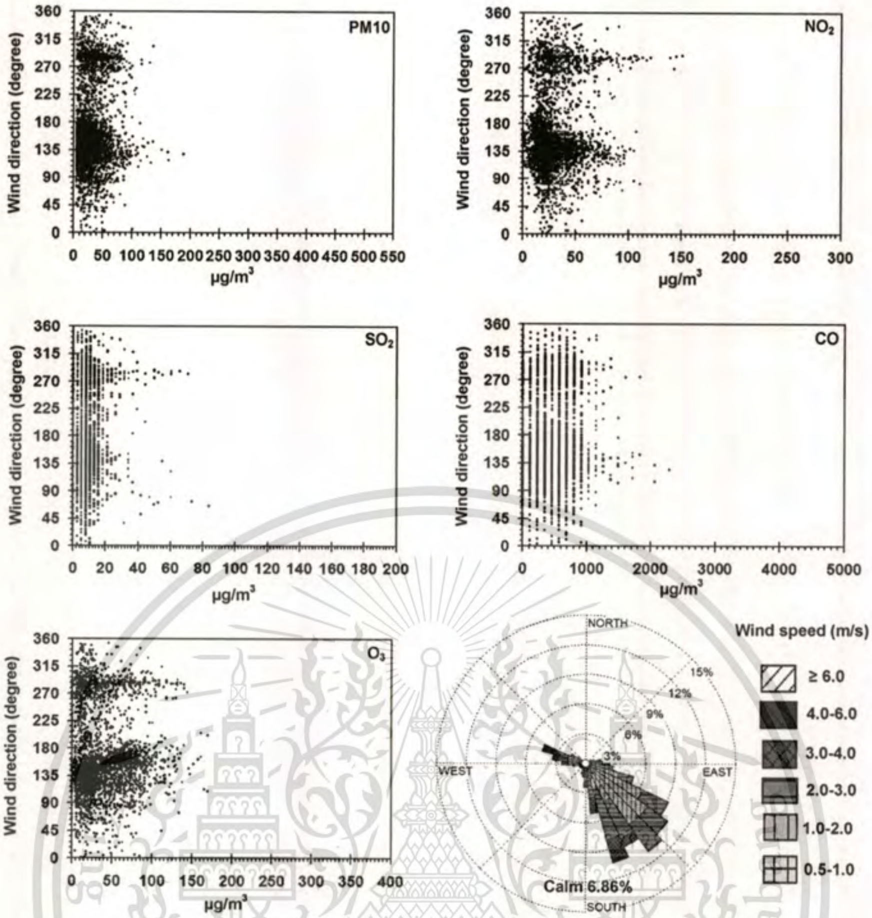

Figure 4.6 Wind direction against hourly averaged concentrations of PM_{10}, NO_2, SO_2, CO and O_3 monitored at Kao Noi station in wet season.

(2) Non-permanent monitoring station

The routine monitorings of TSP, PM_{10}, NO_2 and SO_2 for 7 days continuously in dry and wet seasons by 12 receptors of the Siam City Cement Public Company Limited (SCCC) in accordance with the EIA guidelines were used to evaluate air pollution due to no permanent monitoring station in Kaeng Koi. Figure 4.7 shows the distance between each receptor and the reference point.

The characteristics and performances of 12 receptors to detect pollutant concentrations are the same. The receptors were divided to 3 groups for west and east directions of the study domain in dry and wet seasons. The monitoring periods were shown in Tables 4.11 and 4.12.

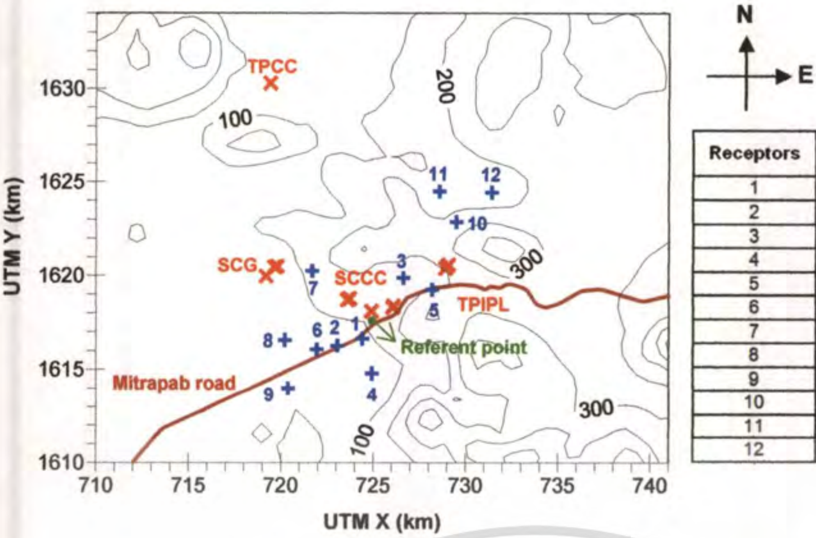

Receptors	Distance from the reference point (km)
1	1.47
2	2.35
3	2.47
4	3.44
5	3.58
6	3.64
7	3.90
8	4.87
9	6.07
10	6.65
11	7.38
12	9.12

Figure 4.7 Locations of 12 receptors nearby 4 cement manufacturers: (+) receptors and (×) stacks of cement plants.

Table 4.11 Monitoring period of the receptors in dry season.

Group number	Receptors on the west of the domain	Receptors on the east of the domain	Monitoring period
1	6, 8	5, 12	2nd – 9th March 2007
2	1, 2, 7	11	9th – 17th March 2007
3	4, 9	3, 10	17th – 24th March 2007

Table 4.12 Monitoring period of the receptors in wet season.

Group number	Receptors on the west of the domain	Receptors on the east of the domain	Monitoring period
1	6, 9	5, 12	12nd – 19th October 2007
2	1, 2, 8	11	20th – 27th October 2007
3	4, 7	3, 10	28th October – 4th November2007

The TSP and PM_{10} were collected by air samplers, as described in section 3.3.2(2) and reported in 24-hour averaged values, not 1-hour averaged values as at the 2 semi-permanent monitoring stations belonging to the Pollution Control Department. Thus, from Figure 4.9-4.19 it was not possible to plot the concentrations of TSP and PM_{10} against wind direction.

Figures 4.8-4.19 show that the concentrations of TSP, PM_{10}, NO_2 and SO_2 at 12 receptors in 360 degrees at west and east directions of the study domain in dry season (calm winds 9-38 %) and wet season (calm winds 3-41 %) were not over the permits of the NAAQS in Table 2.2. It can be seen that wind directions at 12 receptors are not uniform that might be the effects of valley and mountain winds. The dispersion patterns of all pollutants from the receptors in dry and wet seasons were similar even though the dominant winds were different. In the dry season, Figures 4.8-4.13, the dispersion patterns of all pollutants from the receptors at west and east directions of the study domain were similar, except SO_2 in Figure 4.11 at receptor 7. This implied that the emission rates of SO_2 from the cement plants changed because of different sulfur contents in primary and secondary fuels. The overall results could not describe the impact of individual pollutant to the study areas obviously because the data plotted in Figures 4.8-4.19 were obtained from only 7 days continuous measurement. However, we can see that almost of the monitoring concentrations of NO_2 and SO_2 in wet season were lower than those of dry season. These phenomena confirmed the effect of the pollutant deposition in wet season.

In summary, by monitoring it is rather difficult to identify the area of high air pollution impact. We found that only 7-day continuous measurement based on the EIA guidelines and inaccessible locations of the residential areas to install the receptors made them not possible to detect and distinguish the accurate air pollutants emitting from the cement manufacture. Accordingly, in section 4.5, the simulation dispersion models (AERMOD and CALPUFF) were applied to find the aerial impact of the emissions. The trajectories of NO_2 concentrations in dry and wet seasons to indicate the impact areas and suitable locations of the receptors were demonstrated by the CALPUFF.

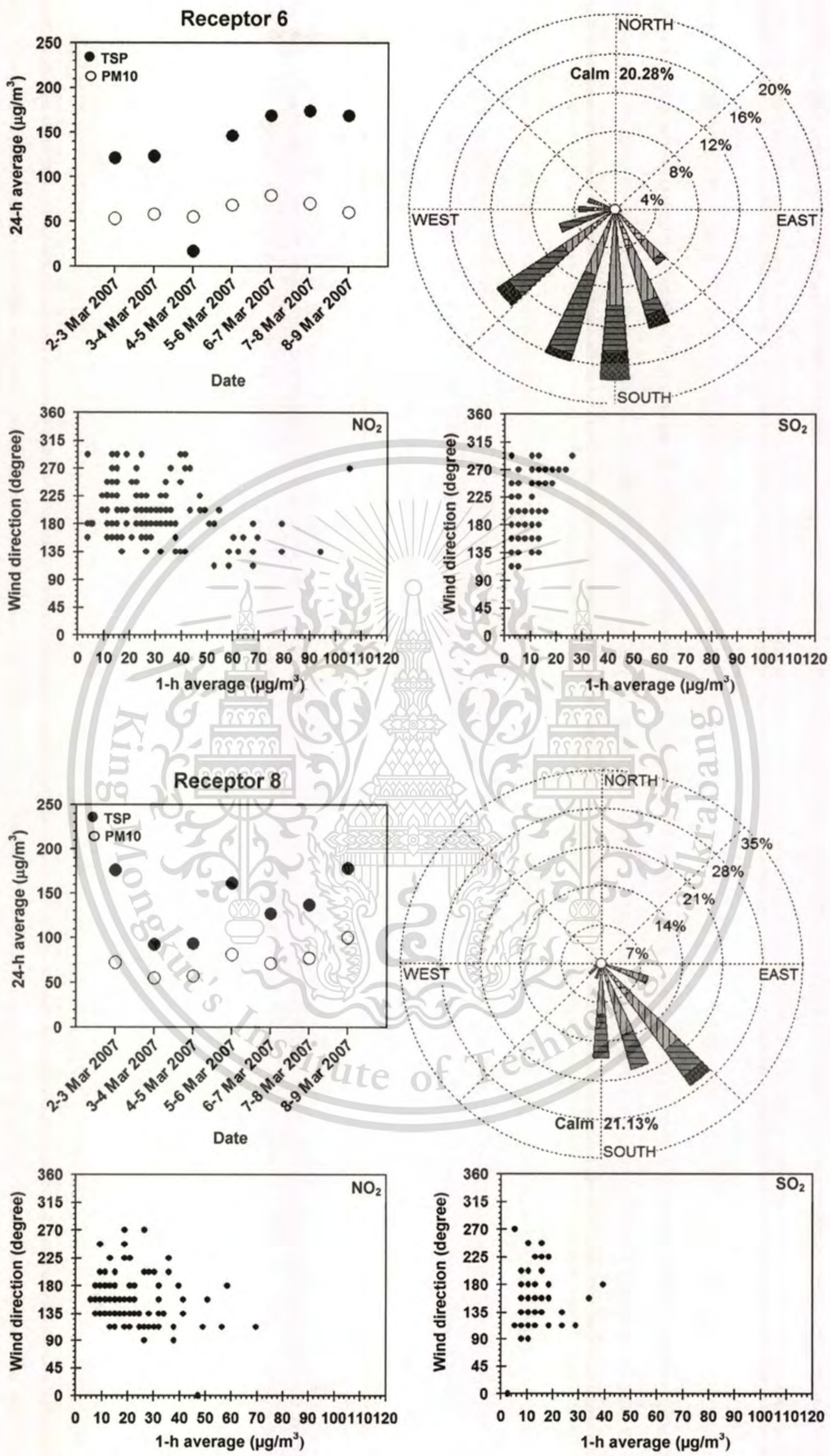

Figure 4.8 Group 1 receptors in the west of the domain in dry season.

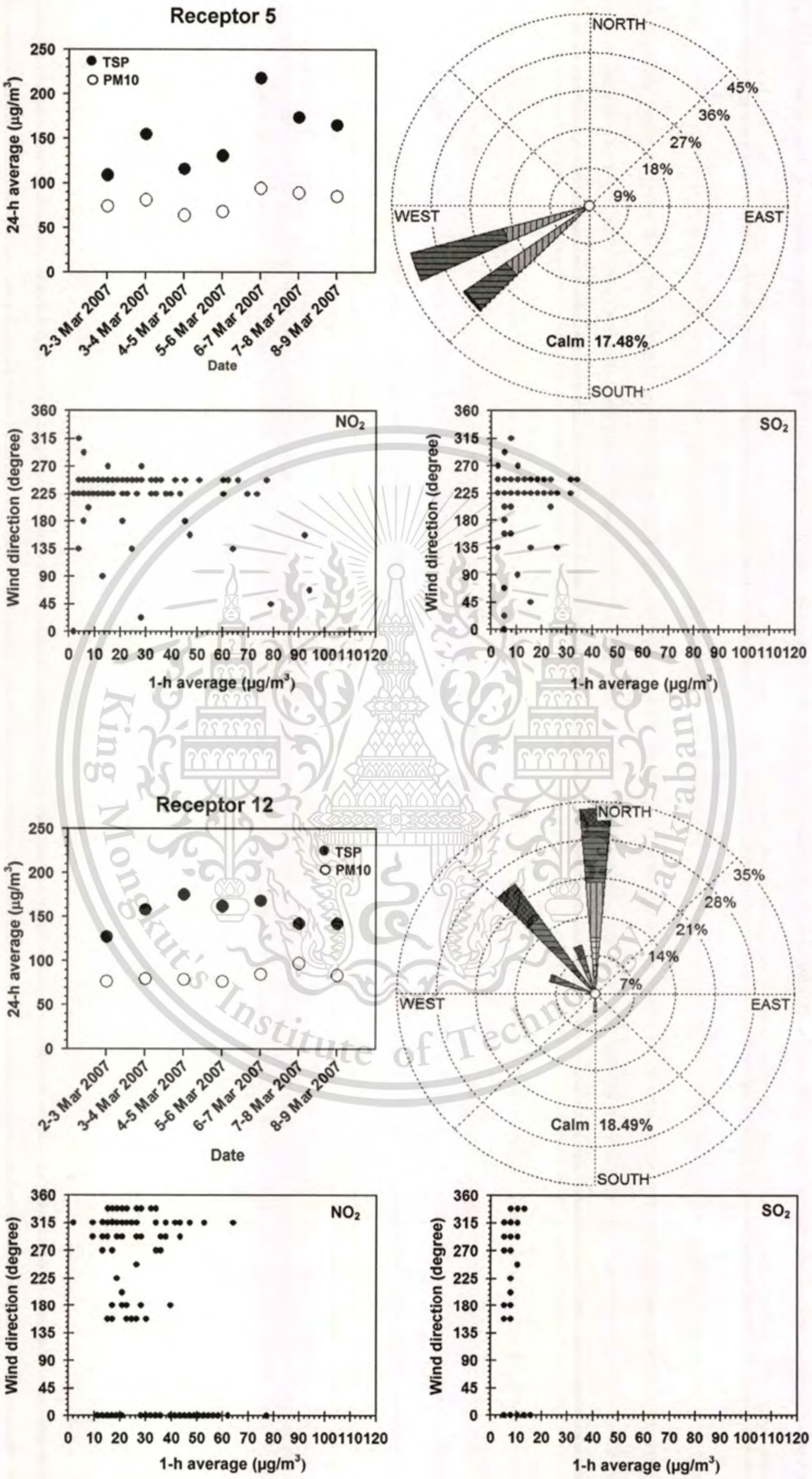

Figure 4.9 Group 1 receptors in the east of the domain in dry season.

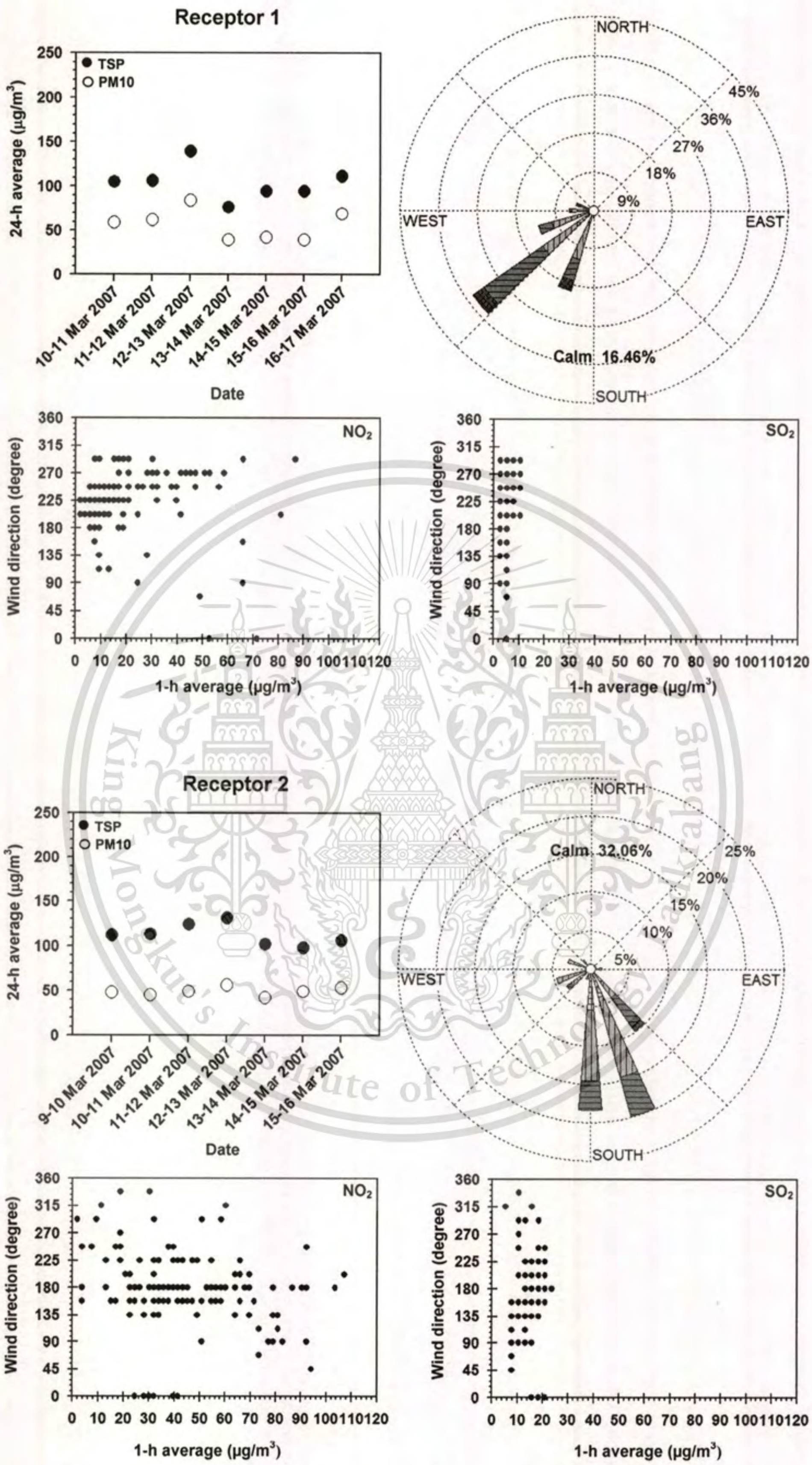

Figure 4.10 Group 2 receptors in the west of the domain in dry season.

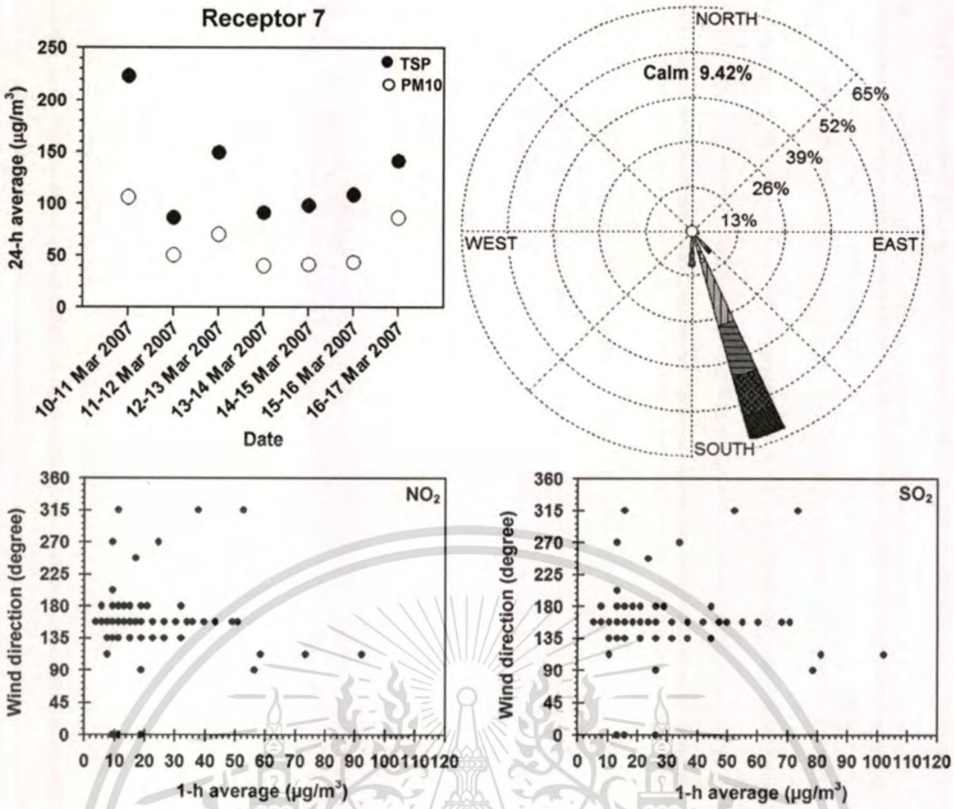

Figure 4.10 Group 2 receptors in the west of the domain in dry season (cont).

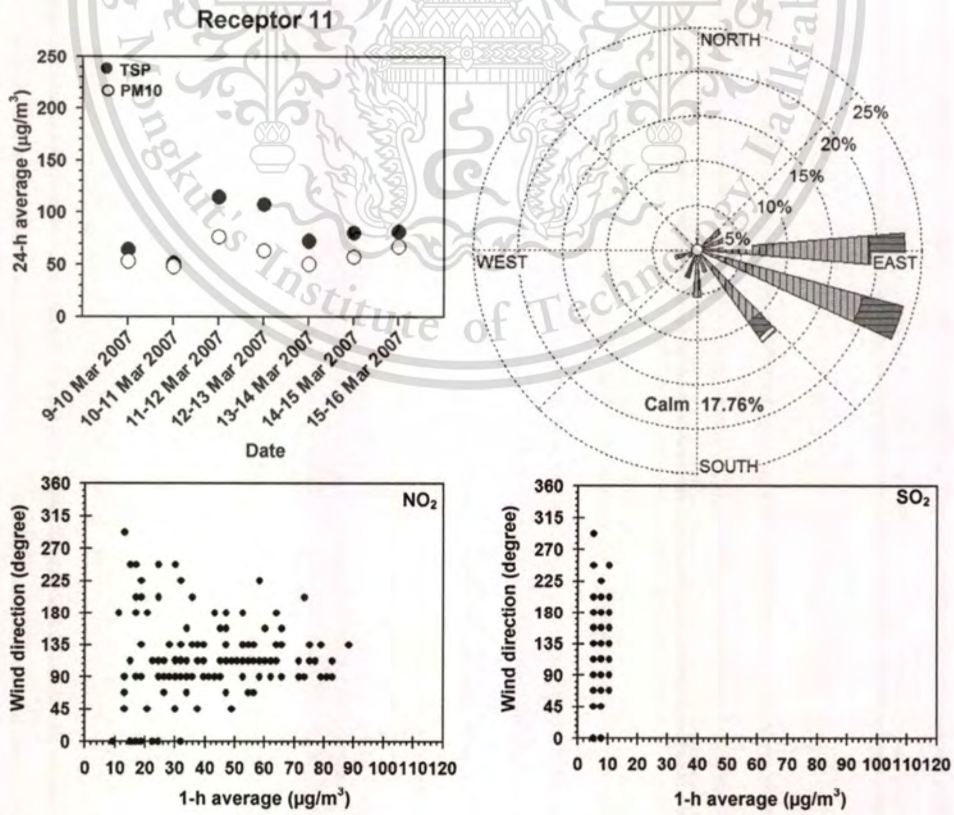

Figure 4.11 Group 2 receptors in the east of the domain in dry season.

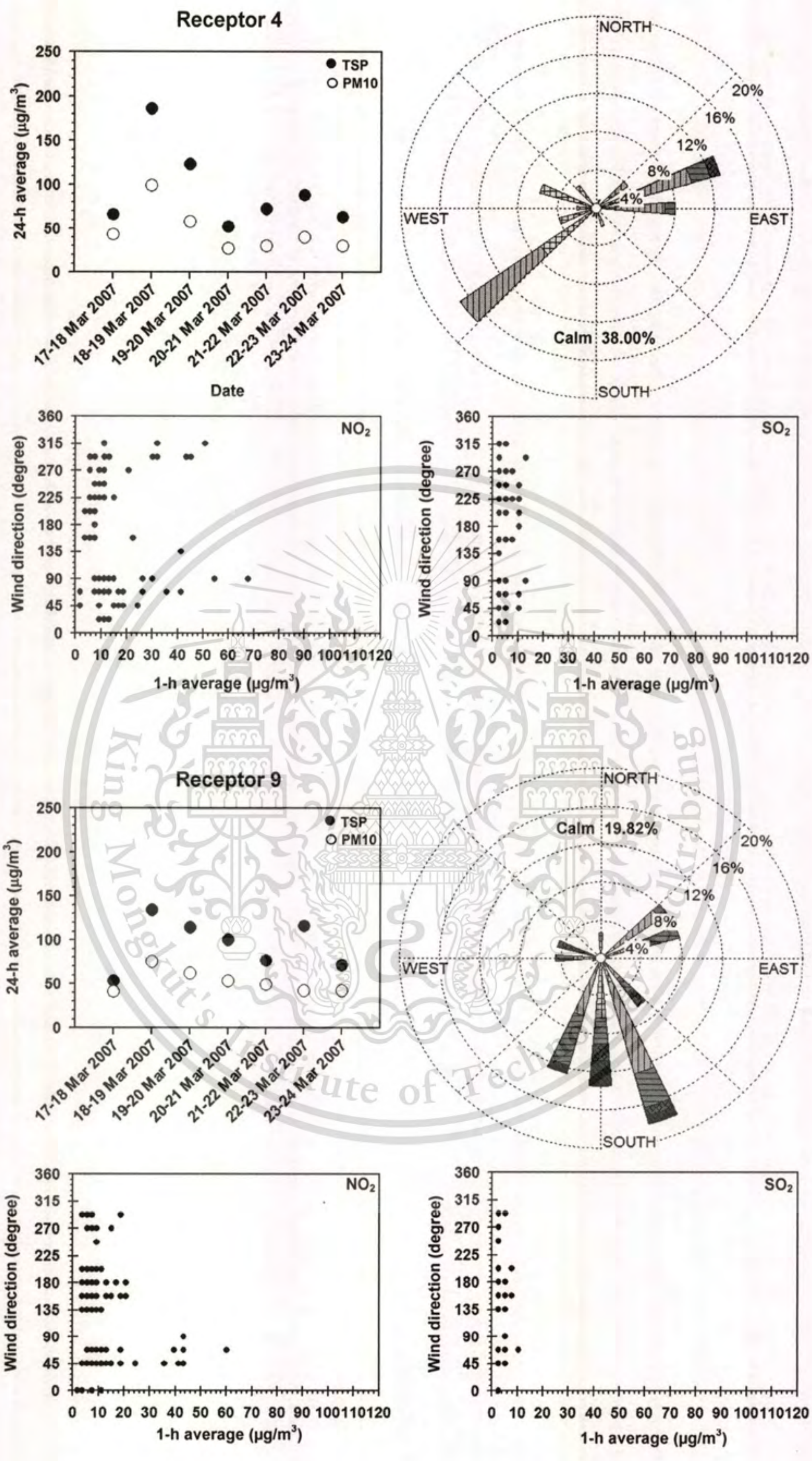

Figure 4.12 Group 3 receptors in the west of the domain in dry season.

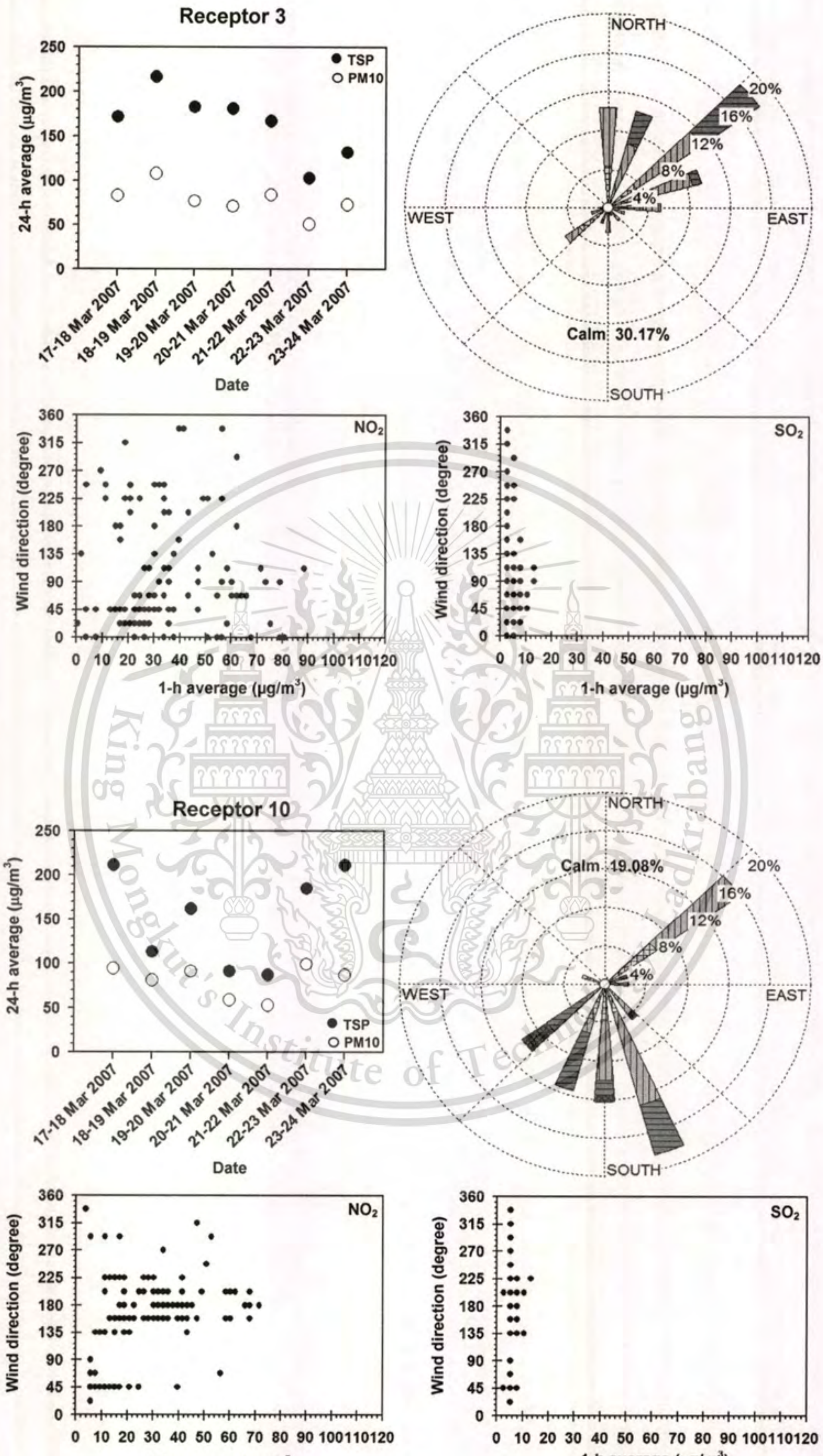

Figure 4.13 Group 3 receptors in the east of the domain in dry season.

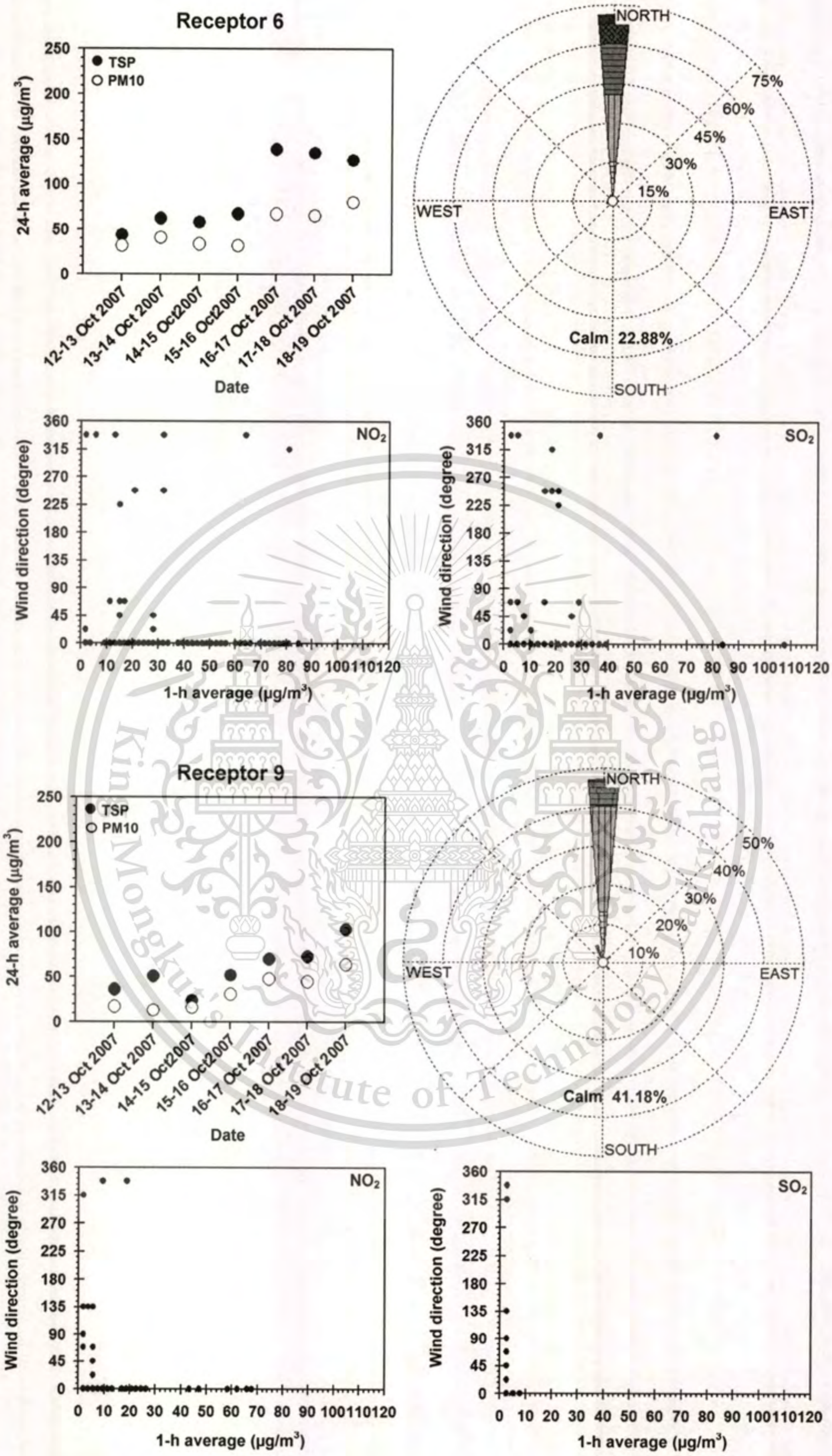

Figure 4.14 Group 1 receptors in the west of the domain in wet season.

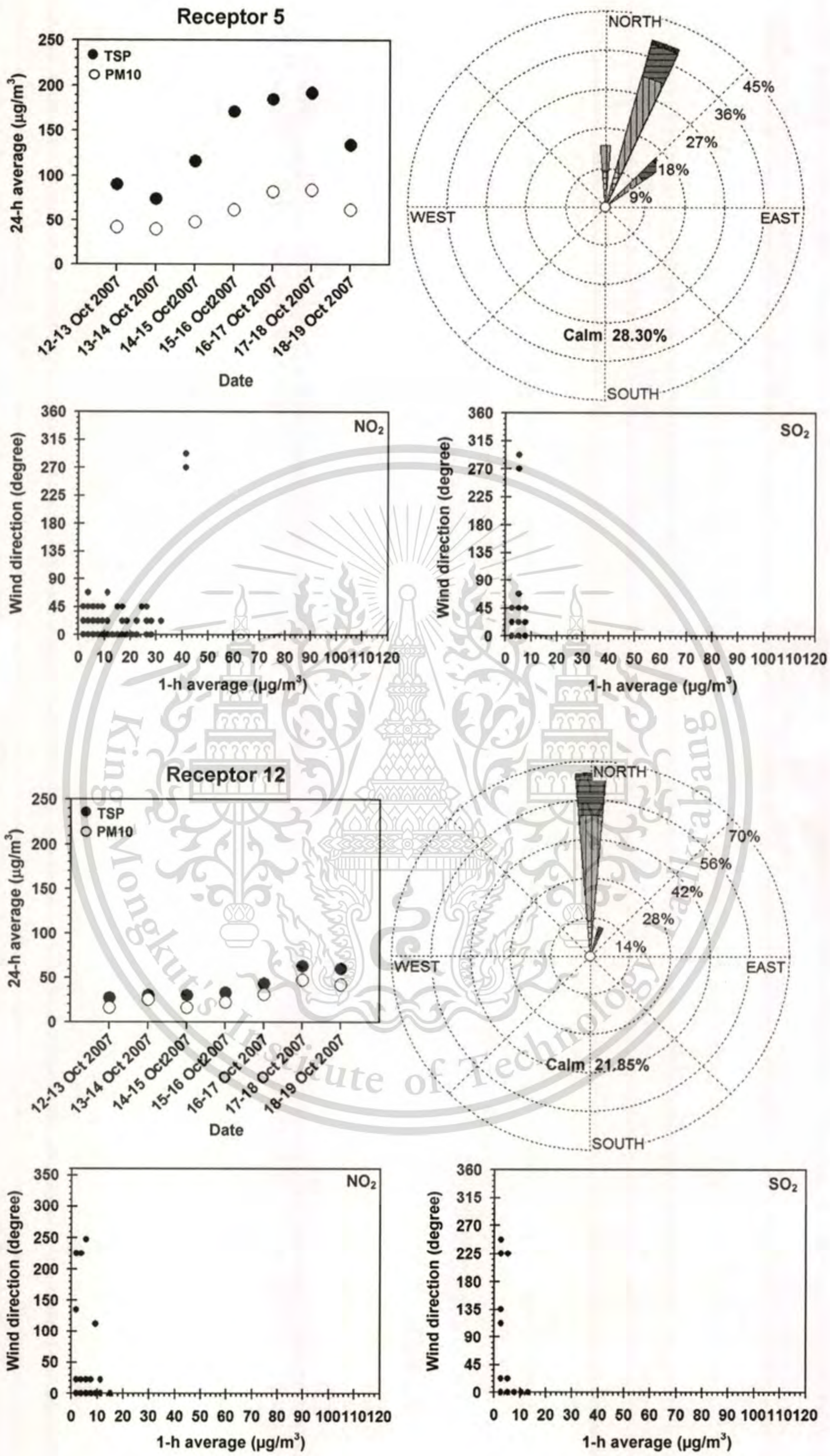

Figure 4.15 Group 1 receptors in the east of the domain in wet season.

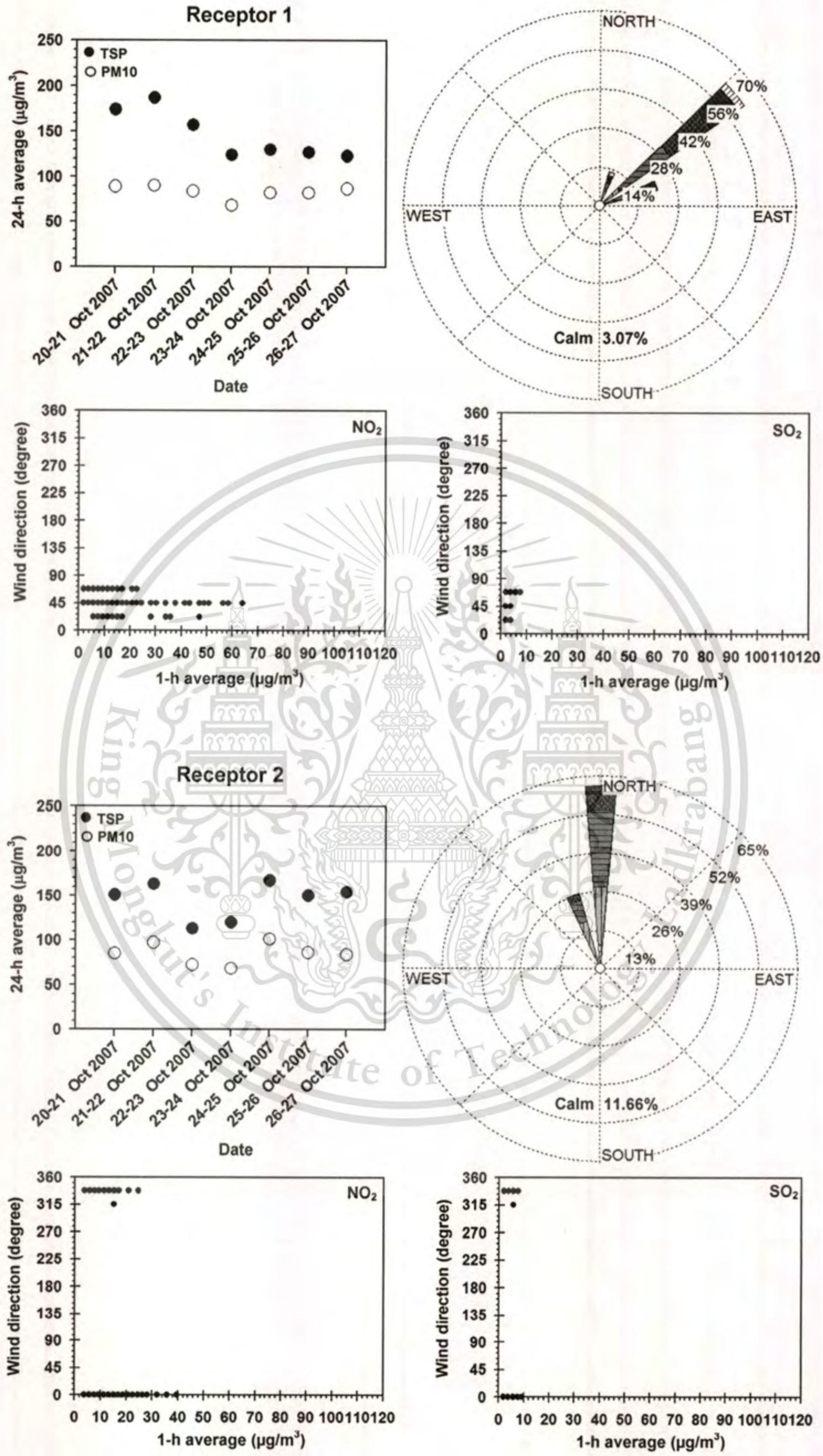

Figure 4.16 Group 2 receptors in the west of the domain in wet season.

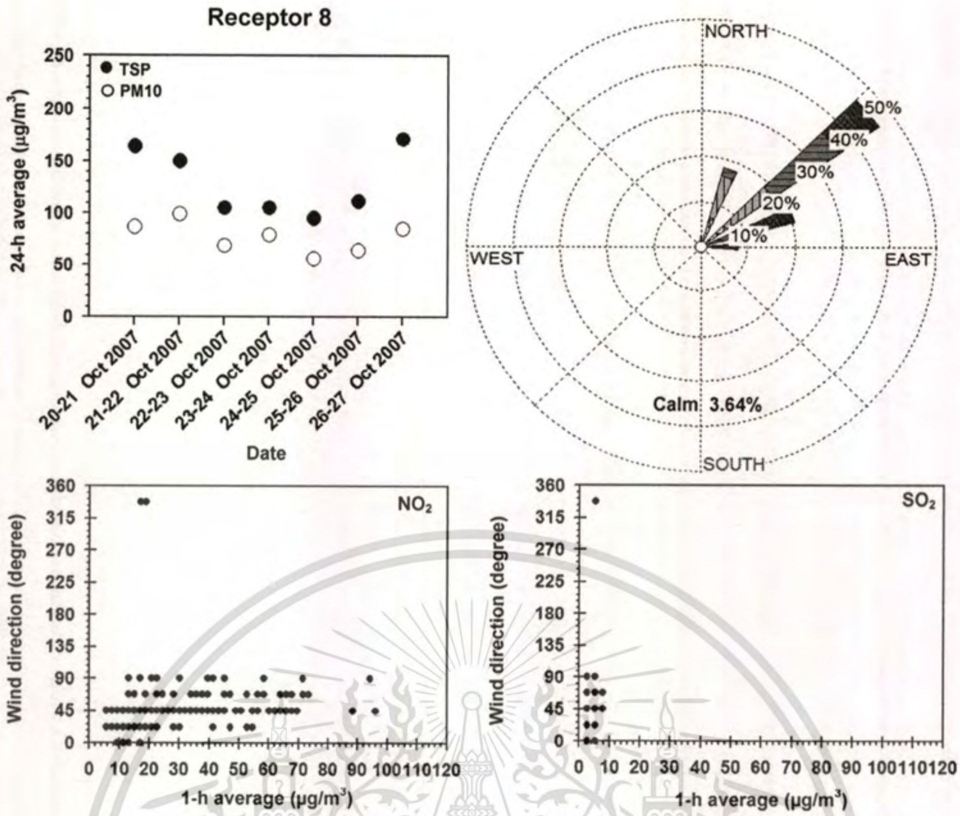

Figure 4.16 Group 2 receptors in the west of the domain in wet season (cont).

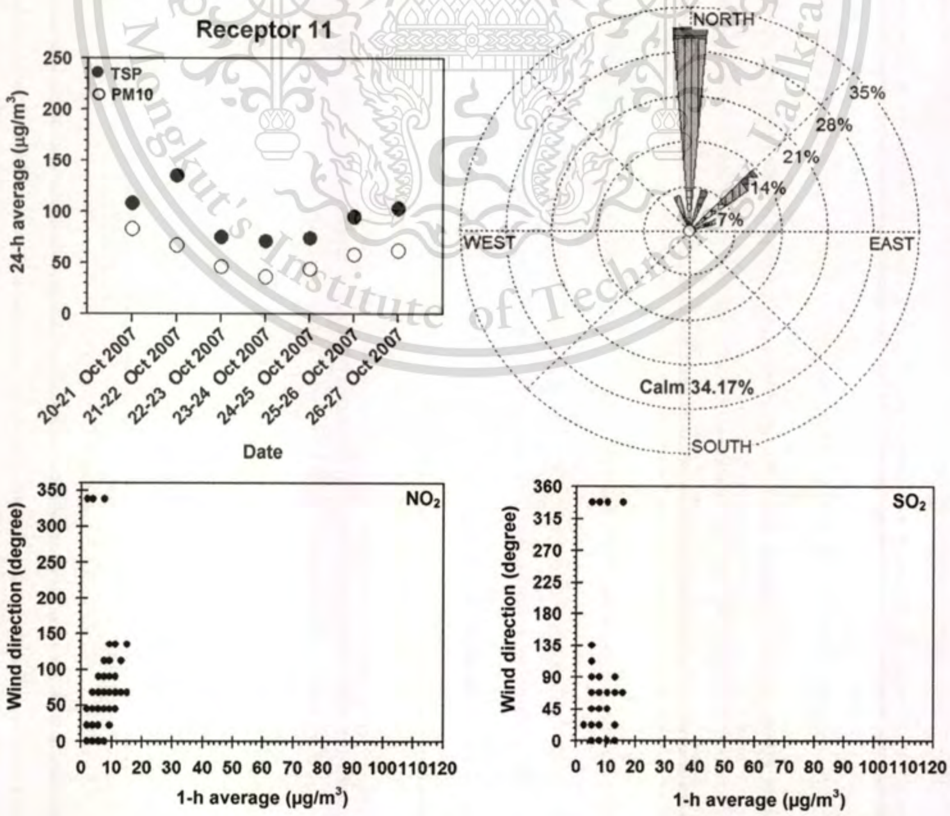

Figure 4.17 Group 2 receptors in the east of the domain in wet season.

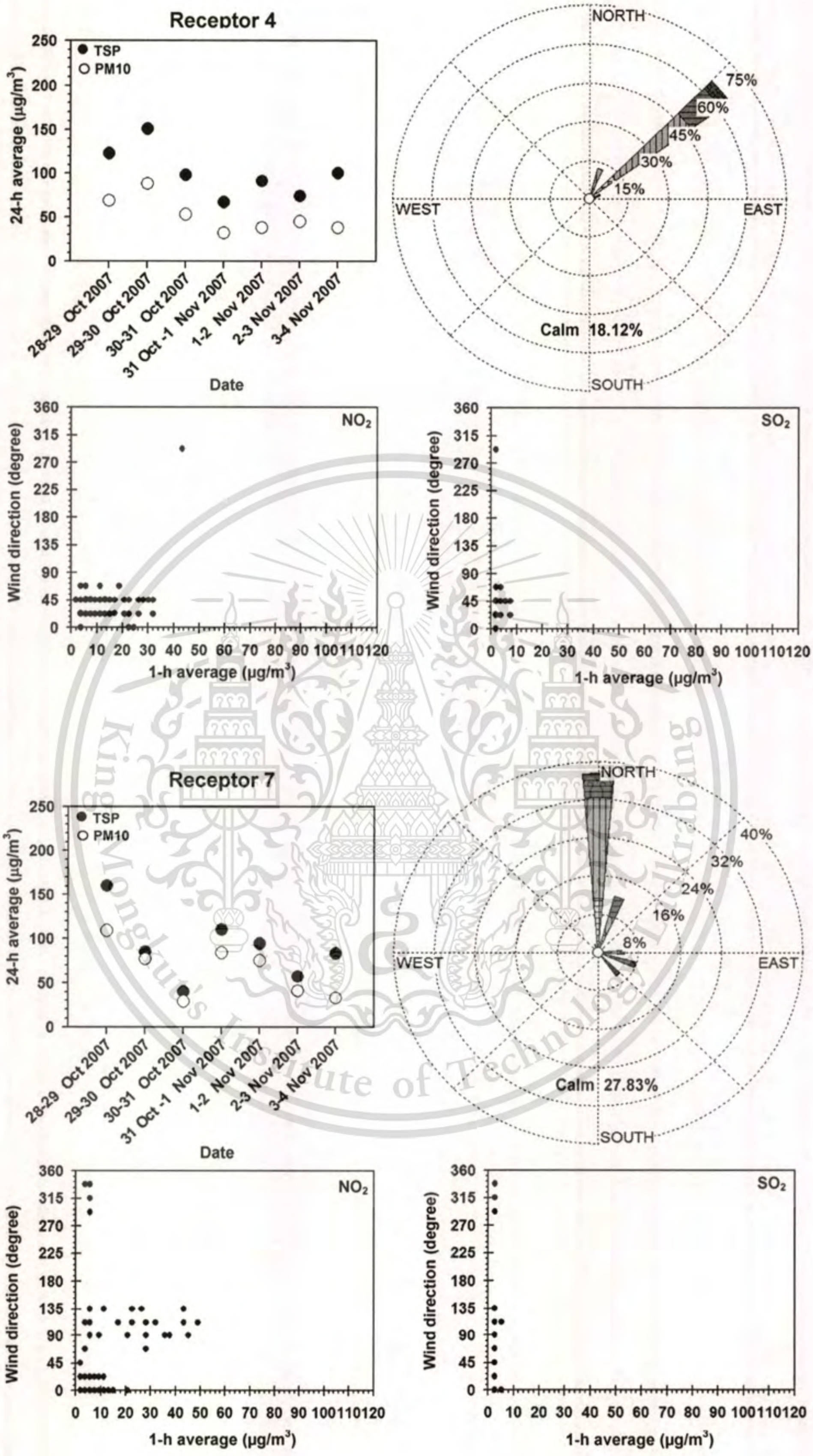

Figure 4.18 Group 3 receptors in the west of the domain in wet season.

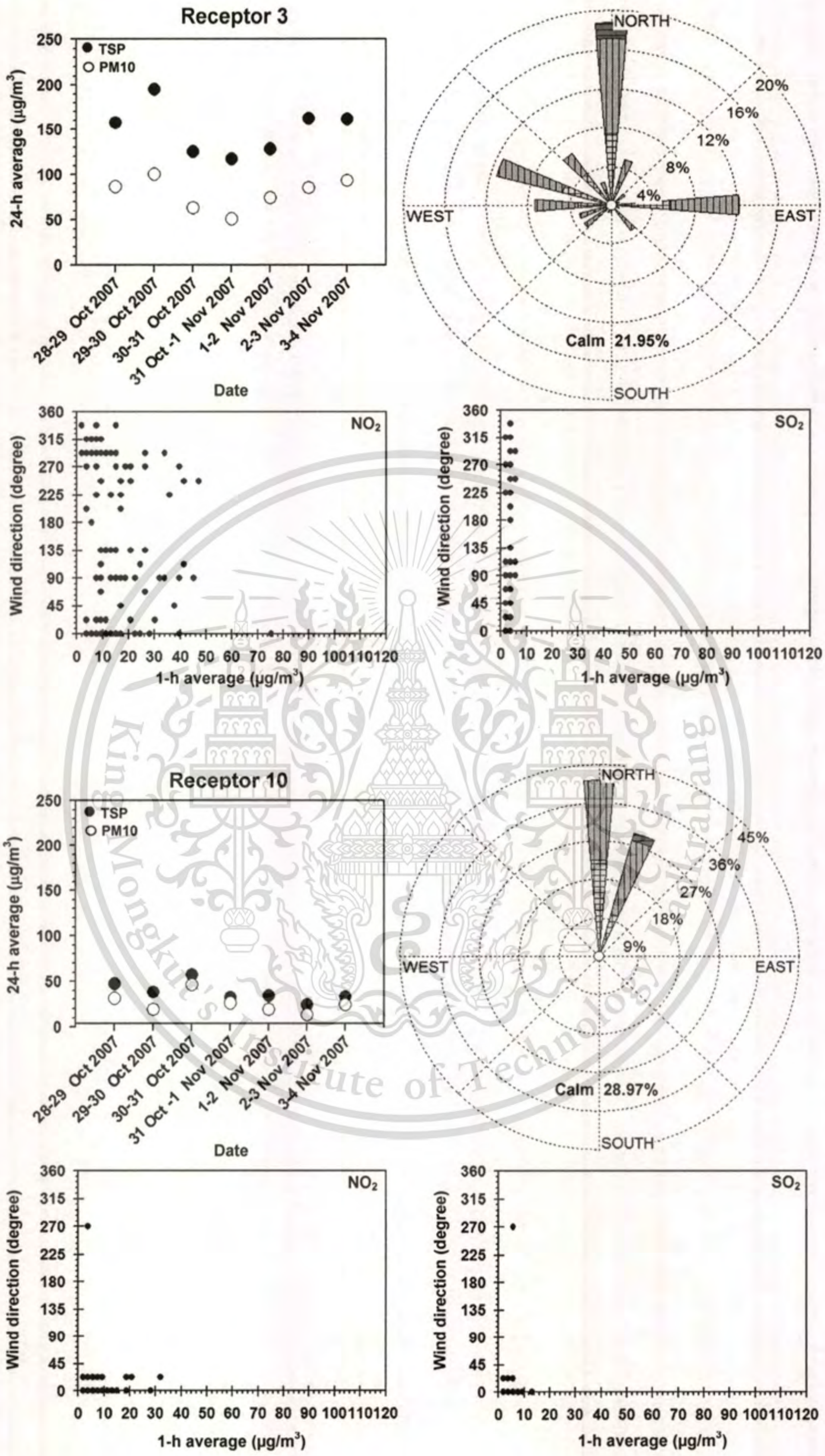

Figure 4.19 Group 3 receptors in the east of the domain in wet season.

4.3 SEM/EDX micrographs of particulate matter

Morphological observation and composition analysis of TSP and PM_{10} on fiber filters collected from the selected receptors of 12 receptors were analyzed by the SEM/EDX. The monitoring time and the selected receptors were in Table 4.13. The reference image of the fiber filter was shown in Figure 4.20. From Figures 4.21-4.22, TSP and PM_{10} particles were irregular shape and poorly-size-distributed. Yue et al. [106] classified the PM particles according to morphology and composition to spherical fly ash, chain-like soot aggregates, elongated particles, irregular-shaped mineral particles, cluster soot aggregates and pollen or spores as shown in Figures 4.23(a)-4.23(f). It can be seen that the TSP and PM_{10} nearby the cement manufacture agreed well with the images of spherical fly ash, irregular-shaped mineral particles and cluster soot aggregates as seen in Figures 4.23(a), 4.23(d) and 4.23(e).

Table 4.13 Monitoring time and receptors.

Receptors	Monitoring time
4	15th November 2007
7	13rd December 2007
10	13rd December 2007
11	15th November 2007

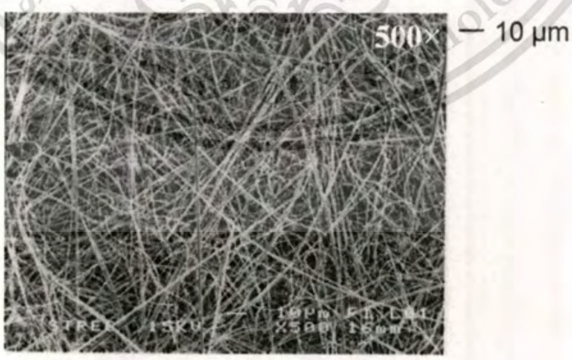

Figure 4.20 SEM micrograph of the reference fiber filter.

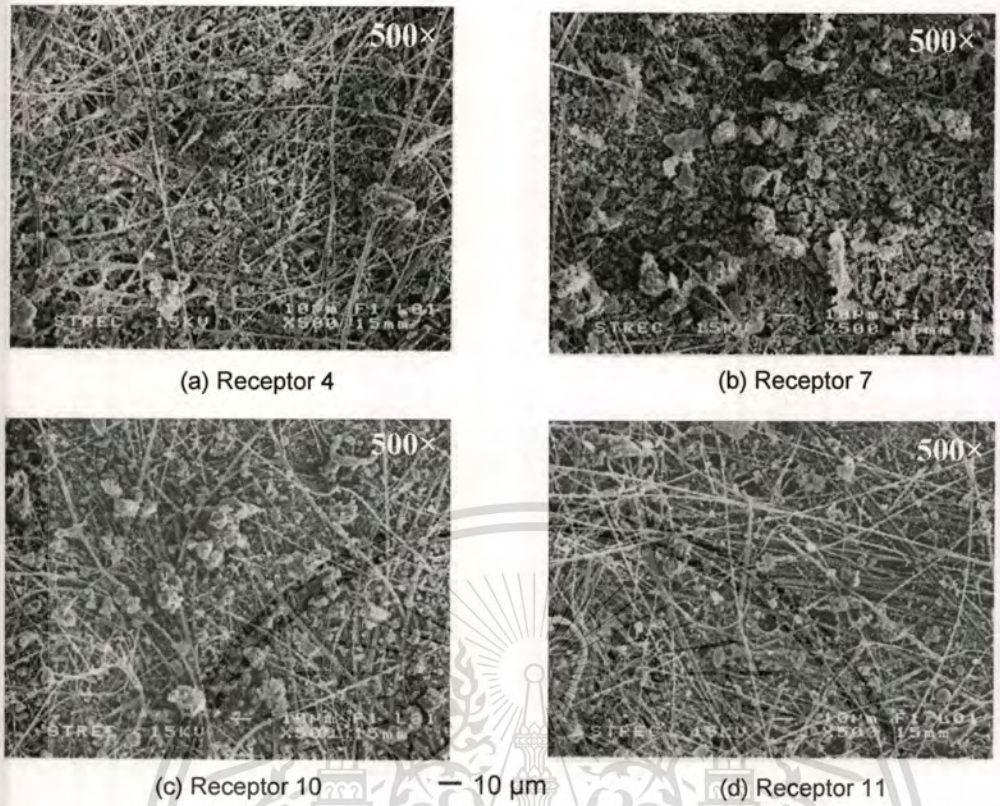

Figure 4.21 SEM micrographs of TSP.

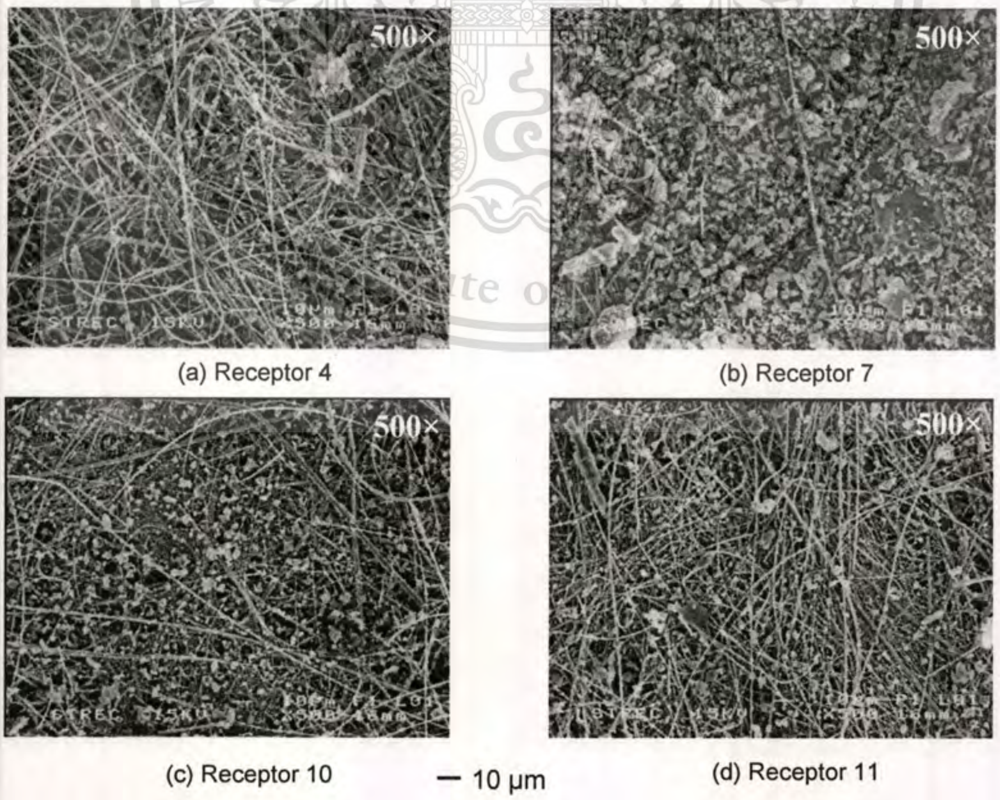

Figure 4.22 SEM micrographs of PM_{10}.

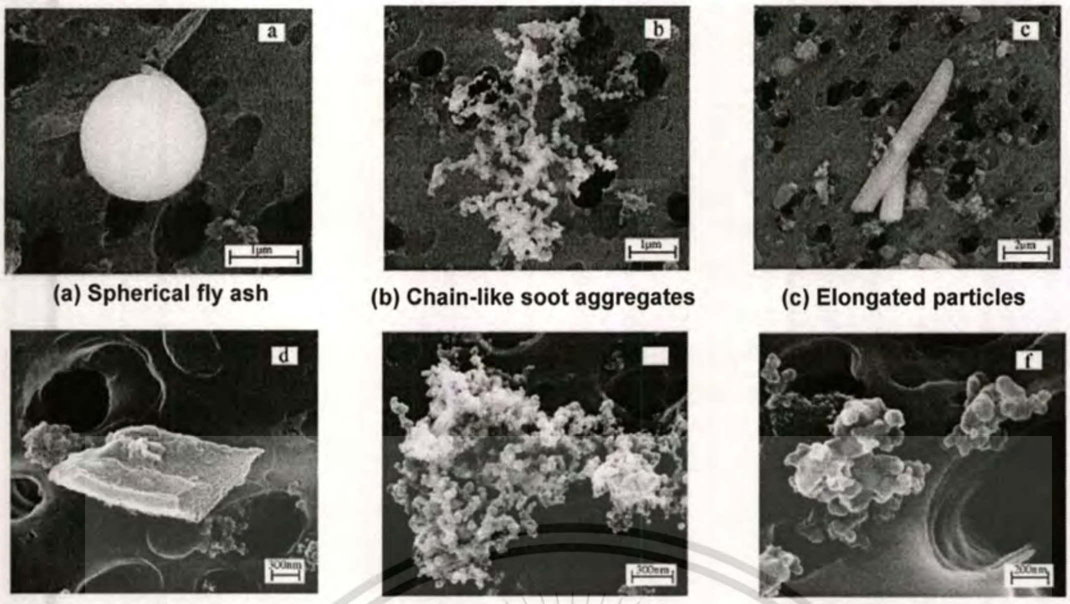

(a) Spherical fly ash (b) Chain-like soot aggregates (c) Elongated particles

(d) Irregular-shaped mineral particles (e) Cluster soot aggregates (f) Biological particles and fragments of pollen or spores

Figure 4.23 SEM micrographs of individual $PM_{2.5}$ [106].

Figures 4.24-4.25 show the elements in TSP and PM_{10} which were collected nearby the cement complex by the EDX. The elemental analysis of the TSP and PM_{10} can serve as a marker of the emitting sources (Table 4.14) [107]. For example, Ca is possible attained from cement industry, soil, and road dust. From the results both TSP and PM_{10} consisted of Al, Ca, Fe, K, Mg, Na, Si and Zn which were often available in raw materials of the cement production. The morphological and elemental analysis can presume that the cement industry is possible emission sources of TSP and PM_{10}, but cannot specify definitely from which cement plants that the TSP and PM_{10} emitted from as the 4 cement manufacturers are located near each other. The simulation by dispersion models can, therefore, help to specify the locations of the emissions.

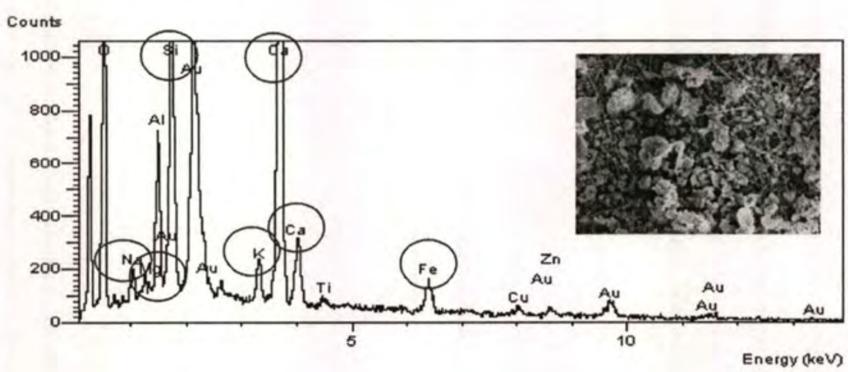

Figure 4.24 EDX result of TSP at receptor 7.

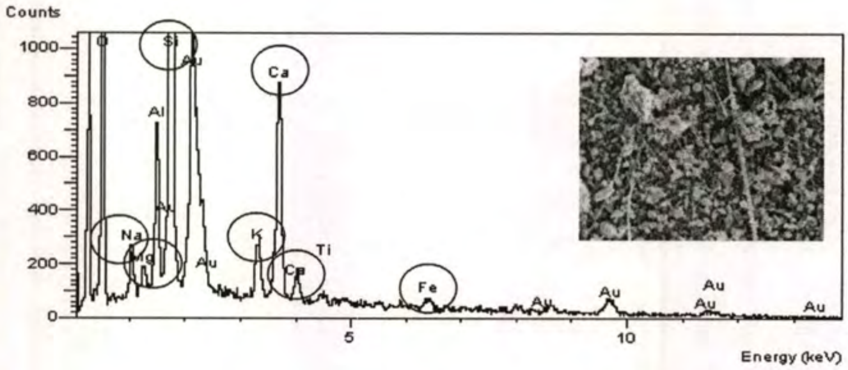

Figure 4.25 EDX result of PM_{10} at receptor 7.

Table 4.14 Marker elements associated with various emission sources [107].

Emission source	Marker element*
Cement industry	Ca
Coal burning	Al, Sc, Se, Co (Cobalt), As, Ti, Th, S
Iron and steel industries	Mn, Cr, Fe, Zn, W (Tungsten), Rb (Rubidium)
Non-ferrous metal industries	Zn, Cu, As, Sb, Pb, Al
Oil burning	V, Ni, Mn, Fe, Cr, As, S, SO_4^{2-}
Refuse incineration	K, Zn, Pb, Sb
Road dust	Ca, Al, Sc, Si, Ti, Fe, Sm
Soil	Al, Si, Sc, Ti, Fe, Sm, Ca

* Marker elements are arranged by priority order.

4.4 Meteorological factor analysis

Wind speed and direction, relative humidity, pressure, temperature, precipitation, ceiling height, cloud cover and global radiation were used to simulate the dispersion of pollutants by the AERMOD and CALPUFF in this study. The data from 4 stations in Saraburi and Lopburi (2 meteorological stations of the Thai Meteorological Department and 2 monitoring and meteorological stations of the Pollution Control Department) were analyzed.

4.4.1 Meteorological data

The meteorological parameters can enhance or diminish the dispersion of pollutants. Two types of meteorological measurements are classified based on the measurement from the ground level. The 'surface data' which directly impact human beings are 10-m measurement above ground level. The 'upper air data' are measured by launching balloon in the sky, recording the temperature and wind from ground level at different pressures from 1,000 to 100 hPa. Detailed results are as follows.

(1) Surface data

The surface data include wind speed and direction, relative humidity, pressure, temperature and global radiation. It is important that high percentage of data completeness is favorable for the AERMOD and CALPUFF. Missing data may cause some errors in simulation results by the model resulting in higher concentrations than the permits and must not report. The possible causes generating missing data are for example:

(i) the limitation of the instrument performance in detecting wind speed and direction, precipitation, etc.

(ii) the damage of instruments

(ii) shut down of station for instrument maintenance.

In this work, missing of one necessary surface data, i.e., wind speed and direction, relative humidity, pressure and temperature during the measuring period was counted as one 'missing data' for the AERMOD and CALPUFF simulations. Figure 4.26 shows the availability of surface data from NPL, KN, PC and LB stations over 90% in 2007. This indicated that the surface meteorological data from these stations were favorable for the AERMOD and CALPUFF. In case of any existing missing data during the simulation, it would be filled by the average of the non-missing values between the missing point.

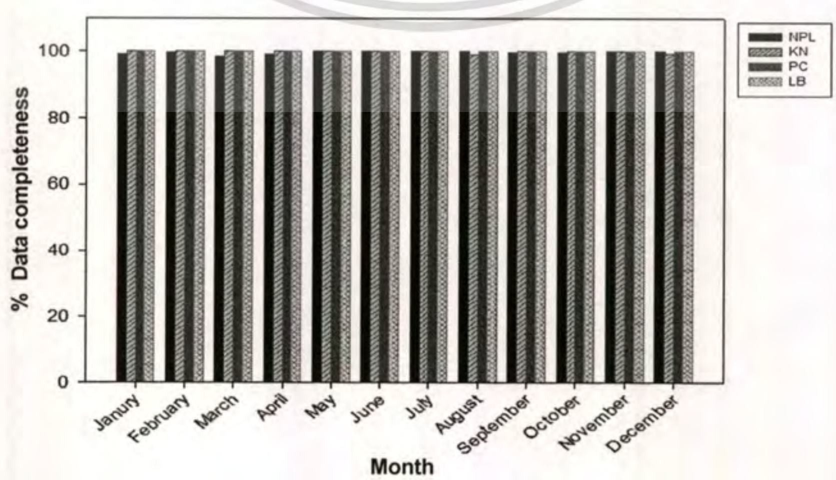

Figure 4.26 The coverage of surface meteorological data from 4 stations in 2007.

- Wind speed and direction

Wind speed and direction were analyzed by plotting of windrose using a software package of the ISC-AERMOD View version 4.6.2 from Lakes Environmental Software (WRPLOT view version 4.6.5). According to the windroses in the Figure 4.27, the maximum wind speeds at NPL, KN, PC and LB stations in 2007 were 5.8, 6.6, 15.4 and 8.8 m/s, while winds below the instrument sensitivity so-called calm winds were 11.29, 6.97, 45.27 and 72.71%, respectively. The dominant wind directions at NPL and KN stations were south-easterly and south-westerly winds. The PC station surrounding by the agriculture and mountain areas was dominated by the westerly and easterly winds. The LB station, 52-km northwest of the study areas, was dominated by the east-northeasterly and southerly winds.

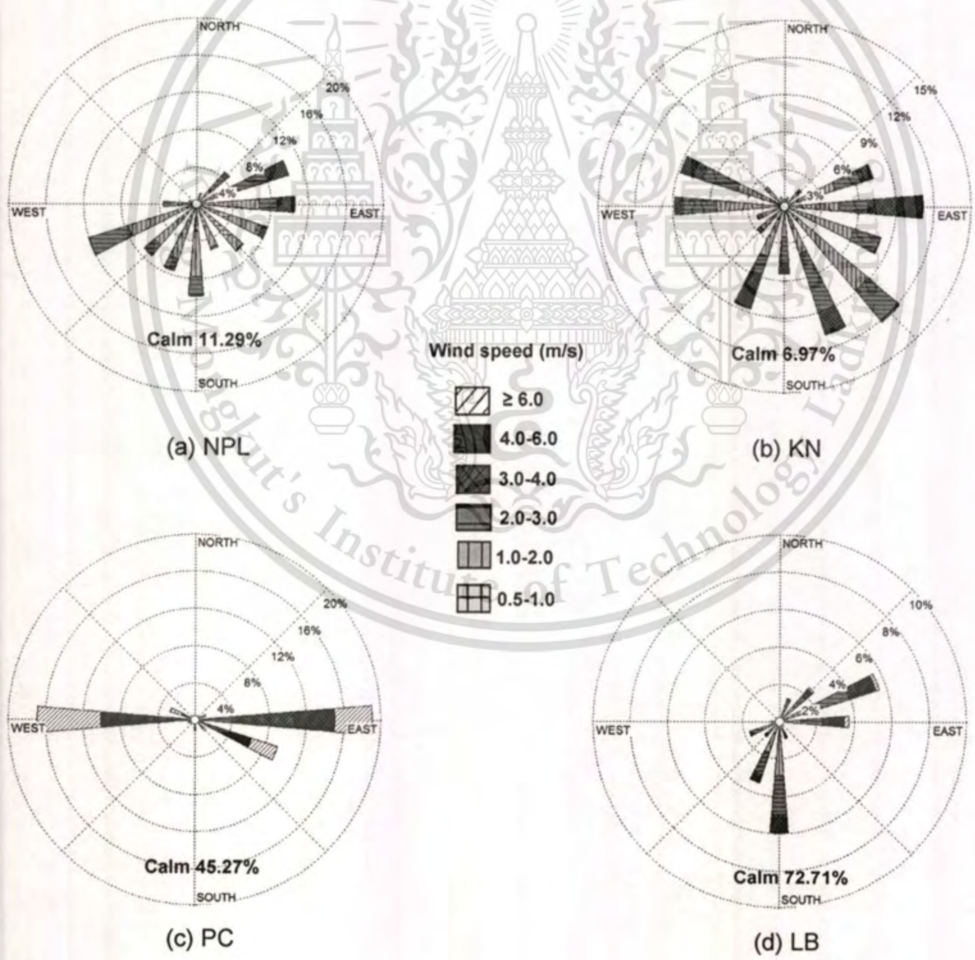

Figure 4.27 Windroses of 4 stations in 2007.

- Calm wind

One of the differences between the AERMOD and CALPUFF models was calm wind manipulation. The CALPUFF can use calm wind to simulate the pollutant concentrations, while the AERMOD cannot. Downwind concentration of the target pollutant from the AERMOD based on Gaussian plume equation (Equation 2.1) becomes infinity because the model defines calm wind at zero m/s. Low percentages of calm winds at NPL and KN stations in Figures 4.27-4.28 showed that the meteorological data at NPL and KN stations were suitable for the simulation.

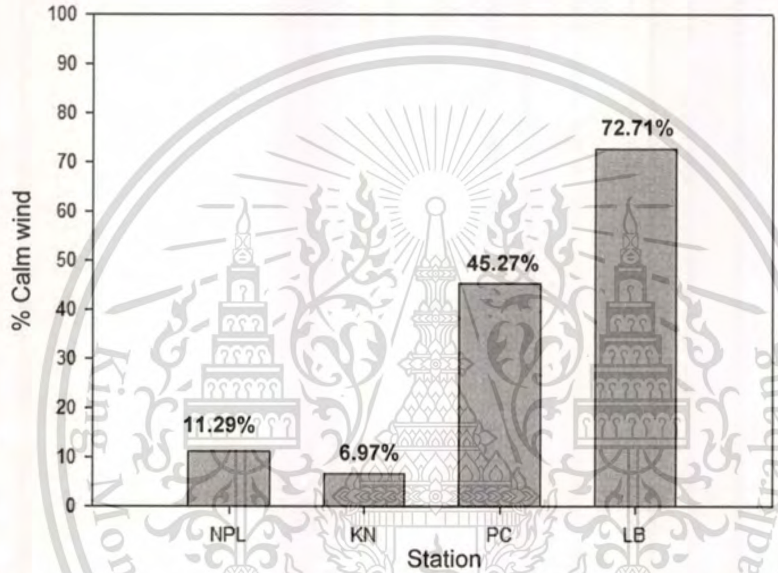

Figure 4.28 Percentages of calm winds at 4 stations in 2007.

- Rain precipitation

Rain precipitation relates to wet scavenging and deposition of pollutants. Rain precipitation at NPL, KN, PC and LB were measured in dry and wet seasons for model operation. Figure 4.29 show monthly rain precipitation which in accordance that dry months are January to April and November to December but wet months are May to October.

(2) Upper air data

The upper air data for model simulation in this study includes wind speed and direction, and temperature at a pressure of 1,000-100 hPa. The percentage of completeness of upper air data at Bang Na meteorological station in 2007 was higher than 95%, as seen in Figure 4.30. This indicated that the upper air data at Bang Na station were sufficient to run the AERMOD and CALPUFF. The upper air data at Bang Na station were recorded once a day at 7 am (0 UT). The missing data at 12 UT were used the data at 7 am by assuming a constant profile. Table 4.15 illustrates the missing upper air data at Bang Na station in 20 days of 2007 and their adjustments.

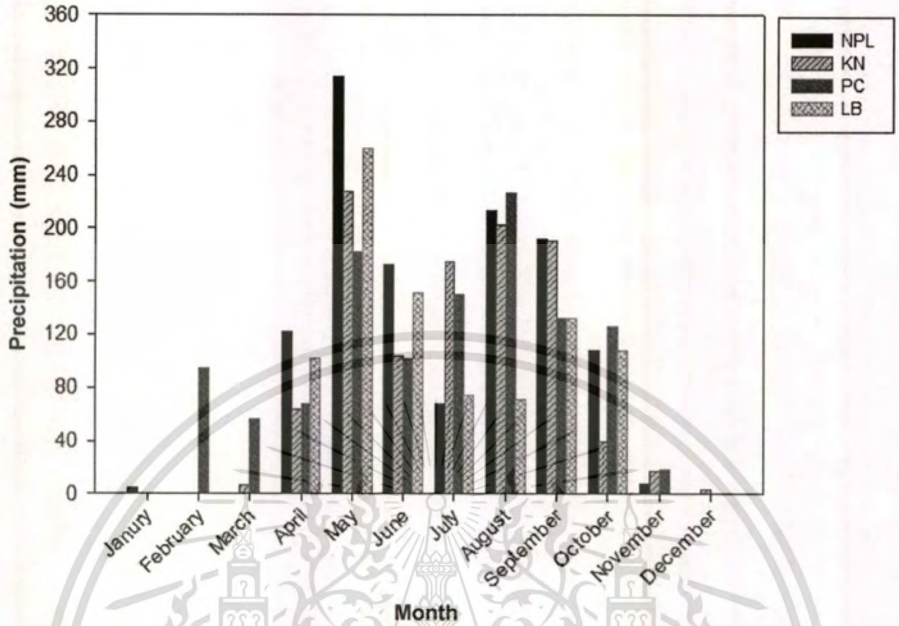

Figure 4.29 Monthly rain precipitation data in 2007.

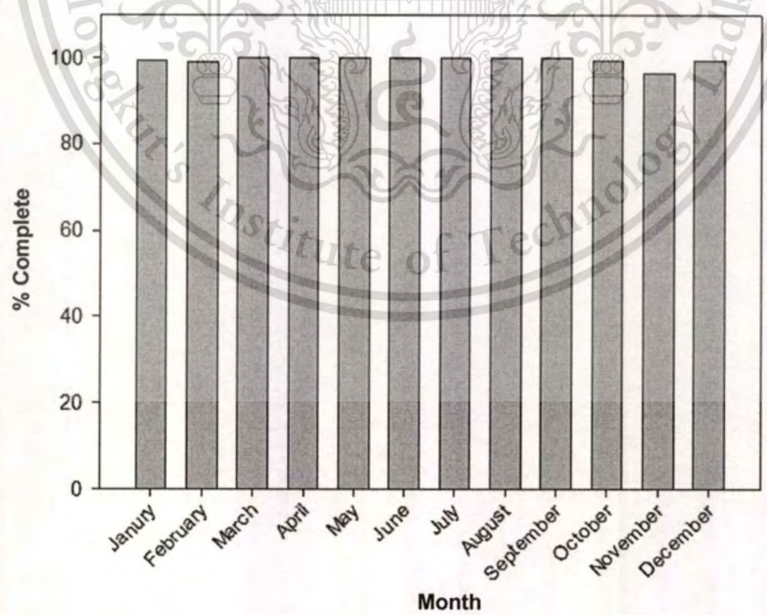

Figure 4.30 The coverage of upper air data at Bang Na station in 2007.

Table 4.15 Information of missing upper air data at Bang Na station and the adjustments.

Date	Time	Type of missing data	Adjustment
1st January 2007	12 am	all	Taken from 31st December 2006
2nd January 2007	12 am	all	Taken from 3rd January 2007
1st February 2007	12 am	WS, WD at pressure of 149, 145, 142, 137, 129, 123 hPa	-
7th February 2007	12 am	WS, WD at pressure of 200, 150, 100 hPa	-
13rd February 2007	12 am	all	Taken from 12 nd February 2007
12 nd October 2007	12 am	all	Taken from 11st February 2007
2nd November 2007	12 am	all	Taken from 1st November 2007
13rd-23rd November 2007	12 am	all	Taken from 13 rd-23rd November 2006
25th November 2007	12 am	all	Taken from 24th November 2007
23rd December 2007	12 am	all	Taken from 22nd December 2007

4.4.2 Meteorological outputs from the CALMET

CALMET is a meteorological module for preparing the hour-by-hour meteorological data and the hourly surface wind patterns in the study areas to run the CALPUFF.

(1) Model validation

The outputs of the CALMET were verified by the scatter plots of the simulated meteorological parameters against their measurement. Table 4.16 shows the number of wind speeds, wind directions and temperatures at 3 stations for the scatter plots. The middle line of the scatter plots shows equal values of the measurement and the simulation. The other two lines (below and above the middle line) marks half and double levels of the measurement and the simulation. They show half-under and double-over predictions, respectively. If most or all of the measured data are in line with the middle line of the scatter plots, it indicates that the simulation by the CALMET is reliable. In this work, the CALMET was run under two conditions with and without rain precipitation input data.

Table 4.16 Number of input data for the scatter plots.

Meteorological stations	Number of data taken to plot (hours)		
	Wind speed	Wind direction	Temperature
NPL	8,641	8,640	8,658
KN	8,745	8,672	8,758
PC	4,793	4,794	8,760

For the simulation without rain precipitation, most of the measured and simulated temperatures in 2007 at 3 stations were on the middle line as shown in Figure 4.31. This is clear that the CALMET can simulate the temperature very well. The scatter plots of measured and simulated wind speeds and wind directions in Figures 4.32-4.33 from about 8,600 data (Table 4.16) showed a few under and over estimations at NPL and KN stations but good estimation at PC station.

In case the simulation with rain precipitation, the 1-hour averaged rain records from NPL and KN stations were used in simulation, not 3-h averaged rain record at PC station. Detailed data can avoid the error in simulation. About 100-120 days in the study areas were rainy days (Table 4.17). The scatter plots of temperatures, wind speeds and wind directions in Figures 4.34-4.36 were found to be similar to those without rain precipitation. From this work it is worth to note that rain precipitation does not much affect the simulations of temperatures, wind speeds and wind directions. As a result, the meteorological simulated outputs from the CALMET were verified for running the CALPUFF.

Table 4.17 Number of rainy days.

Meteorological stations	Number of rainy days (days)
NPL	118
KN	101
PC	114

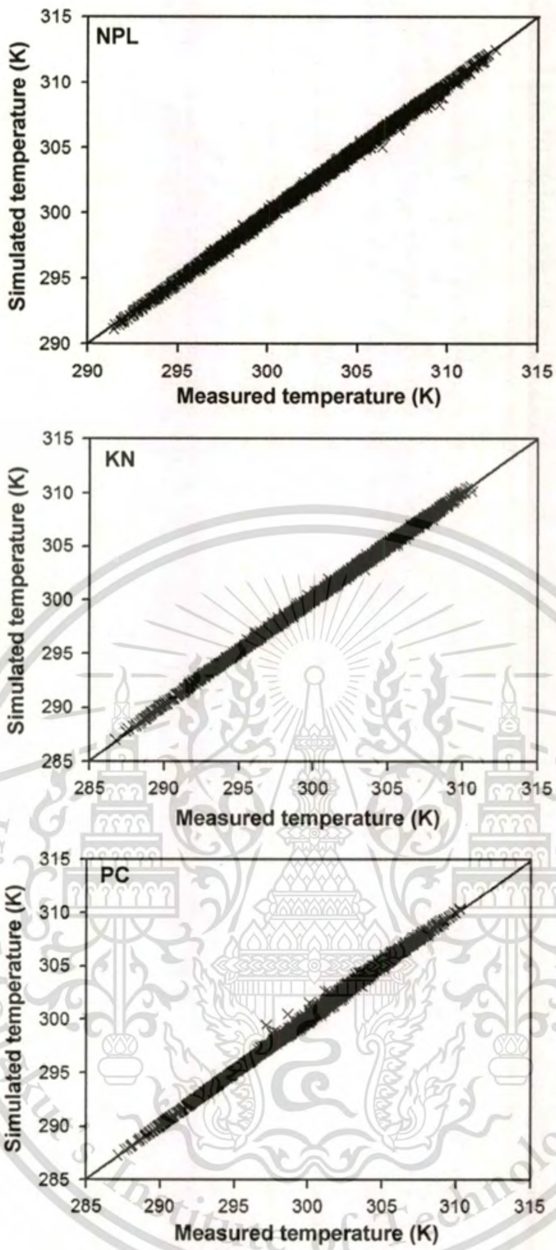

Figure 4.31 Scatter plots of simulated and measured temperatures at 3 stations without rain precipitation in 2007.

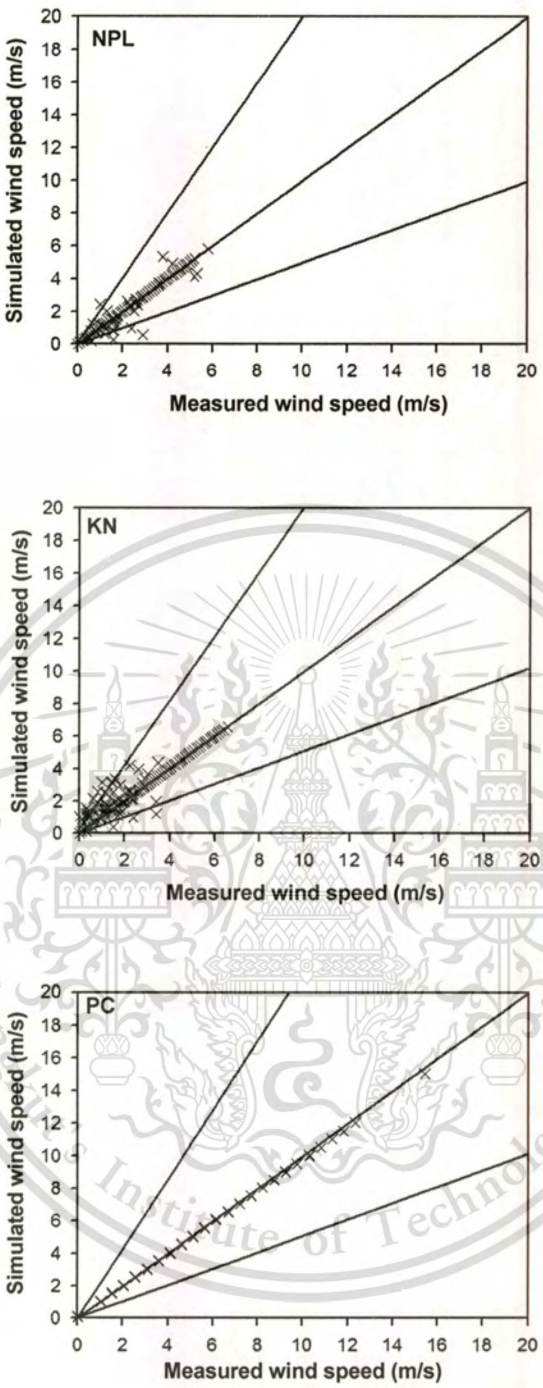

Figure 4.32 Scatter plots of simulated and measured wind speeds at 3 stations without rain precipitation in 2007.

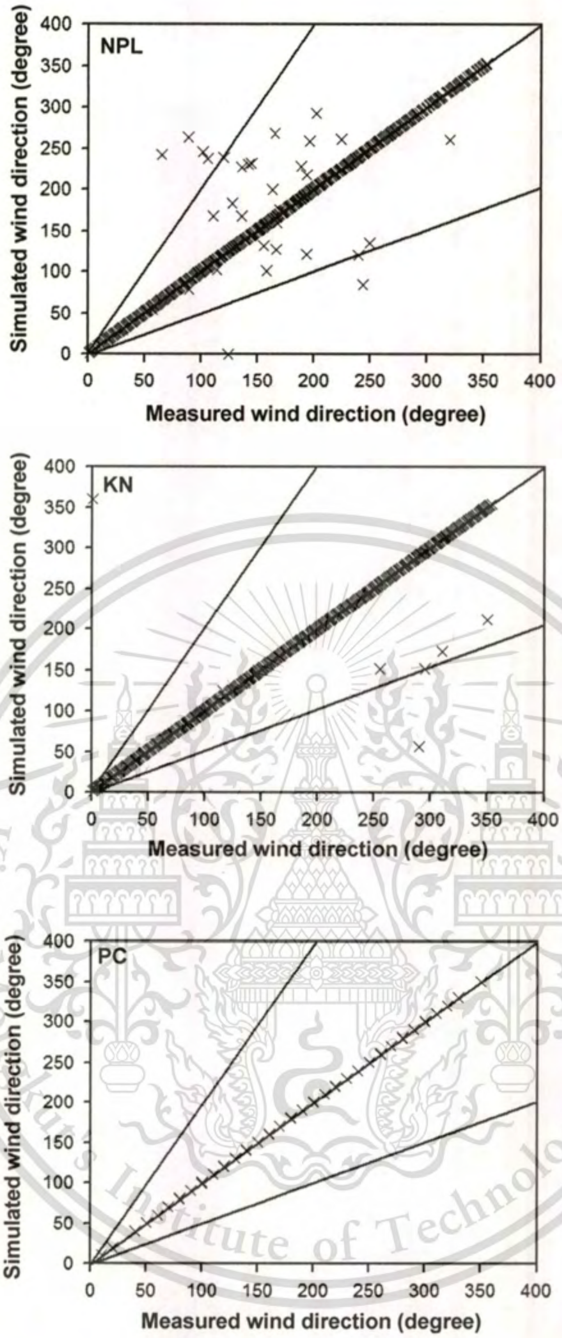

Figure 4.33 Scatter plots of simulated and measured wind directions at 3 stations without rain precipitation in 2007.

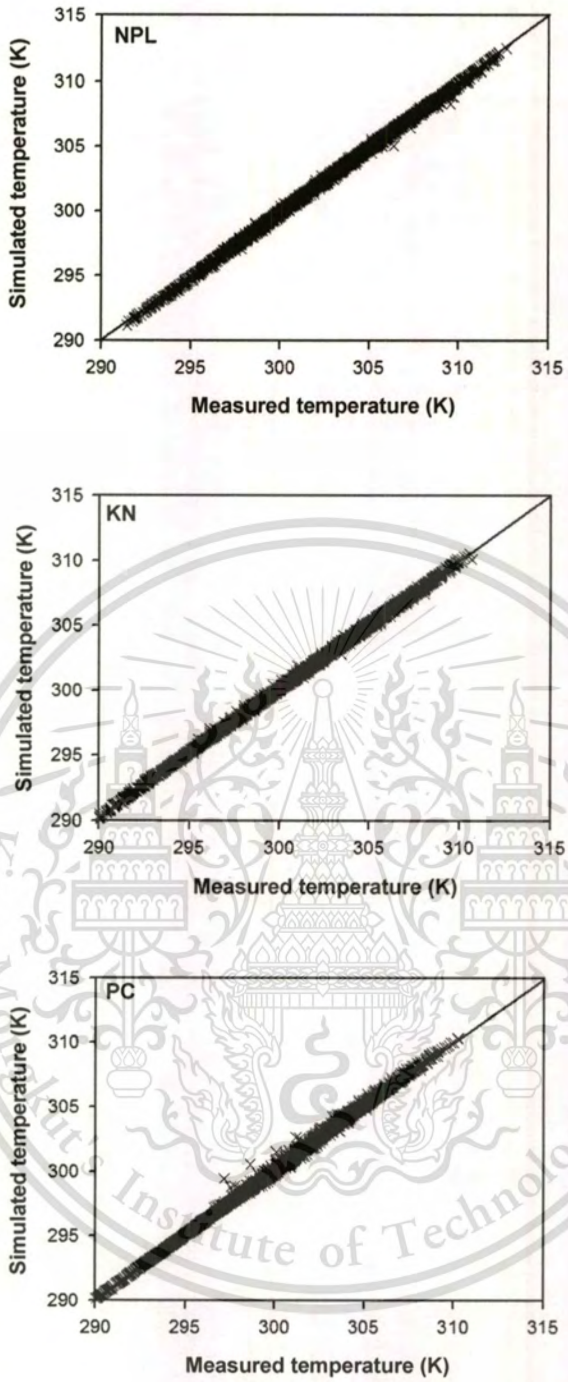

Figure 4.34 Scatter plots of simulated and measured temperatures at 3 stations with rain precipitation in 2007.

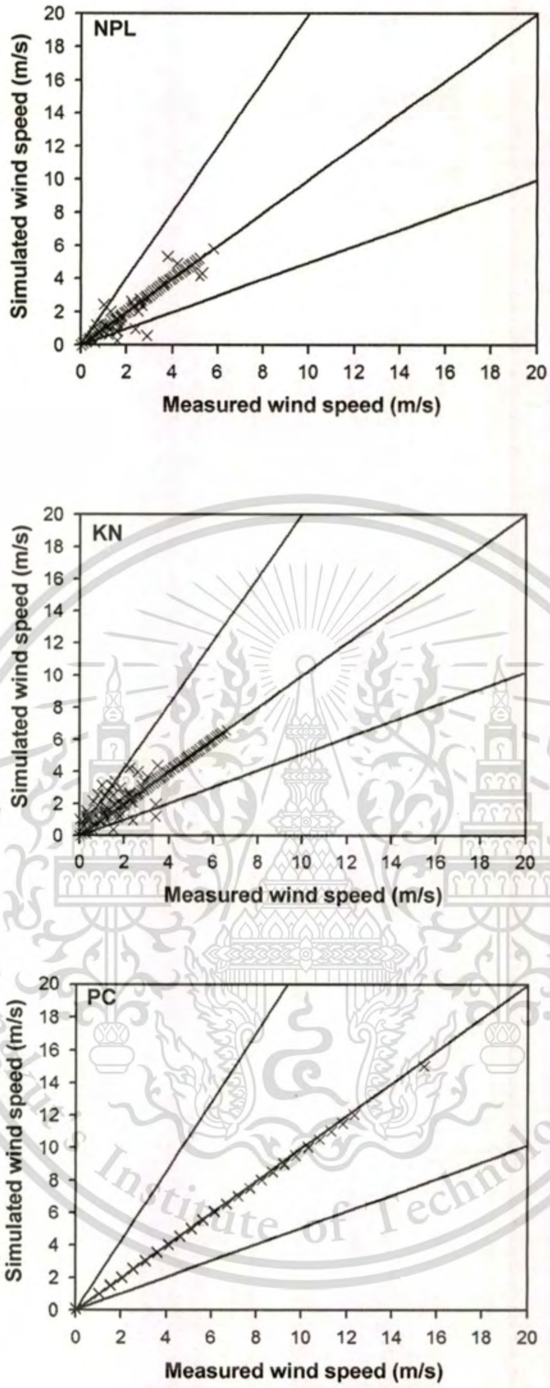

Figure 4.35 Scatter plots of simulated and measured wind speeds at 3 stations with rain precipitation in 2007.

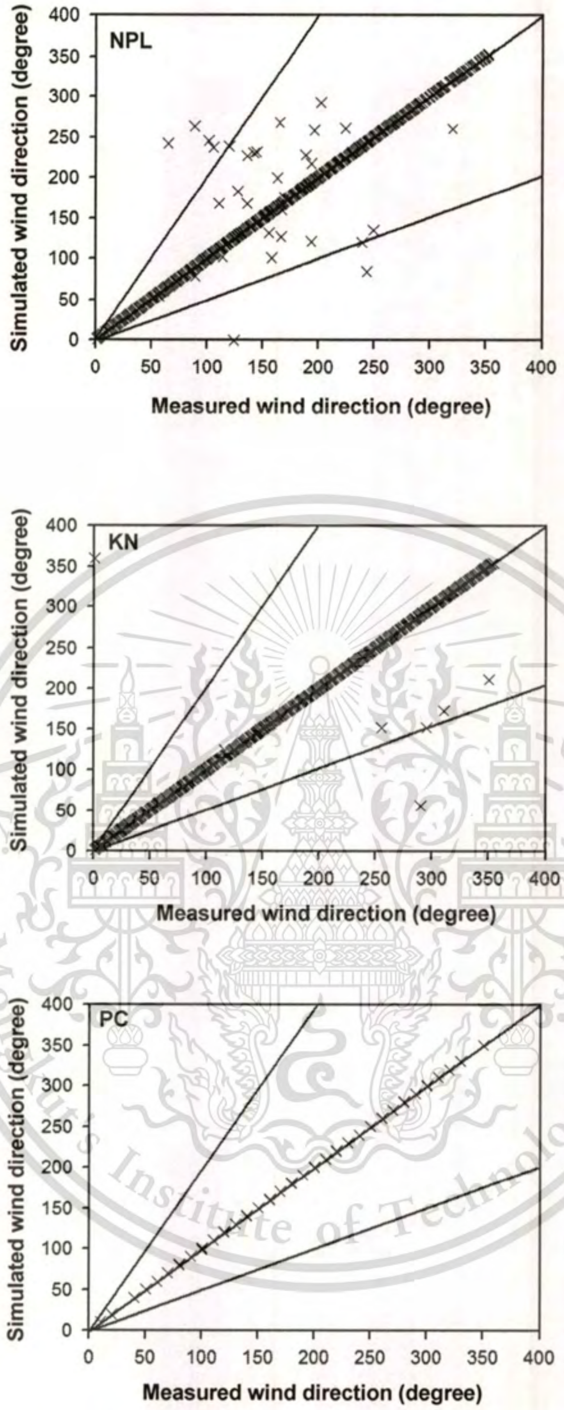

Figure 4.36 Scatter plots of simulated and measured wind directions at 3 stations with rain precipitation in 2007.

(2) Wind field analysis by the CALMET

The overall of wind speed and direction in the study areas can be viewed and explained by the wind field by the CALMET. The surface wind field of 1-hour averaged wind speed and 1-

hour averaged wind direction is generated by the measured surface meteorological data (10-m above the ground level from NPL, KN and PC stations) and the measured upper meteorological data from Bang Na station. Figures 4.37 and 4.38 show surface wind fields in dry season on 2nd March 2007 and in wet season on 4th November 2007, respectively.

As mentioned earlier, dry season is influenced by the northeast monsoon. From Figure 4.37, it can be seen that at the 1st hour the winds on the flat area partially blew to the southeast while at the same time different direction from the mountain areas to the flat terrain was observed. From the 4th to 10th hours the winds blew from flat terrain to mountain area in the east direction. The wind fields at the 13rd hour were similar to those of the 1st hour. Subsequently, in the 16th hour the winds blew from the mountain areas to the lower area. In the 19th to 22nd hours, the winds blew from the flat terrain to the mountain areas as well as from the mountain areas to the flat terrain.

In case of wet season, the plateau is influenced by the southwest monsoon. The wind field patterns are shown in Figure 4.38. From the 1st to 22nd hours, the winds blew from mountain areas to flat terrain all day. More wind field plots in dry season on 24th March 2007 and in wet season on 12nd October 2007 are shown in Appendix E.

In summary, the wind distribution in the study areas was not uniform. It was obvious that the seasonal winds (northeaster and southwester monsoons) and local circulation significantly affected the wind field patterns in the study areas. In the dry season (March), the simulated wind on the top of the mountains followed the seasonal wind, i.e. northeaster monsoon, while in the valley the wind followed the terrain effect and solar elevation angle contribution to the ground heat flux during the whole day [65].

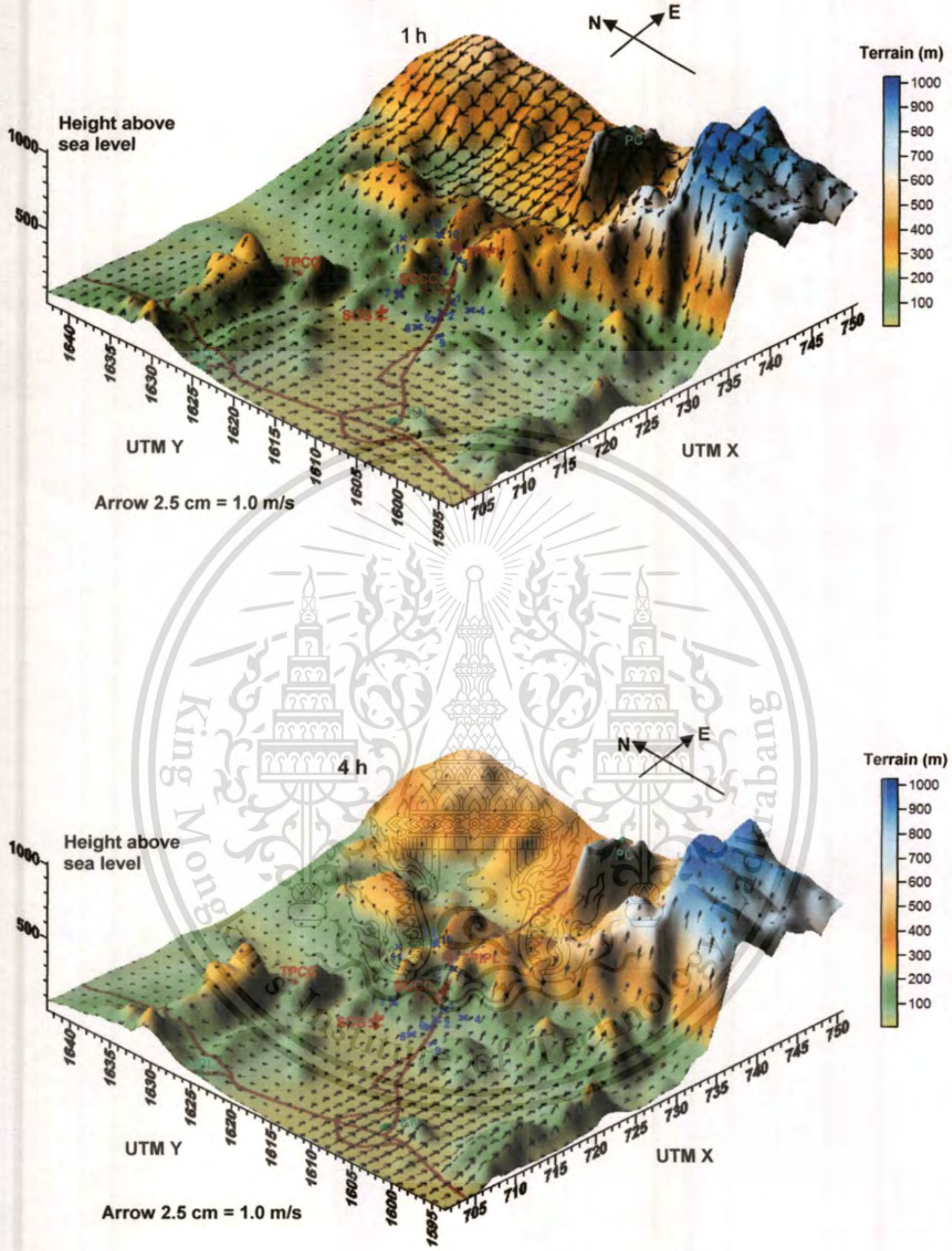

Figure 4.37 Surface wind field simulated by the CALMET on March 2, 2007: (●) meteorological stations, (+) receptors and (×) stacks of cement plants.

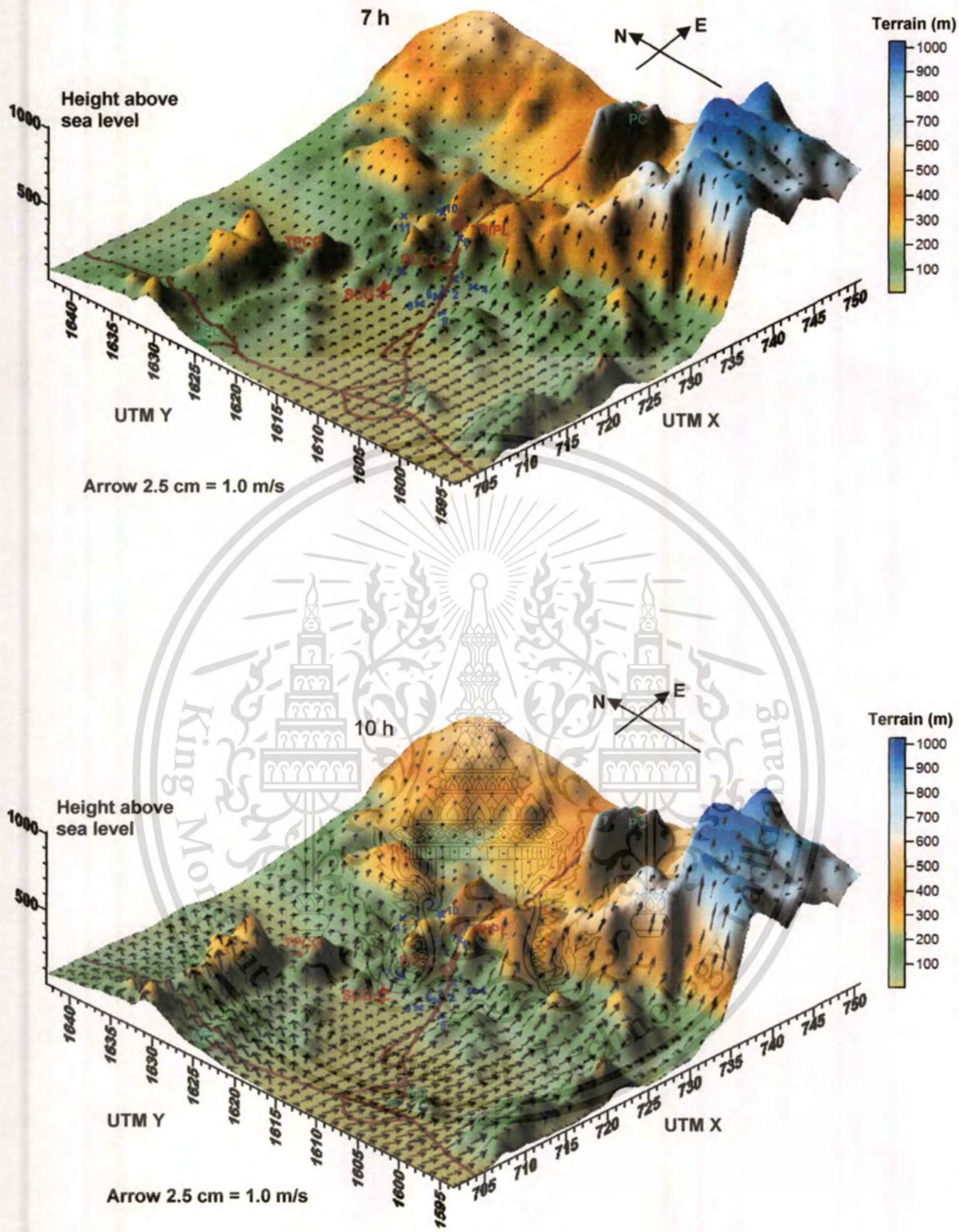

Figure 4.37 Surface wind field simulated by the CALMET on March 2, 2007: (●) meteorological stations, (+) receptors and (×) stacks of cement plants (cont.).

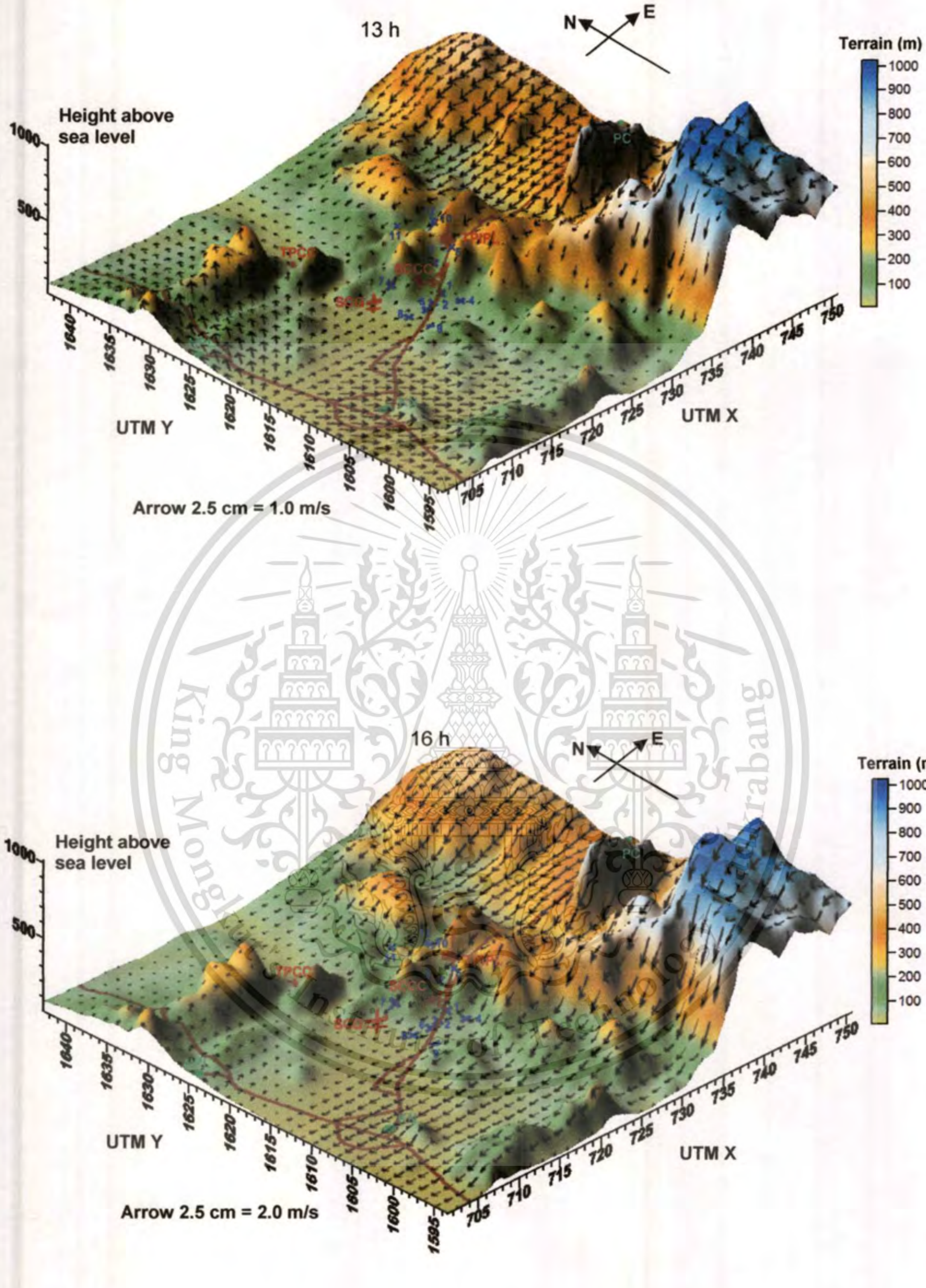

Figure 4.37 Surface wind field simulated by the CALMET on March 2, 2007: (●) meteorological stations, (+) receptors and (×) stacks of cement plants (cont.).

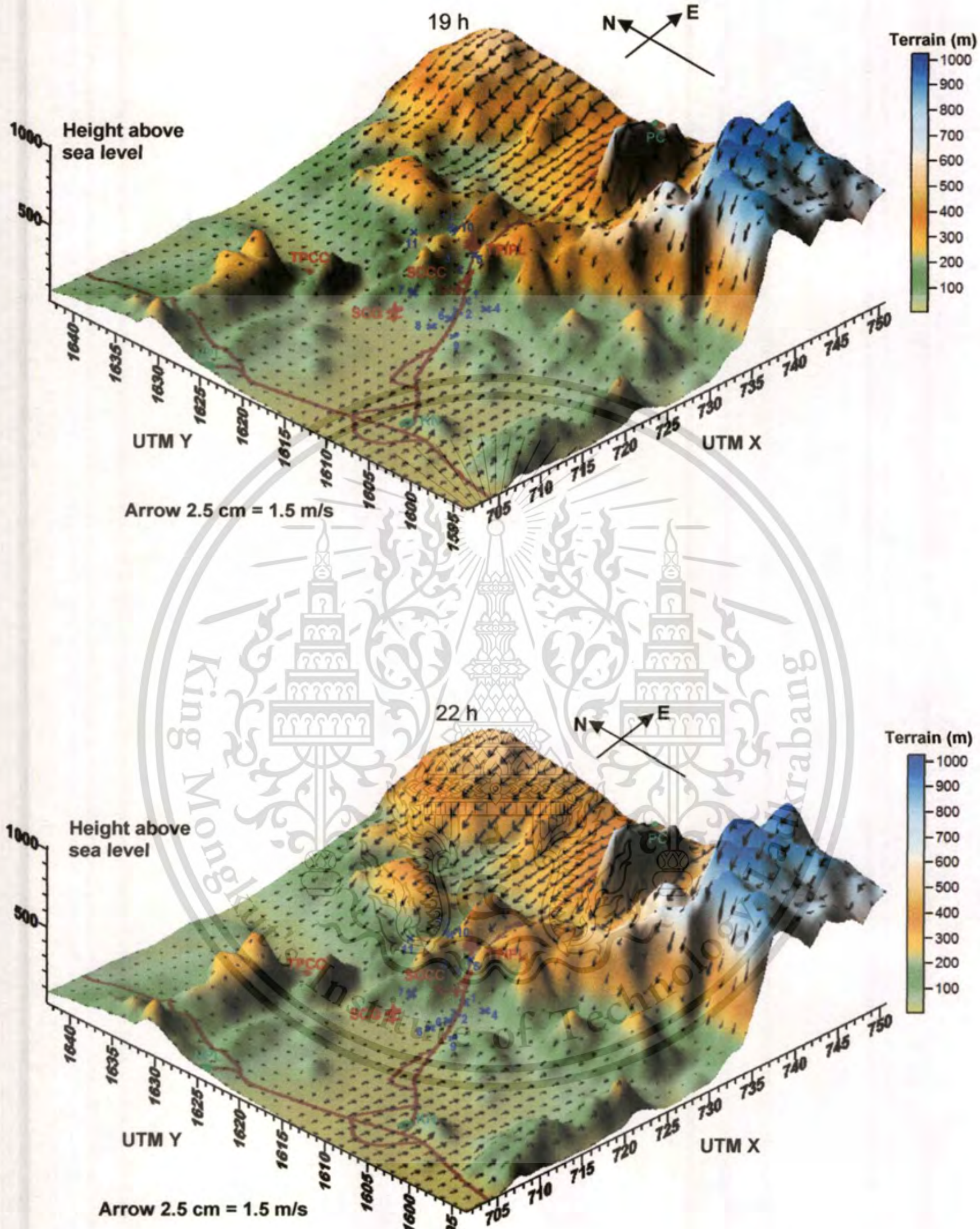

Figure 4.37 Surface wind field simulated by the CALMET on March 2, 2007: (●) meteorological stations, (+) receptors and (×) stacks of cement plants (cont.).

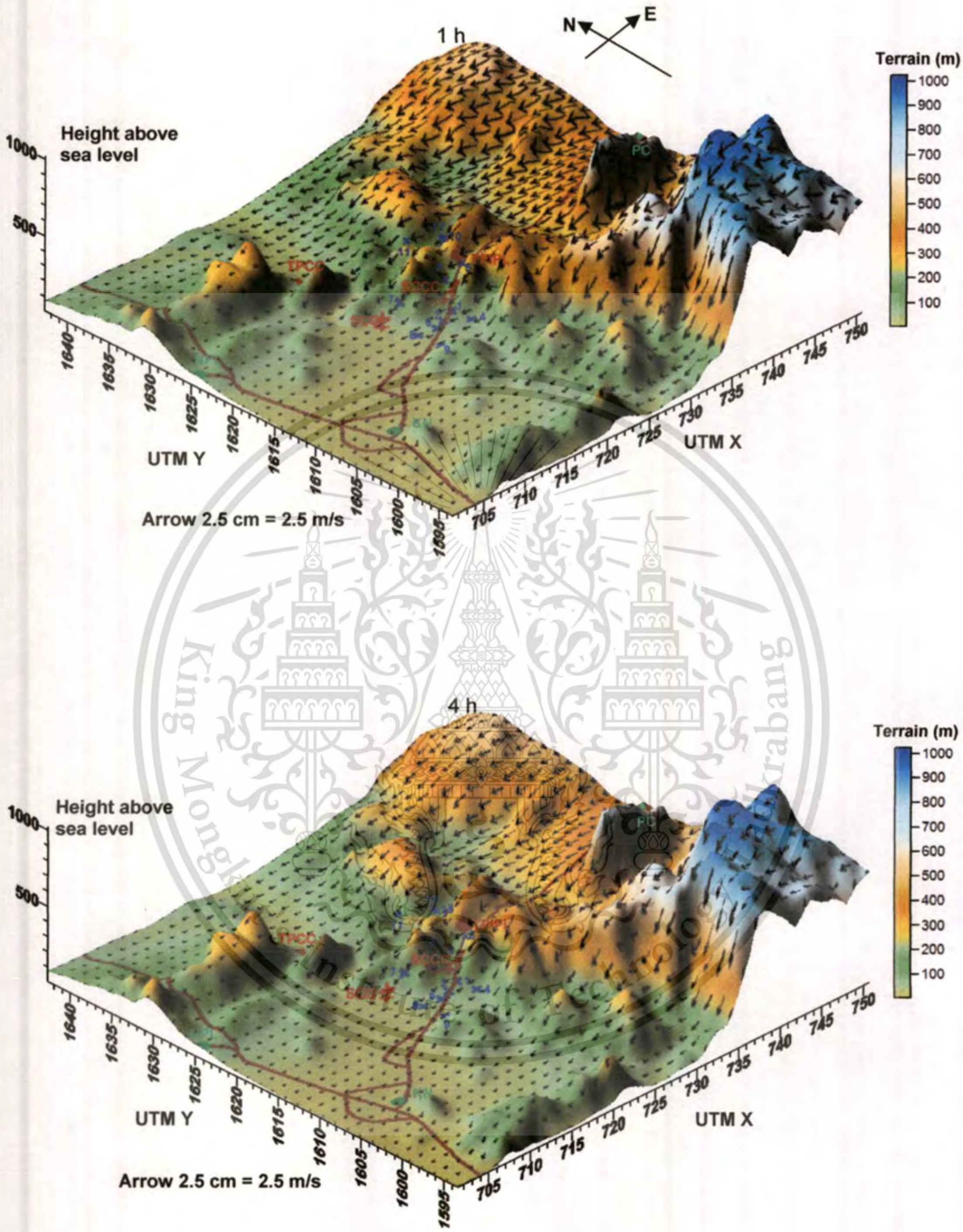

Figure 4.38 Surface wind field simulated by the CALMET on November 4, 2007: (●) meteorological stations, (+) receptors and (×) stacks of cement plants.

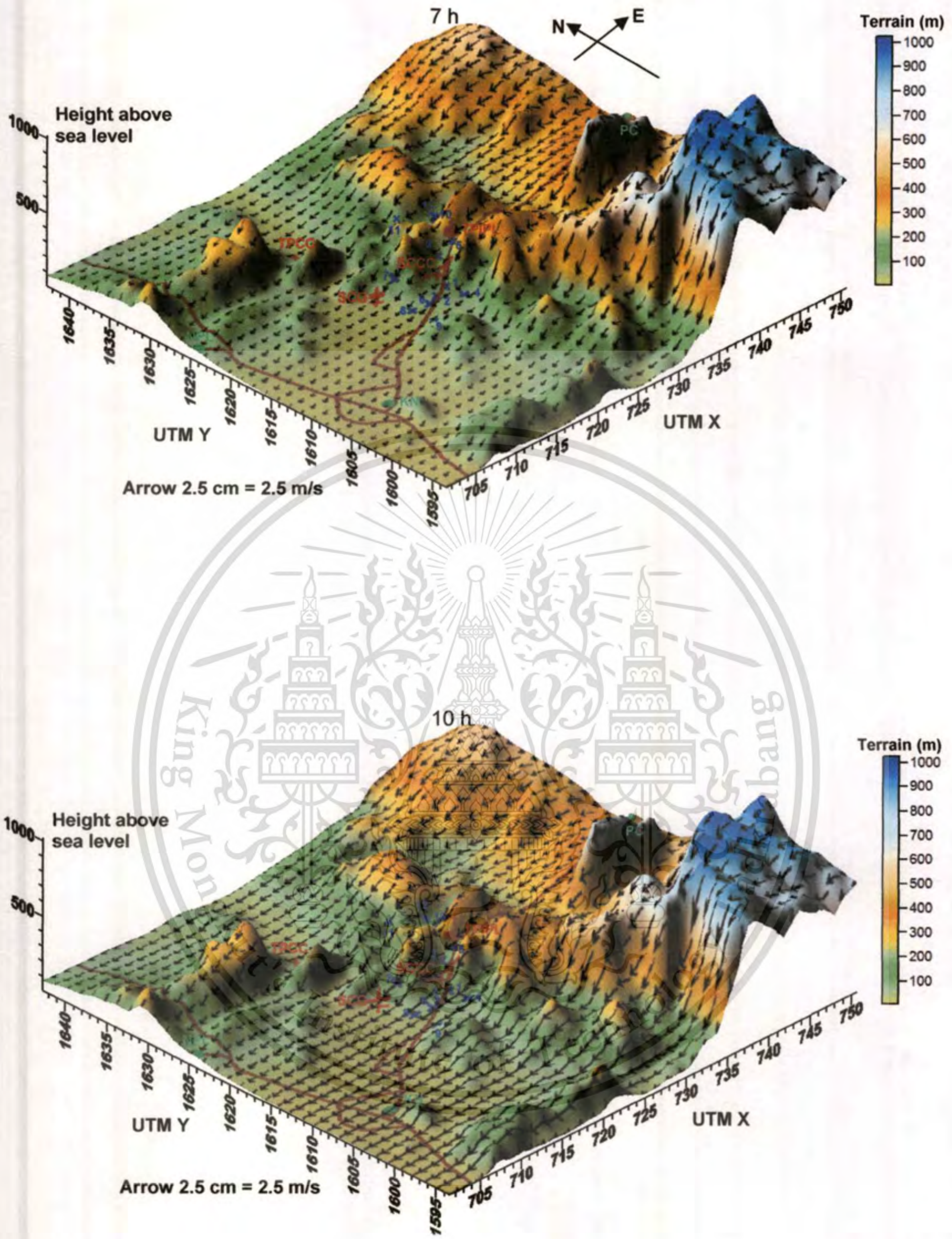

Figure 4.38 Surface wind field simulated by the CALMET on November 4, 2007: (●) meteorological stations, (+) receptors and (×) stacks of cement plants (cont.).

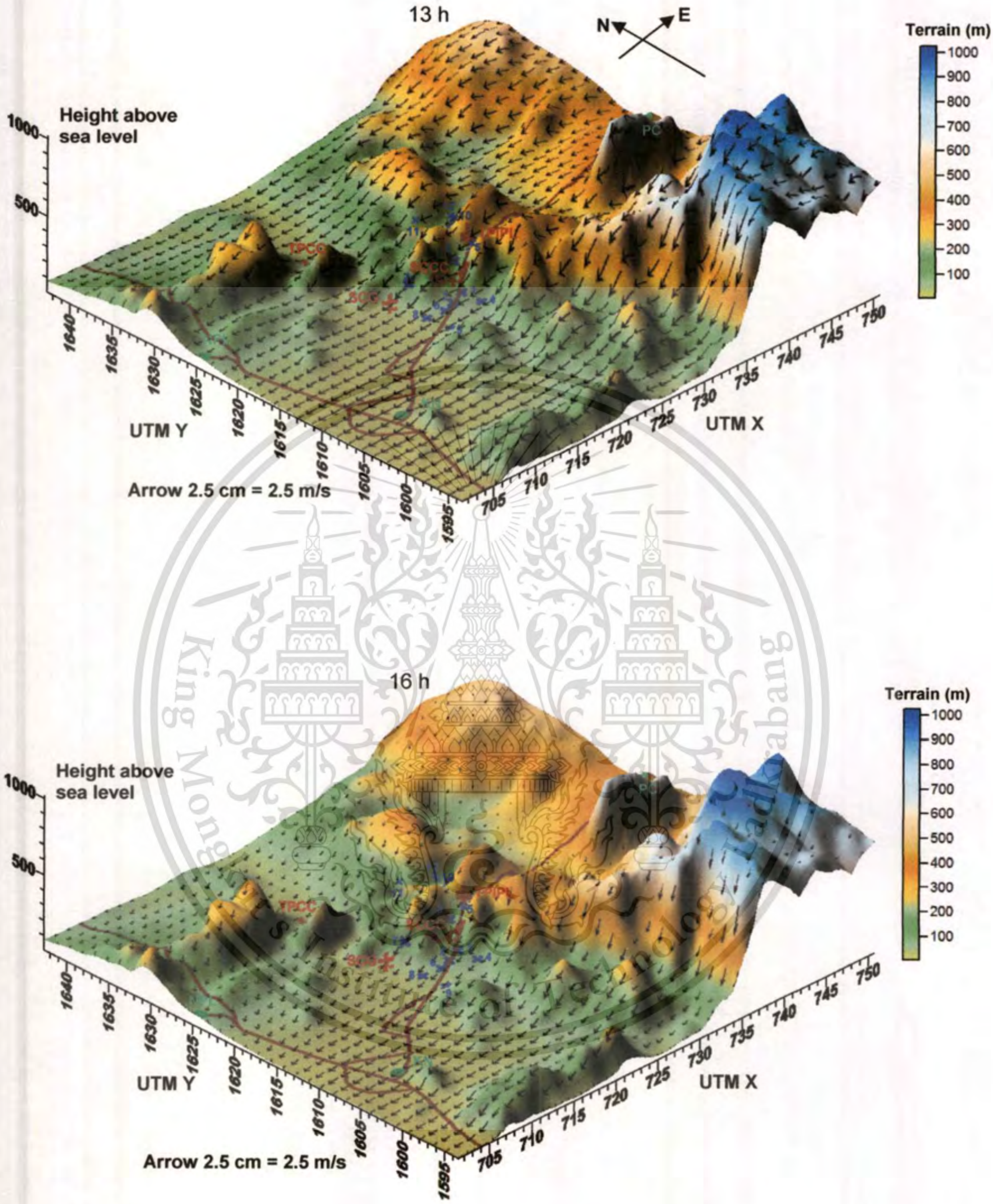

Figure 4.38 Surface wind field simulated by the CALMET on November 4, 2007: (●) meteorological stations, (+) receptors and (×) stacks of cement plants (cont.).

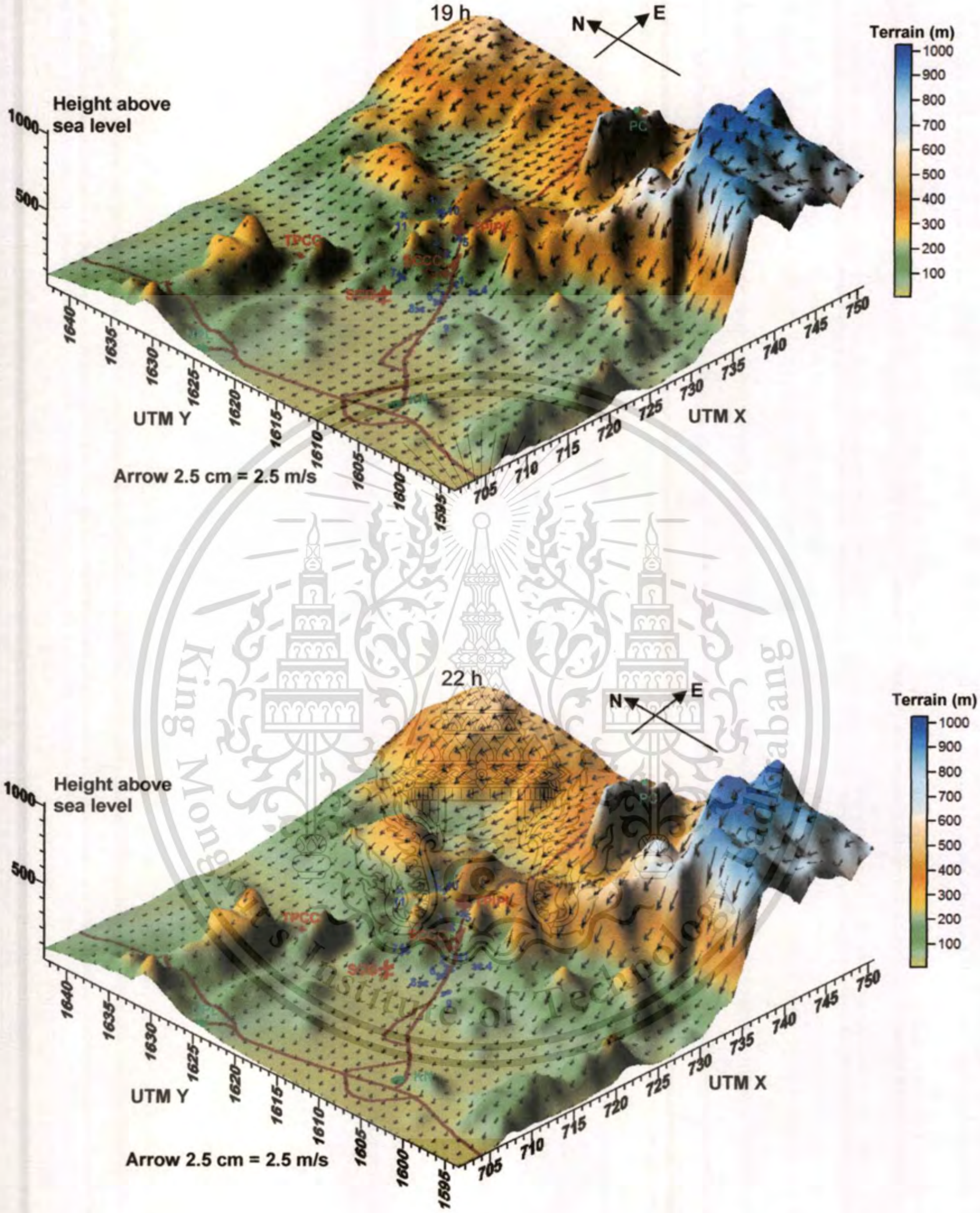

Figure 4.38 Surface wind field simulated by the CALMET on November 4, 2007: (●) meteorological stations, (+) receptors and (×) stacks of cement plants (cont.).

4.5 Estimation results of air pollutants

This section demonstrates the simulation results of 1-hour and 24-hour averaged concentrations of PM_{10}, NO_2 and SO_2 by the AERMOD and CALPUFF on the Cartesian receptor grid and discrete grid (at 2 semi-permanent monitoring stations and 12 receptors (non-permanent monitoring stations)).

4.5.1 Estimation of air pollutants by the AERMOD

The AERMOD is an easy-operated software program compared to the CALPUFF. Different versions of the AERMOD are widely used in Thailand for the EIA from point sources because the AERMET, a meteorological model in the AERMOD, requires the surface data from only 1 station inside or outside the study domain. The commercial AERMOD versions have been developing continuously to support the requirements of the users, e.g., providing a module to estimate the upper air data in the AERMET in case no measured upper air data are available. The different versions are claimed much easier than a free version by the U.S.EPA. The following simulation results are compared between 2 commercial versions (AERMOD 4.6.2 and AERMOD 5.4).

(1) Sensitivity of period averaged meteorological data to the AERMOD prediction

In this part the sensitivities of sources of 1-hour and 3-hour averaged meteorological input data from 4 stations of the Pollution Control Department (NPL and KN stations) and Thai Meteorological Department (PC and LB stations), shown in Table 4.18, were reported. The PC station is 25 km in the east of the reference point and the LB station is about 52 km to the west. To avoid the effect of wet deposition, the AERMOD version 4.6.2 was run without wet deposition covering a domain of 30.5 km × 39.5 km (UTM 701.0, 1602.0 to 740.5, 1641.5) with a grid size of 0.5 km^2. From Table 4.19, the maximum 1-hour averaged concentrations of NO_2 at 4 stations by the AERMOD were shown. The differences of the simulated values between each station were ranged from 12.6 $\mu g/m^3$ (475.5-462.9 $\mu g/m^3$) and 197.3 $\mu g/m^3$ (660.3-462.9 $\mu g/m^3$) showing the significance of 1-hour and 3-hour averaged input data on the output (the maximum 1-hour averaged concentration) by the AERMOD. The difference of 1-hour averaged NO_2 concentrations from NPL and KN stations, located in the domain, was

98.6 μg/m^3. We can see that the areas of high NO_2 impact (higher than 320 μg/m^3 by NAAQS) from NPL, KN, PC and LB stations were 249.7, 289.9, 22.4, and 25.3 km^2, respectively.

Table 4.18 Meteorological stations for the AERMET.

Station	Authority	Averaged period	Distance from the reference point (km)	Status
NPL	PCD	1 hour	20.1	in the domain
KN	PCD	1 hour	24.2	in the domain
PC	TMD	3 hour	25.0	in the domain
LB	TMD	3 hour	51.5	outside the domain

Table 4.19 Summary of the maximum 1-hour averaged concentration of NO_2 by the AERMOD version 4.6.2.

Station	Maximum 1-h averaged NO_2 concentration (μg/m^3)	Location of the maximum impact in UTM (X,Y) (km)	Local station time of the maximum impact	Impact area (km^2)*	Population in the impact area (persons)**
NPL	660.3	718.5, 1620.5	08/05/2007 at 8.00 a.m.	249.7	19,726
KN	561.7	722.5, 1618.5	26/12/2007 at 9.00 a.m.	289.9	22,902
PC	462.9	722.0, 1619.0	17/01/2007 at 10.00 a.m.	22.4	1,770
LB	475.5	724.0, 1617.5	5/01/2007 At 10.00 a.m.	25.3	1,999

* Impact area is the area with the exposure of NO_2 concentration higher than 320 μg/m^3

** Population in the impact area = Impact area (km^2) × 79 (persons/km^2)

Figures 4.39(a) - 4.39(d) show the contours of the maximum 1-hour averaged NO_2 concentrations by the AERMOD using 1-hour averaged surface data from NPL and KN stations and 3-hour averaged surface data from PC and LB as the input data for the AERMET. It was found that NO_2 of 320 μg/m^3 dispersed as far as 10 km from the reference point. The larger impact areas in Figures 4.39(a) - 4.39(b) compared with the impact areas in Figures 4.39(c) - 4.39(d) were attained by using the input data of 1-hour averaged surface data from the stations in the domain (NPL and KN stations) instead of 3-hour averaged surface data from the stations inside and outside the domain (PC and LB stations). It can be indicated that 1-hour averaged surface data provide less missing data to the AEMET than 3-hour averaged surface data.

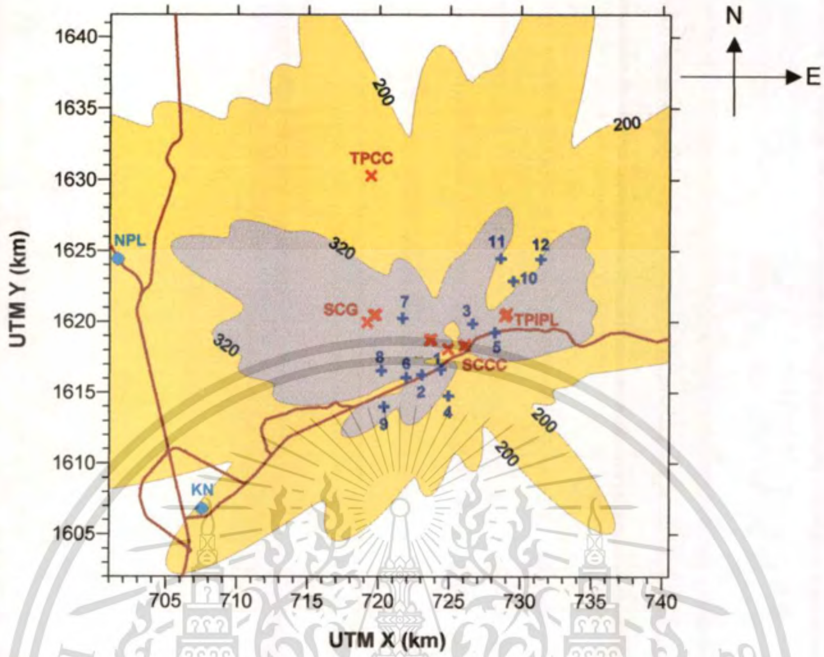

(a) use the surface data from the NPL station

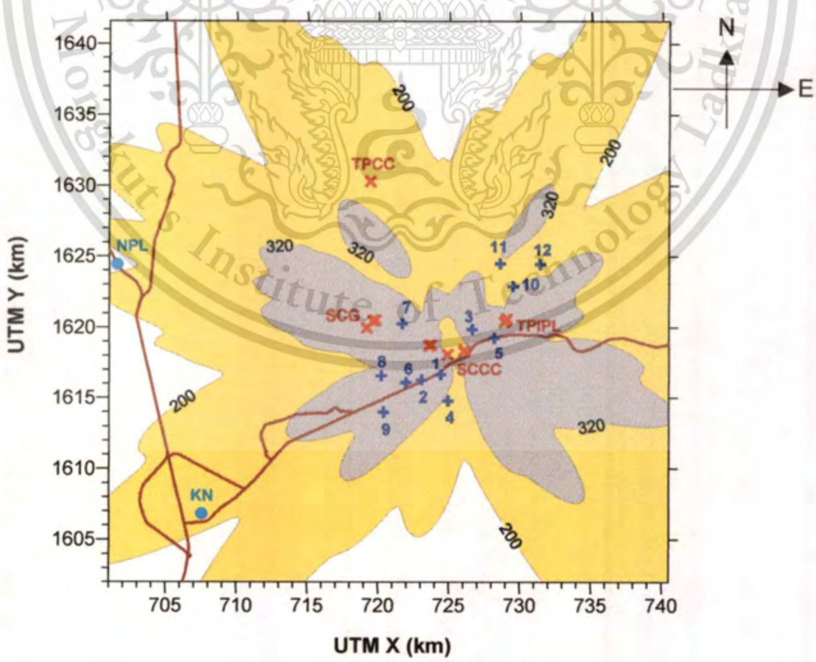

(b) use the surface data from the KN station

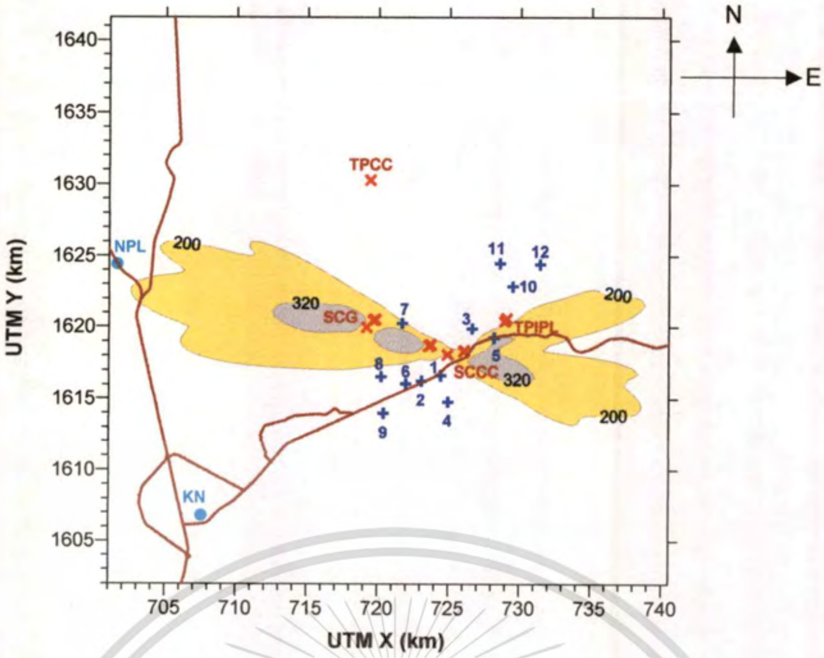

(c) use the surface data from the PC station

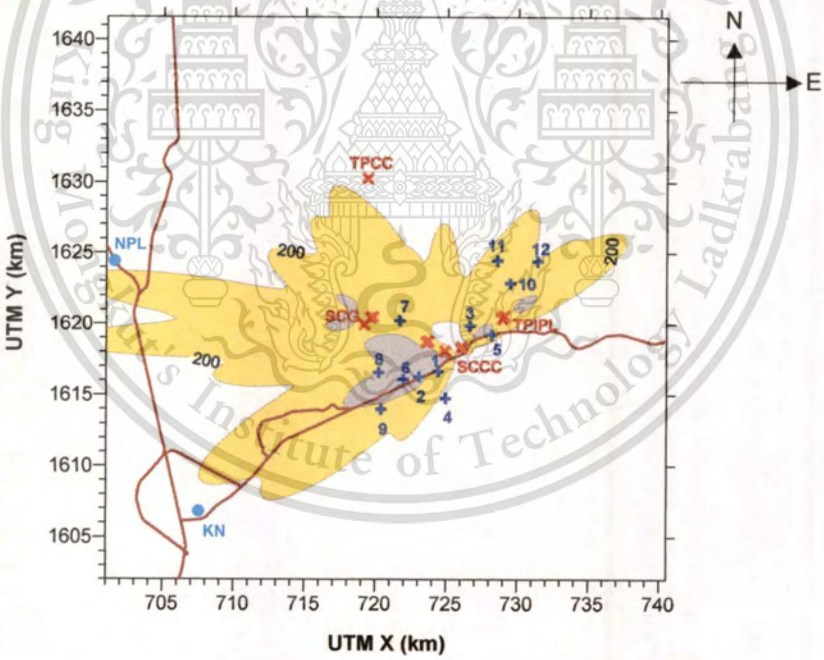

(d) use the surface data from the LB station

Figure 4.39 Contours of the maximum 1-hour averaged concentrations of NO_2 simulated by the AERMOD version 4.6.2 using the surface data from 4 stations: (●) meteorological stations, (+) receptors and (×) stacks of cement plants. (The contour intervals are 200 and 320 μg/m^3 from outermost to the innermost lines.)

(2) Sensitivity of precipitation or wet deposition to the AERMOD prediction

The meteorological data from Kao Noi station were used as the input surface data for the AERMOD version 4.6.2 to study the sensitivity of (rain) precipitation or wet deposition in Kaeng Khoi. The upper air data were obtained from Bang Na station (about 118 km southwest from the reference point). Cloud cover and ceiling height were obtained from Pak Chong station. The same conditions of the AERMOD for a domain 30.5 km × 39.5 km (UTM 701.0, 1602.0 to 740.5, 1641.5) and a grid size of 0.5 km^2 were set.

The maximum 1-hour averaged concentrations of NO_2 without and with precipitation in Table 4.20 were 561.7 and 512.4 $\mu g/m^3$ corresponding to the impact areas of 289.9 and 107.3 km^2, respectively. It is obvious to notice the effect of precipitation on the simulation of pollutant concentrations by the AERMOD. About 3 times of the impact area was observed at the difference maximum 1-hour averaged concentrations of 49.3 $\mu g/m^3$ (561.7-512.4 $\mu g/m^3$). From Figures 4.40(a) and 4.40(b), we can see that the contours of the maximum 1-hour averaged concentrations of NO_2 without precipitation covered a larger area.

Table 4.20 The maximum simulated 1-hour averaged concentrations of NO_2 by the AERMOD version 4.6.2 without and with precipitation.

Conditions	Maximum 1-h averaged concentration of NO_2 ($\mu g/m^3$)	Location of the maximum impact in UTM (X,Y) (km)	Local station time of the maximum impact	Impact area (km^2)	Population in the impact area (persons)
Without precipitation	561.7	722.5, 1618.5	26/12/2007 at 9.00 a.m.	289.9	22,902
With precipitation	512.4	722.0, 1618.5	26/12/2007 at 9.00 a.m.	107.3	8,477

* Impact area is the area with the exposure of NO_2 concentration higher than 320 $\mu g/m^3$

** Population in the impact area = Impact area (km^2) × 79 (persons/km^2)

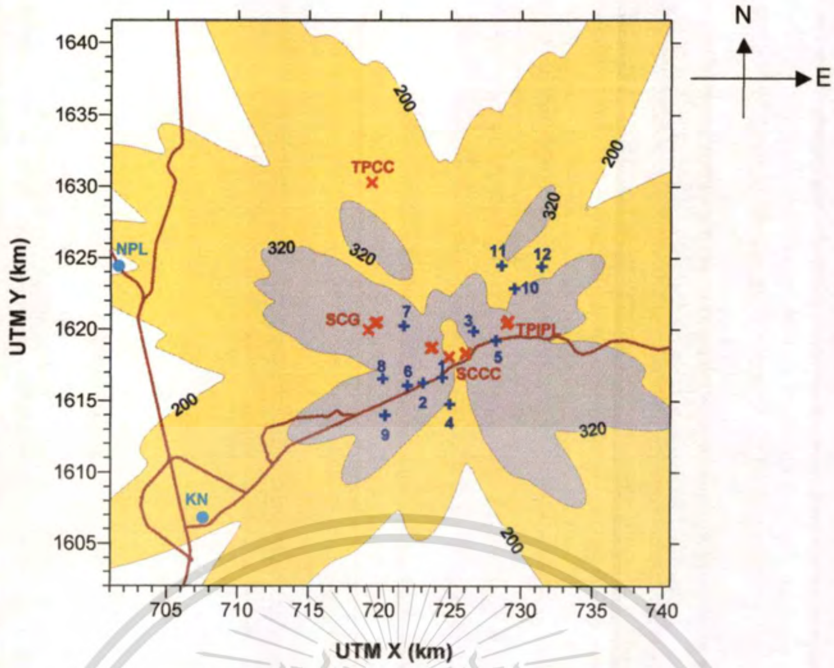

(a) without precipitation

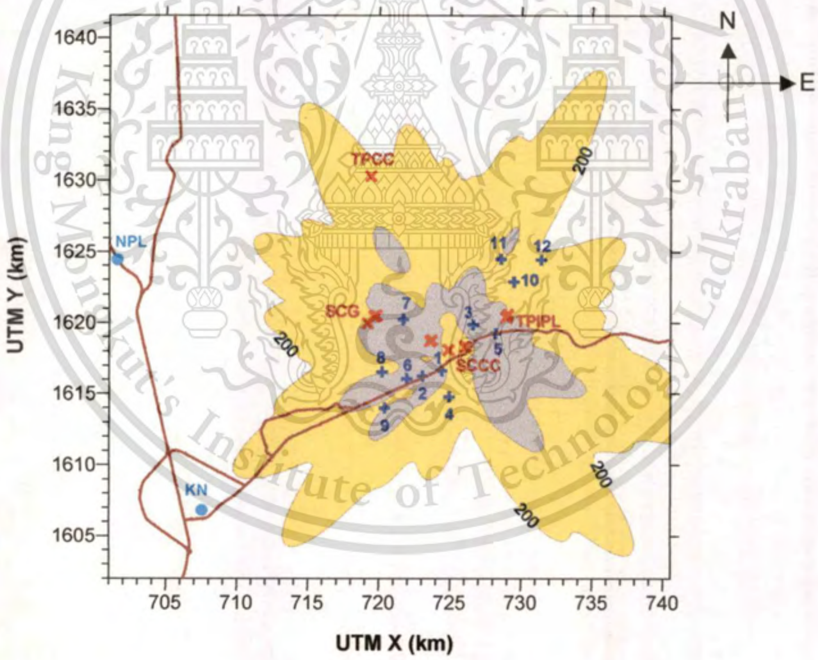

(b) with precipitation

Figure 4.40 Contours of the maximum 1-hour averaged concentrations of NO_2 by the AERMOD version 4.6.2 without and with wet deposition: (●) meteorological stations, (+) receptors and (×) stacks of cement plants. (The contour intervals are 200 and 320 μg/m^3 from the outermost to the innermost lines.)

(3) Sensitivity of the upper air data to the AERMOD prediction

In case the measured upper air data are not available, the commercial AERMOD simulates the upper air data by the meteorological module AERMET using the planetary boundary layers (PBL) similarity theory and the case studies in the U.S. and Europe. The AERMET can be coupled with meso-scale meteorological models, e.g., Eta Models, MM5, RAMS, WRF, etc [108].

In this section, the outputs of the AERMOD (1-hour averaged concentrations of NO_2) using the measured and simulated upper air data were compared. To run the AERMOD version 4.6.2, the 1-hour averaged surface data from Kao Noi station were used. The measured upper air data were obtained from Bang Na station. The precipitation was excluded from the AERMET to avoid the effect of wet deposition. The same conditions of the AERMOD for a domain 30.5 km × 39.5 km (UTM 701.0, 1602.0 to 740.5, 1641.5) and a grid size of 0.5 km^2 were set.

Table 4.21 shows the maximum simulated 1-hour averaged concentrations of NO_2 by using measured and simulated upper air data. It should be noted that the measured and simulated upper air data are significant to the maximum 1-hour averaged concentrations. The maximum 1-hour averaged NO_2 concentrations from the measured and simulated upper air data of 561.7 and 539.3 $\mu g/m^3$ were not much different but significant impact areas of 289.9 and 86.1 km^2 were observed, same as the results in the contours in Figures 4.41(a)-4.41(b). For further study, it is suggested to verify the simulated upper air data by the AERMET for Thailand's cases by coupling the AERMOD with other meteorological models, e.g., MM5, RAMS, WRF, etc.

Table 4.21 The maximum simulated 1-hour averaged concentrations of NO_2 by the AERMOD version 4.6.2 using measured and simulated upper air data.

Source of upper meteorological data	Maximum 1-h averaged concentration of NO_2 ($\mu g/m^3$)	Location of the maximum impact in UTM (X,Y) (km)	Local station time of the maximum impact	Impact area (km^2)	Population in the impact area (persons)
Use measured upper air data from Bang Na station	561.7	722.5, 1618.5	26/12/2007 at 9.00 a.m.	289.9	22,902
Use simulated upper air data from the AERMET	539.3	727.5, 1618.5	22/01/2007 at 4.00 a.m.	86.1	6,802

* Impact area is the area with the exposure of NO_2 concentration higher than 320 $\mu g/m^3$

** Population in the impact area = Impact area (km^2) × 79 (persons/km^2)

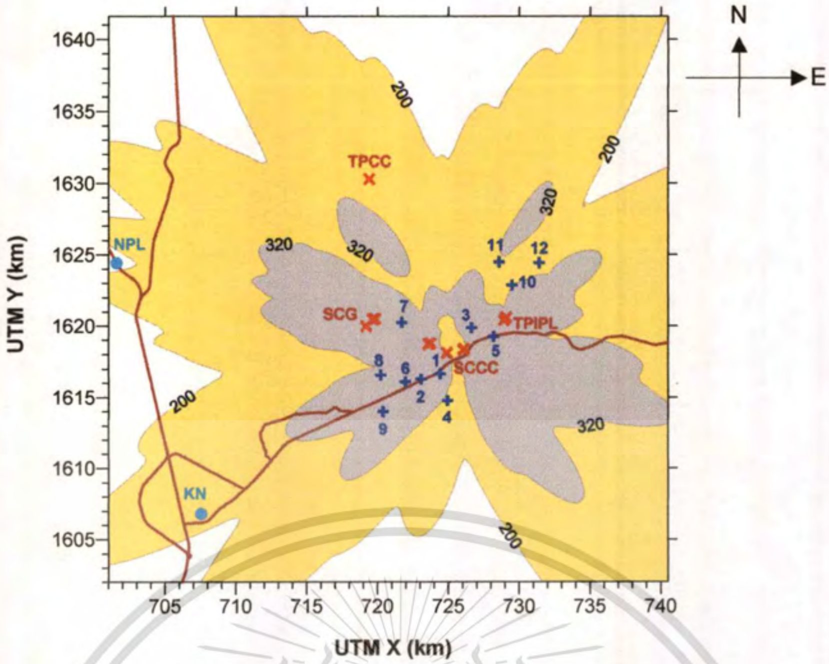

(a) use upper air data measured by Bang Na station

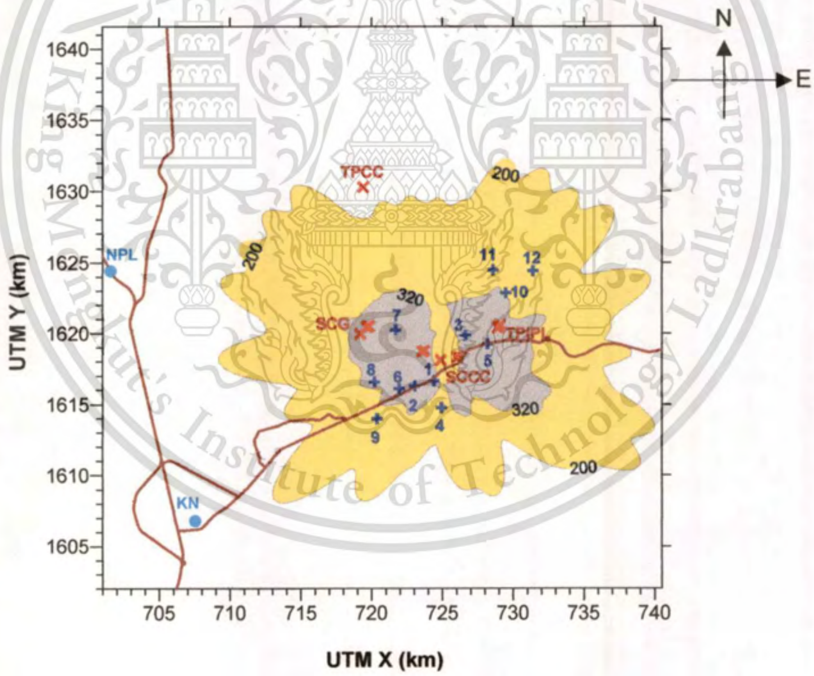

(b) use simulated upper air data

Figure 4.41 Contours of the maximum 1-hour averaged concentrations of NO_2 by the AERMOD version 4.6.2 using measured and simulated upper air data: (●) meteorological stations, (+) receptors and (×) stacks of cement plants. (The contour intervals are 200 and 320 μg/m^3 from outermost to the innermost lines.)

(4) The AERMOD system in air pollution applications

The AERMOD has been replaced the ISCST3 for the EIA evaluation in Thailand. It is an effective Gaussian plume model for flat or complex terrain, particularly the mountain areas like Kaeng Khoi. In this section, the emissions of PM_{10}, NO_2 and SO_2 from 14 stacks of 4 cement manufacturers were evaluated. The 1-hour averaged surface data were used from KN station. The precipitation was included in the AERMET to consider the effect of wet deposition. The upper air data were obtained from Bang Na station.

Table 4.22 shows the maximum 1-hour averaged concentrations of PM_{10}, NO_2 and SO_2 of 96.0, 561.7 and 5.5 $\mu g/m^3$ and the maximum 24-hour averaged concentrations of 11.4, 63.5 and 0.6 $\mu g/m^3$, respectively. Compare to the NAAQSs and the WHO's guidelines in Table 2.2, the maximum 1-hour averaged concentration of NO_2 was higher than the permit of NAAQS (320 $\mu g/m^3$) and the WHO's guidelines (200 $\mu g/m^3$). From Table 4.22, the maximum simulated 1-hour averaged concentrations of PM_{10}, NO_2 and SO_2 were higher than the maximum 24-hour averaged concentrations. The maximum simulated 1-hour averaged concentrations were observed in dry season whereas the maximum simulated 24-hour averaged concentrations were observed in wet season because lower pollutant dispersion in wet season is due to wet deposition. The contours of PM_{10}, NO_2 and SO_2 concentrations from the AERMOD were presented in Figures 4.42-4.44. According to the contours, the pollutants dispersed to all directions because wind directions changed during the day and the whole period of the simulation. The highest concentrations of PM_{10}, NO_2 and SO_2 (in dark color) were noticed in the east and west of the domain. Significant impacts from the emissions were observed in the distance of 5 km away from the reference point, particularly at the connecting area of the SCG and SCCC where the receptor 7 was located. A few pollutants dispersed to the areas of the NPL and KN stations.

Table 4.22 The maximum simulated concentrations of 1-hour and 24-hour averaged by the AERMOD version 4.6.2.

Averaged period	Pollutants	Maximum concentration ($\mu g/m^3$)	Location of the maximum impact in UTM (X,Y) (km)	Local station time of the maximum impact
1-hour average	PM_{10}	96.0	720.0,1621.5	4/01/2007 at 10.00 a.m.
	NO_2	561.7	722.5, 1618.5	26/12/2007 at 9.00 a.m.
	SO_2	5.5	730.5, 1621.0	10/10/2007 at 11.00 a.m.
24-hour average	PM_{10}	11.4	719.5, 1621.0	25/05/2007
	NO_2	63.5	727.5 ,1618.0	24/06/2007
	SO_2	0.6	730.0 1621.0	24/12/2007

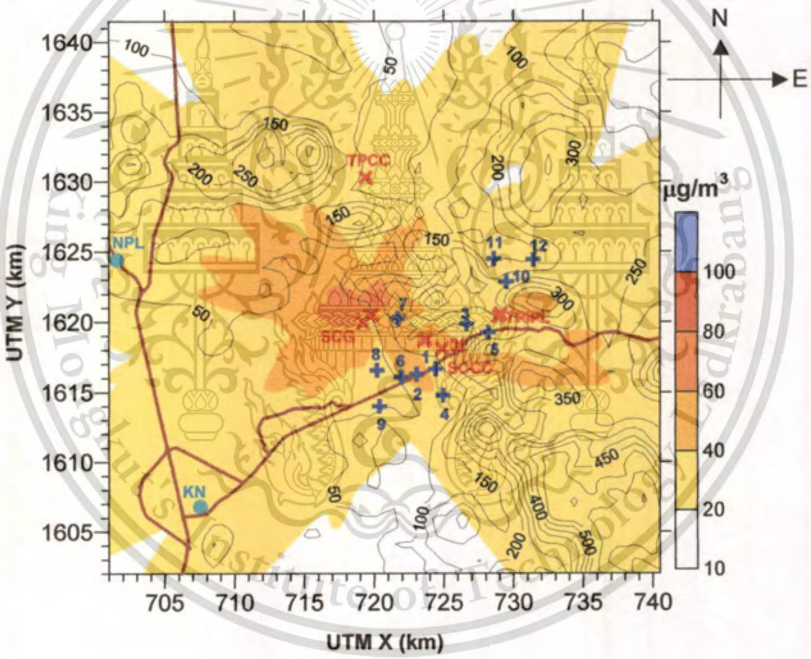

Figure 4.42 Contours of the maximum 1-hour averaged concentrations of PM_{10} by the AERMOD version 4.6.2 with wet deposition: (●) meteorological stations, (+) receptors and (×) stacks of cement plants.

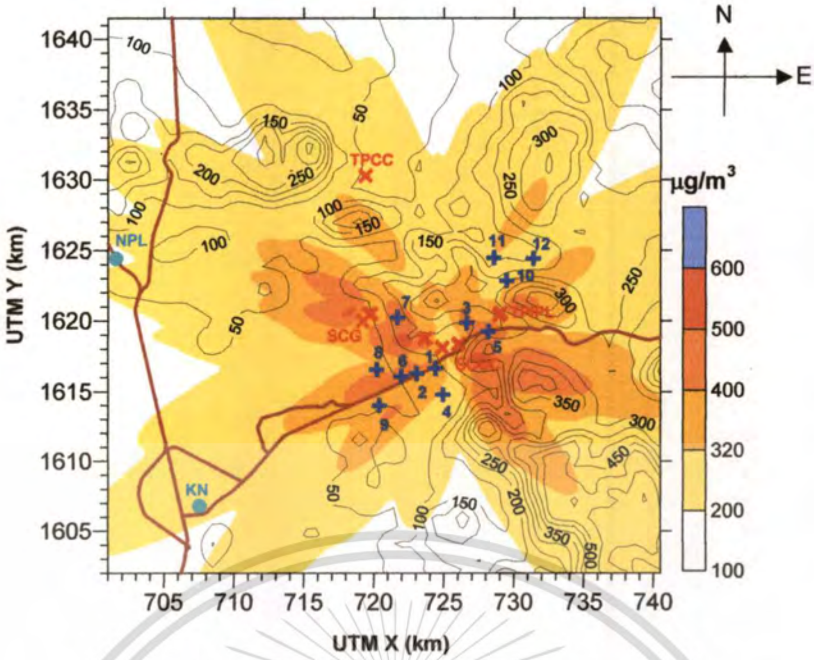

Figure 4.43 Contours of the maximum 1-hour averaged concentrations of NO_2 by the AERMOD version 4.6.2 with wet deposition: (●) meteorological stations, (+) receptors and (×) stacks of cement plants.

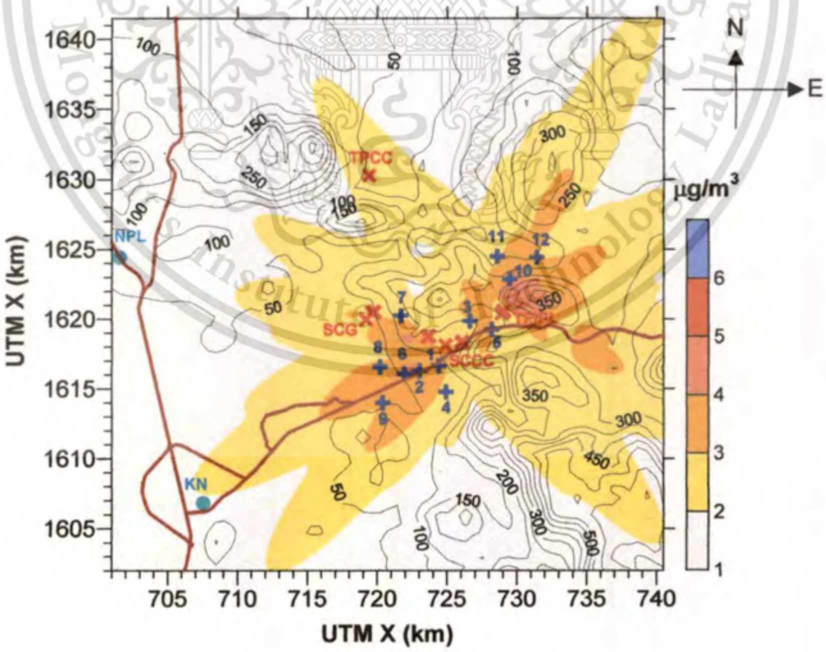

Figure 4.44 Contours of the maximum 1-hour averaged concentrations of SO_2 by the AERMOD version 4.6.2 with wet deposition: (●) meteorological stations, (+) receptors and (×) stacks of cement plants.

(5) Comparison of the outputs by the ISC-AERMOD View 4.6.2 and the AERMOD 5.4

The ISC-AERMOD View by Lakes Environmental Software is now developed to version 7.0 [57]. In Thailand, generally several AERMOD versions are applied for the EIA evaluation, however, no other works compare the output from each version. In this work, the simulation outputs from the AERMOD versions 4.6.2 and 5.4 (an easy-operated version with special graphic options) under the same conditions are reported. The 1-hour averaged surface data were obtained from Kao Noi station. The upper air data were obtained from Bang Na station. The AERMOD was run with wet deposition covering the same domain with in the previous sections (i.e. UTM 47P between 701.0 km, 1602.0 km to 740.5 km, 1641.5 km with a grid size of 0.5 km^2).

Tables 4.23-4.25 show that the maximum 1-hour, 24-hour and 1-year averaged concentrations of PM_{10}, NO_2 and SO_2 by the AERMOD version 4.6.2 were much lower than those by the AERMOD version 5.4. Not only the different maximum pollutant concentrations but also the locations of their maximum concentrations were observed. The users of different AERMOD versions should be aware that the simulated outputs (the maximum concentration of the pollutant and impact area) from a better version agree well with the measured results. Figures 4.45-4.47 show the contours of the maximum concentrations of PM_{10}, NO_2 and SO_2 by the AERMOD version 5.4. The pollutants were likely dispersed to all directions. The maximum concentrations were mostly found in the east of the domain nearby the mountain areas next to the Kao Yai Natural Park. A few pollutants were observed in the west near the mountain areas in Nah Phra Laan. Significant impacts from the emissions were observed in the area nearby the SCCC and TPIPL where the receptors 3, 5, 10, 11 and 12 were located.

As presented in Table 4.26, the AERMOD version 5.4 can calculate more number of sources and grids than the AERMOD version 4.6.2. The higher version can read more details from the DEM resulting in the higher simulated results. This could be a downfall in interpretation if the users are not well aware of the outputs (the maximum concentrations and locations of the pollutants) from different versions.

Table 4.23 The maximum simulated 1-hour averaged pollutant concentrations by the AERMOD versions 4.6.2 and 5.4.

AERMOD version	Pollutants	Maximum concentration ($\mu g/m^3$)	Location of the maximum impact in UTM (X,Y) (km)	Local station time of the maximum impact
Version 4.6.2	PM_{10}	96.0	720.0,1621.5	4/01/2007 at 10.00 a.m.
	NO_2	561.7	722.5, 1618.5	26/12/2007 at 9.00 a.m.
	SO_2	5.5	730.5, 1621.0	10/10/2007 at 11.00 a.m.
Version 5.4	PM_{10}	579.4	723.0, 1621.0	8/09/2007 at 3.00 a.m.
	NO_2	3,820.2	730.0, 1621.5	17/01/2007 at 9.00 p.m.
	SO_2	60.3	730.0, 1621.0	25/12/2007 at 4.00 a.m.

Table 4.24 The maximum simulated 24-hour averaged pollutant concentrations by the AERMOD versions 4.6.2 and 5.4.

AERMOD version	Pollutants	Maximum concentration ($\mu g/m^3$)	Location of the maximum impact in UTM (X,Y) (km)	Local station time of the maximum impact
Version 4.6.2	PM_{10}	11.4	719.5, 1621.0	25/05/2007
	NO_2	63.5	727.5 ,1618.0	24/06/2007
	SO_2	0.6	730.0 1621.0	24/12/2007
Version 5.4	PM_{10}	89.5	725.0, 1618.5	5/01/2007
	NO_2	625.6	725.0, 1619.0	11/01/2007
	SO_2	11.3	730.0 ,1620.5	17/02/2007

Table 4.25 The maximum simulated 1-year averaged pollutant concentrations by the AERMOD versions 4.6.2 and 5.4.

Models	Pollutants	Maximum concentration ($\mu g/m^3$)	Location of the maximum impact in UTM (X,Y) (km)
AERMOD version 4.6.2	PM_{10}	2.9	719.5, 1621.0
	NO_2	16.3	725.5, 1619.5
	SO_2	0.1	728.5, 1621.5
AERMOD version 5.4	PM_{10}	12.1	709.5 1630.0
	NO_2	74.9	730.0, 1620.5
	SO_2	1.4	730.0, 1620.5

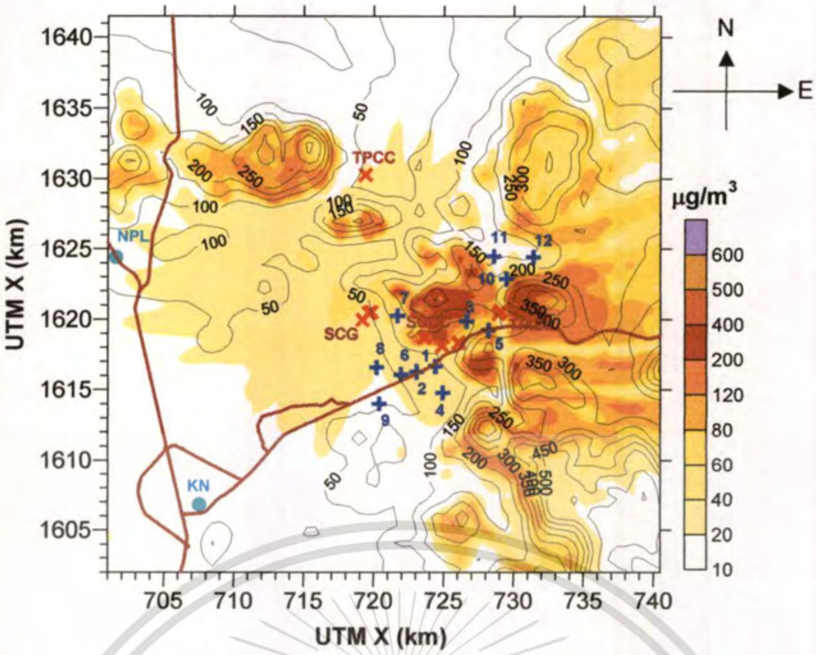

Figure 4.45 Contours of the maximum 1-hour averaged concentrations of PM_{10} by the AERMOD version 5.4 with wet deposition: (●) meteorological stations, (+) receptors and (×) stacks of cement plants.

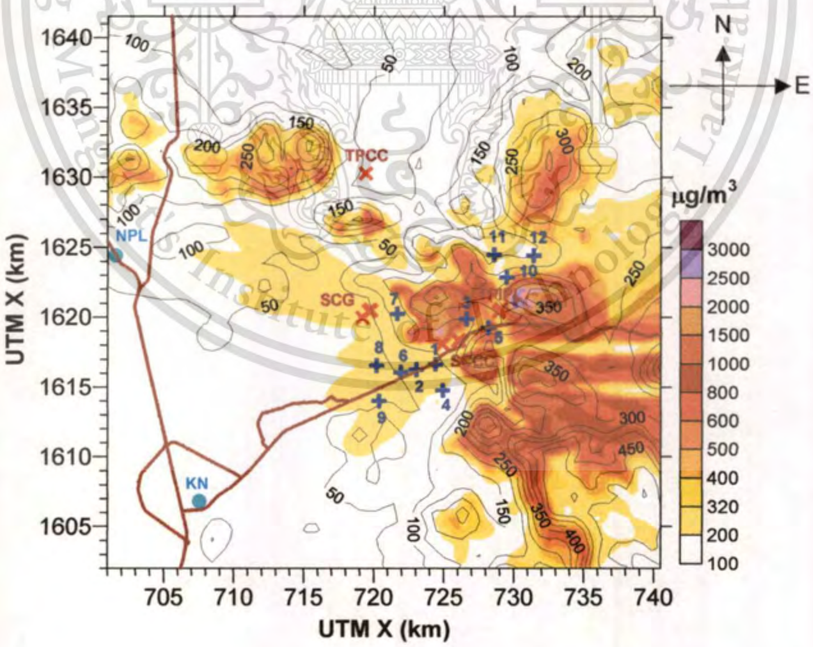

Figure 4.46 Contours of the maximum 1-hour averaged concentrations of NO_2 by the AERMOD version 5.4 with wet deposition: (●) meteorological stations, (+) receptors and (×) stacks of cement plants.

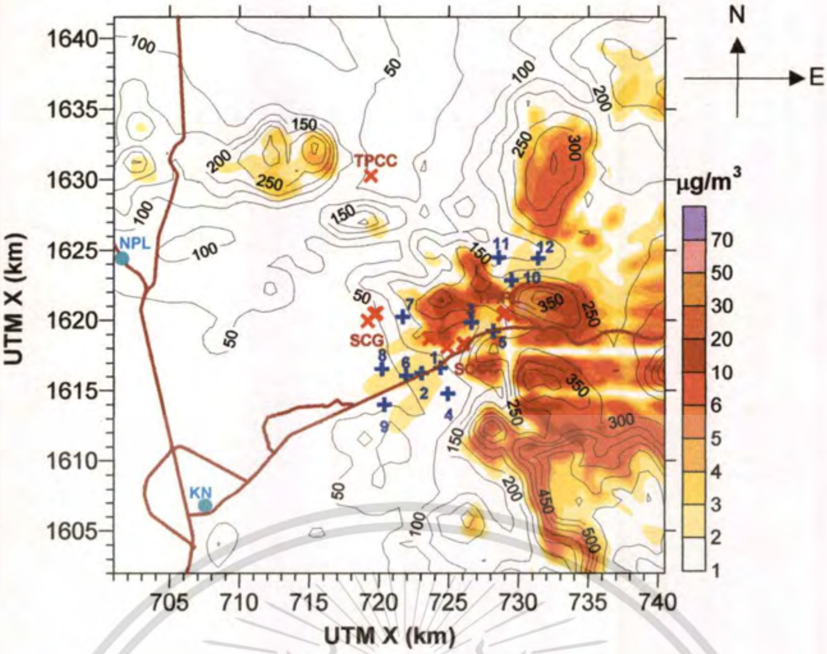

Figure 4.47 Contours of the maximum 1-hour averaged concentrations of SO_2 by the AERMOD version 5.4 with wet deposition: (●) meteorological stations, (+) receptors and (×) stacks of cement plants.

Table 4.26 Comparison of the performances of the AERMOD versions 4.6.2 and 5.4.

Details	Version 4.6.2	Version 5.4
Maximum of source input (points)	300	500
Maximum of grid number (points)	7,200	more than 7,200
Graphical options	less comfortable	more comfortable

(6) PM_{10} dispersion in Kaeng Khoi and Nah Phra Laan by the ISC-AERMOD View 5.4

The PM_{10} dispersion in Kaeng Khoi and Nah Phra Laan were simulated by the AERMOD 5.4. The UTM 689.0E, 1592.0 N to 753.5 E, 1651.5N domain of 64.5 km × 59.5 km with a grid spacing of 0.5 km was larger and covered all the area of the selected cement manufacturers. The emission inputs of PM_{10} to the AERMOD were obtained from 14 stacks of the cement manufacturers in Kaeng Khoi and additional 9 stacks of the cement manufacturers in Nah Phra Laan.

Table 4.27 shows the maximum 1-hour and 24-hour averaged concentrations of PM_{10} of 3,428.6 and 720.7 $\mu g/m^3$. The maximum 24-hour averaged concentration of PM_{10} was about

6 times higher than the NAAQS permit of 120 μg/m^3 (the WHO's guidelines of 50 μg/m^3). From the contours of PM_{10} concentrations in Figures 4.48-4.49, (i) at Kaeng Khoi, the high PM_{10} concentration were observed at the connecting area of the SCCC and TPIPL and the area beside the main road nearby the SCCC. (ii) at Nah Phra Laan, the high PM_{10} concentration was observed at the connecting area of the CMEX and LM nearby Nah Phra Laan station.

The impact areas where PM_{10} concentration exceeded the NAAQS permit and the WHO's guidelines were about 7.3 km^2 with a population density of 577 persons and much lower than the effect of NO_2 concentration in Table 4.20 (107.3 km^2 with a population density of 8,477 persons).

Table 4.27 The maximum simulated 1-hour and 24-hour averaged PM_{10} concentrations by the AERMOD version 5.4.

Averaged period	Concentration (μg/m^3)	Location of the maximum impact in UTM (X,Y) (km)	Local station time of the maximum impact
1	3,428.6	720.5, 1615.0	27/11/2007 at 10.00 p.m.
24	720.7	720.5, 1615.0	2/12/2007

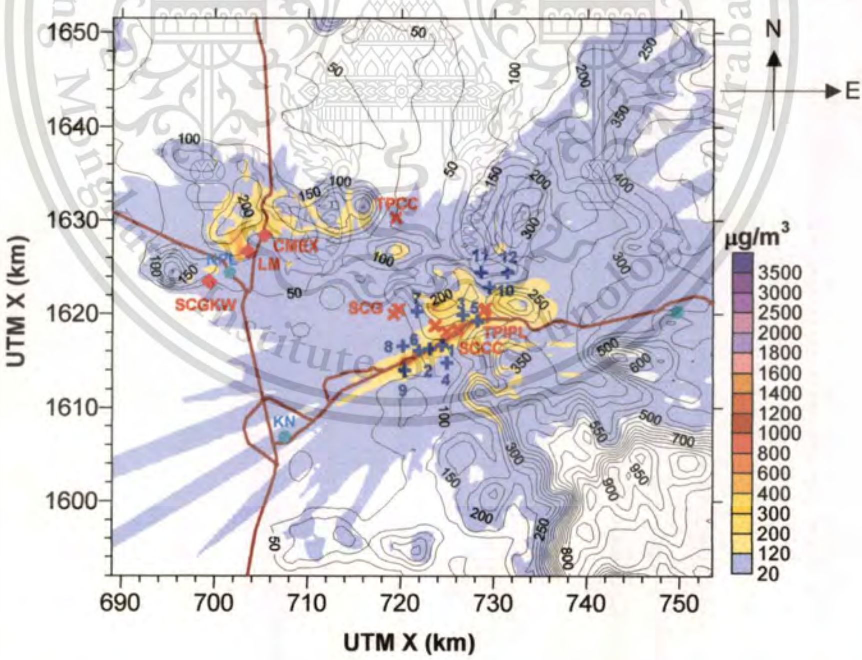

Figure 4.48 Contours of the maximum 1-hour averaged concentrations of PM_{10} by the AERMOD version 5.4 in Kaeng Khoi and Nah Phra Laan: (●) meteorological stations, (+) receptors, (×) stacks of cement plants in Kaeng Khoi and (♦) stacks of cement plants in Nah Phra Laan.

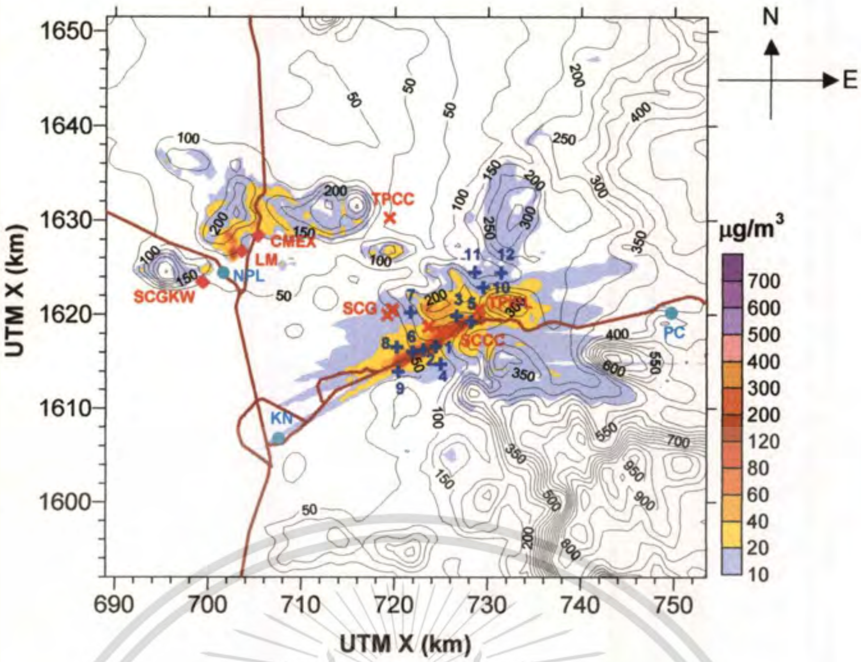

Figure 4.49 Contours of the maximum 24-hour averaged concentrations of PM_{10} by the AERMOD version 5.4 in Kaeng Khoi and Nah Phra Laan: (●) meteorological stations, (+) receptors, (×) stacks of cement plants in Kaeng Khoi and (◆) stacks of cement plants in Nah Phra Laan.

(7) NO_2 dispersion in Kaeng Khoi by the ISC-AERMOD View 4.6.2

Of the total emission from 14 stacks of the cement manufacturers in Kaeng Khoi mentioned in section 4.2, NO_2 was the major emission, therefore the dispersion of NO_2 was simulated by the AERMOD version 4.6.2 in the observation period for the EIA reports in dry and wet seasons. The domain covered 30.5 km × 39.5 km (UTM 701.0, 1602.0 to 740.5, 1641.5) and a grid size of 0.5 km^2. Other settings were the same as the previous sections.

To run the AERMOD, the hourly surface data were obtained from Kao Noi station and the upper air data were obtained from Bang Na station. The time-series plots of hourly measured and simulated NO_2 averaged concentrations were compared with peaks of NO_2 concentrations during the EIA monitoring period. The maximum 1-hour averaged concentrations of NO_2 in dry season (Jan. to Apr. and Nov.-Dec.) and wet season (May to Oct.) from 12 receptors and from the AERMOD were considered in Table 4.28. The impact areas of higher NO_2 concentrations than 320 μg/m^3 were calculated. The stack No. 1 of the SCCC was designated as the reference point for the receptor distances.

From time-series plots of 1-hour averaged concentrations of NO_2 in Figures 4.50-4.51, it was found that the measured NO_2 concentrations at 12 receptors in dry season were 2-135 μg/m^3 and 0-105 μg/m^3 in wet season. The maximum simulated 1-hour averaged concentration of NO_2 in dry season was slightly higher than in wet season (see Table 4.28). At the receptors 1 to 10 about 1 to 7 km from the reference point, the simulation results for the dry season in Figures 4.50 showed higher NO_2 concentration peaks compared to the receptors 11 and 12 about 7.5 km away from the reference point. The measured and simulated results showed almost the same trend in some receptors (e.g., receptors 2, 3, 5, 6). But at some receptors, timing and magnitudes of NO_2 concentration were different (e.g., receptors 1, 8, 10).

In the wet season (Figures 4.51), only a few of NO_2 concentration peaks were found at the receptors (e.g., receptors 4, 5, 6, 7, 9, 12). This can be attributed to high NO_2 wet deposition. According to safety thresholds for 1-hour averaged concentrations of NO_2 issued by the NAAQS of 320 μg/m^3 and by the WHO's Guidelines of 200 μg/m^3, most of NO_2 emissions from 14 stacks of cement manufacturers by measurement and the AERMOD simulation were under the permit values and showed no significant impact at the receptor locations.

As seen in Table 4.28, the maximum 1-hour averaged concentrations of NO_2 by the AERMOD in dry season (562 μg/m^3) and wet season (548 μg/m^3) were higher than the permit value of 320 μg/m^3. These maximum simulated concentrations occurred at short time intervals of approximately 144 hours and 62 hours in the dry and wet seasons. The relevant impacted areas were 123 and 227 km^2 in the study domain, respectively.

However, it is worth to note that the NO_2 emissions depend on several factors, i.e., wind speed and direction, relative humidity, pressure, temperature, ceiling height, cloud cover, global radiation, monitoring location, including wet and dry depositions of NO_2 and the reactions of NO_2 with O_3 and VOCs to secondary PM. The AERMOD coupled with chemical module can simulate the concentration of pollutant having chemical process in the atmospheric.

The simulation results at receptors 7 km further away from the reference point (e.g., the receptor 12) were especially problematic, and it would be uncertain if the U.S. EPA distance threshold of 50 km was applicable for the complex terrain and wind fields of this tropical setting. In short, the current application of the AERMOD is limited due to the following reasons:

(i) There is no module for NO_2 deposition reactions.

(ii) Model output is considered on a 1-hour averaged time scale instead of a longer time scale of 24-hour or more. The AERMOD is highly sensitive to different time scales as reported by Bhardwaj [109] and Zou et al. [81] and our results in section 4.5.1 (1).

(iii) The hourly averaged concentration by the AERMOD is calculated based on the constant emission input which does not change with time or real time input data [13-14].

(iv) The AERMOD cannot effectively simulate the dispersion of a pollutant or the transport of a pollution plume of low wind speed less than 1 m/s.

Table 4.28 The maximum simulated 1-hour averaged NO_2 concentrations in dry and wet seasons by the AERMOD version 4.6.2.

Scenarios	NO_2 maximum concentration (μg/m^3)	Local station time of the maximum impact	Location of the maximum impact in UTM (X,Y) (km)	Impact area (km^2)*	Details of the impact areas
Dry season	562	26th December 2007 at 9.00 a.m.	722.5, 1618.5	123	Agricultural area between cement plants SCCC and TPIPL
Wet season	548	8th October 2007 at 8.00 a.m.	727.5, 1617.0	227	Agricultural area near cement plant SCCC and beside the main road

* Impact area is the area with the exposure of NO_2 concentration higher than 320 μg/m^3

Population in the impact area = Impact area (km^2) × 79 (persons/km^2)

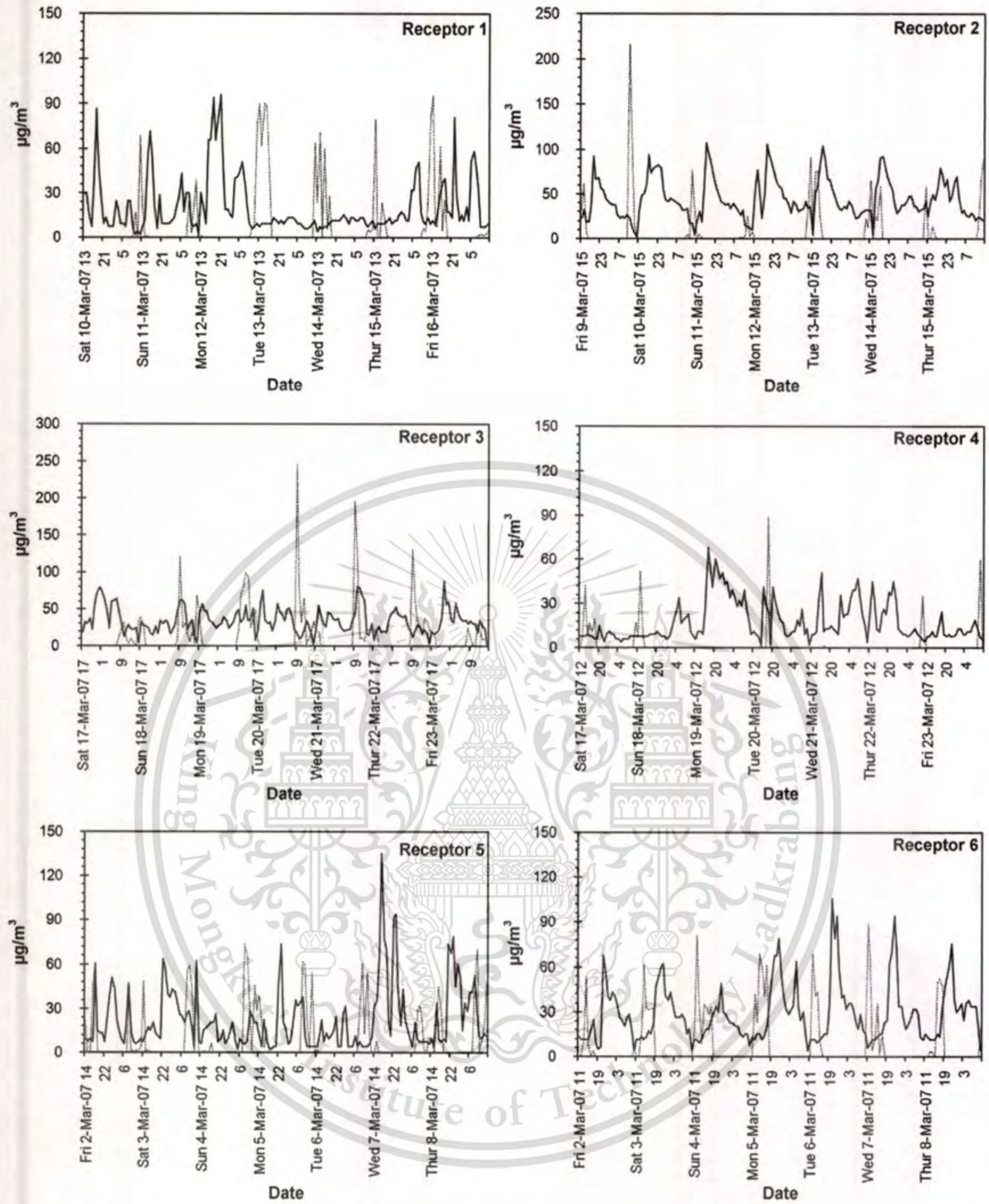

Figure 4.50 1-hour averaged concentration of NO_2 in dry season: solid line by measurements and dashed line by the AERMOD version 4.6.2.

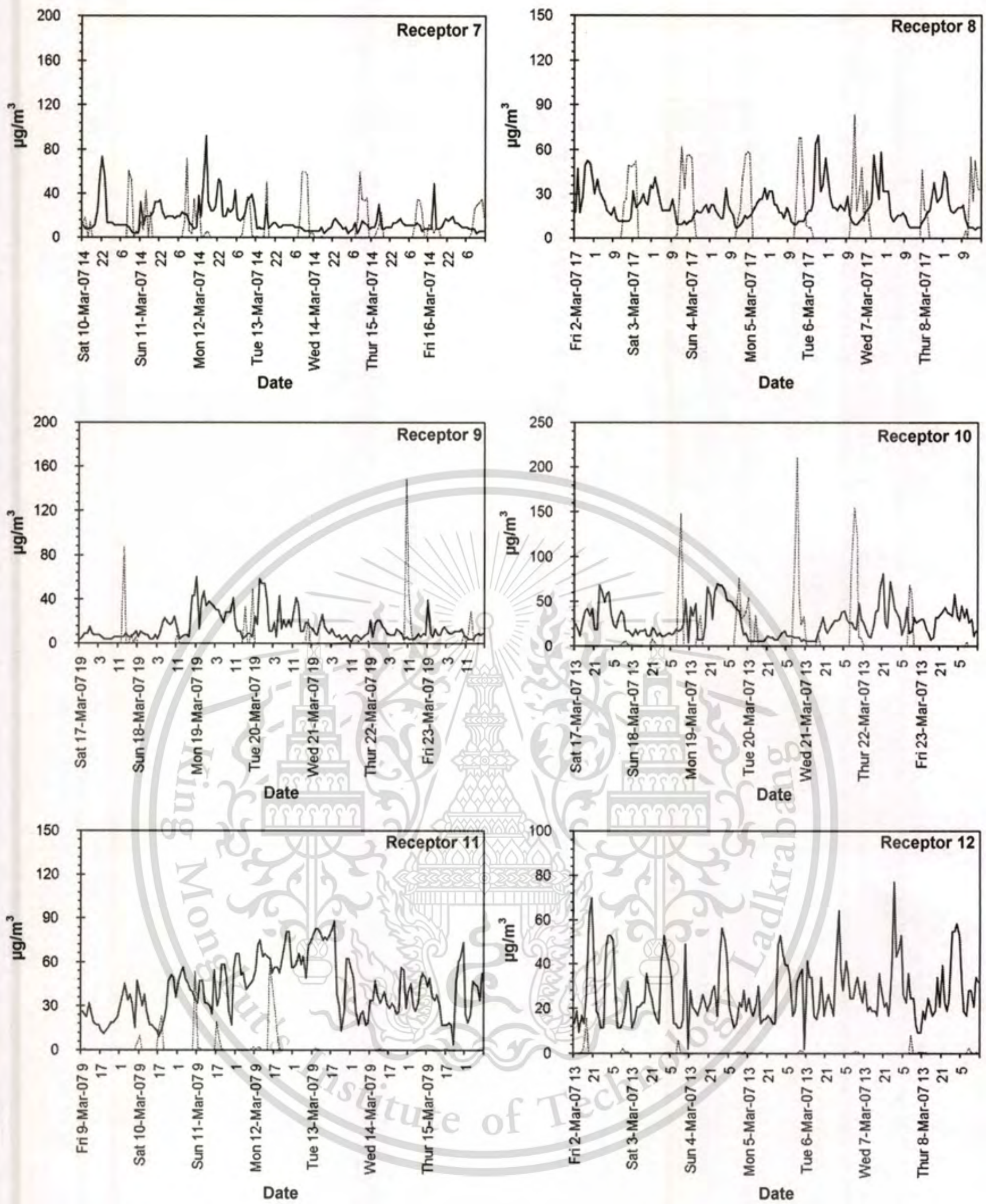

Figure 4.50 1-hour averaged concentration of NO_2 in dry season: solid line by measurements and dashed line by the AERMOD version 4.6.2. (cont.).

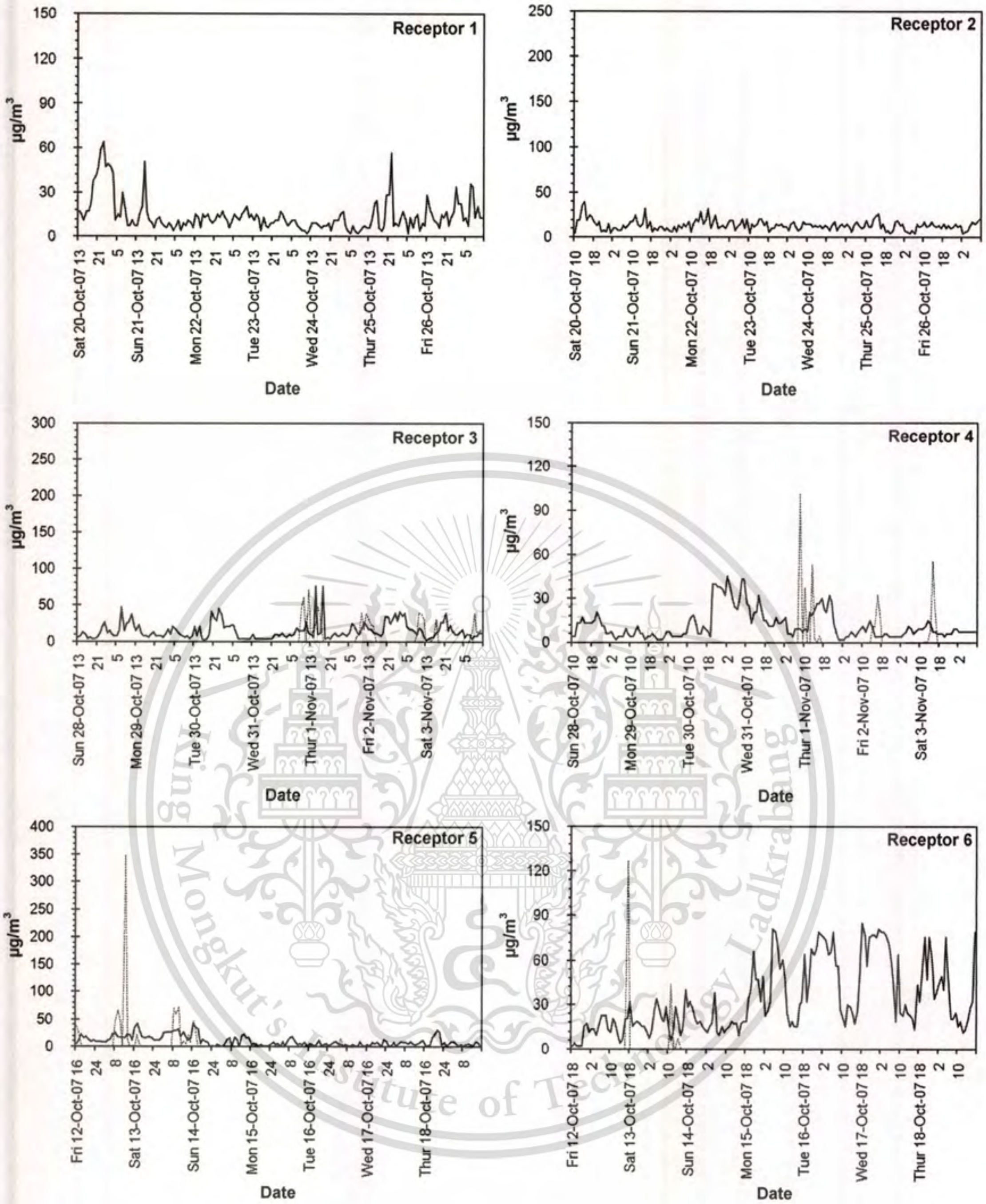

Figure 4.51 1-hour averaged concentration of NO_2 in wet season: solid line by measurements and dashed line by the AERMOD version 4.6.2.

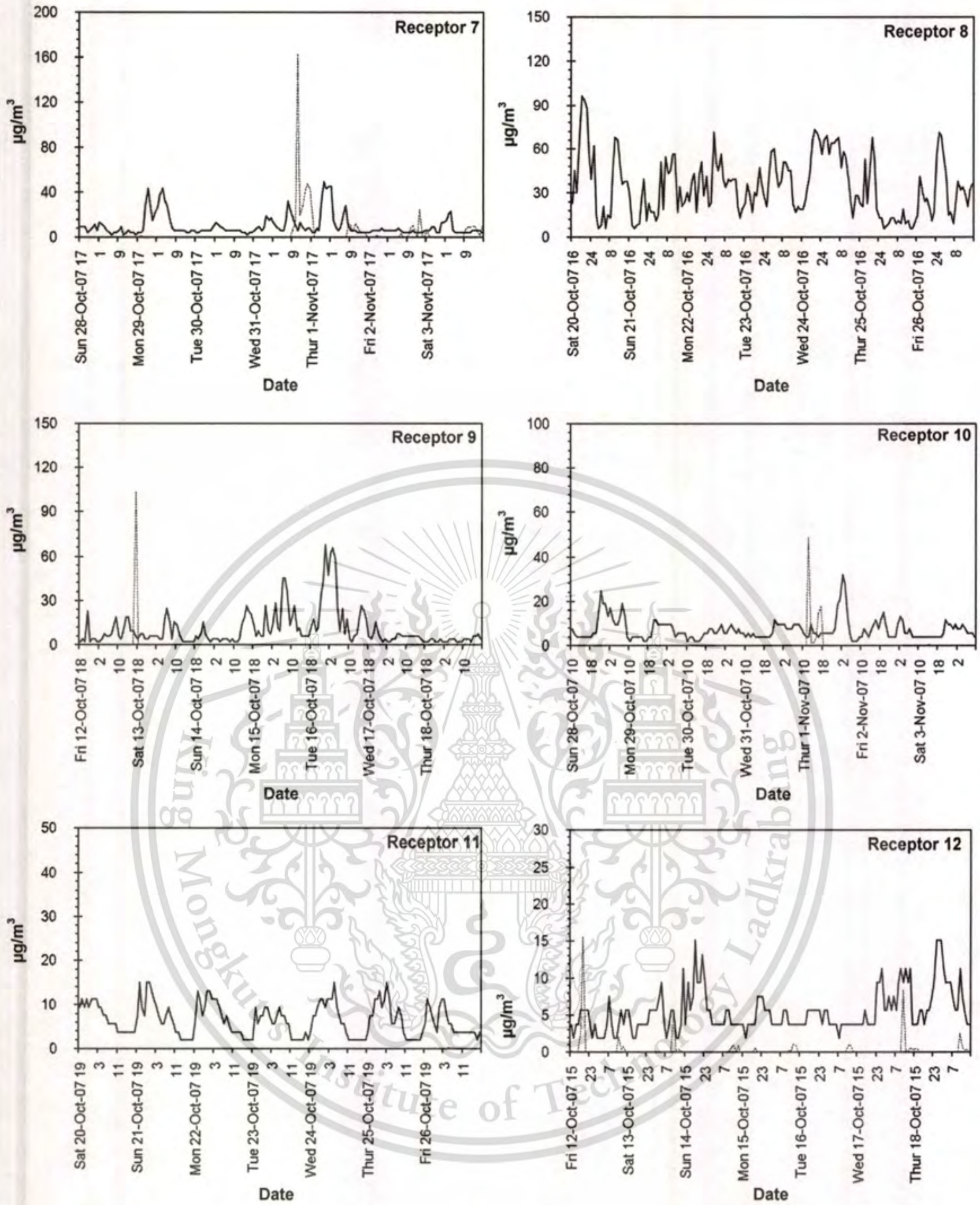

Figure 4.51 1-hour averaged concentration of NO_2 in wet season: solid line by measurements and dashed line by the AERMOD version 4.6.2 (cont.).

Figures 4.52-4.53 illustrate the performance of the AERMOD by the Q-Q plots of monitored and simulated NO_2 at 12 receptors in dry and wet seasons. The Q-Q plots of the receptors 1 to 8 (5 km from the reference point) in the dry season were mostly fitted to the middle line compared to those in the wet season. The Q-Q plots highlight the higher performance of the AERMOD in simulation of NO_2 concentration for dry season in comparison with wet season due to high deposition reactions in wet environment. High humidity and low temperature in the atmosphere in wet season resulted in low NO_2 dispersion due to the uptake by vegetative and ground sources. However, it is found that most of the receptors are under-predicted.

Even though there were some difficulties in the model simulations of extreme NO_2 concentrations and the maximum AERMOD concentrations were not necessarily supported by the measured data, the simulation results agreed with the Q-Q plots. Because the maximum 1-hour averaged concentration of NO_2 monitoring at the receptors was 1-hour average in 7-day continuous measurement and because of the constraints of inaccessibility receptor locations, it is therefore possible that the maximum 1-hour averaged concentration of NO_2 concentration was not likely detected during the measurement period.

In summary, a 7-day continuous measurement of NO_2 emissions showed no significant impact on the environment but it was clearly observed by the AERMOD simulation. It is most likely attributed to the limitation of a short-time measurement. The simulation results can help the policy makers to identify the areas of high pollution exposure risk for the EIA guidelines. However, in this work it is found that the AERMOD program is limited in prediction air pollutants at the distance 5 km further away from the reference point, particularly in wet season. It is noteworthy to be aware that the AERMOD is a dispersion model without the reaction module while NO_2 deposition reactions certainly occur in wet and dry environments. For a more precise estimation of NO_2 concentrations, the AERMOD model incorporating with the reaction module is required. Eventually, in order to estimate more precise impact from NO_2 emissions, it is recommended to evaluate the NO_2 dispersion by the multi-layer, multi-species and non-steady-state CALPUFF dispersion modeling in the following section.

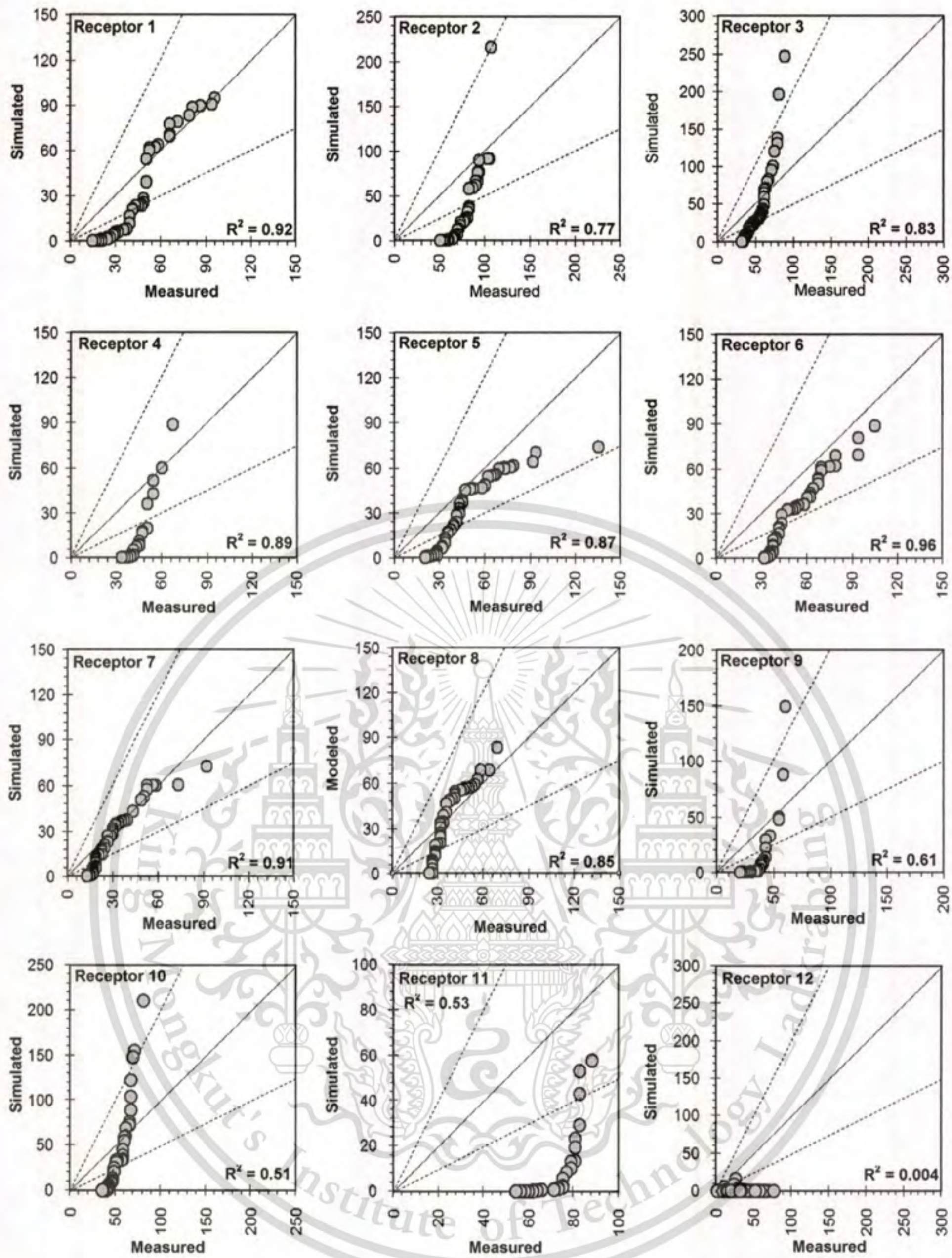

Figure 4.52 The Q-Q plots of hourly monitored NO_2 and simulated NO_2 in dry season by the AERMOD: slope = 1 (solid line); slope = 2 and 0.5 (dashed lines for the factor-of-two, model acceptable limit, within the over and under prediction, respectively).

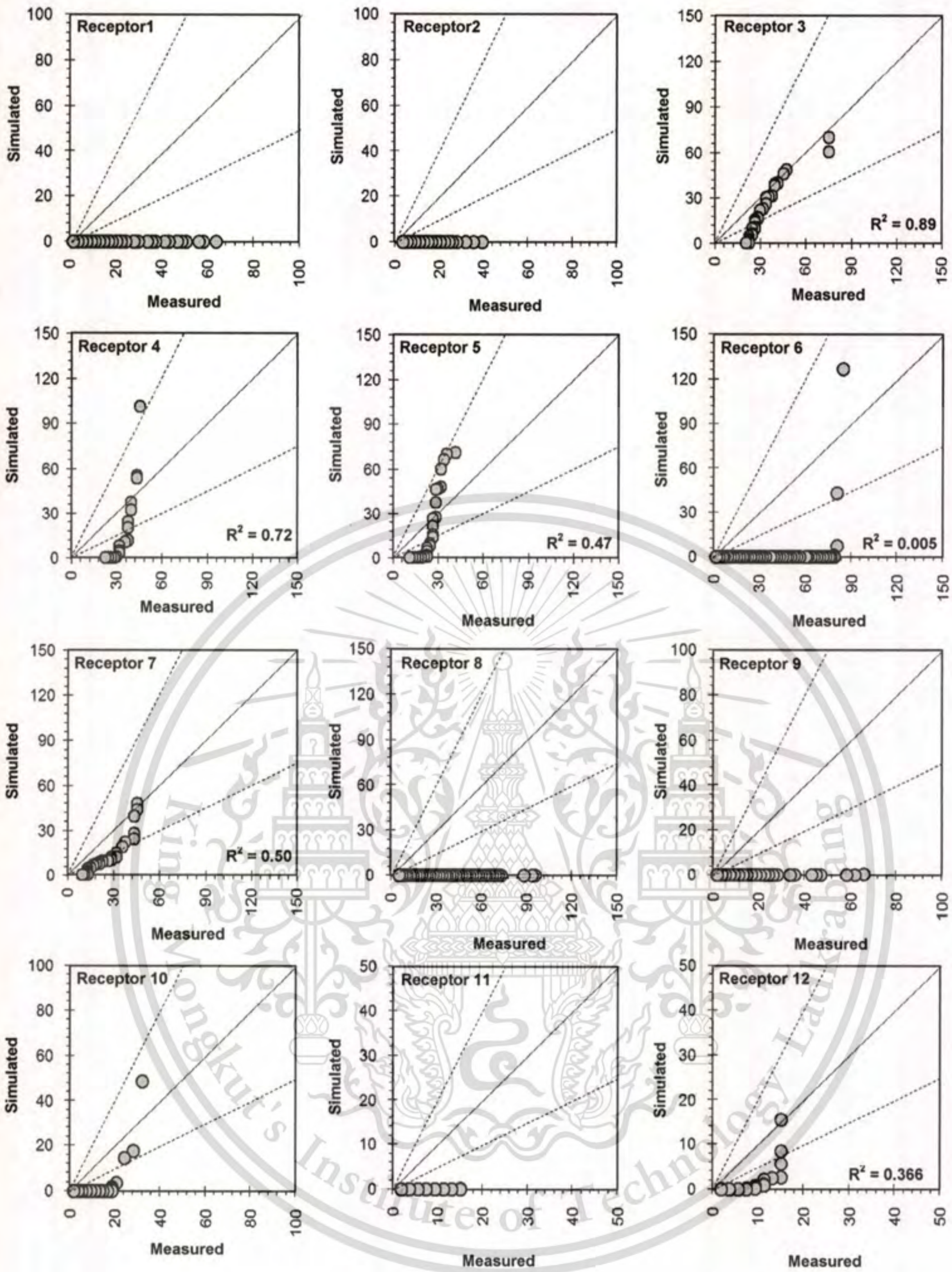

Figure 4.53 The Q-Q plots of hourly monitored NO_2 and simulated NO_2 in wet season by the AERMOD: slope = 1 (solid line); slope = 2 and 0.5 (dashed lines for the factor-of-two, model acceptable limit, within the over and under prediction, respectively).

4.5.2 Estimation of air pollutants by the CALPUFF

According to the monitoring results reported in section 4.2.2, it is found that the concentrations of air pollutants, as indicated by PM_{10}, NO_2 and SO_2, in Kaeng Khoi are not high. Nevertheless, the simulation results by the AERMOD show that the NO_2 emission is significant to the communities in Kaeng Khoi. As a result, the CALPUFF is applied to evaluate the PM_{10}, NO_2 and SO_2 from 14 stacks of the cement manufacturers in Kaeng Khoi.

Five case studies in Table 4.29 under the conditions of wet deposition and chemically reactive modules such as RIVAD/ARM3 and MESOPUFF were simulated by the CALPUFF. It is expected that cases 1 and 2, not including chemically reactive modules, might give the simulation outputs similar to the AERMOD without functions for chemical reactions. For the reactions of NO_2 with VOCs and/or O_3 during the dispersion, we applied cases 3-5 which included chemical reaction modules. The time-series of 1-hour averaged concentrations between monitoring and simulation results were plotted to observe the outputs by the CALPUFF. The monitoring data at Nah Phra Laan and Kao Noi stations were selected to plot with the simulation results by the CALPUFF. These two stations monitored rain and ozone continuously.

Table 4.29 Details of 5 case studies for the simulation by the CALPUFF.

Case study	Reactive module	Precipitation	Hourly background ozone*	Default background ozone**
1	Not included	No	No	No
2	Not included	Yes	No	No
3	RIVAD/ARM3	Yes	No	Yes
4	RIVAD/ARM3	Yes	Yes	No
5	MESOPUFF	Yes	Yes	No

* Hourly background ozone is obtained from NPL station or KN station.

** Default background ozone is monthly averaged ozone of 150 $\mu g/m^3$ (80 ppb). This default value is provided by the CALPUFF.

(1) PM_{10} dispersion by the CALPUFF

As seen in Tables 4.30-4.31, the maximum of 1-hour and 24-hour averaged concentrations of PM_{10} at the same location and simulation period by the CALPUFF in case studies 1 and 2 are about 275.960 and 31.600 $\mu g/m^3$ and case studies 3-5 are about 276.200 and 31.616 $\mu g/m^3$, respectively. The results of 5 cases showed not much difference corresponding to almost no effects of wet deposition and chemically reactive module on the maximum 1-hour and

24- hour averaged concentrations of PM_{10}. The maximum 24-hour averaged concentration of PM_{10} from 5 cases were about 31.6 μg/m^3 (less than 120 μg/m^3 permitted by the NAAQS). No impact areas in Kaeng Khoi were affected by PM_{10} emissions from 14 stacks of the cement complex. In summary, the results of the CALPUFF with the chemically reactive modules (either RIVAD/ARM3 or MESOPUFF) and hourly background ozone agreed well with those of the AERMOD. The time-series plots (Figures 4.54-4.61) and contours of 1-hour averaged concentrations of PM_{10} (Figures 4.62-4.66) are shown.

Table 4.30 Summary of the maximum 1-hour averaged concentrations of PM_{10} by the CALPUFF.

Condition	Maximum concentration (μg/m^3)	Location of the maximum impact in UTM (X,Y) (km)	Local station time of the maximum impact
Case 1	275.960	721.75, 1618.75	21/10/2007 at 6.00 a.m.
Case 2	275.960	721.75, 1618.75	21/10/2007 at 6.00 a.m
Case 3	276.200	721.75, 1618.75	21/10/2007 at 6.00 a.m
Case 4	276.200	721.75, 1618.75	21/10/2007 at 6.00 a.m
Case 5	276.200	721.75, 1618.75	21/10/2007 at 6.00 a.m

Table 4.31 Summary of the maximum 24-hour averaged concentrations of PM_{10} by the CALPUFF.

Condition	Maximum concentration (μg/m^3)	Location of the maximum impact in UTM (X,Y) (km)	Local station time of the maximum impact
Case 1	31.600	728.25, 1620.25	19/11/2007
Case 2	31.610	728.25, 1620.25	19/11/2007
Case 3	31.616	728.25, 1620.25	19/11/2007
Case 4	31.616	728.25, 1620.25	19/11/2007
Case 5	31.616	728.25, 1620.25	19/11/2007

From Figures 4.54-4.55, the simulated 1-hour averaged PM_{10} concentrations at NPL and KN decreased in the rainy days. It can be concluded that the precipitation influences on the simulated PM_{10}.

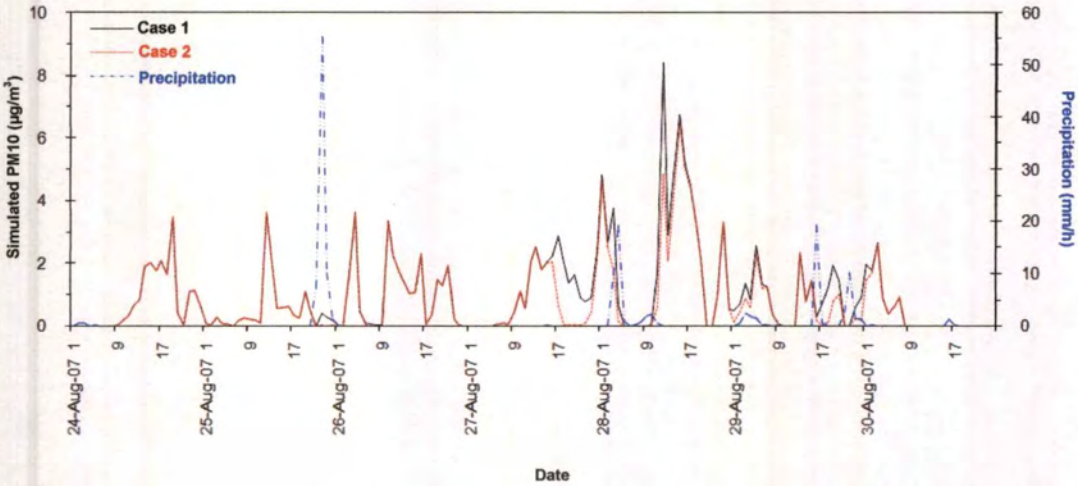

Figure 4.54 Time-series plots of simulated PM_{10} concentrations at Nah Phra Laan station for cases 1 and 2 by the CALPUFF (left axis) with hourly precipitation (right axis).

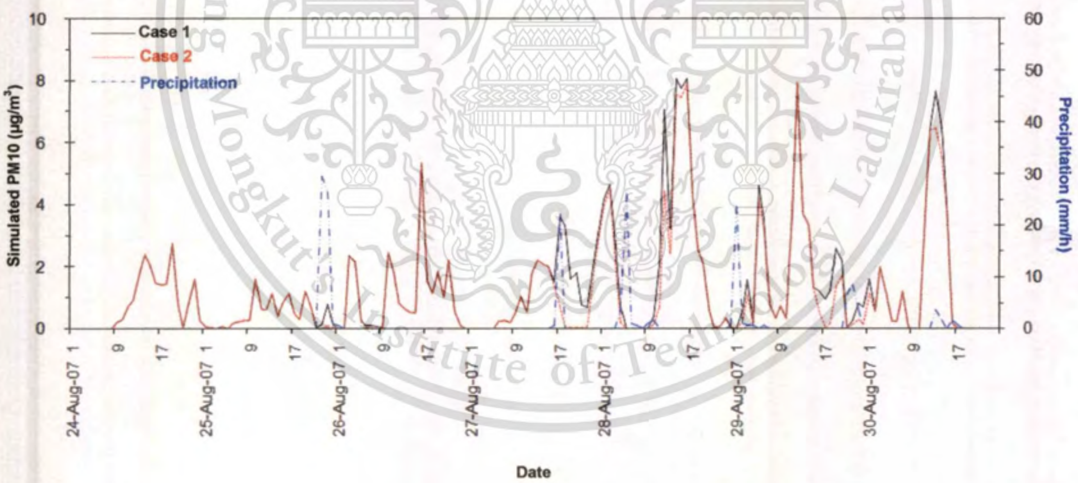

Figure 4.55 Time-series plots of simulated PM_{10} concentrations at Kao Noi station for cases 1 and 2 by the CALPUFF (left axis) with hourly precipitation (right axis).

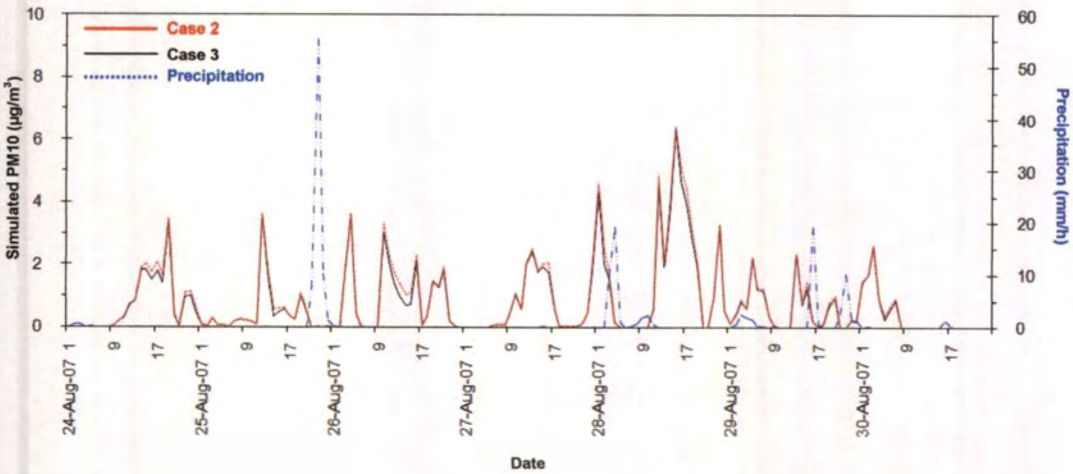

Figure 4.56 Time-series plots of simulated PM_{10} concentrations at Nah Phra Laan station for cases 2 and 3 by the CALPUFF (left axis) with hourly precipitation (right axis).

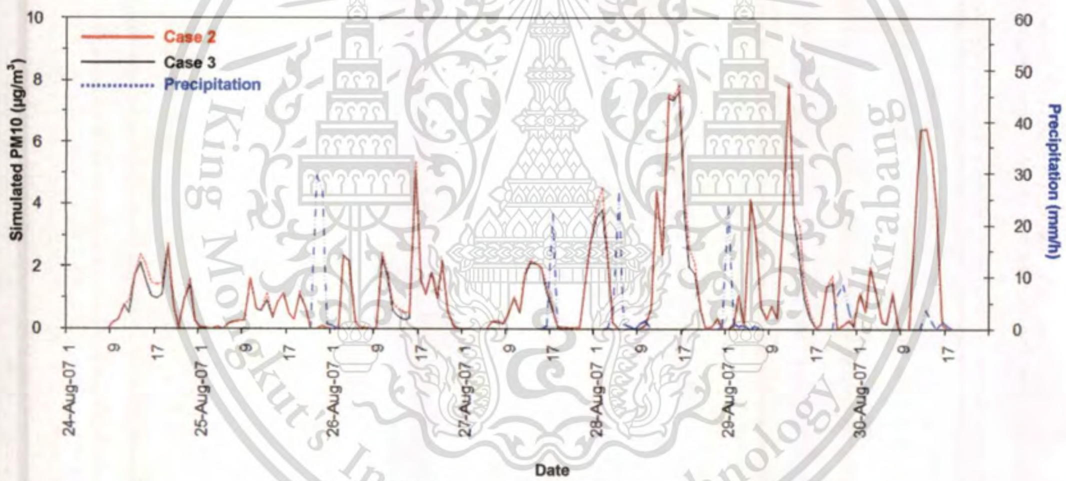

Figure 4.57 Time-series plots of simulated PM_{10} concentrations at Kao Noi station for cases 2 and 3 by the CALPUFF (left axis) with hourly precipitation (right axis).

Figures 4.56-4.57 show that the RIVAD/ARM3 chemically reactive module and default background ozone has almost no effect on the simulated 1-hour averaged PM_{10} concentrations. The simulated 1-hour averaged PM_{10} concentrations from case 3 are slightly lower than case 2.

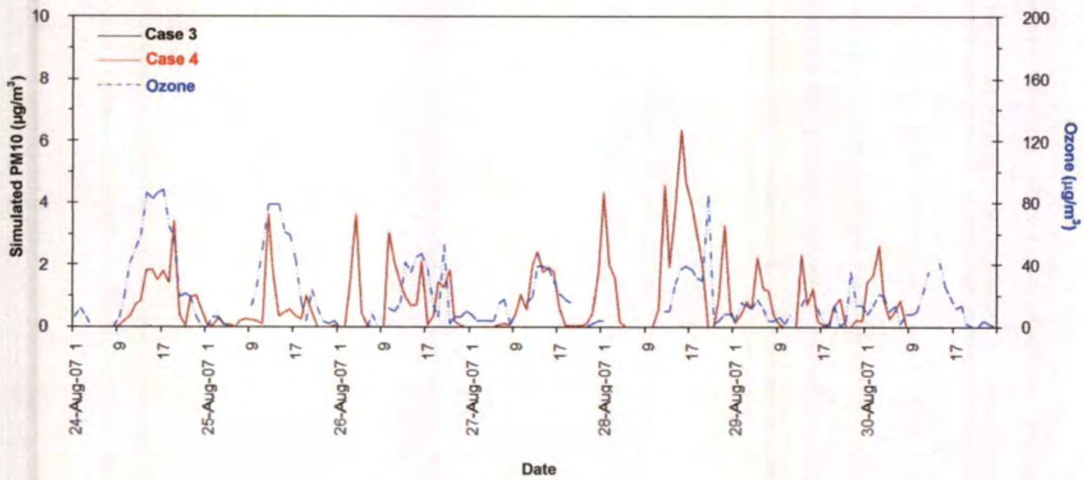

Figure 4.58 Time-series plots of simulated PM_{10} concentrations at Nah Phra Laan station for cases 3 and 4 by the CALPUFF (left axis) with hourly background ozone (right axis).

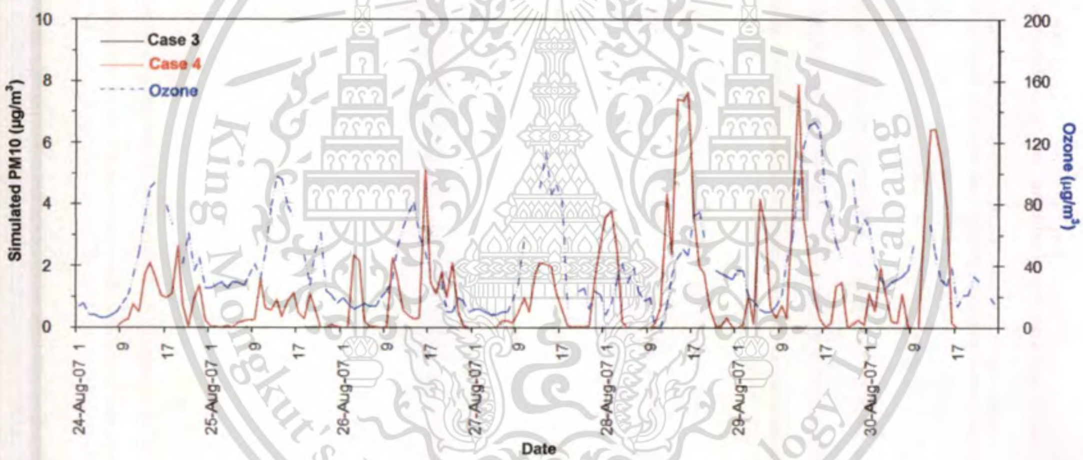

Figure 4.59 Time-series plots of simulated PM_{10} concentrations at Kao Noi station for cases 3 and 4 by the CALPUFF (left axis) with hourly background ozone (right axis).

The hourly background ozone in case 4 and default background ozone in a case 3 for the CALPUFF had no effect on the maximum simulated 1-hour and 24-hour averaged PM_{10} concentrations. Almost no differences between two cases at both stations were observed in Figures 4.58-4.59.

No effects of typically reactive modules of the RIVAD/ARM3 in case 4 and the MESOPUFF in case 5 on 1-hour averaged PM_{10} concentration because no different outputs were shown in Figures 4.60-4.61.

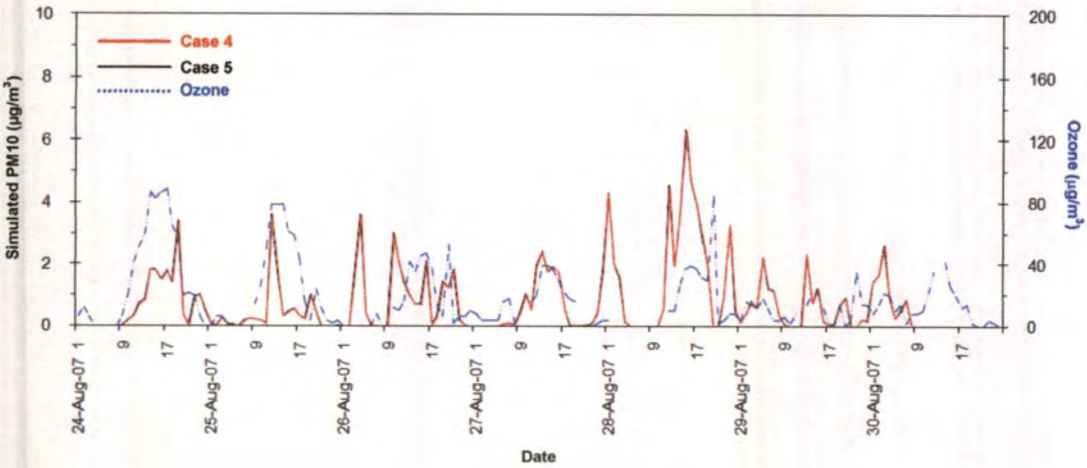

Figure 4.60 Time-series plots of simulated PM_{10} concentrations at Nah Phra Laan station for cases 4 and 5 by the CALPUFF (left axis) with hourly background ozone (right axis).

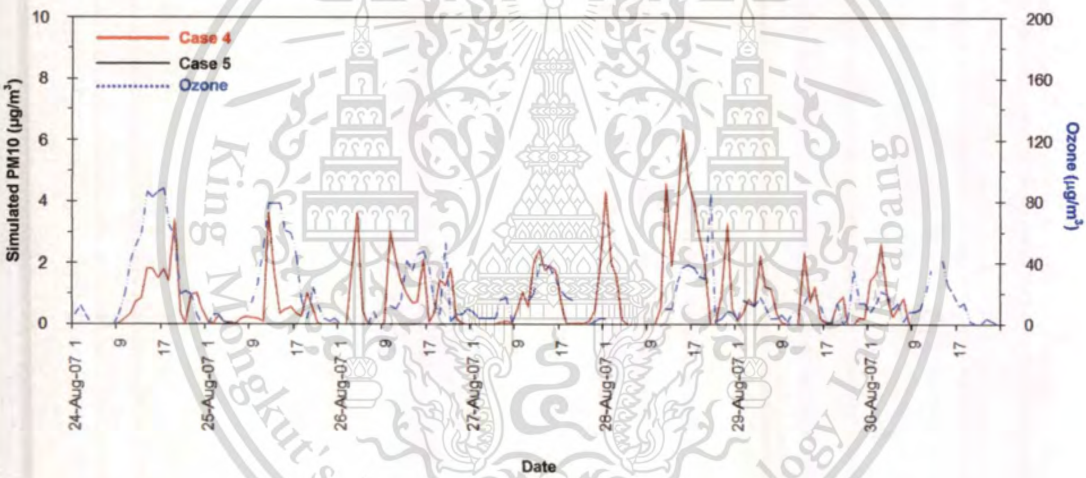

Figure 4.61 Time-series plots of simulated PM_{10} concentrations at Kao Noi station for cases 4 and 5 by the CALPUFF (left axis) with hourly background ozone (right axis).

From contours of the maximum simulated 1-hour averaged PM10 concentration from 5 cases by the CALPUFF in Figures 4.62-4.66, we can see that PM_{10} dispersed to all directions. The maximum concentrations were mostly observed in the northwest of the reference point and the area between the SCCC and SCG near the main road (receptors 1, 2, 6 and 8).

In summary, using the chemically reactive module and ozone background are not important to the simulation of PM_{10} dispersion by the CALPUFF, It is obviously that the precipitation has an effect on PM_{10} wet deposition but not a significant effect due to few rainy days in the study areas, as detailed in Table 4.17.

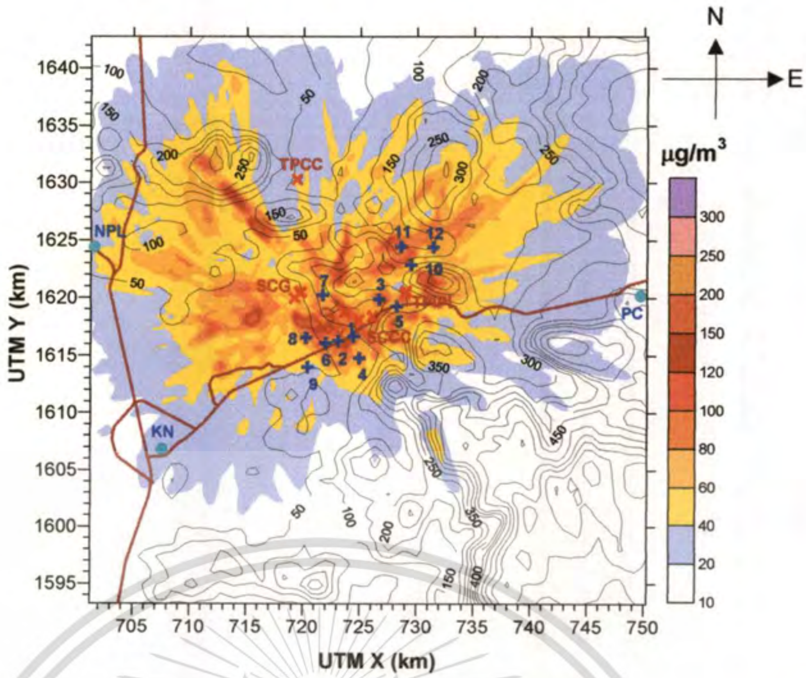

Figure 4.62 Contours of the maximum 1-hour averaged concentrations of PM_{10} by the CALPUFF case 1: (●) meteorological stations, (+) receptors and (×) stacks of cement plants.

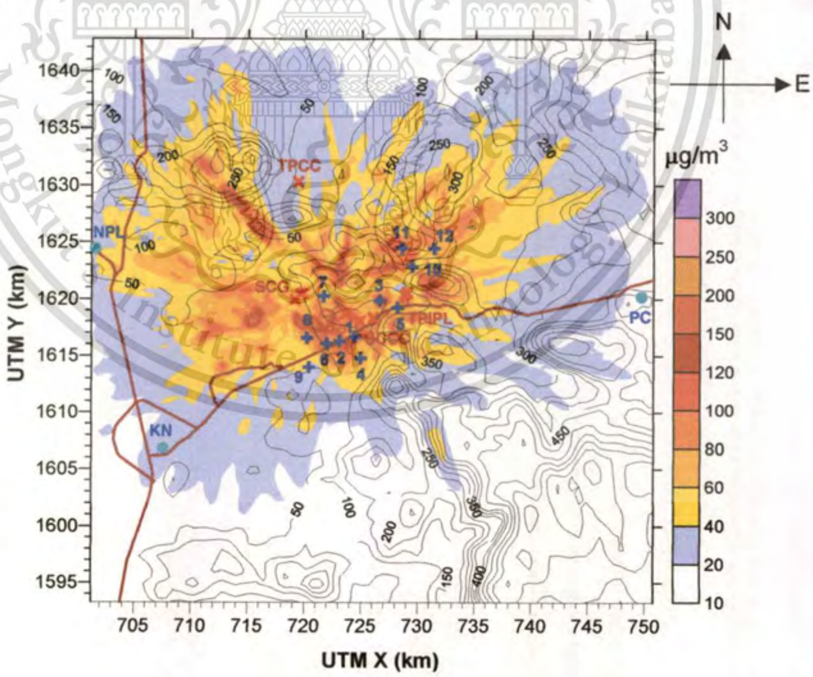

Figure 4.63 Contours of the maximum 1-hour averaged concentrations of PM_{10} by the CALPUFF case 2: (●) meteorological stations, (+) receptors and (×) stacks of cement plants.

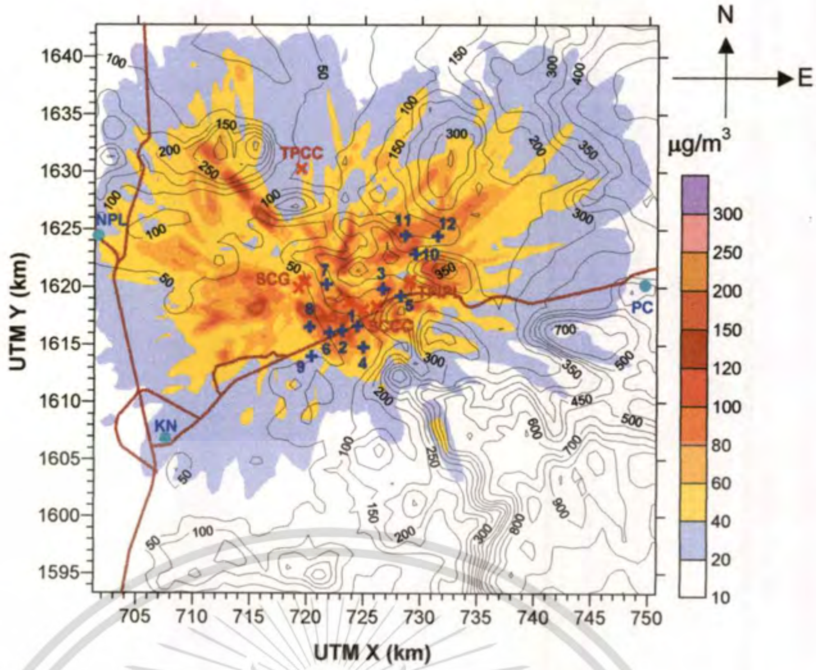

Figure 4.64 Contours of the maximum 1-hour averaged concentrations of PM_{10} by the CALPUFF case 3: (●) meteorological stations, (+) receptors and (×) stacks of cement plants.

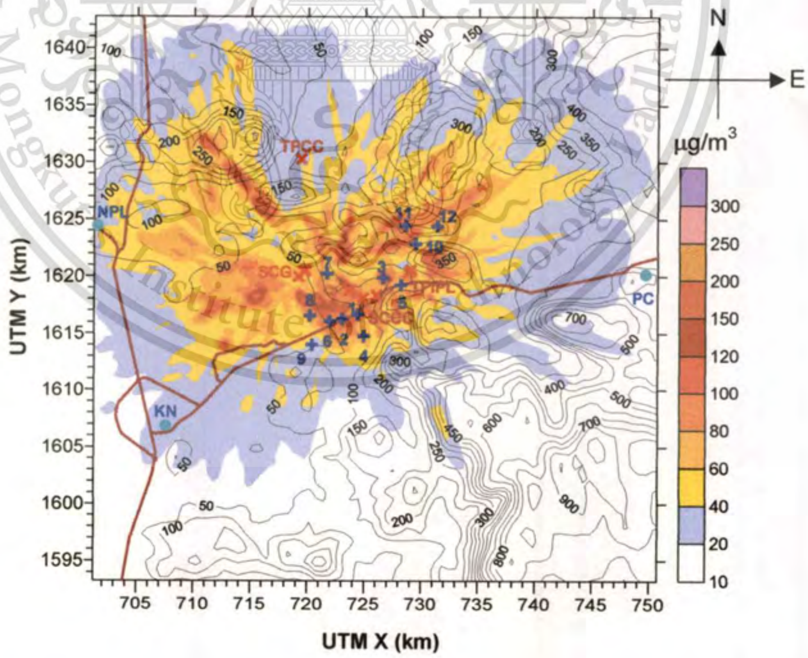

Figure 4.65 Contours of the maximum 1-hour averaged concentrations of PM_{10} by the CALPUFF case 4: (●) meteorological stations, (+) receptors and (×) stacks of cement plants.

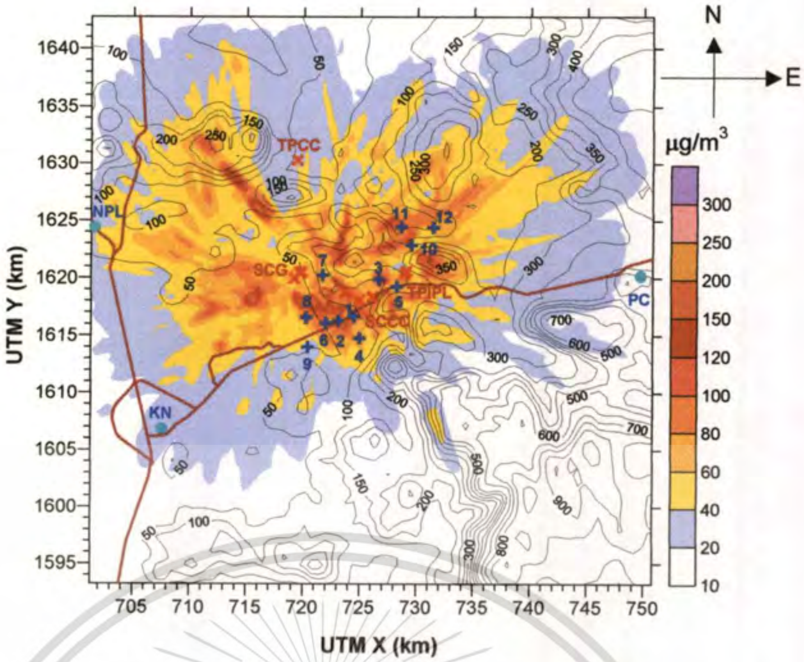

Figure 4.66 Contours of the maximum 1-hour averaged concentrations of PM_{10} by the CALPUFF case 5: (●) meteorological stations, (+) receptors and (×) stacks of cement plants.

(2) NO_2 dispersion by the CALPUFF

In section 4.2.2, a large amount of NO_2 emission from the stacks of the cement complex in Kaeng Khoi corresponding to a significant NO_2 concentration simulated by the AERMOD in section 4.5.1 was observed. In contrast, the maximum monitoring 1-hour averaged concentrations of NO_2 from 12 receptors did not exceed the NAAQS of 320 µg/m^3. Normally, NO_2 reacted with ozone and VOCs in the atmosphere to secondary PM. In this case, the CALPUFF with the chemically reactive modules was applied to verify the simulation results by the AERMOD. More precise simulation results were expected.

The maximum simulated 1-hour averaged concentrations of NO_2 by the CALPUFF for all 5 different cases in Table 4.32 exceeded the permit of the NAAQS. The simulation results by the CALPUFF confirmed a potential air pollution problem by NO_2 emission in the study areas. From Tables 4.32-4.33 and Figures 4.67-4.74 (the maximum 1-hour averaged concentrations of NO_2), we can see that the wet deposition in cases 1 (without precipitation) and 2 (with precipitation) had no effect on the maximum 1- hour and 24-hour averaged concentrations of NO_2 and almost no effect on the impact area.

The effects of chemical reaction of NO_2 with VOCs and ozone, case 2 (included the precipitation but no chemically reactive module and no default background ozone) and case 3 (included precipitation and a chemically reactive module, namely RIVAD/ARM3 and high default background ozone of 80 ppb) were examined. Low NO_2 concentration from case 3 was apparently observed but still exceeded the permit of the NAAQS (shown in Table 4.32). In addition, from the different chemical reaction modules in case 4 (RIVAD/ARM3) and case 5 (MESOPUFF), the simulated NO_2 concentration from case 5 was higher than that of case 4.

From the contours of maximum 1-hour averaged concentrations in Figures 4.75-4.79, the NO_2 dispersed in all directions. The maximum simulated 1-hour concentrations of NO_2 exceeding the permit of the NAAQS (320 $\mu g/m^3$) were mostly observed in the areas around the cement complex.

In the view point of air quality concern, the simulated NO_2 concentration should be justified by the CALPUFF with important parameters on NO_2 dispersion (e.g., the chemical module) for more precise evaluation. Without using the precipitation data (wet deposition) and reactive modules in the simulation may result in immense errors because these input data significantly relate to the NO_2 dispersion. In our study, for example, the impact areas from cases 1 (no precipitation, chemical module and background ozone) was 780 km^2 and case 3 (included precipitation, RIVAD/ARM3 and default background ozone) was 366 km^2.

Table 4.32 Summary of the maximum 1-hour averaged concentrations of NO_2 by the CALPUFF.

Condition	Maximum concentration ($\mu g/m^3$)	Location of the maximum impact in UTM (X,Y) (km)	Local station time of the maximum impact	Impact area (km^2)	Population in the impact area (persons)
Case 1	4,763.1	723.25, 1617.25	19/10/2007 at 5.00 a.m.	780	61,634
Case 2	4,763.1	723.25, 1617.25	19/10/2007 at 5.00 a.m.	769	60,774
Case 3	3,079.3	723.25, 1617.25	19/10/2007 at 5.00 a.m.	366	28,899
Case 4	3,730.3	723.25, 1617.25	19/10/2007 at 5.00 a.m.	678	53,581
Case 5	4,070.4	723.25, 1617.25	19/10/2007 at 5.00 a.m.	765	60,460

* Impact area is the area with the exposure of NO_2 concentration higher than 320 $\mu g/m^3$

** People in the impact area = Impact area (km^2) × 79 (persons/km^2)

Table 4.33 Summary of the maximum 24-hour averaged concentrations of NO_2 by the CALPUFF.

Condition	Maximum concentration ($\mu g/m^3$)	Location of the maximum impact in UTM (X,Y) (km)	Local station time of the maximum impact
Case 1	401.1	723.25, 1617.75	18/01/2007
Case 2	401.1	723.25, 1617.75	18/01/2007
Case 3	310.0	723.25, 1617.75	18/01/2007
Case 4	323.2	723.25, 1617.75	18/01/2007
Case 5	331.9	723.25, 1617.75	18/01/2007

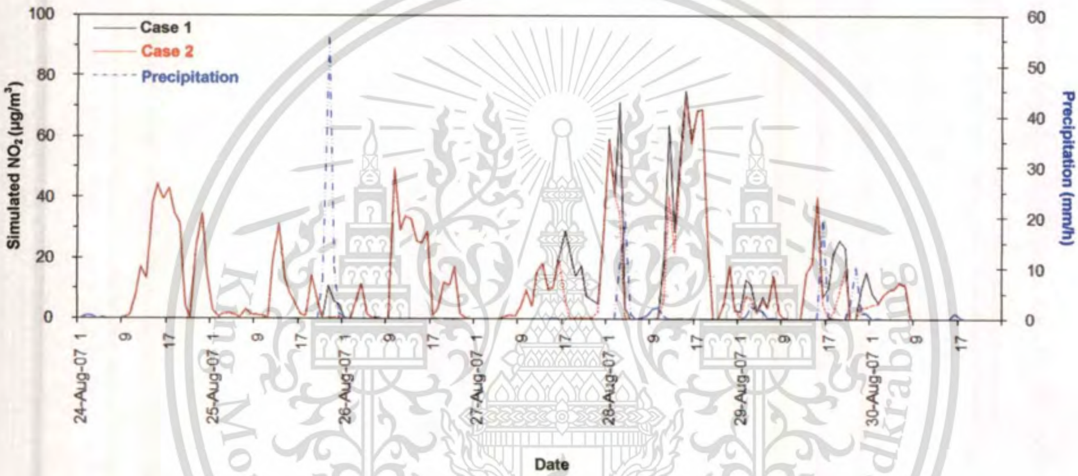

Figure 4.67 Time-series plots of simulated NO_2 concentrations at Nah Phra Laan station for cases 1 and 2 by the CALPUFF (left axis) with hourly precipitation (right axis).

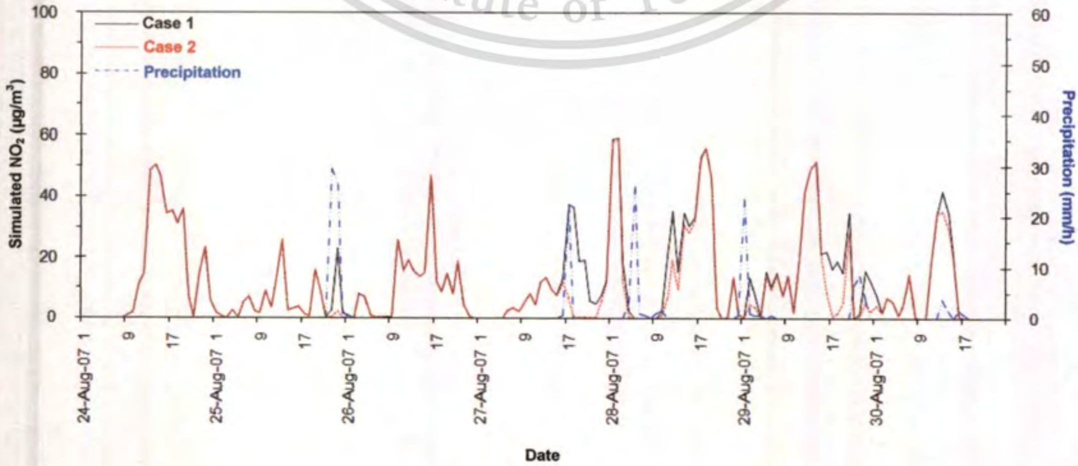

Figure 4.68 Time-series plots of simulated NO_2 concentrations at Kao Noi station for cases 1 and 2 by the CALPUFF (left axis) with hourly precipitation (right axis).

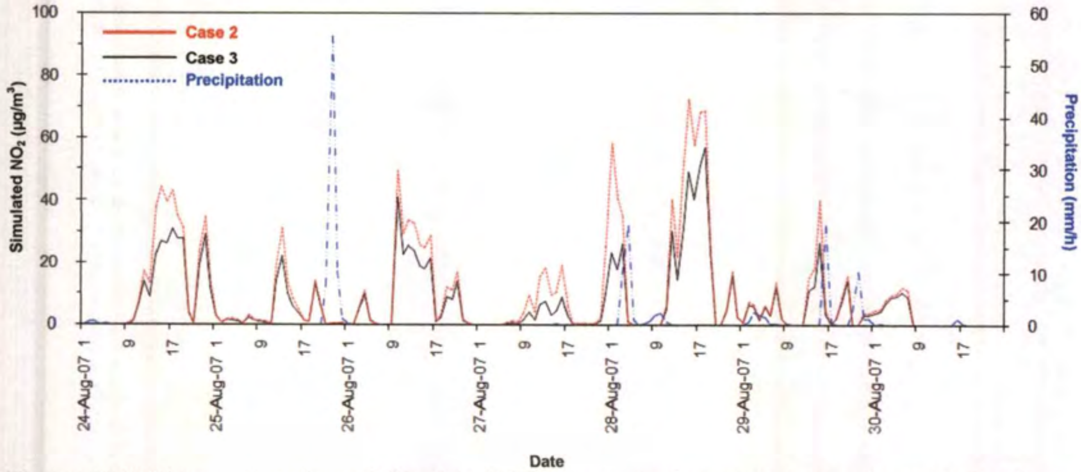

Figure 4.69 Time-series plots of simulated NO_2 concentrations at Nah Phra Laan station for cases 2 and 3 by the CALPUFF (left axis) with hourly precipitation (right axis).

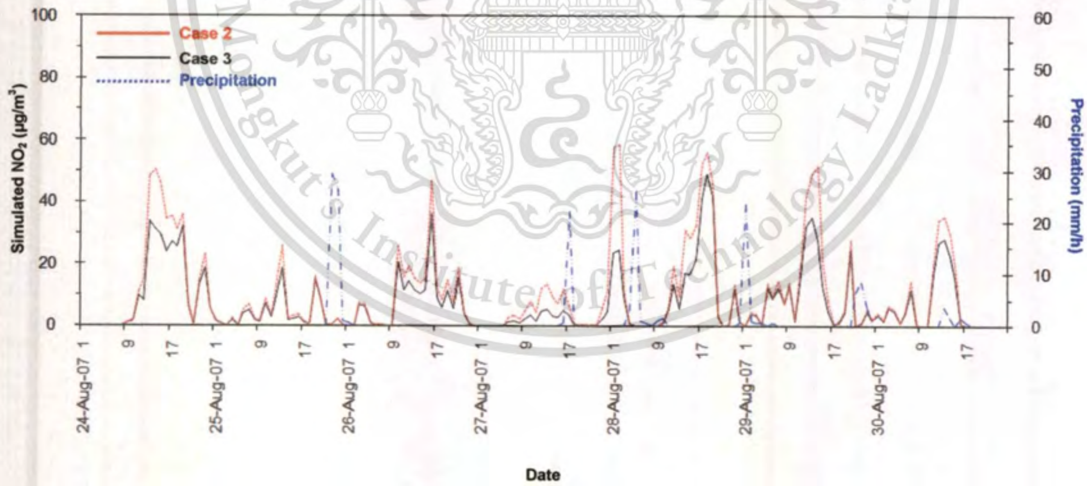

Figure 4.70 Time-series plots of simulated NO_2 concentrations at Kao Noi station for cases 2 and 3 by the CALPUFF (left axis) with hourly precipitation (right axis).

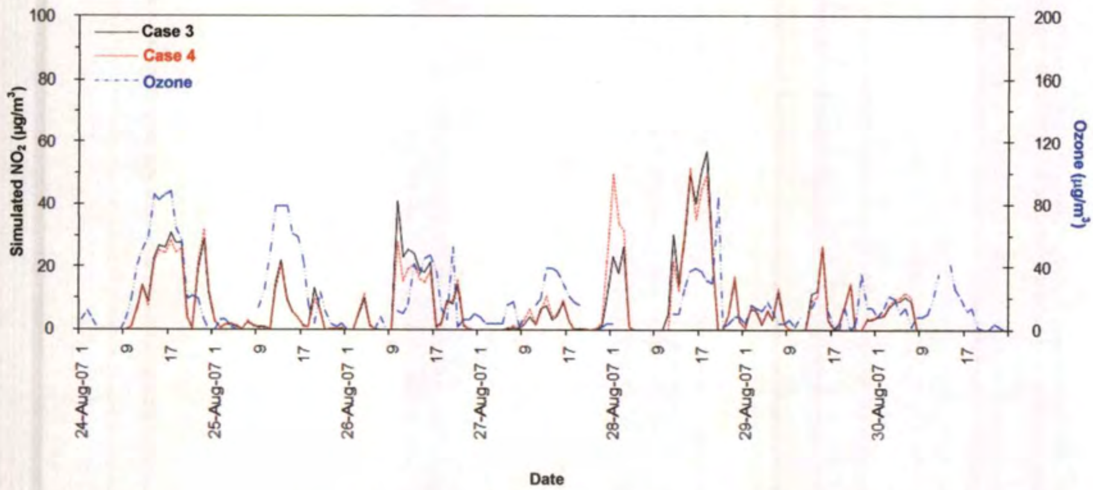

Figure 4.71 Time-series plots of simulated NO_2 concentrations at Nah Phra Laan station for cases 3 and 4 by the CALPUFF (left axis) with hourly background ozone (right axis).

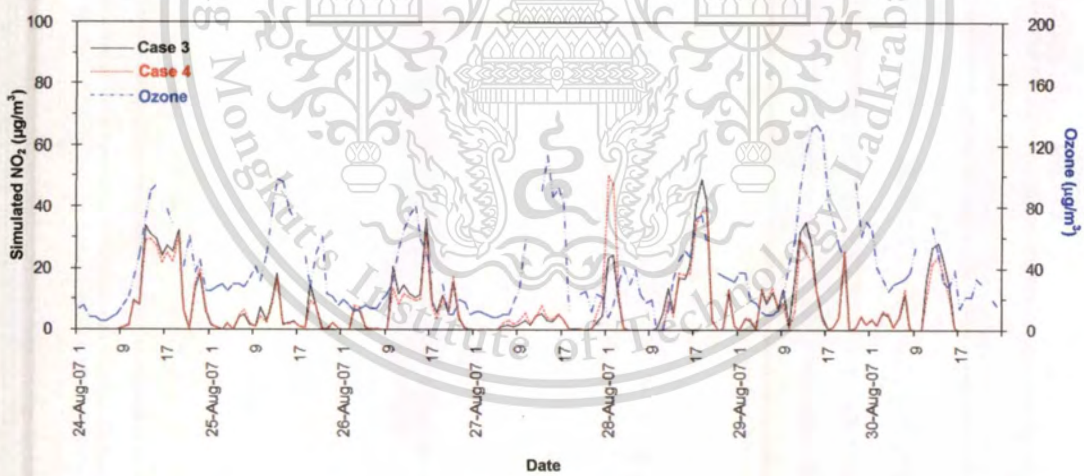

Figure 4.72 Time-series plots of simulated NO_2 concentrations at Kao Noi station for cases 3 and 4 by the CALPUFF (left axis) with hourly background ozone (right axis).

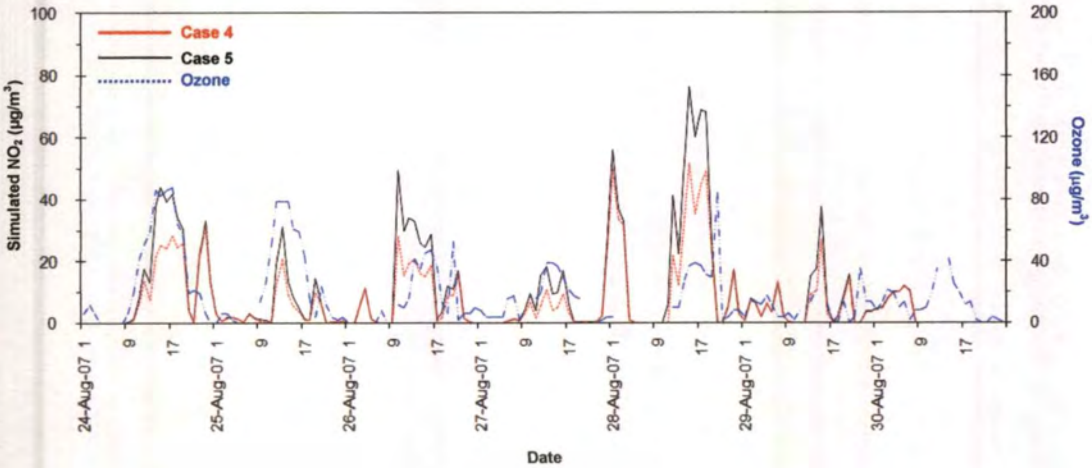

Figure 4.73 Time-series plots of simulated NO_2 concentrations at Nah Phra Laan station for cases 4 and 5 by the CALPUFF (left axis) with hourly background ozone (right axis).

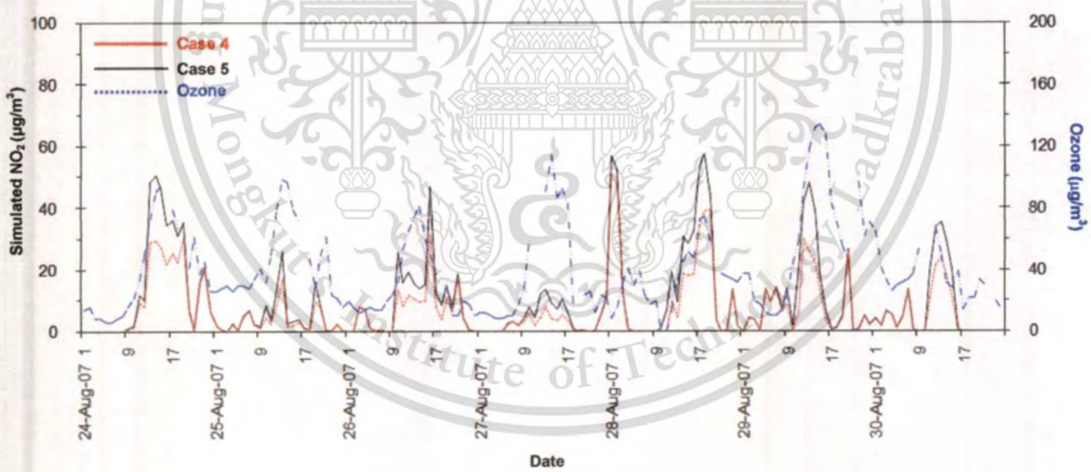

Figure 4.74 Time-series plots of simulated NO_2 concentrations at Kao Noi station for cases 4 and 5 by the CALPUFF (left axis) with hourly background ozone (right axis).

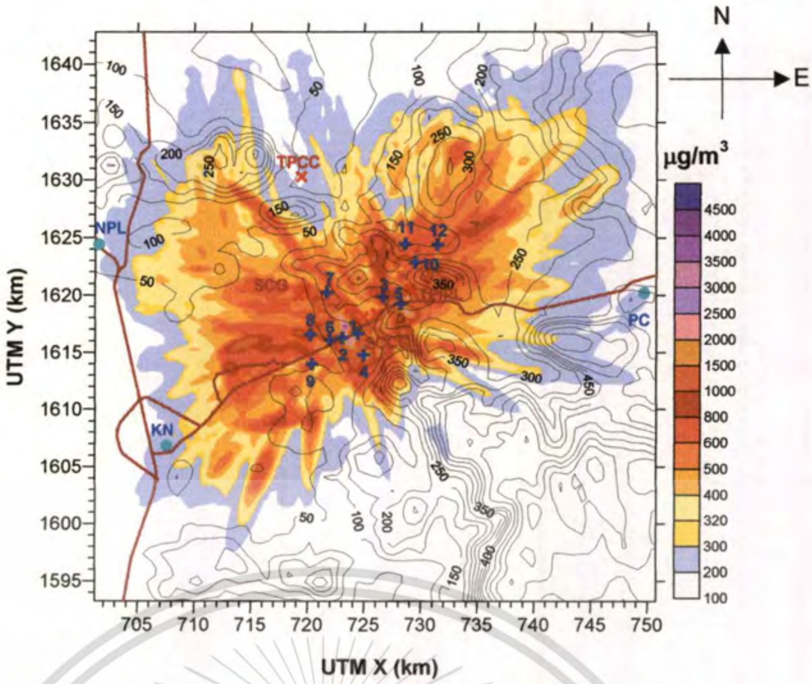

Figure 4.75 Contours of the maximum 1-hour averaged concentrations of NO_2 by the CALPUFF case 1: (●) meteorological stations, (+) receptors and (×) stacks of cement plants.

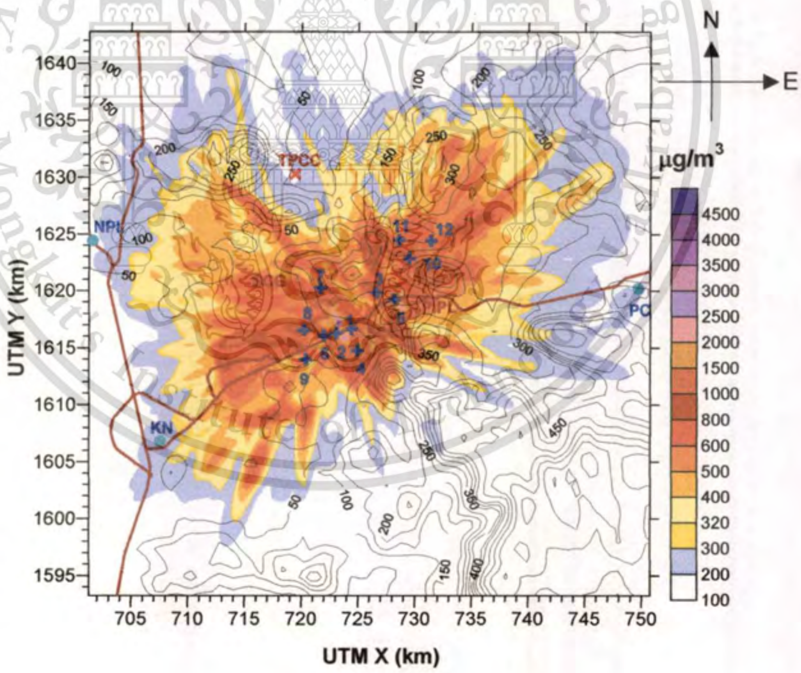

Figure 4.76 Contours of the maximum 1-hour averaged concentrations of NO_2 by the CALPUFF case 2: (●) meteorological stations, (+) receptors and (×) stacks of cement plants.

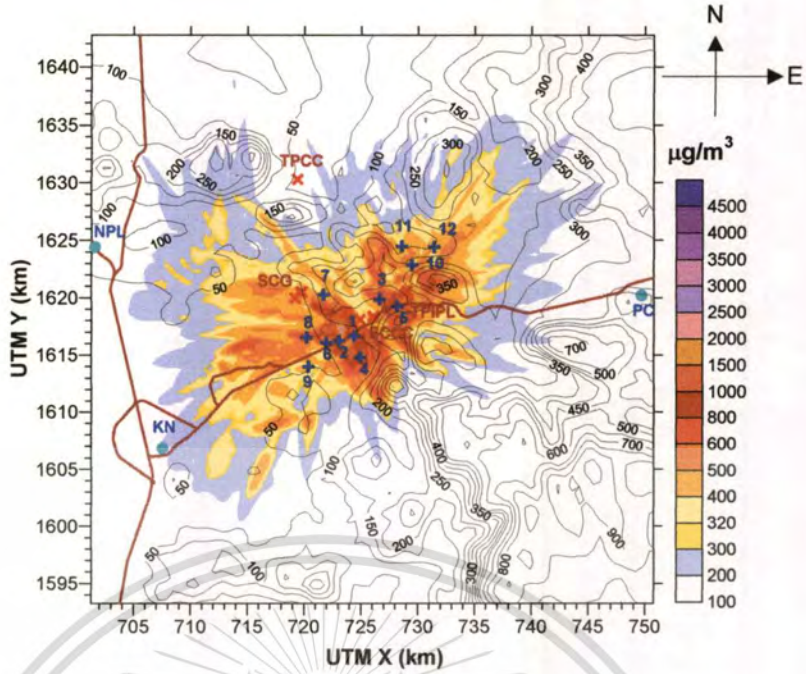

Figure 4.77 Contours of the maximum 1-hour averaged concentrations of NO_2 by the CALPUFF case 3: (●) meteorological stations, (+) receptors and (×) stacks of cement plants.

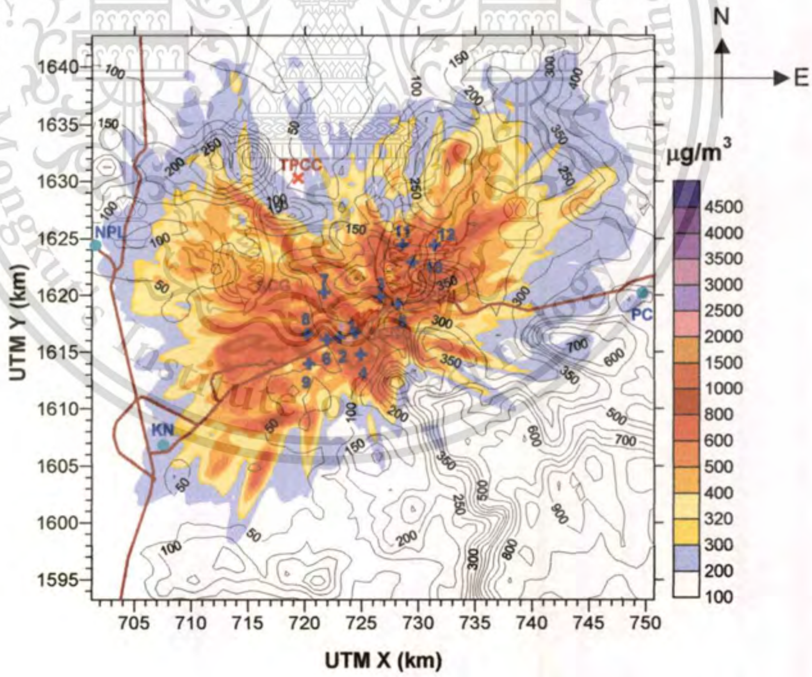

Figure 4.78 Contours of the maximum 1-hour averaged concentrations of NO_2 by the CALPUFF case 4: (●) meteorological stations, (+) receptors and (×) stacks of cement plants.

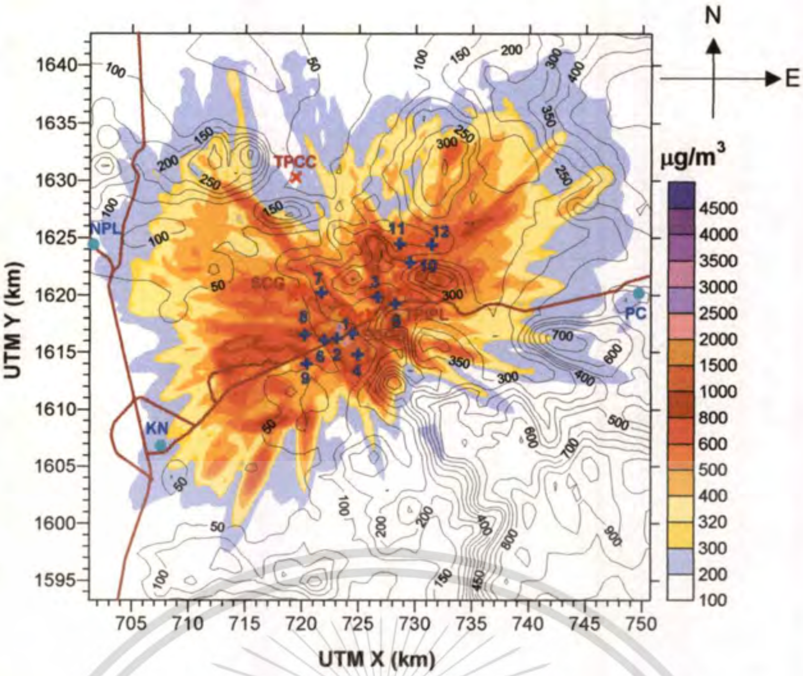

Figure 4.79 Contours of the maximum 1-hour averaged concentrations of NO_2 by the CALPUFF case 5: (●) meteorological stations, (+) receptors and (×) stacks of cement plants.

(3) SO_2 dispersion by the CALPUFF

From the results in section 4.2.2, the monitoring SO_2 concentrations from 14 stacks of the cement complex and the SO_2 concentration simulated by the AERMOD are very low. In the same way as PM_{10} and NO_2, we verify the results by using the CALPUFF.

As seen in Tables 4.34-4.35 the maximum of 1-hour and 24-hour averaged concentrations of SO_2 by the CALPUFF for 5 case studies are extremely lower than the permit by the NAAQS of 780 µg/m^3 and 300 µg/m^3, respectively (WHO's guideline of 20 µg/m^3 for 24-hour averaged). The SO_2 emissions from 14 stacks of the cement complex in the study areas have no significant impact on the nearby communities and environment.

The time-series plots of simulated SO_2 concentrations were shown in Figures 4.80-4.87. From Figures 4.80-4.81, the simulated SO_2 at NPL and KN stations decreased in rainy days. This implies that precipitation affects SO_2 wet deposition.

In case of other interested study area of high SO_2, it is suggested to include the important parameters that relate to the SO_2 dispersion, e.g., precipitation data in the CALPUFF for a precise simulation. In our work due to very low SO_2 concentration, the reactive modules (RIVAD/ARM3 and MESOPUFF) and background ozone had almost no effect on the simulated SO_2 concentrations.

Table 4.34 Summary of the maximum 1-hour averaged concentrations of SO_2 by the CALPUFF.

Condition	Maximum concentration ($\mu g/m^3$)	Location of the maximum impact in UTM (X,Y) (km)	Local station time of the maximum impact
Case 1	27.600	723.25, 1617.25	19/10/2007 at at 5.00 a.m.
Case 2	27.602	723.25, 1617.25	19/10/2007 at at 5.00 a.m.
Case 3	23.622	723.250, 1617.25	19/10/2007 at at 5.00 a.m.
Case 4	23.622	723.25, 1617.25	19/10/2007 at at 5.00 a.m.
Case 5	23.622	723.25, 1617.25	19/10/2007 at at 5.00 a.m.

Table 4.35 Summary of the maximum 24-hour averaged concentrations of SO_2 by the CALPUFF.

Condition	Maximum concentration ($\mu g/m^3$)	Location of the maximum impact in UTM (X,Y) (km)	Local station time of the maximum impact
Case 1	4.1633	728.25, 1620.25	19/11/2007
Case 2	4.1609	728.25, 1620.25	19/11/2007
Case 3	4.1606	728.25, 1620.25	19/11/2007
Case 4	4.1607	728.25, 1620.25	19/11/2007
Case 5	4.1601	728.25, 1620.25	19/11/2007

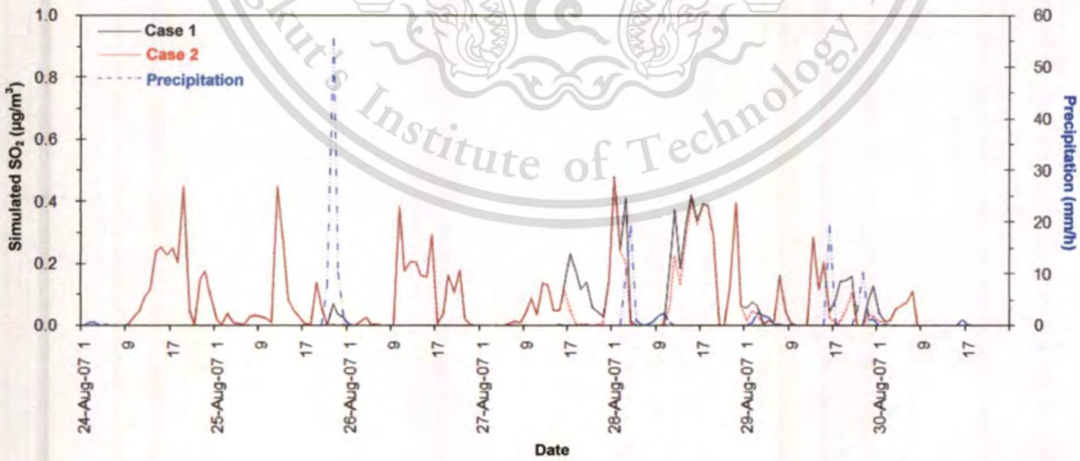

Figure 4.80 Time-series plots of simulated SO_2 concentrations at Nah Phra Laan station for cases 1 and 2 by the CALPUFF (left axis) with hourly precipitation (right axis).

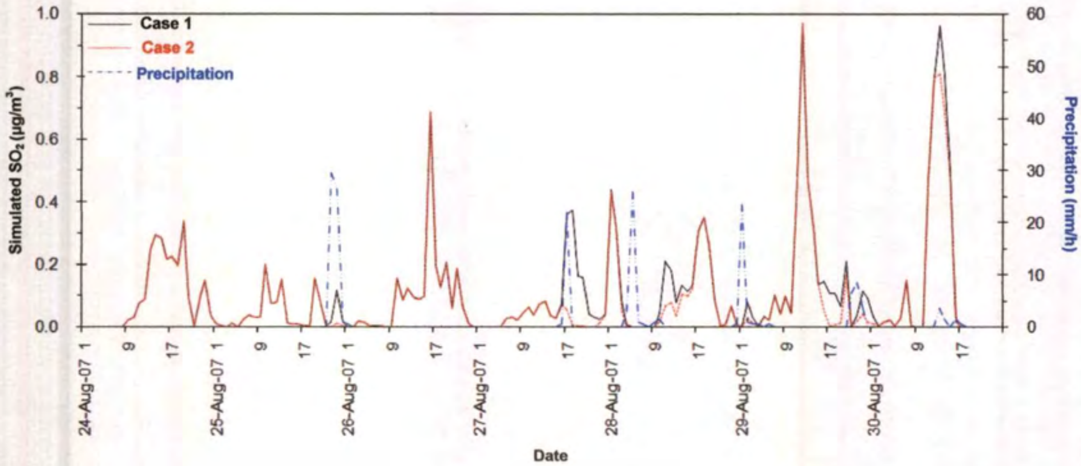

Figure 4.81 Time-series plots of simulated SO_2 concentrations at Kao Noi station for cases 1 and 2 by the CALPUFF (left axis) with hourly precipitation (right axis).

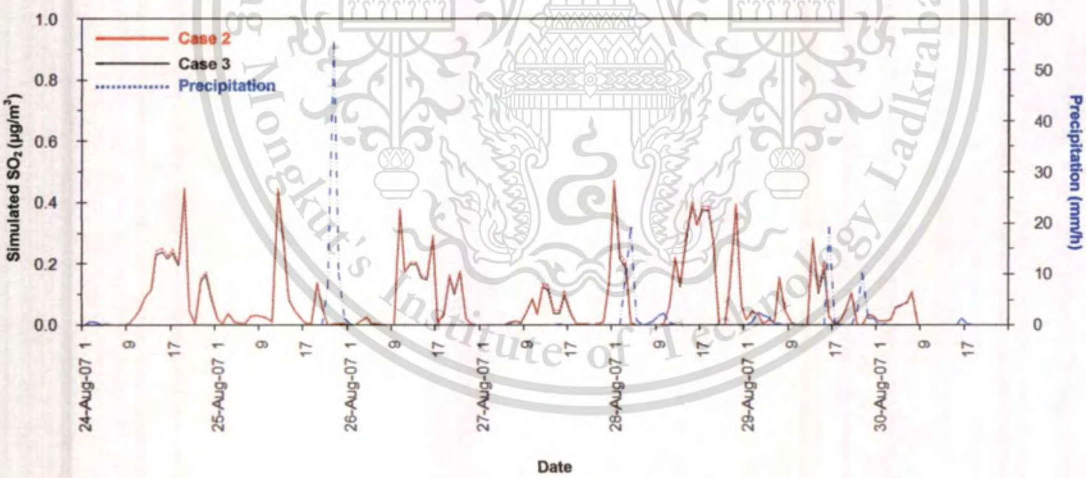

Figure 4.82 Time-series plots of simulated SO_2 concentrations at Nah Phra Laan station for cases 2 and 3 by the CALPUFF (left axis) with hourly precipitation (right axis).

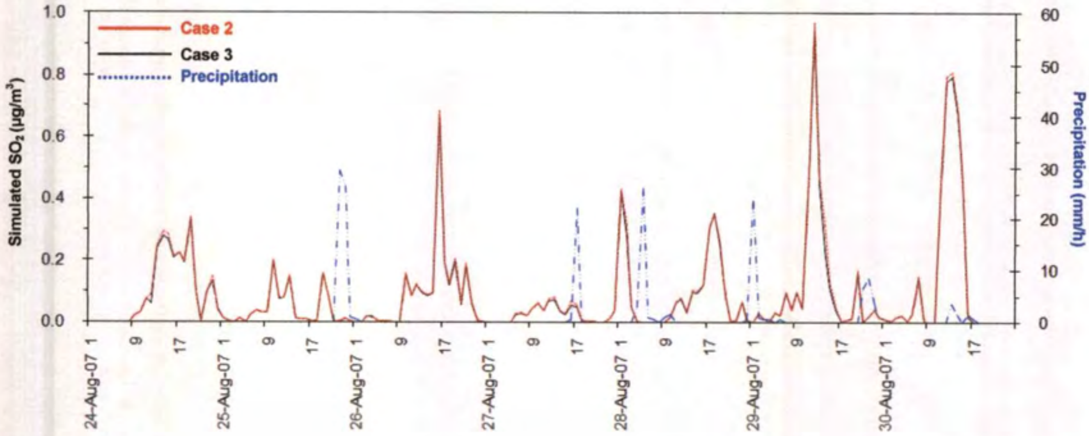

Figure 4.83 Time-series plots of simulated SO_2 concentrations at Kao Noi station for cases 2 and 3 by the CALPUFF (left axis) with hourly precipitation (right axis).

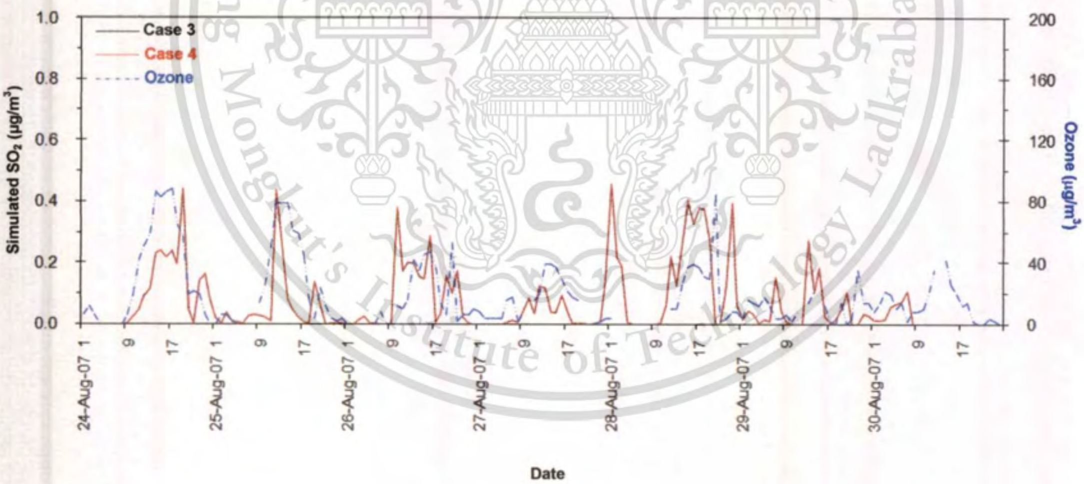

Figure 4.84 Time-series plots of simulated SO_2 concentrations at Nah Phra Laan station for cases 3 and 4 by the CALPUFF (left axis) with hourly background ozone (right axis).

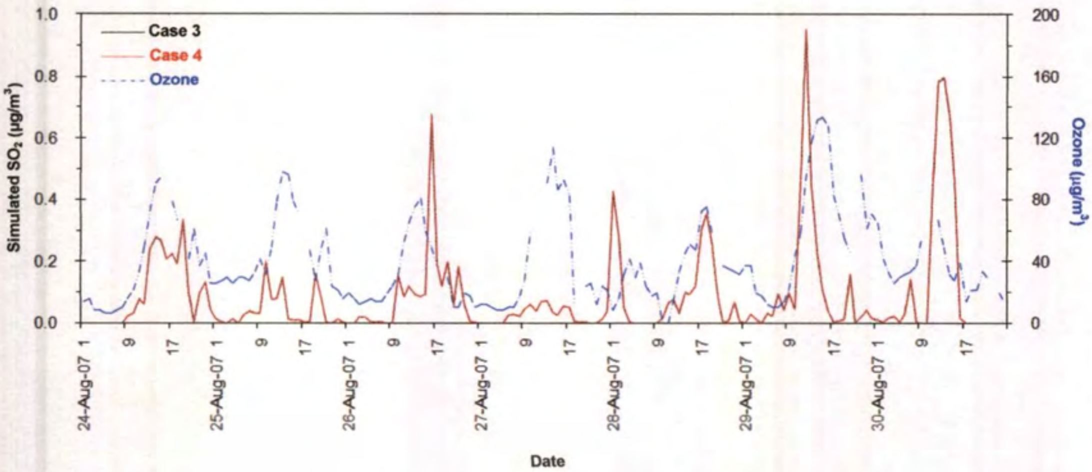

Figure 4.85 Time-series plots of simulated SO_2 concentrations at Kao Noi station for cases 3 and 4 by the CALPUFF (left axis) with hourly background ozone (right axis).

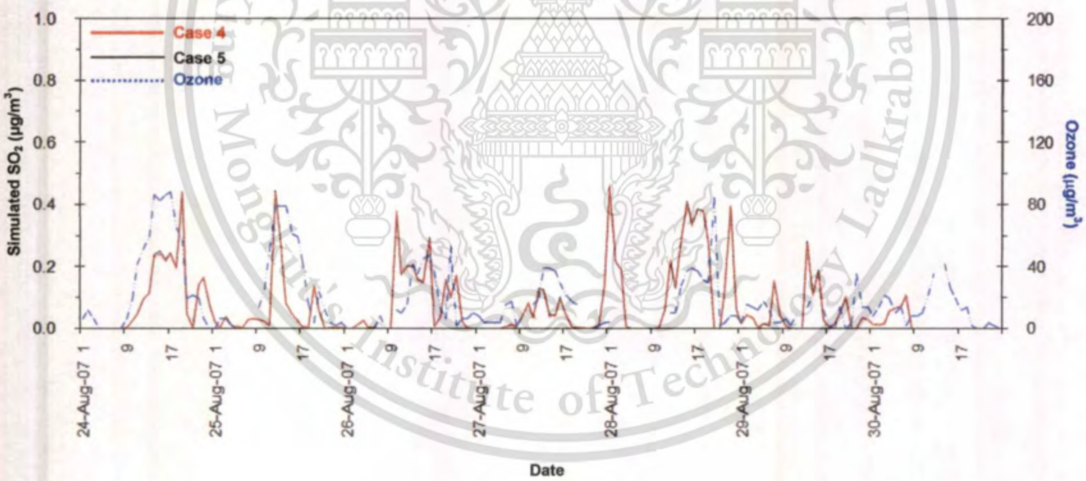

Figure 4.86 Time-series plots of simulated SO_2 concentrations at Nah Phra Laan station for cases 4 and 5 by the CALPUFF (left axis) with hourly background ozone (right axis).

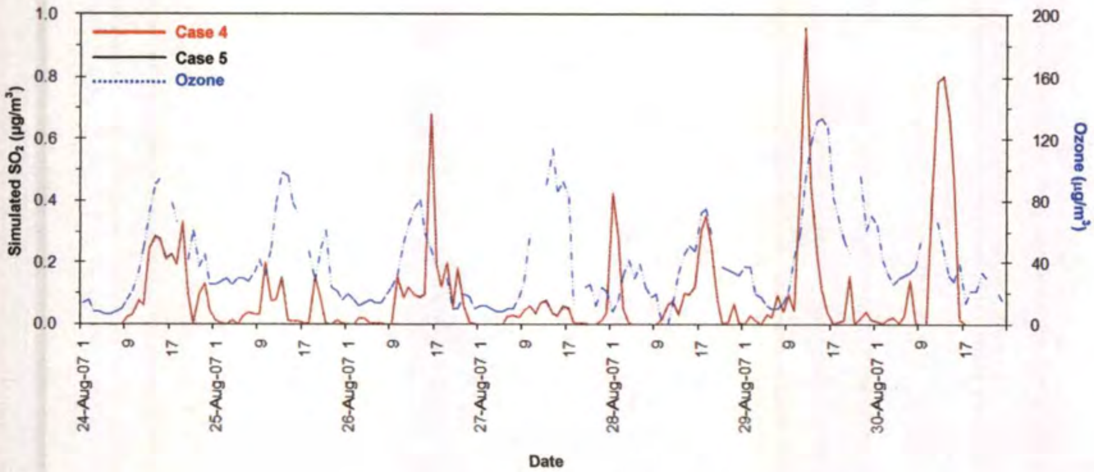

Figure 4.87 Time-series plots of simulated SO_2 concentrations at Kao Noi station for cases 4 and 5 by the CALPUFF (left axis) with hourly background ozone (right axis).

The contours of the maximum 1-hour averaged SO_2 concentrations were shown in Figures 4.88-4.92. The simulated SO_2 dispersed to all directions around the area of 4 cement manufacturers. The maximum concentrations, not exceeding the NAAQS of 780 µg/m^3, were mostly found in the areas around the SCCC, SCG and TPIPL.

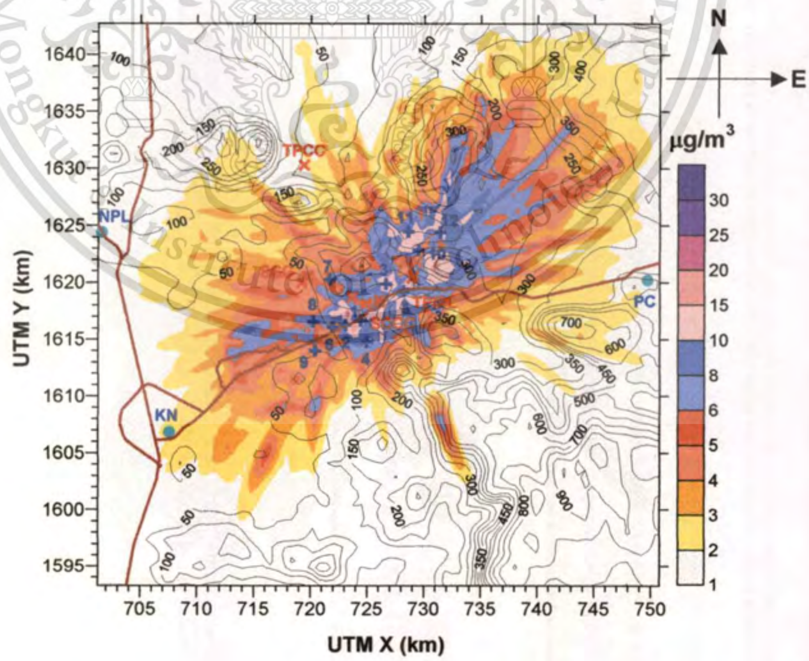

Figure 4.88 Contours of the maximum 1-hour averaged concentrations of SO_2 by the CALPUFF case 1: (●) meteorological stations, (+) receptors and (×) stacks of cement plants.

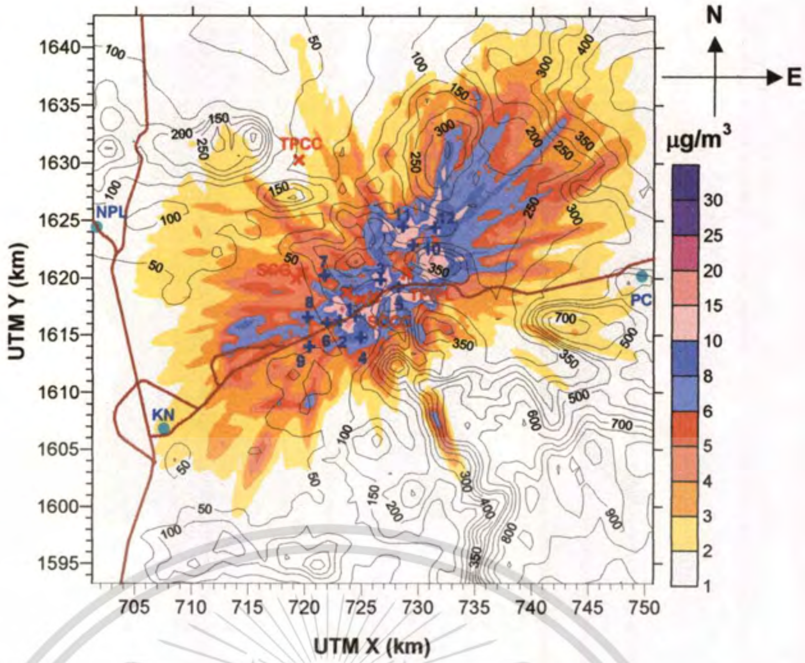

Figure 4.89 Contours of the maximum 1-hour averaged concentrations of SO_2 by the CALPUFF case 2: (●) meteorological stations, (+) receptors and (×) stacks of cement plants.

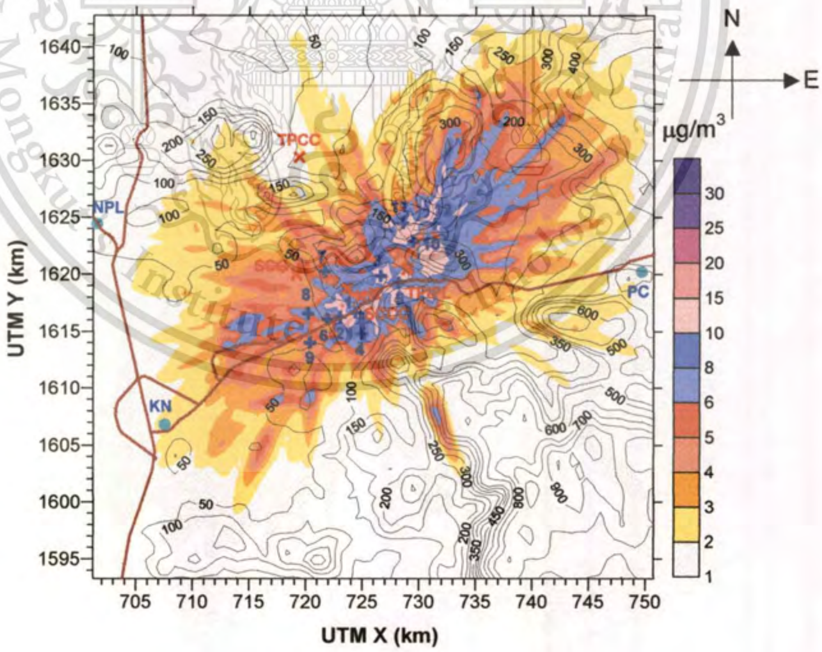

Figure 4.90 Contours of the maximum 1-hour averaged concentrations of SO_2 by the CALPUFF case 3: (●) meteorological stations, (+) receptors and (×) stacks of cement plants.

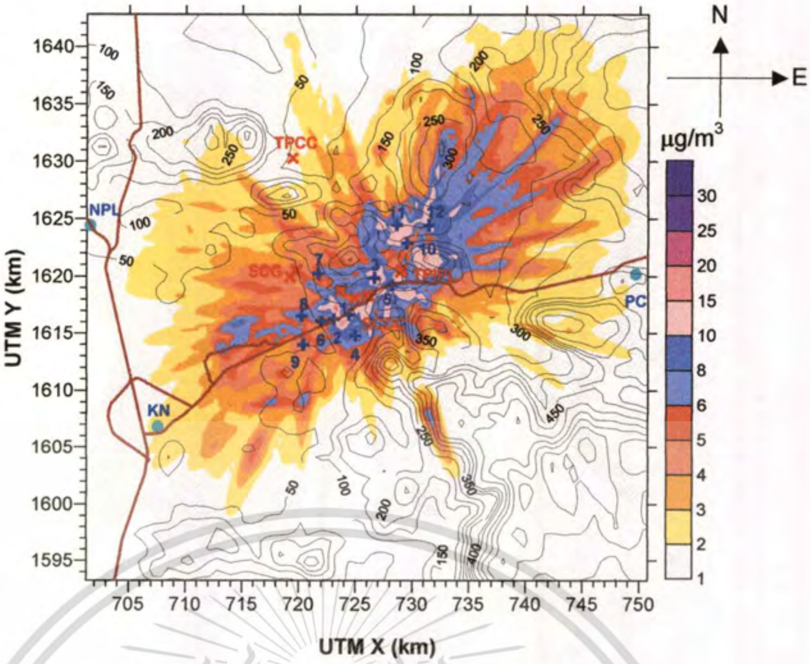

Figure 4.91 Contours of the maximum 1-hour averaged concentrations of SO_2 by the CALPUFF case 4: (●) meteorological stations, (+) receptors and (×) stacks of cement plants.

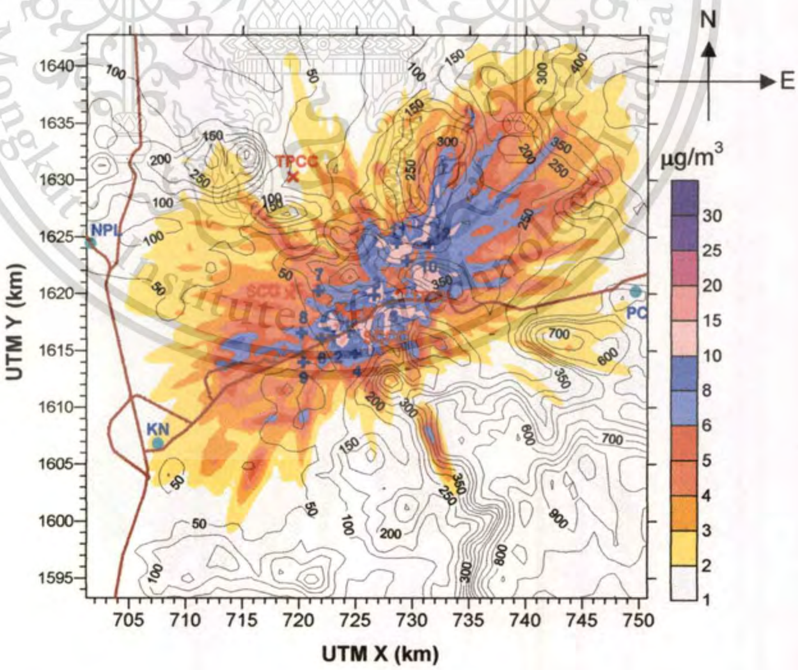

Figure 4.92 Contours of the maximum 1-hour averaged concentrations of SO_2 by the CALPUFF case 5: (●) meteorological stations, (+) receptors and (×) stacks of cement plants.

(4) Evaluation of NO_2 dispersions by the CALPUFF

In a similar way to the AERMOD in section 4.5.2, the performance of CALPUFF PROfessional Beta 5.2.0 was validated by the Q-Q plots of NO_2 dispersion from 14 stacks of the cement complex in Kaeng Khoi. The input surface data were obtained from Nah Phra Laan, Kao Noi and Pak Chong stations whereas the upper air data were obtained from Bang Na station. The precipitation data were prepared from the rain record at Nah Phra Laan and Kao Noi stations. The CALPUFF included RIVAD/ARM3 and hourly background ozone (monitored at NPL and KN stations) was applied.

From Table 4.36, the maximum 1-hour averaged NO_2 concentrations in dry and wet seasons of 2,285.6 $\mu g/m^3$ and 3,730.3 $\mu g/m^3$, respectively were exceeded the permit by the NAAQS. In dry season, the maximum simulated concentration of NO_2 was observed on the east of the domain (in the area between the SCCC and TPIPL near receptors 3 and 5) while in wet season it was observed on the west of the domain (in the area between the SCCC and SCG near receptor 8) due to the effects of the seasonal winds (northeasterly and southwesterly monsoons) over the domain. The impact areas in the dry and wet seasons are 541 and 438 km^2, respectively.

Table 4.36 The maximum of 1-hour averaged NO_2 concentrations in dry and wet seasons predicted by the CALPUFF.

Scenario	NO_2 maximum concentration ($\mu g/m^3$)	Local station time of the maximum impact	Location of the maximum impact in UTM (X,Y) (km)	Impact area (km^2)*	Details of impact areas
Dry season	2,285.6	10th March 2007 at 3.00 a.m.	728.75, 1619.75	541	Agricultural area between SCCC and TPIPL near receptors 3 and 5
Wet season	3,730.3	19th October 2007 at 5.00	723.25, 1617.25	438	Agricultural area near SCCC and SCG near receptor 8

* Impact area is the area with the exposure of NO_2 concentration higher than 320 $\mu g/m^3$

From Figures 4.93-4.94, we can observe higher peaks of simulated NO_2 in dry season than in wet season same as the simulation results by the AERMOD. This attributed to the effect of the wet depositions.

The performance of the CALPUFF can be seen from the Q-Q plots in Figures 4.95-4.96. The simulation results agreed well with the monitoring data at some receptors, for example, receptors 5, 7 and 10 in dry season and receptors 3 and 4 in wet season. In this regards, it is possible that there might be error in the monitoring. Difficult-accessible or inaccessible locations of the receptors made them not possible to detect and distinguish the air pollutants emitting from the cement complex exactly. The trajectories or plumes of the simulated 1-hour averaged concentrations of NO_2 can help to determine the areas of high impact hit by the plumes.

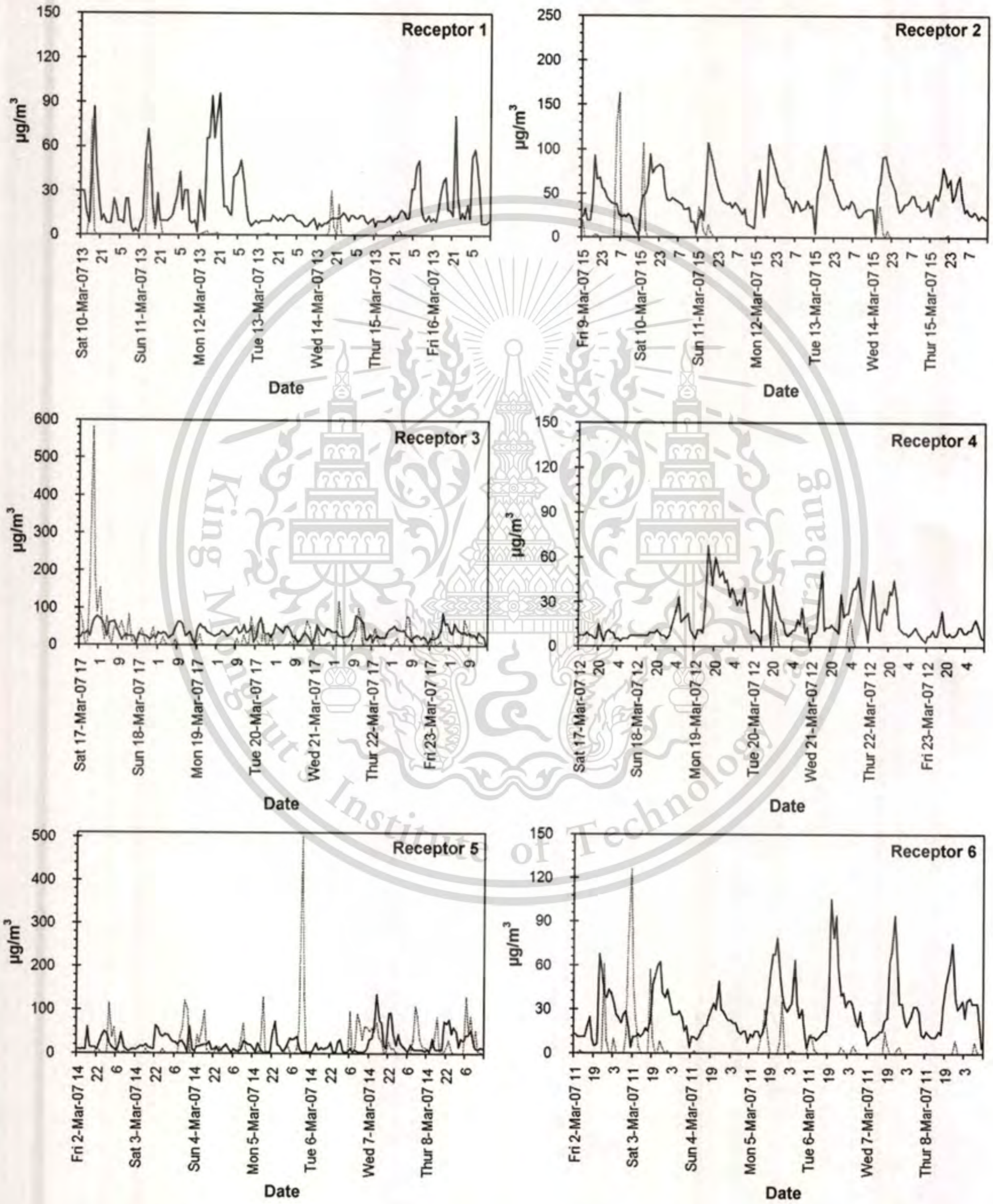

Figure 4.93 NO_2 concentrations in dry season: solid line by measurements and dashed line by CALPUFF.

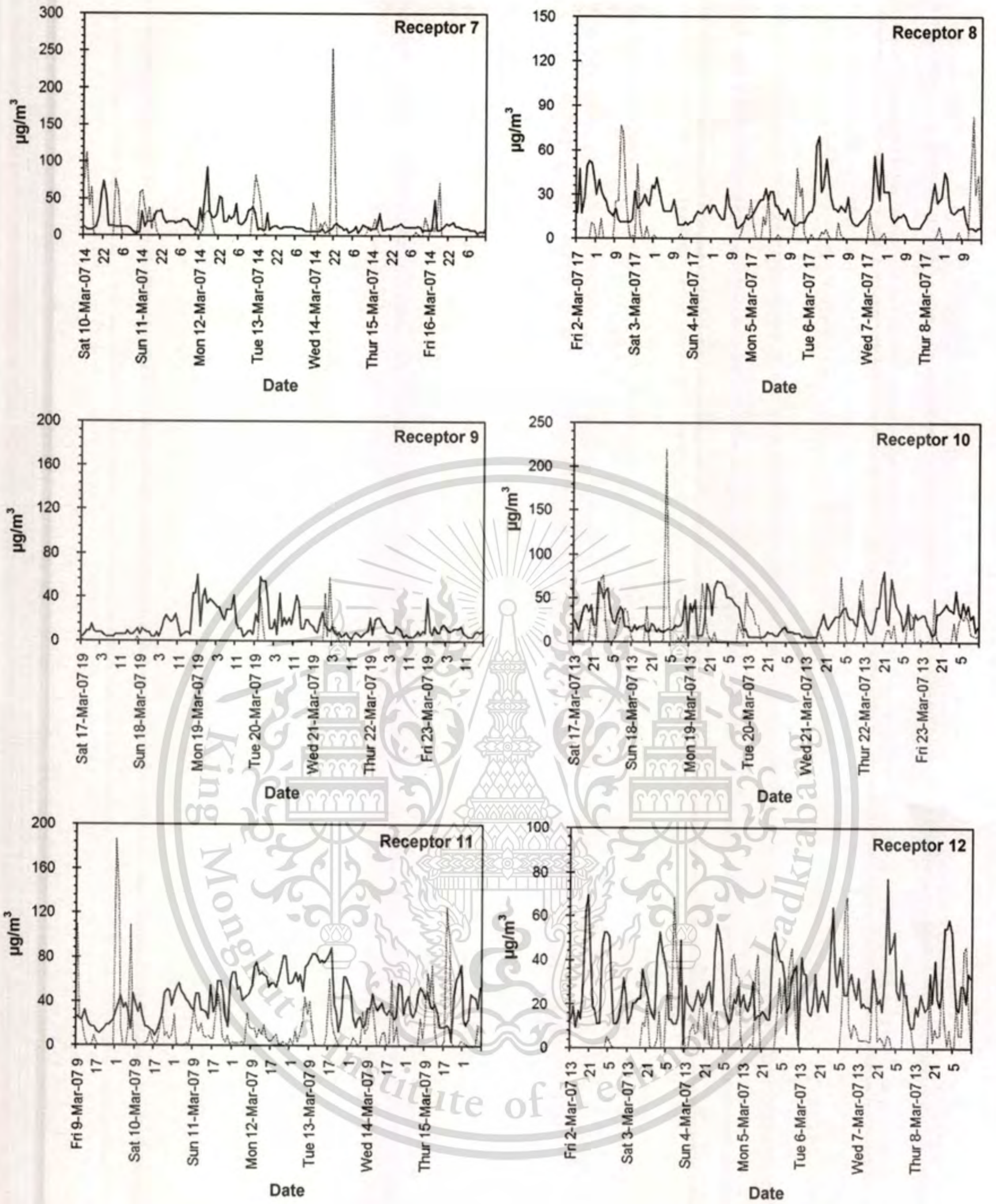

Figure 4.93 NO_2 concentrations in dry season: solid line by measurements and dashed line by CALPUFF (cont.).

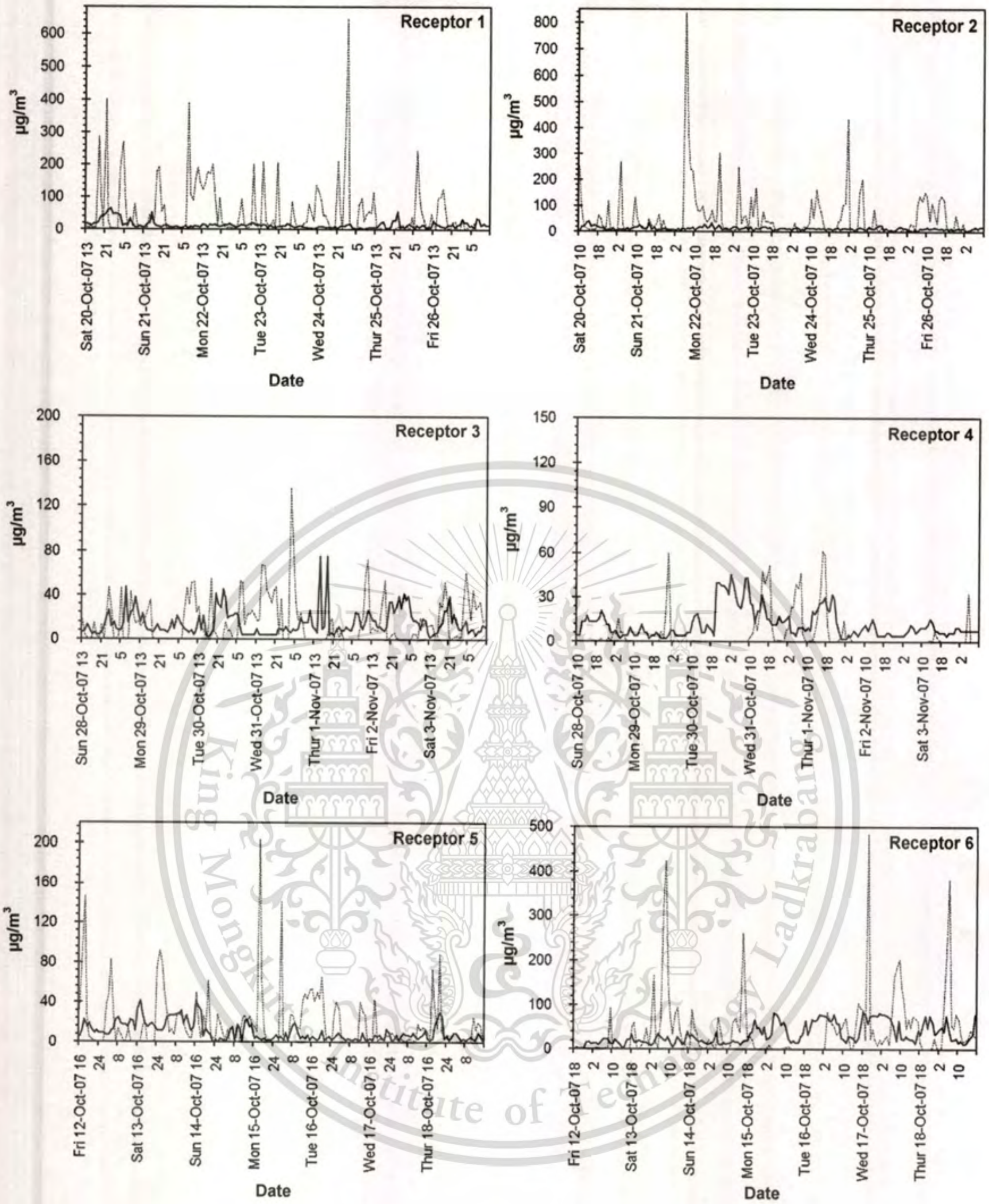

Figure 4.94 NO_2 concentrations in wet season: solid line by measurements and dashed line by CALPUFF.

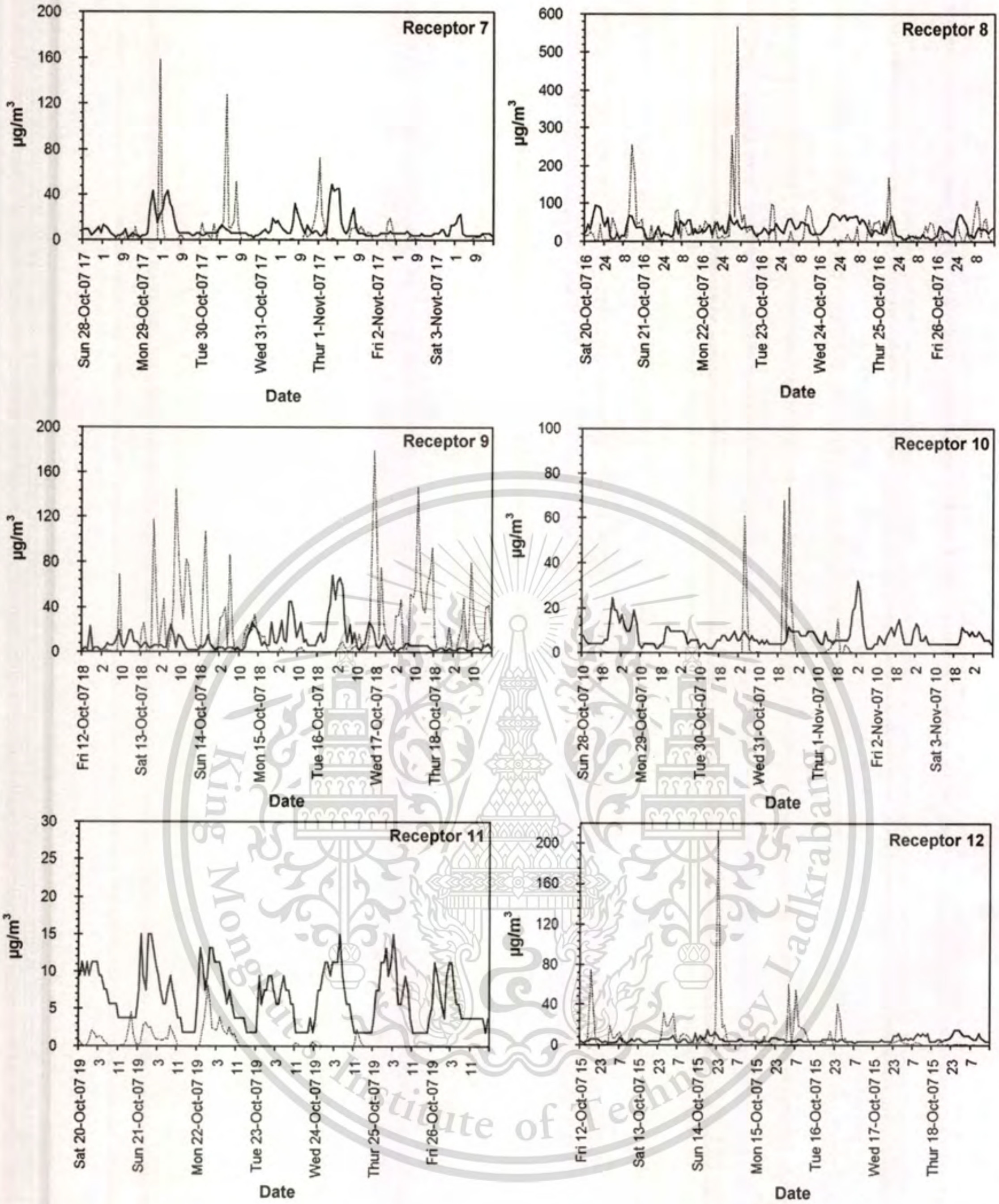

Figure 4.94 NO_2 concentrations in wet season: solid line by measurements and dashed line by CALPUFF (cont).

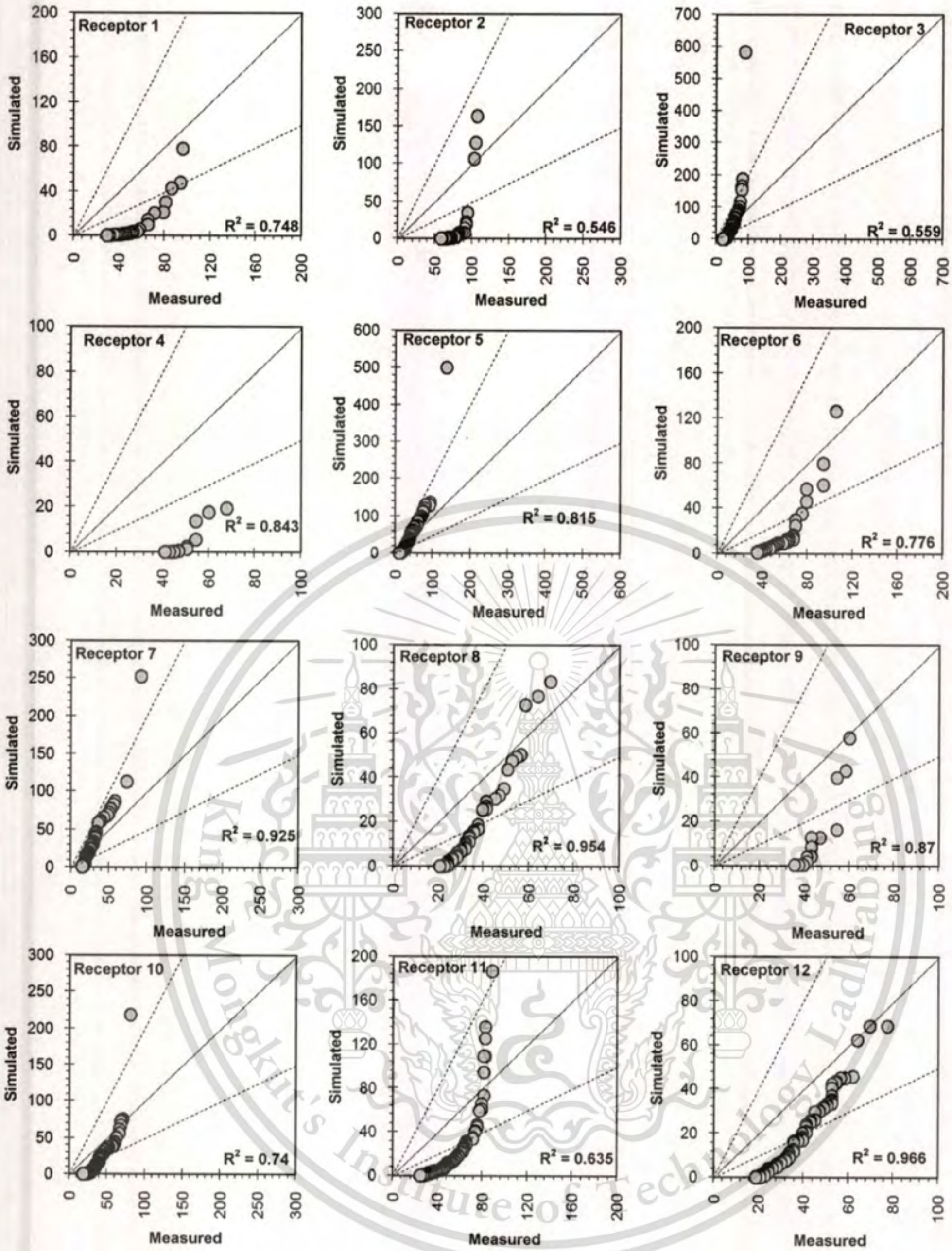

Figure 4.95 The Q-Q plots of hourly monitored NO_2 and simulated NO_2 in dry season by CALPUFF: slope = 1 (solid line); slope = 2, 0.5 (dashed lines for the factor-of-two, model acceptable limit, within the over and under prediction, respectively).

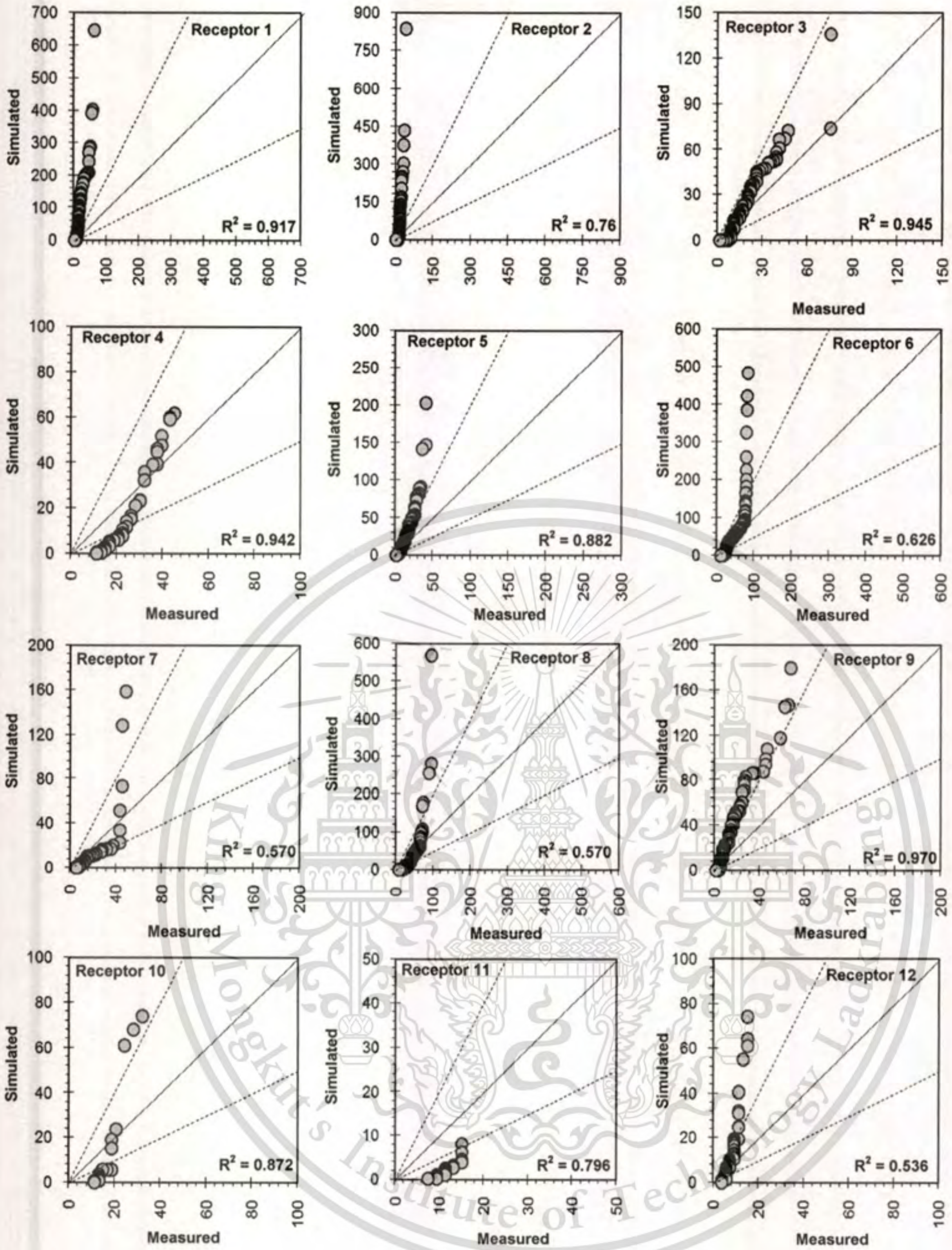

Figure 4.96 The Q-Q plots of hourly monitored NO_2 and simulated NO_2 in wet season by CALPUFF: slope = 1 (solid line); slope = 2, 0.5 (dashed lines for the factor-of-two, model acceptable limit, within the over and under prediction, respectively).

4.5.3 Ground concentration distribution analysis by the CALPUFF

The ground concentration distribution of the pollution emitted from 14 stacks of the cement manufacturers in Kaeng Khoi were analyzed by the CALPUFF. Since the NO_2 plays the most important role in the area with the highest emission, the emission of NO_2 is selected as the input for the CALPUFF. The hourly simulated ground concentration distribution of NO_2, hereafter called 'plume', is plotted against the 1-hour averaged concentrations of NO_2 and time. The CALPUFF were operated with the RIVAD/ARM3, a chemical transformation module, including wet deposition. The ozone monitoring data at NPL and KN stations were taken as background for the model. The 1-hour averaged concentration plume of NO_2 was plotted every 3 hours to observe 'NO_2 hit or land on' at the receptors and nearby the study areas. As NO_2 was monitored twice a year (in the dry and wet seasons) the plumes from 1^{st} to 22^{nd} hours in the beginning and last days of the monitoring period in dry season (2^{nd} and 24^{th} Mar. 2007) and wet season (12^{nd} Oct. and 4^{th} Nov. 2007) were observed.

All day on 2^{nd} Mar. 2007 in dry season, as seen in Figure 4.97, the NO_2 plumes dispersed to the north, sometimes switched to the west and east of the domain. It can be seen that the receptors 3, 5, 7, 10, 11 and 12 were hit by the NO_2 plumes. While in wet season on 4^{th} Nov. 2007, the NO_2 plumes were likely to disperse to the west or southwest of the domain and land on the areas in NPL and KN sometimes as shown in Figure 4.98. The NO_2 plumes covered the receptors 1, 2, 4, 6, 8 and 9. It is clear that the directions of NO_2 plumes change with the seasonal monsoons. The NO_2 plumes of 24^{th} Mar. and 12^{nd} Oct. 2007 are shown in Appendix F.

From the plume analysis, it can be seen that the locations of the receptors were not always hit by the trajectories of NO_2 plumes in dry and wet seasons. It is suggested that the performances of the AERMOD and CALPUFF in simulation of NO_2 concentrations at 12 receptors do not relate to the distance from the emission sources. As the plumes randomly hit the receptors, the accurate concentrations of NO_2 at the receptors might not be detected. Accordingly, suitable locations of the receptors should be considered to match 1-year trajectories of NO_2 plumes.

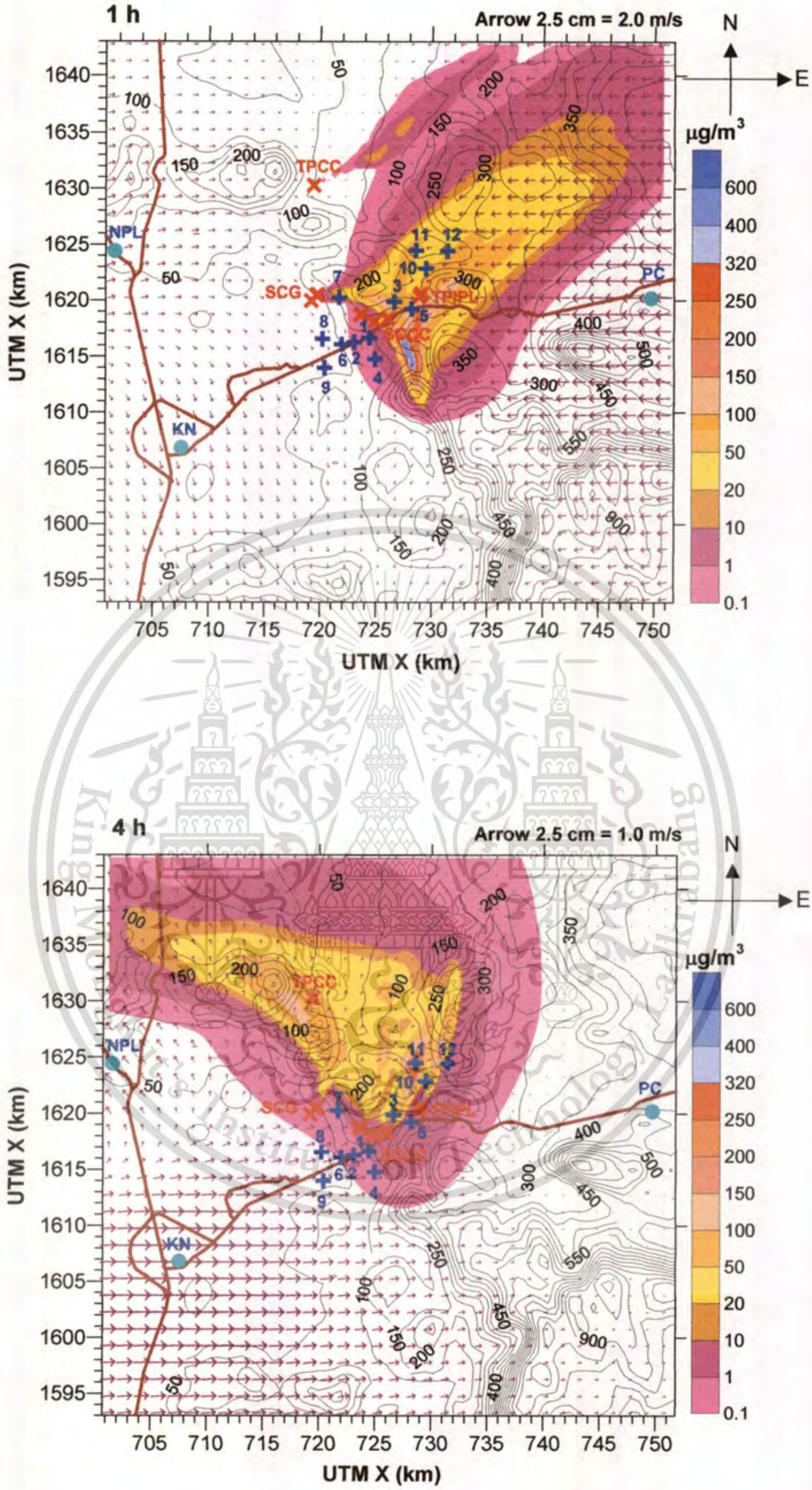

Figure 4.97 Plumes of NO_2 simulated by CALPUFF on March 2, 2007: (●) meteorological stations, (+) receptors and (×) stacks of cement plants.

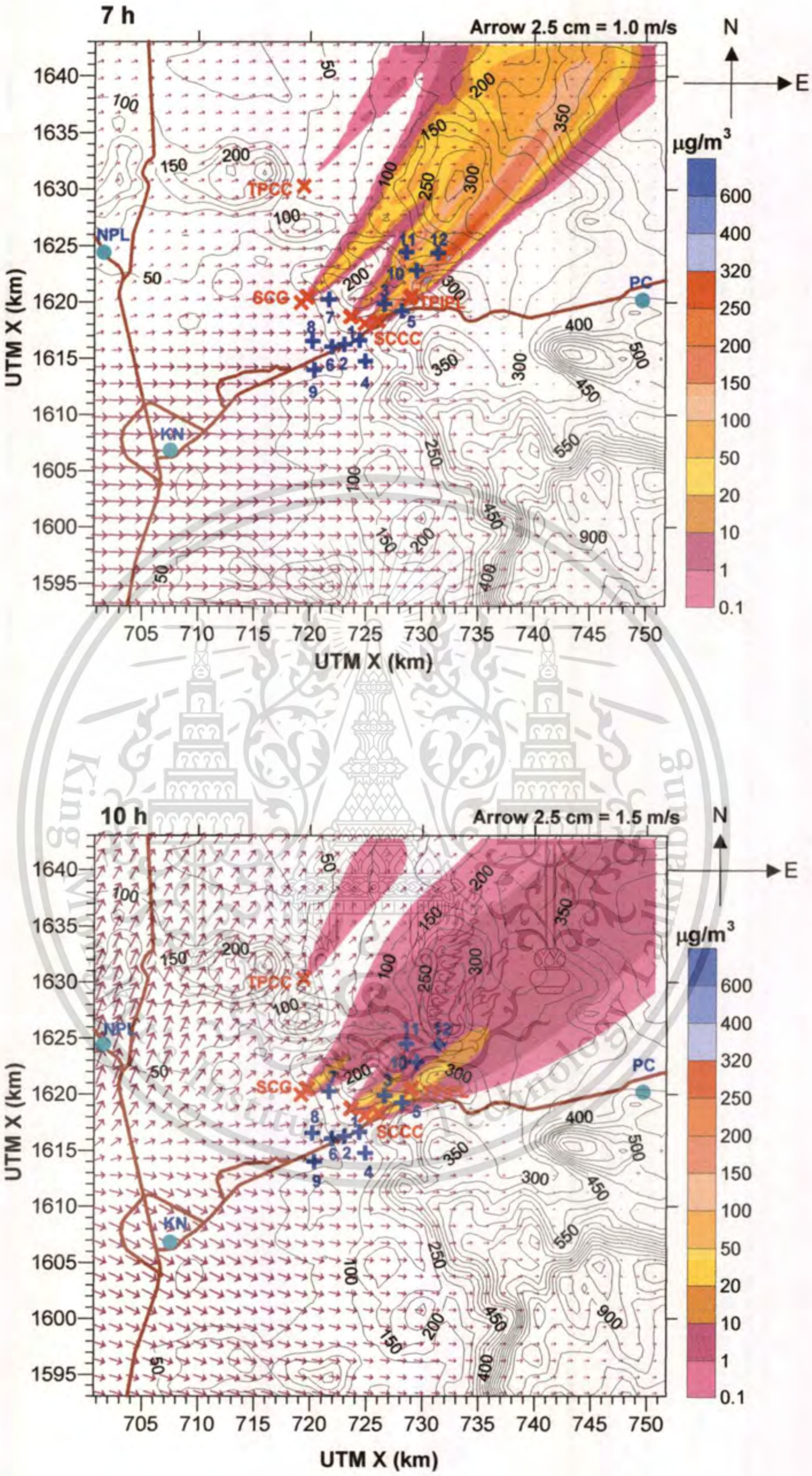

Figure 4.97 Plumes of NO_2 simulated by CALPUFF on March 2, 2007: (●) meteorological stations, (+) receptors and (×) stacks of cement plants (cont.).

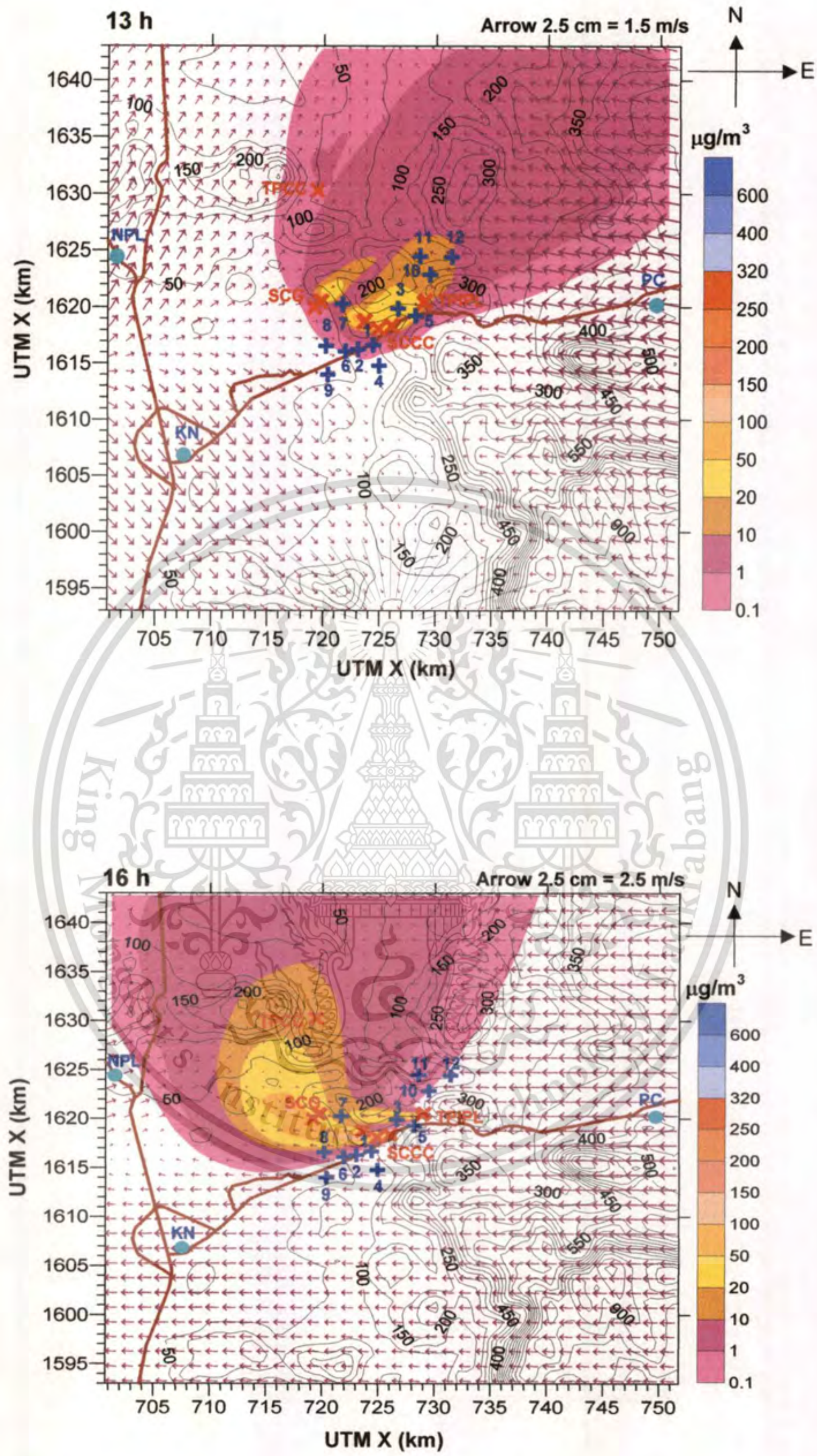

Figure 4.97 Plumes of NO_2 simulated by CALPUFF on March 2, 2007: (●) meteorological stations, (+) receptors and (×) stacks of cement plants (cont.).

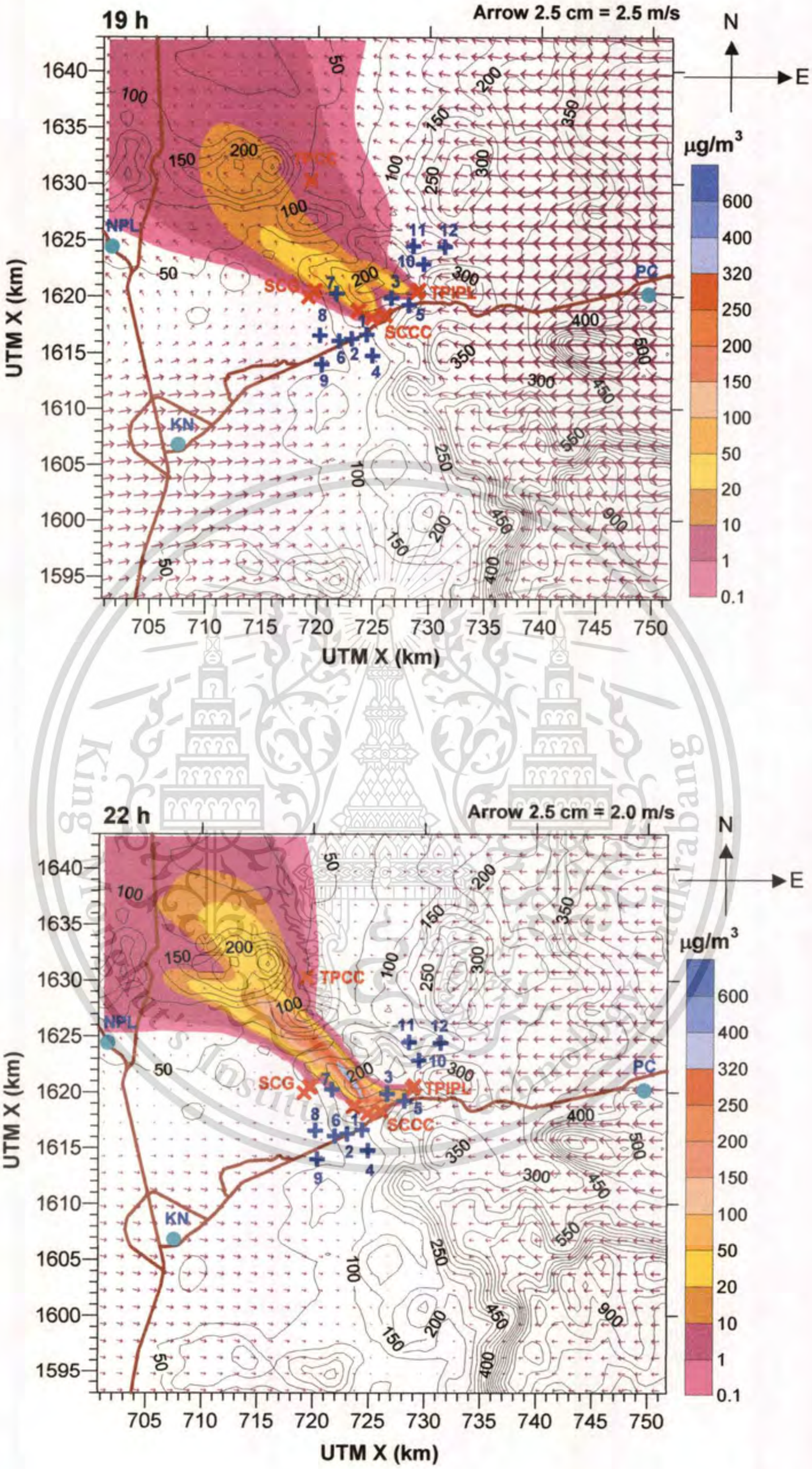

Figure 4.97 Plumes of NO_2 simulated by CALPUFF on March 2, 2007: (●) meteorological stations, (+) receptors and (×) stacks of cement plants (cont.).

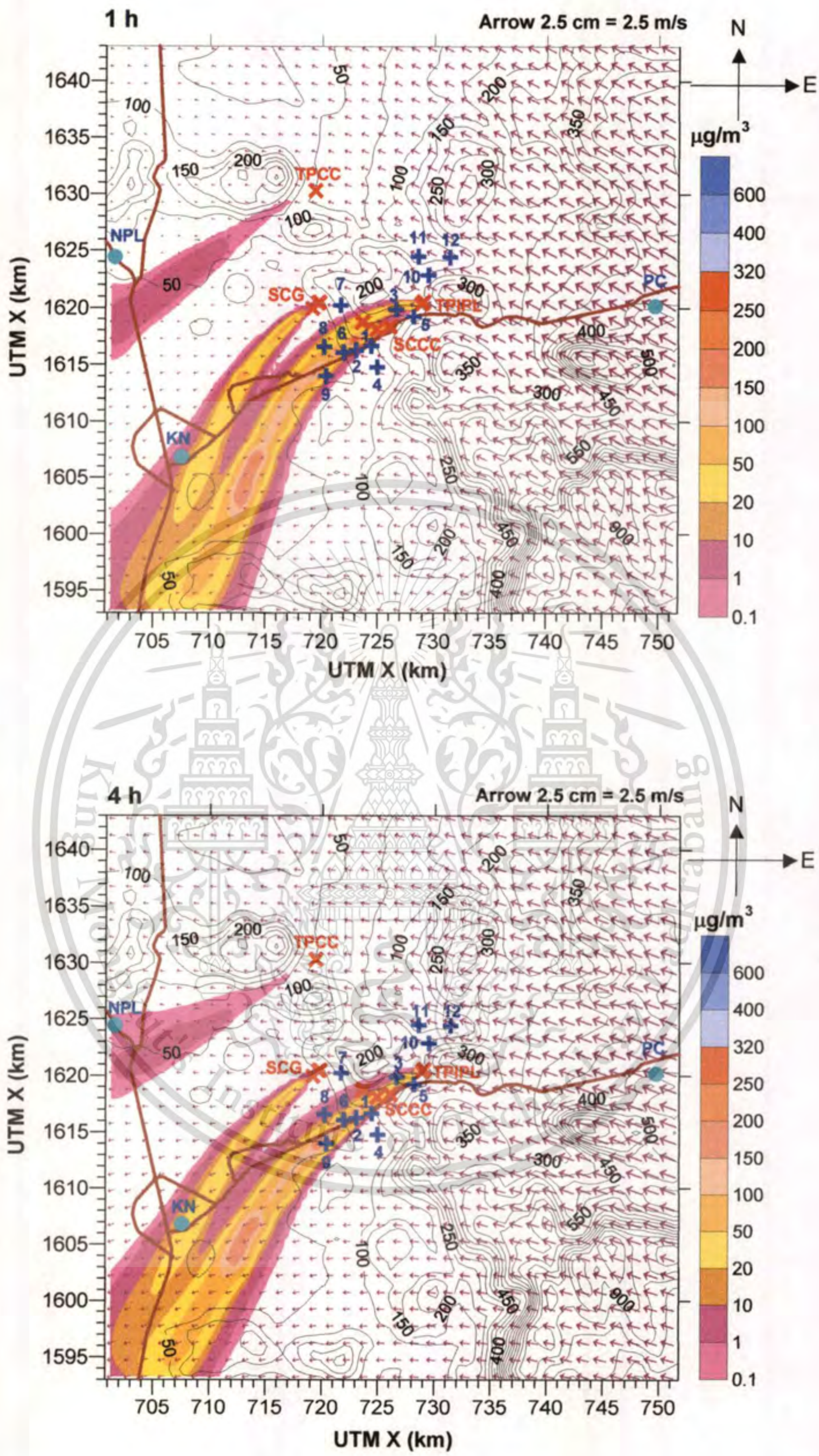

Figure 4.98 Plumes of NO_2 simulated by CALPUFF on November 4, 2007: (●) meteorological stations, (+) receptors and (×) stacks of cement plants.

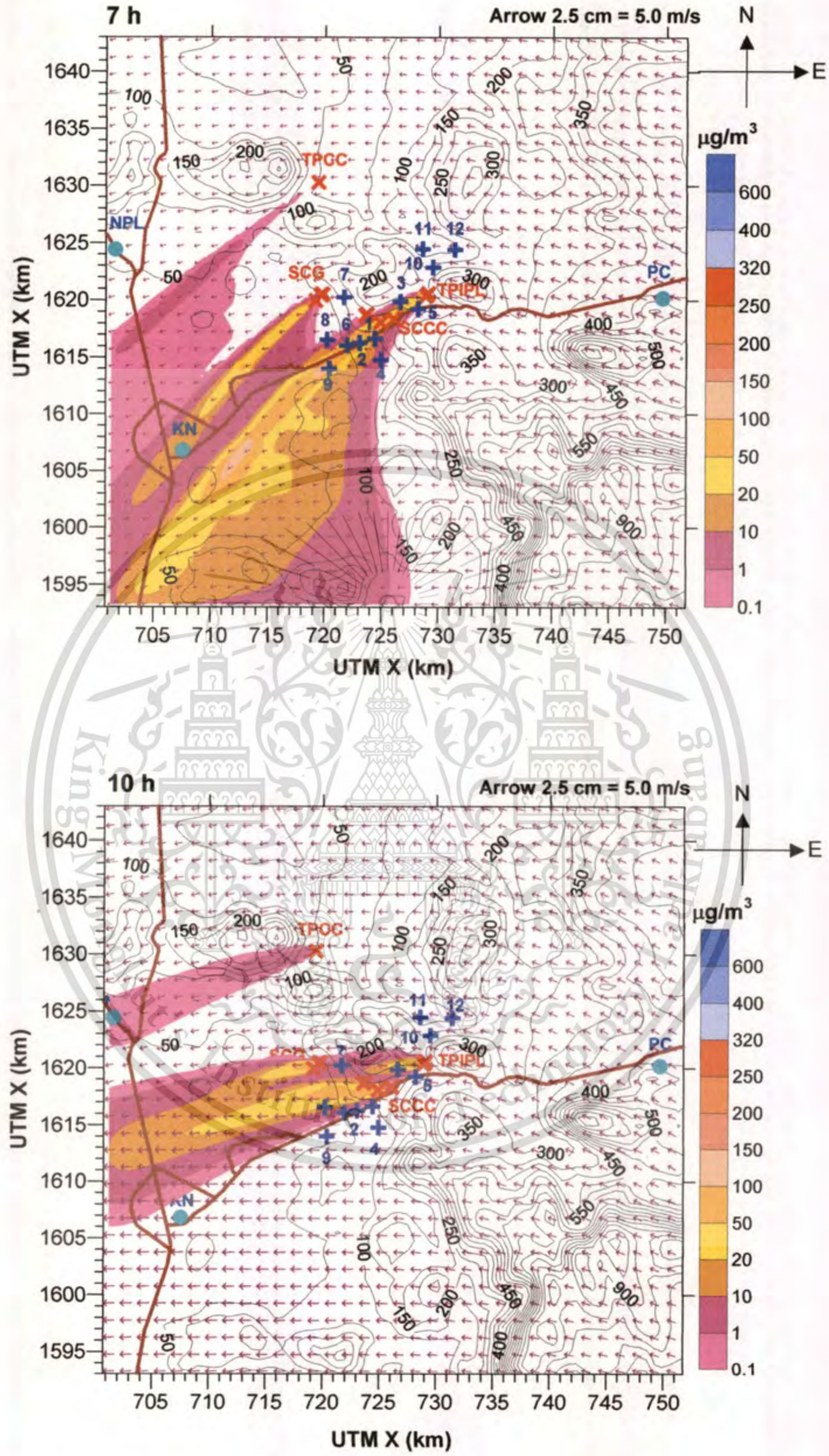

Figure 4.98 Plumes of NO_2 simulated by CALPUFF on November 4, 2007: (●) meteorological stations, (+) receptors and (×) stacks of cement plants.

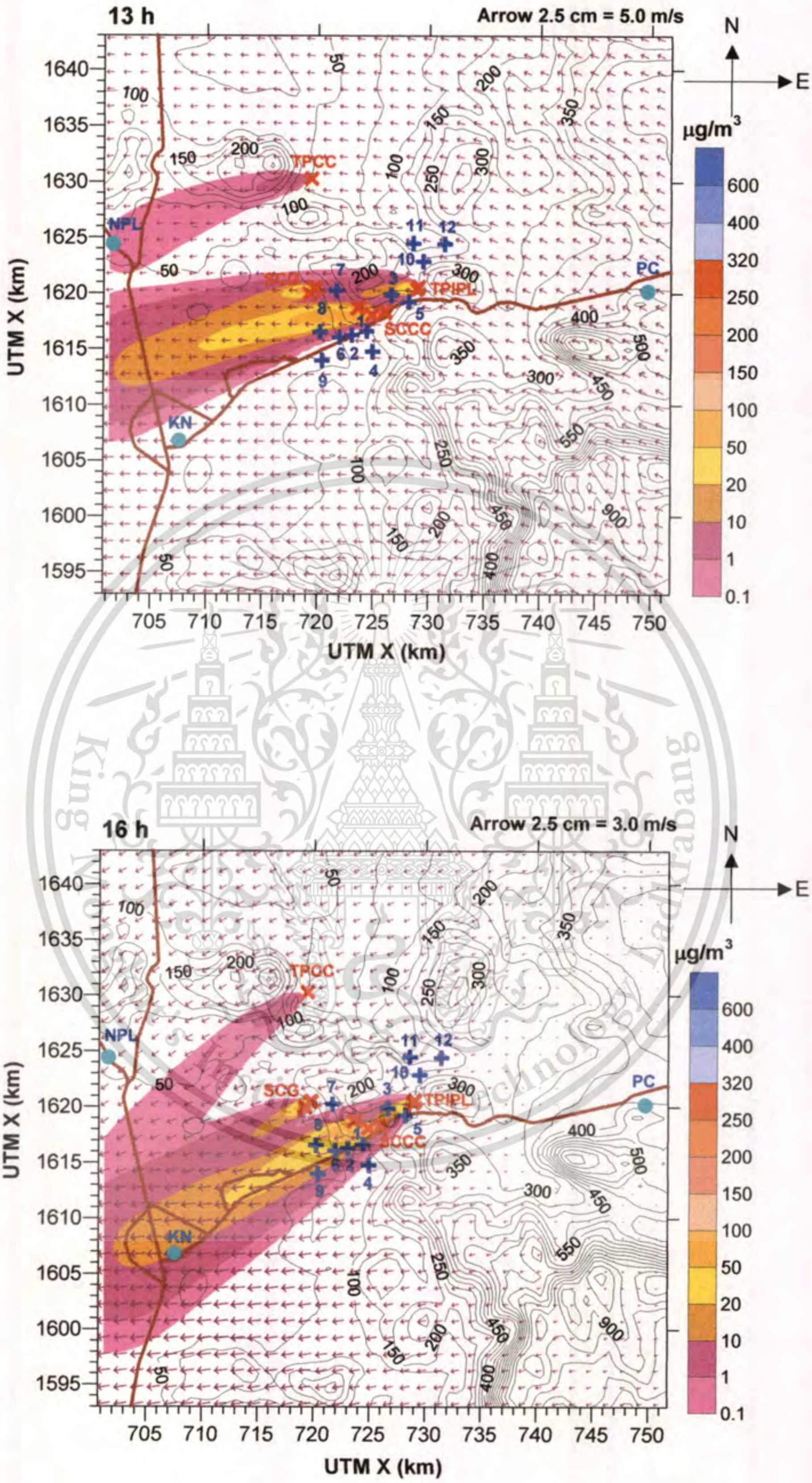

Figure 4.98 Plumes of NO_2 simulated by CALPUFF on November 4, 2007: (●) meteorological stations, (+) receptors and (×) stacks of cement plants (cont.).

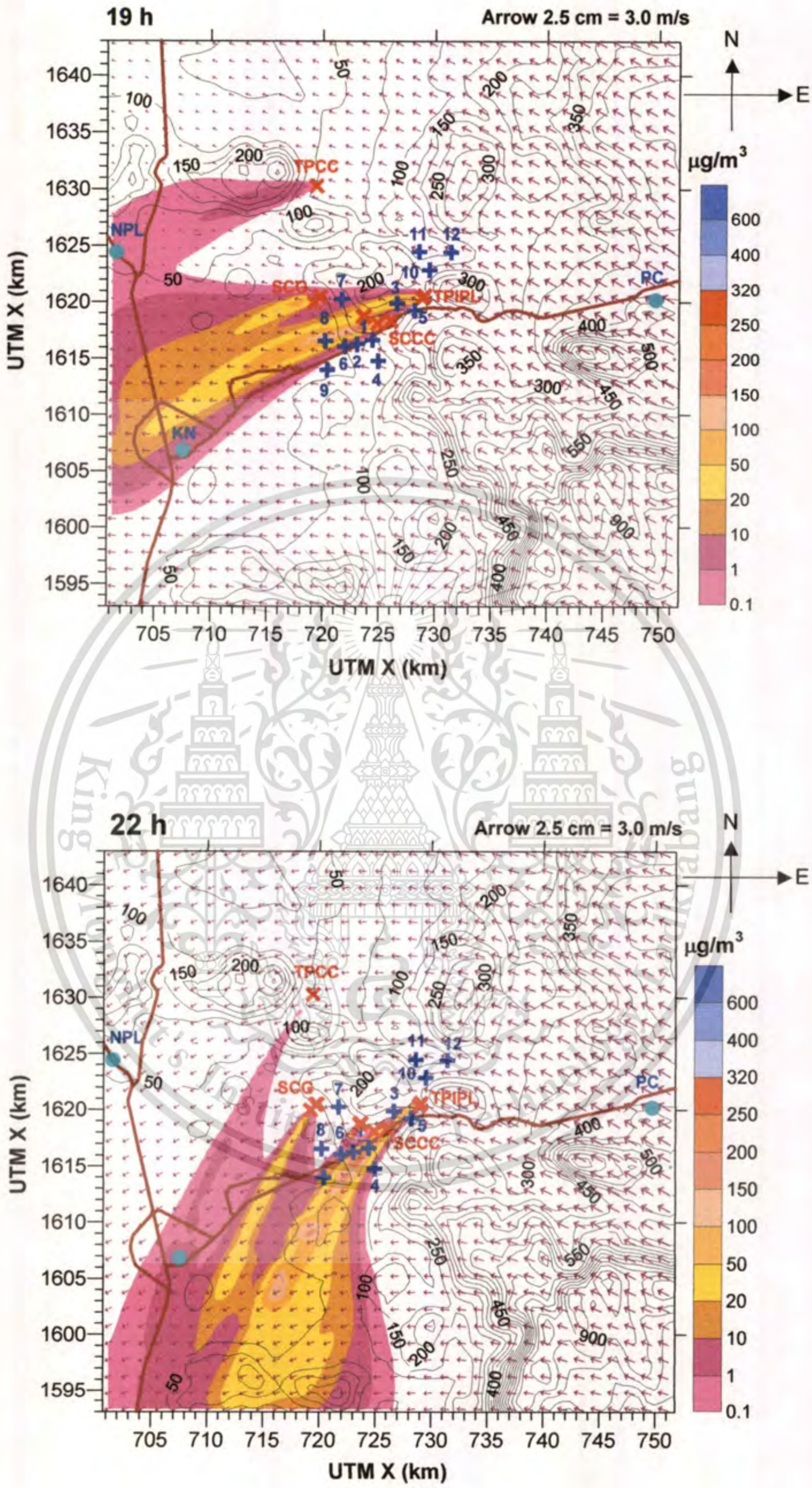

Figure 4.98 Plumes of NO_2 simulated by CALPUFF on November 4, 2007: (●) meteorological stations, (+) receptors and (×) stacks of cement plants (cont.).

4.5.4 Comparison results between the AERMOD and the CALPUFF

The simulated results from the commercial AERMOD, ISC-AERMOD View versions 4.6.2 and 5.4 and the free accessible CALPUFF, CALPUFF PROfessional Beta 5.2.0, were compared. The maximum concentrations simulated by the CALPUFF were higher than those obtained by the ISC-AERMOD View version 4.6.2 at every averaged scale but were lower than those obtained by the ISC-AERMOD View version 5.4, as shown in Tables 4.37-4.39.

Time-series plots of the monitored and simulated of NO_2 concentrations by the AERMOD version 4.6.2 and the CALPUFF PROfessional Beta 5.2.0 are shown in Figures 4.99-4.100. The AERMOD and CALPUFF could simulate NO_2 peaks at the receptors located in a short- and long- distance from the reference point. For example, a number of NO_2 peaks were generated at the receptor 6, 2.5 km away from the reference point, and at the receptor 11, 7.5 km away from the reference point. In dry season, some parts of NO_2 plumes landed on the receptors 3 and 11. More NO_2 peaks were detected by the CALPUFF than by the AERMOD. As a result, it revealed that the AERMOD provided the statistical calculation whereas the CALPUFF detected hourly time values.

Table 4.37 The maximum simulated 1-hour averaged concentrations by the AERMOD and CALPUFF.

Model	Pollutants	Maximum concentration ($\mu g/m^3$)	UTM (X,Y) (km)	Local station time
AERMOD Version 4.6.2	PM_{10}	96.0	720.00,1621.50	4/01/2007 at 10.00 a.m.
	NO_2	561.7	722.50, 1618.50	26/12/2007 at 900 a.m.
	SO_2	5.5	730.50, 1621.00	10/10/2007 at 11.00 a.m.
AERMOD Version 5.4	PM_{10}	579.4	723.00, 1621.00	8/09/2007 at 300 a.m.
	NO_2	3,820.2	730.00, 1621.50	17/01/2007 at 9.00 p.m.
	SO_2	60.3	730.00, 1621.00	25/12/2007 at 4.00 a.m.
CALPUFF	PM_{10}	276.2	721.75, 1618.75	21/10/2007 at 6.00 a.m.
	NO_2	3,730.3	723.25, 1617.25	19/10/2007 at 5.00 a.m.
	SO_2	23.6	723.25, 1617.25	19/10/2007 at 5.00 a.m.

Table 4.38 The maximum simulated 24-hour averaged concentrations by the AERMOD and CALPUFF.

Model	Pollutant	Maximum concentration ($\mu g/m^3$)	Location of the maximum impact in UTM (X,Y) (km)	Local station time of the maximum impact
AERMOD Version 4.6.2	PM_{10}	11.4	719.50, 1621.00	25/05/2007
	NO_2	63.5	727.50 ,1618.00	24/06/2007
	SO_2	0.6	730.00, 1621.00	24/12/2007
AERMOD Version 5.4	PM_{10}	89.5	725.00, 1618.50	5/01/2007
	NO_2	625.6	725.00, 1619.00	11/01/2007
	SO_2	11.3	730.00 ,1620.50	17/02/2007
CALPUFF	PM_{10}	31.6	728.25, 1620.25	19/11/2007
	NO_2	323.2	723.25, 1617.75	18/01/2007
	SO_2	4.2	728.25, 1620.25	19/11/2007

Table 4.39 The maximum simulated 1-year averaged concentrations by the AERMOD and CALPUFF.

Model	Pollutant	Maximum concentration ($\mu g/m^3$)	Location of the maximum impact in UTM (X,Y) (km)
AERMOD Version 4.6.2	PM_{10}	2.9	719.50, 1621.00
	NO_2	16.3	725.50, 1619.50
	SO_2	0.1	728.50, 1621.50
AERMOD Version 5.4	PM_{10}	12.1	709.50, 1630.00
	NO_2	74.9	730.00, 1620.50
	SO_2	1.4	730.00, 1620.50
CALPUFF	PM_{10}	5.9	728.25, 1620.25
	NO_2	43.4	728.25, 1620.25
	SO_2	0.7	728.25, 1620.25

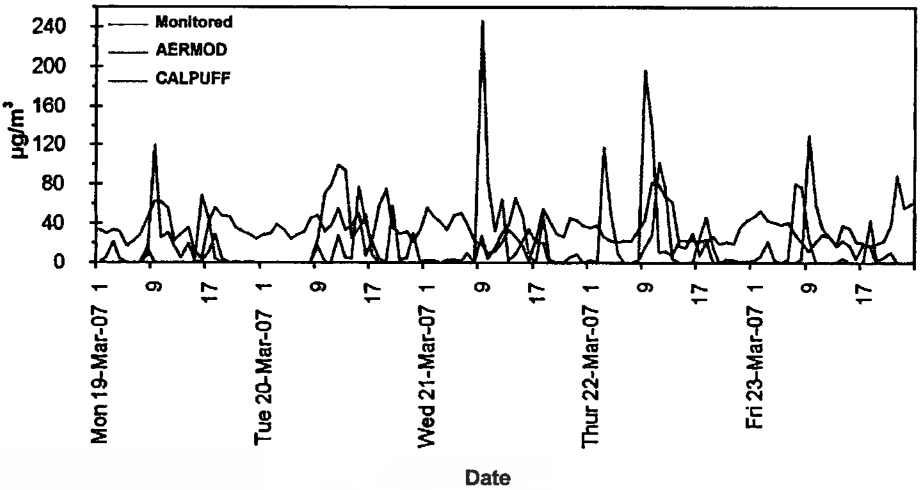

Figure 4.99 Time-series plots between 1-hour averaged of monitored and simulated NO_2 at receptor 3.

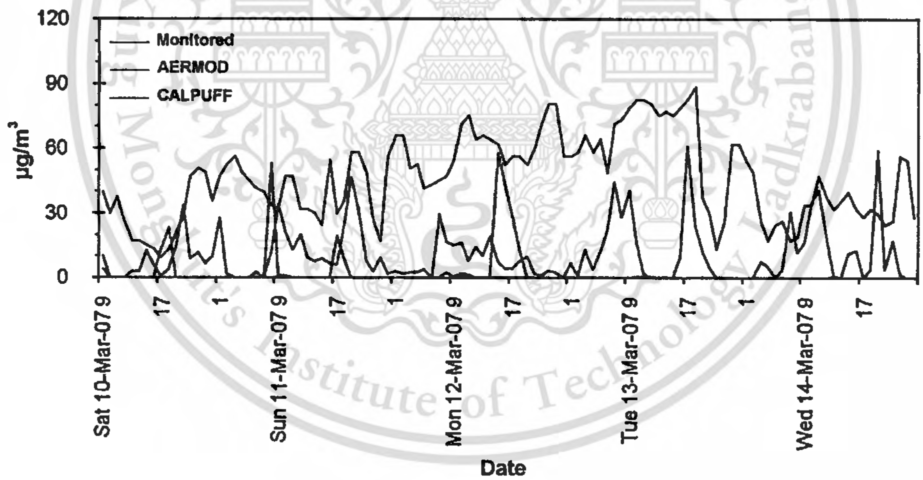

Figure 4.100 Time-series plots between 1-hour averaged of monitored and simulated NO_2 at receptor 11.

Chapter 5

Conclusions and recommendations

5.1 Conclusions

Gaseous and particulate air pollutants are troublesome to human beings. For the study areas of the cement complex in Kaeng Khoi, Saraburi, NO_2 contributes a major air pollution emission although the monitoring results of TSP, PM_{10}, NO_2 and SO_2 show no serious air pollution in the areas. Nevertheless, Nah Phra Laan-the connecting area faces serious PM_{10} emission. Higher PM_{10} concentration in the ambient air than the permit by the National Ambient Air Quality Standards (NAAQS) of Thailand is regularly observed. Knowing the location of the source relative to the receptor would allow us to estimate the pollutant concentration at a particular downwind receptor using a dispersion model.

In this work, the American Meteorological Society-Environmental Protection Agency Regulatory Model (AERMOD) and the California Puff Dispersion Model (CALPUFF) demonstrate that the 24-hour averaged concentration of PM_{10}, the maximum 1-hour averaged concentrations of NO_2 and SO_2 from the cement complex in Kaeng Khoi are in the NAAQS. In the mean time, PM_{10} and SO_2 do not show significant impact on the nearby communities but NO_2 is of most concern because the hourly averaged concentrations of NO_2, not in 7 days of the EIA measurement, exceed the permit by the NAAQS. This may bring Kaeng Khoi a new risky area in the near future if serious pollutant-emission-regulating mechanisms are not active.

The performances of the AERMOD and CALPUFF were validated by the Quantile-Quantile plots of 1-hour averaged NO_2 concentrations in dry and wet seasons. Compare to wet season, the simulated 1-hour averaged NO_2 concentrations in dry season agreed well with their monitoring data. It was attributed to the effects of NO_2 deposition reactions in wet environment. The CALPUFF is known to be more suitable for a complex terrain than the AERMOD because it is a multi-layer, multi-species and non-steady-state dispersion modeling. It contains the reactive modules which can calculate chemical reactions of the NO_x, SO_x, VOCs, etc in the atmosphere. Moreover, the CALPUFF detects hourly time variations whereas the AERMOD provides the statistical simulation. Difficult-accessible or inaccessible locations of the receptors made them not possible to detect and distinguish the air pollutants emitting from the cement complex exactly. The trajectories or plumes of the simulated 1-hour averaged concentrations of NO_2 can help to determine the areas of high impact. It should be noted that the air circulation and NO_2 dispersion are not controlled only by local and seasonal winds but also the complex topography of the study areas. Because the locations of the receptors were not always hit by the trajectories of NO_2 plumes in dry and wet seasons so the concentrations of NO_2 at the receptors might not be accurate. Suitable locations of the receptors should be considered with respect to NO_2 trajectories.

5.2 Comments and recommendations

1. The monitoring for the EIA report should be collected in the middle period of dry and wet seasons. No emission inventory is provided for Kaeng Khoi so all-inclusive record should be prepared. The line sources or transportations-related information are highly recommended to be included.

2. Since a 7-day continuous measurement of NO_2 concentration in ambient air showed no significant impact on the environment, in contrast its impact was observed by the simulation. It is most likely attributed to insufficient monitoring data due to a short-time measurement. Longer period than 7-day monitoring to assure the air pollution in the area is recommended.

3. Regards to a noticeable difference of the simulation results by the AERMOD, CALPUFF and the monitoring pollutant concentrations, it is possible that the maximum pollutant concentrations do not exist at 12 receptors. It is strongly recommended to set up the receptors around the cement manufacturers at the pollutant trajectory of highly risk area nearby the communities.

4. Due to no available precipitation data in Kaeng Khoi, the data collected at Nah Phra Laan and Kao Noi stations (25 km away from the reference point) were used for the simulations by the AERMOD and CALPUFF. Consequently, some errors may occur because of the effect of precipitation. For better outputs from the AERMOD and CALPUFF, the precipitation in Kaeng Khoi should be collected.

5. The chemical transport regional models, i.e., WRF-chem and CMAQ should be studied for simulating pollution in Kaeng Khoi as is the complex terrain of mountain areas with various activities (e.g., transportations, open burning, etc) that affect air pollutant dispersions.

6. Corresponding to the U.S. EPA, 5-year meteorological data are the minimum requirement for air dispersion models. Further work to use 5-year meteorological input data with the AERMOD and CALPUFF for a better simulation of pollutant concentration should be studied.

7. It is recommended to apply meteorological models, e.g., MM5, WRF, RAMS, etc to predict meteorological data and determine the possible risk areas from the emissions of cement industry. The simulated results can be used as primary information for preventive management.

8. The concentrated plumes on the ground can be calculated according to the basic equation of Gaussian plume model as shown in Appendix G. More-refined models such as the AERMOD and CALPUFF can predict the effect of NO_2 plume approximately to the actual dispersion.

References

[1] Department of Industrial Work (DIW). **"ข้อมูลโรงงานอุตสาหกรรม."** [Online]. Available : http://www.diw.go.th/diw/query.asp. 2010.

[2] Phajon-Aripai K. **"Stochastic Study of Fugitive Dust Concentration from Stone-processing Plants at Nah Phra Laan using Monte-Carlo Simulation of ISCST3 Model"** Master Thesis, Department of Chemical Engineering, Faculty of Engineering, Chulalongkorn University. 2001. (in Thai).

[3] Moondee S., bualert S., Phewnil O. and Jiamjarasragsi W. "Prevalence of Respiratory Symptoms and Lung Function of Students in Rock-crushing Industrial Area, Saraburi Province" **Thailand Journal of Health Promotion and Environmental Health.** Vol. 27, No.3, July-September 2004. (in Thai).

[4] Pimonsree S., Wongwises P., Pan-Aram R., P.A. and Meigen Z. "Dispersion Modeling of PM_{10} During Winter Episode over a Mineral Products Industrial Area in Saraburi, Thailand" **Proceedings of the International Conference on Environmental Research and Technology, Penang, Malaysia.** 28-30 May 2008. pp. 637-641. [Online]. Available : http://www.ppti.usm.my/ ICERT_website/ index.html. 2009.

[5] Pimonsree S., Wongwises P., Pan-Aram R., and Meigen Z. "Model Analysis of PM_{10} Concentration Variations Over a Mineral Products Industrial Area in Saraburi, Thailand" **Water, Air, & Soil Pollution.** Vol. 201, N0. 1-4, 2008. pp. 239-251.

[6] Pimonsree S. **"Study on PM_{10} Dispersion in Saraburi."** Doctoral thesis, The Joint Graduate School of Energy and Environment, King Mongkut's University of Technology Thonburi. 2008. (in English).

[7] Pollution Control Department (PCD). **Project of Studying the Problem and Impact of PM_{10} in Saraburi: Surveying, Measuring and Developing Database of PM_{10} Emission Sources in Nah Phra Laan.** 2006. (in Thai).

[8] กรมควบคุมมลพิษ กระทรวงทรัพยากรธรรมชาติและสิ่งแวดล้อม. "ประกาศกรมควบคุมให้หน้าพระลานเป็นพื้นที่ควบคุม ประกาศคณะกรรมการสิ่งแวดล้อมแห่งชาติฉบับที่ ๒๓ (พ.ศ. ๒๕๔๗) เรื่อง กำหนดให้ท้องที่เขตตำบลหน้าพระลาน อำเภอเฉลิมพระเกียรติ จังหวัดสระบุรี เป็นเขตควบคุมมลพิษ" **ราชกิจจานุเบกษา ฉบับประกาศ**

ทั่วไป เล่ม ๑๒๑ ตอนพิเศษ ๑๐๔ ง วันที่ ๒๒ กันยายน ๒๕๔๗ ประกาศ ณ วันที่ ๑๓ สิงหาคม พ.ศ. ๒๕๔๗ [online]. Available : http://www.pcd.go.th/Download/regulation.cfm?task=s6. 2010.

[9] สำนักจัดการคุณภาพอากาศและเสียง กรมควบคุมมลพิษ กระทรวงทรัพยากรธรรมชาติและสิ่งแวดล้อม. **สถานการณ์และการจัดการปัญหามลพิษทางอากาศและเสียง ปี 2552.** [online]. Available : http://www.pcd.go.th. 2010.

[10] Bison Engineering. **Best Available Retrofit Technology (Bart) Analysis Helena for Holcim (U.S.) Inc., MT. July 6, 2007.** [online]. Available: http://www.epa.gov/region8/air/pdf/HolcimBARTReport.pdf. 2010.

[11] Thai Cement Manufacturers Association (TCMA). **Thai Cement Manufacturers Association Report.** [online]. Available : http://www.thaicma.or.th/Background%20Dec.htm. 2008.

[12] U.S.EPA. **Revision to the Guideline on Air Quality Models: Adoption of a Preferred General Propose (Flat and Complex Terrain) Dispersion Model and Other Revisions: Final Rule (Federal Register).** Washington DC, 9th November 2005. [Online]. Available : http://www.epa.gov/scram001/guidance/guide/appw_05.pdf. 2010.

[13] U.S.EPA. **AERMOD Implementation Guide: Last Revised (March 19, 2009).** [Online]. Available : http://www.epa.gov/scram001/7thconf/aermod/aermod_implmtn_guide_19March2009.pdf. 2009.

[14] U.S. EPA. **AERMOD Implementation Guide (Last Revised: October 19, 2007).** Research Triangle Park, North Carolina. . [Online]. Available : http://hpe4.anamai.moph.go.th/hia/data/cat1/aermod_19oct2007.pdf. 2009.

[15] Department of Provincial Administration (DOPA). **"รายงานสถิติจำนวนประชากรและบ้านรายจังหวัด รายอำเภอ และรายตำบล ณ เดือน ธันวาคม พ.ศ. 2550."** [Online]. Available : http://www.dopa.go.th/xstat/p5019_01.html. 2010.

[16] Hidore J. J. and Oliver J. E. **Climatology: An Atmospheric Science.** New York, U.S.: Macmillan, Inc. 1993. pp 136-137.

[17] Alsop P. A. **The Cement Plant Operations Handbook: The Concise Guide to Cement Manufacture.** 4th ed. Dubai, United Arab Emirates : Printing Press. 2005. p. 42.

[18] Kääntee U., Zevenhoven R., Backman R. and Hupa M. "Cement Manufacturing Using Alternative Fuels and the Advantages of Process Modelling" **Fuel Processing Technology.** Vol. 85, 2004. pp. 293–301.

[19] Szabó L., Hidalgo I., Ciscar J. C. and Soria A. "CO_2 Emission Trading within the European Union and Annex B Countries: the Cement Industry Case" **Energy Policy.** Vol. 34, 2006. pp. 72-87.

[20] Schnelle K. B. and Brown C. A. **Air Pollution Control Technology Handbook.** U.S. : CRC Press LLC. 2002. pp. 13-22.

[21] WHO. **"Air Quality Guidelines for Particulate Matter, Ozone, Nitrogen Dioxide and Sulfur Dioxide."** [Online]. Available : http://whqlibdoc.who.int/hq/2006/WHO_SDE_PHE_OEH_06.02_eng.pdf. 2010.

[22] The Pollution Control Department (PCD). **"Air Quality and Noise Standard."** [Online]. Available : www.pcd.go.th. 2010.

[23] The Pollution Control Department (PCD). **"มาตรฐานคุณภาพอากาศและเสียง: มาตรฐานจากแหล่งกำเนิดอยู่กับที่."** [Online]. Available : http://www.pcd.go.th/info_serv/reg_std_airsnd03.html. 2010.

[24] U.S. EPA. **"News Releases Issued by the Office of Air and Radiation EPA Sets First National Limits to Reduce Mercury and Other Toxic Emissions from Cement Plants."** [Online]. Available : http://yosemite.epa.gov/opa/admpress.nsf/7ebdf4d0b217978b852573590040443a/ef62ba1cb3c8079b8525777a005af9a5!OpenDocument. 2010.

[25] McMurry P., Shepherd M., and Vickery J., Editors. **Particulate Matter Science for Policy Makers : A NARSTO Assessment.** Cambridge University Press. 2004.

[26] Heinsohn R. J. and Kabel R. L. **Sources and Control of Air Pollution.** U.A. : Prentice-Hall, Inc. 1999.

[27] Wark K., Warner G. F. and Davis W. T. **Air Pollution: Its Original and Control.** 3rd ed. United States of America : Addison Wesley Longman, Inc. 1998.

[28] U.S.EPA. **" Six Common Air pollutants."** [Online]. Available: http://www.epa.gov/air/urbanair/. 2007.

[29] Bal M., Bell P., and Fernandes J., Editors. **Cement Plant Environmental Handbook 2003.** Tradeship Publication Ltd. pp 101-108.

[30] U.S. EPA. **"Emissions Factors & AP 42, Compilation of Air Pollutant Emission Factors."** [online]. Available : http://www.epa.gov/ttnchie1/ap42/. 2009.

[31] Gieré R. and Stille P. **Energy, Waste and the Environment: A Geochemical Perspective.** Trowbridge, UK : Cromwell Press. 2004.

[32] Essom Equipment for Engineering. **"Heating Values of Hydrogen and Fuels."** [Online]. Available: http://www.essom.com/backend/data-file/engineer/engin21_1.pdf. 2004.

[33] Worldcoal Institute. **"Climate Change."** [Online]. Available: http://www.worldcoal.org/coal-the-environment/climate-change/. 2009.

[34] WMO. **"WMO Greenhouse Gas Bulletin, No. 1: 14 March 2006."** [Online]. Available: ftp://ftp.wmo.int/Documents/PublicWeb/arep/gaw/ghg-bulletin-en-03-06_000.pdf. 2008.

[35] WMO. **"WMO Greenhouse Gas Bulletin, No. 3:23 November 2007."** [Online]. Available : http://www.wmo.int/pages/prog/arep/gaw/ghg/documents/ghg-bulletin-3.pdf. 2008.

[36] Maria Hood. "A Carbon Sink That Can No Longer Cope?" **A World of Science.** Vol. 2, No. 4, October–December 2004. [Online]. Available : http://unesdoc.unesco.org/images/0013/001372/137292e.pdf. 2010.

[37] Pigeat M. "GGBS: The World's Most Sustainable Building Material?" **World Cement.** September 2009. pp. 151-155.

[38] Moonaw W. R. "Industrial Emissions of Greenhouse Gases" **Energy Policy.** Vol. 24, 1996. pp.951-968.

[39] Karstensen K. H. "Formation, Release and Control of Dioxins in Cement Kilns" **Chemosphere.** Vol. 70, 2008. pp. 543-560.

[40] World Business Council for Sustainable Development (WBCSD). **"Dioxins and the Cement Industry in Australia."** [Online]. Available: http://www.wbcsdcement.org/pdf/tf4/CIF-dioxin-tech-note.pdf. 2010.

[41] Murray A. and Price L. **"Use of Alternative Fuels in Cement Manufacture: Analysis of Fuel Characteristics and Feasibility for Use in the Chinese Cement Sector."** [Online]. Available : http://ies.lbl.gov/iespubs/LBNL-525E.pdf. 2010.

[42] European Environment Agency (EEA). "EMEP/EEA Air Pollutant Emission Inventory Guidebook-2009" **Technical Report No. 9/2009.** [Online]. Available: http://www.eea.europa.eu/publications/emep-eea-emission-inventory-guidebook-2009. 2010.

[43] Olivier J. G. J., Bloos J. P. J., Berdowski J. J. M., Visschedijk A. J. H., and A. F Bouwman. "A 1990 Global Emission Inventory of Anthropogenic Sources of Carbon Monoxide on $1^{\circ} \times 1^{\circ}$ Developed in the Framework of EDGAR/GEIA" **Chemosphere-Global Change Science.** Vol. 1, Issues 1-3, August 1999, pp 1-17.

[44] Graedel T. E., Bates T.S., Bouwman A.F., Cunnold D., Dignon J., Fung I., Jacob D.J., Lamb B.K., Logan J.A., Marland G., Middleton P., Pacyna J.M., Placet M., and Veldt C. "A Compilation of Inventories of Emissions to the Atmosphere" **Global Biogeochemical Cycles.** Vol 7, 1993. pp. 1-26.

[45] Streets D. G., Bond T. C., Carmichael G. R., Fernandes S. D., Fu Q., He D., Klimont Z., Nelson S. M., Tsai N. Y., Wang M. Q., Woo J. H. and Yarber K.F. "An Inventory of Gaseous and Primary Aerosol Emissions in Asia in the Year 2000" **Journal of Geophysical Research.** Vol. 108, No. D21, 2003. pp GTE30-1 – GTE30-23. [Online]. Available : http://www.cgrer.uiowa.edu/ACESS/papers/Streets_emission_jgr_2002JD003093.pdf. 2010

[46] Frontier Research Center for Global Change (FRCGC). **"Regional Emissions Inventory in Asia."** [online]. Available : http://www.jamstec.go.jp/frcgc/research/d4/emission.htm. 2010.

[47] Supaporn Chesomboon. **"Thai Cement Market."** [Online]. Available: http:// http://www.scb.co.th/LIB/th/article/ktb/data/k8-38.html. 2008. (in Thai).

[48] K. Wark, Warner G. F. and Davis W. T. **Air Pollution: Its Original and Control.** 3rd ed. United States of America : Addison Wesley Longman, Inc., 1998.

[49] Schnelle K.B. and Dey P.R. **Atmospheric Dispersion Modeling Compliance Guide.** United States of America : McGraw-Hill Companies, Inc., 1999.

[50] Heinsohn R. J. and Kabel R. L. **Sources and Control of Air Pollution.** U.S. : Prentice-Hall Inc., 1999.

[51] Arthur C.S. **Air Pollution: Air Pollutants, Their Transformation and Transport.** 3rd ed. New York : Academic Press, Inc., 1976.

[52] J. Colls. **Air Pollution: An Introduction.** 1st ed. Padstow, Cornwall, Great Britain: TJ International Ltd., 1997.

[53] Perkins H. C. **Air Pollution.** New York : McGraw-Hill Inc., 1974.

[54] Ministry for the Environment, New Zealand. **Good Practice Guide for Atmospheric Dispersion Modelling.** June 2004. [online]. Available : http://www.mfe.govt.nz/publications/air/atmospheric-dispersion-modelling-jun04/atmospheric-dispersion-modelling-jun04.pdf. 2010.

[55] Department of Environmental Protection (DEP), State of Maine, U.S. **"Modeling Protocols and Submittals."** [online]. Available : http://www.maine.gov/dep/air/meteorology/protocol.html. 2010.

[56] U.S.EPA. **"Prefer/Recommend Models."** [Online]. Available: http://www.epa.gov/scram001/dispersion_prefrec.htm#aermod. 2010.

[57] Lakes Environnemental. **"AERMOD View™: Gaussian Plume Air Dispersion Model."** [online]. Available: http://www.weblakes.com/. 2010.

[58] Thé J. L., Thé C. L. and Johnson M. A. **User's Guide: ISC AERMOD View AERMOD.** Waterloo, Ontario, Canada: Lakes Environmental Software. 1996-2002.

[59] Thé J. L., Thé C. L. and Johnson M. A. **User's Guide: ISC AERMOD View AERMOD Tutorials.** Waterloo, Ontario, Canada: Lakes Environmental Software. 1996-2002.

[60] U.S.EPA. **User's Guide for the AMS/EPA Regulatory Model-AERMOD (Revised Draft).** 10th November 1998 [online]. Available : www.epa.gov/scram001/7thconf/ aermod/aermodug.pdf. 2010.

[61] U.S.EPA. **User's Guide for the AERMOD Meteorological Preprocessor (AERMET) (Revised Draft).** 10th November 1998 [online]. Available: www.epa.gov/scram001/7thconf/ aermod/aermetug.pdf. 2010.

[62] TRC Environmental Corporation. **"The CALPUFF Modeling System."** [Online]. Available : http://www.src.com/calpuff/calpuff1.htm. 2010.

[63] Scire J. S., Strimaitis D. G. and Yamartino R. J. **A User Guide for the CALPUFF Dispersion Model (version 5).** MA, U.S.: Earth Tech, Inc., 1998-2000. [online]. Available : www.src.com/calpuff/download/CALPUFF_UsersGuide.pdf. 2007.

[64] Scire J. S., Robe F. R., Fernau M. E. and Yamartino R. J. **CALMET Meteorological Model (version 5).** MA, U.S. : Earth Tech, Inc., 1998-2000. [online]. Available: www.src.com/calpuff/download/**CALMET_UsersGuide**.pdf. 2007.

[65] Aguado E. and Burt J. E. **Understanding Weather and Climate.** 2[nd] ed., New Jersey: Orebtuce-Hall Inc., 2001.

[66] Windfinder. **"Windfinder, Wind Speed Units & Wind Directions."** [Online]. Available : http://www.windfinder.com/wind/windspeed.htm. 2010.

[67] LPD Lab Services. **"Contaminant Particle Identification and Elimination."** [Online]. Available : http://www.lpdlabservices.co.uk/documents/07-113en01.pdf. 2010.

[68] สำนักจัดการ คุณภาพอากาศและเสียง กรมควบคุมมลพิษ กระทรวงทรัพยากรธรรมชาติและสิ่งแวดล้อม. **สถานการณ์และการจัดการปัญหามลพิษทางอากาศและเสียงปี 2551.** หน้า 69-71. [Online]. Available: http://aqnis.pcd.go.th/report/annualreport2551.pdf. 2010.

[69] Hung N. T. **"Assessment of Air Pollution Emission from Waste Co-fueling Cement Kilns."** Master Thesis, Asian Institute of Technology. 2007. (in English)

[70] Prakitcharoensuk A. **"Assessment of Atmospheric Impact of POPs Emission from the Cement Industry: A Case Study of Siam City Cement Company."** Master Thesis, Asian Institute of Technology. 2008. (in English)

[71] Sax T. and Isakov V. "A Case Study for Assessing Uncertainty in Local-scale Regulatory Air Quality Modeling Applications" **Atmospheric Environment.** Vol. 37, 2003. pp. 3481-3489.

[72] Caputo M., Giménez M. and Schlamp M. "Intercomparison of Atmospheric Dispersion Models" **Atmospheric Environment.** Vol. 37, 2003. pp. 2435-2449.

[73] Venkatram A., Isakov V., Yuan J. and Pankratz D. "Modeling Dispersion at Distances of Meters from Urban Sources" **Atmospheric Environment.** Vol. 38, 2004. pp. 4633-4641.

[74] Bhardwaj K. S. **"Examination of Sensitivity of Land Use Parameters and Population on the Performance of the AERMOD Model for and Urban Area."** Master Thesis, Civil Engineering, University of Toledo. 2005. (in English).

[75] Orloff K.G., Kaplan B. and Kowalski P. "Hydrogen Cyanide in Ambient Air Near a Gold Heap Leach Field: Measured vs. Modeled Concentrations" **Atmospheric Environment.** Vol. 40, 2006. pp. 3022-3029.

[76] Stein A. F., Isakov V., Godowitch J. and Draxler R. R. "A Hybrid Modeling Approach to Resolve Pollutant Concentrations in an Urban Area" **Atmospheric Environment.** Vol. 41, 2007. pp. 9410-9426.

[77] Kesarkara A. P., Dalvi M., Kaginalkar A., and Ojha A. "Coupling of the Weather Research and Forecasting Model with AERMOD for Pollutant Dispersion Modeling. A Case Study for PM_{10} Dispersion Over Pune, India" **Atmospheric Environment.** Vol. 41, 2007. pp. 1976-1988.

[78] Isakov V., Venkatram A., Touma J. S., Koracin D. and Otte T. L. "Evaluating the Use of Outputs from Comprehensive Meteorological Models in Air Quality Modeling Applications" **Atmospheric Environment.** Vol. 41, 2007. pp. 1689–1705.

[79] Mazur M., Mintz R., Lapalme M. and Wiens B. "Ambient Air Total Gaseous Mercury Concentrations in the Vicinity of Coal-fired Power Plants in Alberta, Canada" **Science of the Total Environment.** Vol. 408, 2009. pp. 373-381.

[80] Venkatram A., Isakov V., Seila R. and Baldauf R. "Modeling the Impacts of Traffic Emissions on Air Toxics Concentrations Near Roadways" **Atmospheric Environment.** Vol. 43, 2009. pp. 3191–3199.

[81] Zou B., Zhan F. B., Wilson J. G. and Zeng Y. "Performance of AERMOD at Different Time Scales" **Simulation Modelling Practice and Theory.** Vol. 18, 2010. pp. 612–623.

[82] Doolgindachbaporn T. **"Calpuff Dispersion Model Study of Ambient SO_2 Concentrations around the Mae Moh Thermal Power Plant in Thailand."** Master Thesis, Faculty of Engineering, Asian Institute of Technology. 1995. (in English).

[83] Godfrey J. J. and Clarkson T. S. "Air Quality Modelling in a Stable Polar Environment-Ross Island, Antarctica" **Atmospheric Environment.** Vol 32, No.17, 1998. pp 2899-2911.

[84] Barna M. G. and Gimson N. R. "Dispersion Modelling of a Wintertime Particulate Pollution Episode in Christchurch, New Zealand" **Atmospheric Environment.** Vol. 36 2002. pp. 3531–3544.

[85] Levy J. I., Spengler J. D., Hlinka D., Sullivan D. and Moon D. "Authors' Response", **Atmospheric Environment.** Vol. 36, 2002. pp. 2267-2270. (Letter to the editor).

[86] Surapipith V. **"Air Pollution in Northern Czech Republic."** Doctoral Thesis, Environmental Sciences, University of East Anglia. 2002.

[87] Jiang G., Lamb B., Westberg H. "Using Back Trajectories and Process Analysis to Investigate Photochemical Ozone Production in the Puget Sound Region" **Atmospheric Environment.** Vol. 37, 2003. pp. 1489-1502.

[88] Elbir T. "Comparison of Model Predictions with the Data of an Urban Air Quality Monitoring Network in Izmir, Turkey" **Atmospheric Environment.** Vol. 37, 2003. pp. 2149-2157.

[89] Kanokkanjana K. **"Modelling Tool for Air Quality Management of the Laem Chabang Industrial Estate."** School of Environment, Resources and Development, Asian Institute of Technology. 2004.

[90] Song Y., Zhang M., Cai X. "PM_{10} modeling of Beijing in the Winter" **Atmospheric Environment.** Vol. 40, 2006. pp. 4126-4136.

[91] Wang L., Parker D. B., Parnell C. B., Lacey R. E. and Shaw B. W. "Comparison of CALPUFF and ISCST3 Models for Predicting Downwind Odor and Source Emission Rates" **Atmospheric Environment.** Vol. 40, 2006. pp. 4663-4669.

[92] Yang D., Han Y., Gao J. and Thé J. "Transport of Airborne Particulate Matters Originating from Mentougou, Beijing, China" **China Particuology.** Vol. 5, No. 6, December 2007. pp. 408-413.

[93] Indumati S., Oza R.B., Mayya Y.S., Puranik V.D., and Kushwaha H.S. "Dispersion of Pollutants Over Land–water–land Interface: Study Using CALPUFF Model" **Atmospheric Environment.** Vol. 43, 2009. pp. 473-478.

[94] MacIntosh D. L., Stewart J. H., Myatt T. A., Sabato J. E., Flowers G. C., Brown K. W., Hlinka D.J. and Sullivan D. A. "Use of CALPUFF for Exposure Assessment in a Near-field, Complex Terrain Setting" **Atmospheric Environment.** Vol. 44, 2010. pp. 262-270.

[95] Goyal P., Singh M. P. and Gulạti A. "Air Quality Assessment of the Environment Over a Cement Industrial Complex" **Atmospheric Environment.** Vol. 30, No. 7, 1996. pp. 1159-1166.

[96] Baroutian S., Mohebbi A. and Goharrizi A.S. "Measuring and Modeling Particulate Dispersion: A Case Study of Kerman Cement Plant" **Journal of Hazardous Materials.** Vol. A136, 2006. pp. 468-474.

[97] Silvester S. A., Lowndes I. S. and Hargreaves D. M. "A Computational Study of Particulate Emissions from an Open Pit Quarry Under Neutral Atmospheric Conditions" **Atmospheric Environment.** Vol. 43, 2009. pp. 6415–6424.

[98] Code of Federal Regulations (CFR). **40 CFR Part 60, App. A, Office of the Federal Register, Jul. 1, 1993.** National Archives and Records Administration, Washington DC, U.S. [Online]. Available : http://www.deq.state.or.us/aq/forms/ sourcetest/appendix_a1.pdf. 2010.

[99] Wilks D. S. **Statistical Methods in the Atmospheric Sciences.** 2nd ed. U.S.: Elsevier Inc., 2006. pp. 113-114.

[100] Bich Thao P. T. **"Development of Emission Inventory and Representative Temporal Allocation Profiles for Power Plants and Major Emission Point Sources in the Central and Eastern Regions of Thailand."** Master thesis, The Joint Graduate School of Energy and Environment, King Mongkut's University of Technology Thonburi, 2006. (in English).

[101] บริษัท เทคนิคสิ่งแวดล้อมไทย จำกัด. **รายงานผลการปฏิบัติตามมาตรการป้องกัน และลดผลกระทบสิ่งแวดล้อม และการติดตามตรวจสอบคุณภาพสิ่งแวดล้อม เหมืองแร่หินปูนเพื่ออุตสาหกรรมปูนซีเมนต์ ของบริษัท ภูมิใจไทยซีเมนต์ จำกัด.** ระหว่างเดือนมกราคม-มิถุนายน 2549.

[102] แผนกสิ่งแวดล้อม ฝ่ายควบคุมคุณภาพ บริษัท ทีพีไอ โพลีน จำกัด (มหาชน). **รายงานผลการติดตามตรวจสอบคุณภาพสิ่งแวดล้อม บริษัท ทีพีไอ โพลีน จำกัด (มหาชน).** ระหว่างเดือนมกราคม-มิถุนายน 2550.

[103] ห้องปฏิบัติการสิ่งแวดล้อม (ว035) ศูนย์มาตรวิทยา บริษัทเอสซีจี ซิเมนต์ จำกัด. **รายงานการปฏิบัติตามมาตรการป้องกัน แก้ไข และลดผลกระทบสิ่งแวดล้อม และมาตรการติดตามตรวจสอบคุณภาพสิ่งแวดล้อม บริษัท ปูนซิเมนต์ไทย (แก่งคอย) จำกัด.** ระหว่างเดือนมกราคม-มิถุนายน 2550.

[104] SGS. **รายงานผลการปฏิบัติตามมาตรการด้านสิ่งแวดล้อมโครงการบริหารพลังงานทดแทนเพื่อการผลิตปูนซีเมนต์ โรงงาน 2 และ 3 บริษัท ปูนซีเมนต์นครหลวง จำกัด (มหาชน).** ระหว่างเดือนมกราคม-มิถุนายน 2550.

[105] Fan S., Horowitz L. W., Levy II H., and Moxim W. J. "Impact of Air Pollution on Wet Deposition of Mineral Dust Aerosols" **Geophysical Research Letters.** Vol. 31, L02104, 2004.

[106] Yue W., Li X., Liu J., Li Y., Yu X., Deng B., Wan T., Zhang G., Huang Y., He W., Hua W., Shao L., Li W. and Yang S. "Characterization of $PM_{2.5}$ in the Ambient Air of Shanghai City by Analyzing Individual Particle" **Science of the Total Environment.** Vol. 368, 2006. pp. 916-925.

[107] Energy Sector Management Assistance Program (ESMAP). **Tools for Improving Air Quality Management: Formal Report 339/11.** [Online]. Available: March 2011. http://www.esmap.org/esmap/sites/esmap.org/files/7607-Source%20Web (Small).pdf. 2011.

[108] Thé J. L., Russell L., Brode R. W. **Worldwide Data Quality Effects on PBL Short-range Regulatory Air Dispersion Models.** [Online]. Available: http://www.weblakes.com/support/resources/WorldQualityADM3.pdf. 2010.

[109] Bhardwaj K. S. **"Examination of Sensitivity of Land Use Parameters and Population on the Performance of the AERMOD Model for and Urban Area."** Master thesis, Department of Civil Engineering, Faculty of Engineering, University of Toledo, 2005. (in English).

APPENDIXES

Appendix A

Industries and population in Saraburi

Table A.1 Industries in Saraburi [1].

District		Number of industries								
		Grey cement	White cement	Stone crushing	Stone production	Concrete production	Power plant	Agriculture production	Others	Total
1	Nong Kae	0	0	0	1	24	1	6	303	**335**
2	Kaeng Khoi	4	4	3	2	15	7	3	179	**217**
3	Chaloem Phra Kiat	1	19	57	12	21	0	14	82	**206**
4	Mueang Saraburi	0	1	1	7	14	0	12	131	**166**
5	Phra Phutthabat	2	7	14	1	23	1	15	97	**160**
6	Wihan Daeng	0	0	2	4	7	0	13	61	**87**
7	Sao Hai	0	0	0	4	7	0	30	33	**74**
8	Ban Mo	1	0	3	0	6	1	12	44	**67**
9	Muak Let	0	0	0	0	1	0	20	29	**50**
10	Wang Muang	0	0	0	0	4	0	15	9	**28**
11	Nong Saeng	0	0	0	0	0	0	12	9	**21**
12	Nong Don	0	0	0	0	0	0	5	0	**5**
13	Don Phut	0	0	0	0	3	0	0	1	**4**
	Total	**8**	**31**	**80**	**31**	**125**	**10**	**157**	**978**	**1,420**

Table A.2 Districts, areas and population in Saraburi [15].

District		Area (km^2)	Number of homes	Population	Population density
1	Nong Kae	262.9	22,285	63,766	243
2	Sao Hai	111.8	6,328	21,086	189
3	Mueang Saraburi	301.6	15,634	49,753	165
4	Chaloem Phra Kiat	150.6	8,635	23,750	158
5	Wihan Daeng	204.5	9,065	30,764	150
6	Ban Mo	203.6	9,234	30,284	149
7	Nong Saeng	87.1	3,366	12,718	146
8	Nong Don	88.1	3,352	11,408	129
9	Phra Phutthabat	287.1	8,768	27,877	97
10	Kaeng Khoi	801.1	22,066	63,217	79
11	Muak Let	681.4	16,190	44,718	66
12	Wang Muang	338.0	5,029	14,097	42
13	Don Phut	58.7	580	2,050	35
	Total	**3576.4**	**130,532**	**395,488**	**111**

Appendix B

Emission factors

Table B.1 Tier 1 emission factors for source category 2.A.1 Cement production [42].

<table>
<tr><th colspan="6">Tier 1 emission factors</th></tr>
<tr><td></td><td>Code</td><td colspan="4">Name</td></tr>
<tr><td>NFR source category</td><td>2.A.1</td><td colspan="4">Cement production</td></tr>
<tr><td>Fuel</td><td colspan="5">NA</td></tr>
<tr><td>Not applicable</td><td colspan="5">NH_3, Aldrin, Chlordane, Chlordecone, Dieldrin, Endrin, Heptachlor, Heptabromo-biphenyl, Mirex,Toxaphene, HCH, DDT, PCB, PCP, SCCP</td></tr>
<tr><td>Not estimated</td><td colspan="5">NO_x, CO, NMVOC, SO_x, Pb, Cd, Hg, As, Cr, Cu, Ni, Se, Zn, PCDD/F, Benzo(a)pyrene, Benzo(b)fluoranthene, Benzo(k)fluoranthene, Indeno(1,2,3-cd)pyrene, Total 4 PAHs, HCB</td></tr>
<tr><td rowspan="2">Pollutants</td><td rowspan="2">Values</td><td rowspan="2">Units</td><td colspan="2">95% confidence interval</td><td rowspan="2">References</td></tr>
<tr><td>Lower</td><td>Upper</td></tr>
<tr><td>TSP</td><td>220</td><td>kg/Mg cement produced</td><td>110</td><td>440</td><td>European commission (2007)</td></tr>
<tr><td>PM_{10}</td><td>100</td><td>kg/Mg cement produced</td><td>100</td><td>400</td><td>European commission (2007)</td></tr>
<tr><td>$PM_{2.5}$</td><td>110</td><td>kg/Mg cement produced</td><td>55</td><td>220</td><td>European commission (2007)</td></tr>
</table>

Table B.2 Tier 2 emission factors for source category 1.A.2.f.i, Cement production [42].

Tier 2 emission factors						
	Code	**Name**				
NFR source category	**1.A.2.f.i**	**Stationary combustion in manufacturing industries and construction**				
Fuel	coal/pet. coke/gas/oil/recovered wastes					
Technologies/practices	Cement manufacture					
Region or regional conditions	NA					
Abatement technologies	NA					
Not applicable	Aldrin, Chlordane, Chlordecone, Dieldrin, Endrin, Heptachlor, Heptabromo-biphenyl, Mirex,					
Not estimated	NH_3, TSP, PM_{10}, $PM_{2.5}$, Total 4 PAHs					
Pollutants	**Values**	**Units**	**95% confidence interval**		**References**	
			Lower	**Upper**		
NO_x	1,550	g/ton clinker	400	6,000	EIPPCB 2007	
CO	2,000	g/ton clinker	1000	4,000	EIPPCB 2007	
NMVOC	100	g/ton clinker	10	1,000	EIPPCB 2007	
SO_x	374	g/ton clinker	20	7,000	EIPPCB 2007	
Pb	0.098	g/ton clinker	0.024	0.4	EIPPCB 2007	
Cd	0.008	g/ton clinker	0.004	0.016	EIPPCB 2007	
Hg	0.11	g/ton clinker	0.012	0.11	EIPPCB 2007	
As	0.0265	g/ton clinker	0.014	0.05	EIPPCB 2007	
Cr	0.041	g/ton clinker	0.028	0.06	EIPPCB 2007	
Cu	0.0647	g/ton clinker	0.022	0.19	EIPPCB 2007	
Ni	0.049	g/ton clinker	0.016	0.15	EIPPCB 2007	
Se	0.0253	g/ton clinker	0.016	0.04	EIPPCB 2007	
Zn	0.424	g/ton clinker	0.2	0.9	EIPPCB 2007	
PCB	1	µg/ton clinker	0.5	10	EMEP/CORINAIR B3311	
PCDD/F	0.05	µg I-TEQ/ton clinker	0.03	0.5	UNEP 2005	
Benzo(a)pyrene	0.000065	g/ton clinker	0.000033	0.000098	US EPA 1995, chapter 11.6	
Benzo(b)fluoranthene	0.00028	g/ton clinker	0.00014	0.00042	US EPA 1995, chapter 11.6	
Benzo(k)fluoranthene	0.000077	g/ton clinker	0.000039	0.00012	US EPA 1995, chapter 11.6	
Indeno(1,2,3-cd)pyrene	0.000043	g/ton clinker	0.000022	0.000065	US EPA 1995, chapter 11.6	
HCB	11	µg/ton clinker	6	17	Kakareka 2005	

Appendix C

Details of the AERMOD input data

Table C.1 Examples of hourly surface data in terms of SAMSON format for the RAMMET View program.

Year	Month	Day	Hour	Ceiling Height (ft)	Cloud Cover (tenths)	Global Radiation (w/m^2)	P (mbar)	Rain (mm)	RH	WD (deg)	WS (m/s)	T (°C)
07	1	1	01	2000	7	0	996	0	78	204	0.8	20.4
07	1	1	02	2000	7	0	996	0	77	197	0.9	20.4
07	1	1	03	2000	7	0	995	0	81	198	1.1	19.4
07	1	1	04	2000	7	0	995	0	77	208	1.6	19.8
07	1	1	05	2000	7	0	995	0	77	204	1.9	19.4
07	1	1	06	2000	7	0	995	0	77	202	1.5	19.4
07	1	1	07	2000	5	8	995	0	80	202	1.4	18.8
07	1	1	08	2000	5	126	997	0	76	204	1.9	19.5
07	1	1	09	2000	5	327	999	0	66	204	1.8	22.8
07	1	1	10	2000	10	462	1000	0	54	203	2.5	26.3
07	1	1	11	2000	10	632	1000	0	47	200	3.2	28.2
07	1	1	12	2000	10	733	1000	0	43	192	3.2	29.5
07	1	1	13	2000	8	782	999	0	43	184	3.1	30.0
07	1	1	14	2000	8	631	997	0	40	196	2.4	30.3
07	1	1	15	2000	8	674	997	0	37	175	2	31.2
07	1	1	16	2000	6	421	996	0	36	185	1.5	31.1
07	1	1	17	2000	6	193	996	0	37	157	0.5	30.5
07	1	1	18	2000	6	38	996	0	43	111	1.1	28.9
07	1	1	19	2000	5	0	996	0	51	113	1.9	26.7
07	1	1	20	2000	5	0	996	0	57	117	1.5	25.7
07	1	1	21	2000	5	0	997	0	65	92	1.1	24.4
07	1	1	22	2000	6	0	997	0	69	144	0.6	23.4
07	1	1	23	2000	6	0	996	0	75	197	1	22.1
07	1	1	24	2000	6	0	996	0	79	204	0.8	21.1

Examples of upper air data in terms of FSL format for the AERMET program.

254	0	1	JAN	2007		
1	48455	72518	13.72	100.55	86	0
2	100	220	145	35	32767	0
3		BKK			32767	kt
9	1012	4	220	179	0	0
4	1000	110	228	128	180	2
4	962	448	242	102	222	3
5	925	790	222	112	265	4
4	866	1357	172	92	222	1
5	850	1515	158	68	210	0
5	808	1942	124	-6	209	4
5	788	2152	116	-114	208	7
5	767	2377	124	-246	207	9
5	700	3138	100	-390	205	17
5	670	3500	88	-402	226	17
5	646	3801	80	-410	243	17
4	555	5032	0	-390	315	18
5	548	5133	-5	-455	321	18
5	507	5750	-31	-521	358	19
5	500	5860	-35	-525	5	19
5	437	6912	-95	-575	359	38
5	400	7590	-137	-607	355	50
5	353	8525	-197	-647	340	36
5	334	8932	-217	-657	333	30
5	300	9710	-275	-705	320	18
5	287	10028	-291	-711	299	18
5	250	11000	-365	-765	235	18
5	200	12490	-501	-681	220	21
4	150	14290	-667	-847	200	29
5	143	14577	-693	-863	191	27
4	117	15746	-791	-941	154	17
5	112	15993	-801	-971	146	15
5	106	16304	-809	-989	136	12
5	101	16574	-823	-993	127	9
5	100	16630	-823	-993	125	9

Examples of upper air data in terms of FSL format can be explained as follows.

FSL Rawinsonde data format

The official FSL data format is similar to the format used by the National Severe Storms Forecast Center (NSSFC) in Kansas City. The first 4 lines of the sounding are identification and information lines. All additional lines are data lines. An entry of 32767 (original format) or 99999 (new format) indicates that the information is either missing, not reported, or not applicable.

--COLUMN NUMBER---

1	2	3	4	5	6	7		
LINTYP								
header	lines							
254	HOUR	DAY	MONTH	YEAR	(blank)	(blank)		
1	WBAN#	WMO#	LAT	D	LON	D	ELEV	RTIME
2	HYDRO	MXWD	TROPL	LINES	TINDEX	SOURCE		
3	(blank)	STAID	(blank)	(blank)	SONDE	WSUNITS		
data	lines							
9	PRESSURE	HEIGHT	TEMP	DEWPT	WIND DIR	WIND SPD		
4								
5								
6								
7								
8								

LEGEND

LINTYP: type of identification line

254 = indicates a new sounding in the output file

1 = station identification line

2 = sounding checks line

3 = station identifier and other indicators line

4 = mandatory level

5 = significant level

6 = wind level (PPBB) (GTS or merged data)

7 = tropopause level (GTS or merged data)

8 = maximum wind level (GTS or merged data)

9 = surface level

HOUR: time of report in UTC

LAT: latitude in degrees and hundredths

LON: longitude in degrees and hundredths

D: direction latitude ('N' or 'S') or longitude ('E' or 'W') -note this only appears in the online archive containing international observations.

ELEV: elevation from station history in meters

RTIME: is the actual release time of radiosonde from TTBB. Appears in GTS data only.

HYDRO: the pressure of the level to where the sounding passes the hydrostatic check (see section 4.3).**

MXWD: the pressure of the level having the maximum wind in the sounding. If within the body of the sounding there is no "8" level then MXWN is estimated (see section 3.2).

TROPL: the pressure of the level containing the tropopause. If within the body of the sounding there is no "7" level, then TROPL is estimated (see section 3.3)**

LINES: number of levels in the sounding, including the 4 identification lines.

TINDEX: indicator for estimated tropopause. A "7" indicates that sufficient data was available to attempt the estimation; 11 indicates that data terminated and that tropopause is a "suspected" tropopause.

SOURCE:
- 0 = National Climatic Data Center (NCDC)
- 1 = Atmospheric Environment Service (AES), Canada
- 2 = National Severe Storms Forecast Center (NSSFC)
- 3 = GTS or FSL GTS data only
- 4 = merge of NCDC and GTS data (sources 2,3 merged into sources 0,1)

SONDE: type of radiosonde code from TTBB. Only reported with GTS data
- 10 = VIZ "A" type radiosonde
- 11 = VIZ "B" type radiosonde
- 12 = Space data corp. (SDC) radiosonde.

WSUNITS: wind speed units (selected upon output)
- ms = tenths of meters per second
- kt = knots

PRESSURE: in whole millibars (original format)
in tenths of millibars (new format)

HEIGHT: height in meters (m)

TEMP: temperature in tenths of degrees Celsius

DEWPT: dew point temperature in tenths of a degree Celsius

WIND DIR: wind direction in degrees

WIND SPD: wind speed in either knots or tenths of a meter per second (selected by user upon output)

Appendix D

Details of the CALPUFF input data

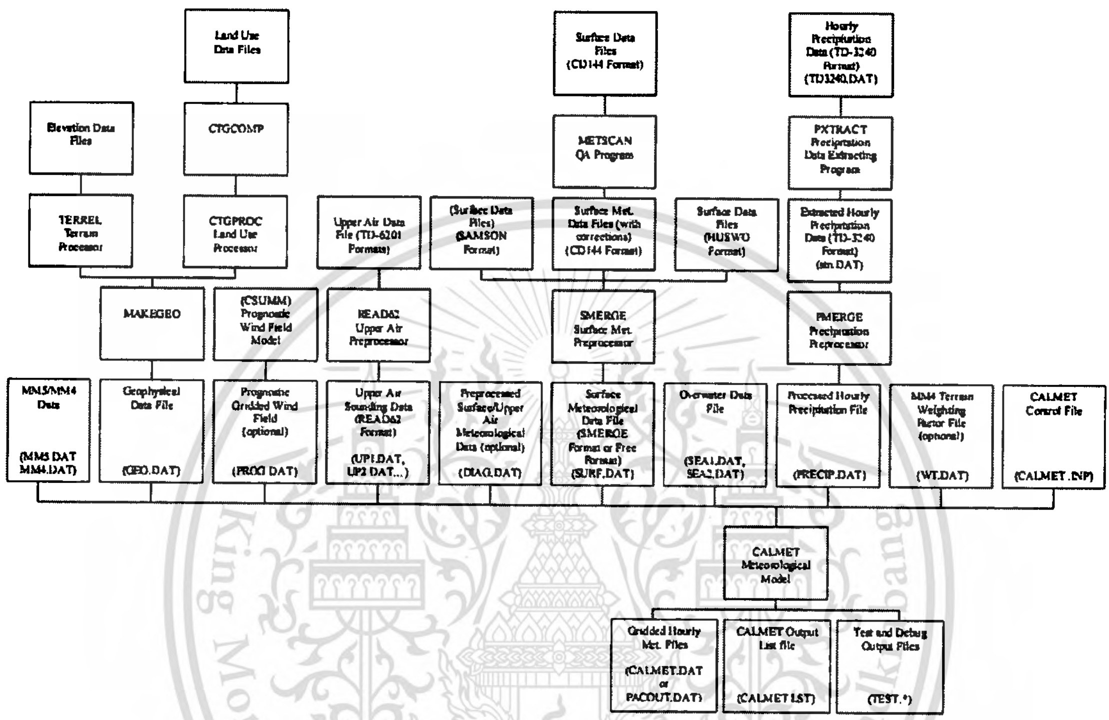

Figure D.1 Meteorological modeling: CALMET modeling flow diagram [64].

Land use and elevation data

```
GEO.DAT         2.0             Header structure with coordinate parameters
   2
Produced by MAKEGEO Version: 2.2  Level: 030402
simplified GEO.DAT
UTM
  47N
WGS-G   25-12-2007
     100      100      701.000    1593.000        0.50        0.50
KM  M
0          - LAND USE DATA - (0 = default categories)
20,20,20,20,20,20,20,20,20,20,10,20,20,20,20,20,20,20,20,20,20,20,20,20,20,20,20,20
,20,20,20,20,20,20,20,20,20,20,20,20,20,10,20,10,20,20,20,50,50,50,20,20,20,20,20,20,2
0,20,20,20,20,20,20,20,20,20,20,20,20,20,20,20,20,20,20,20,40,40,40,40,20,20,20,20,
20,20,10,20,20,20,20,20,20,20,20,20,40,40,20,20,20,20,20,20,10,10,10,10,10,20,10,10,10
,10,20,10,20,20,20,20,20,20,10,20,10,10,20,20,20,20,20,20,20,20,20,10,10,10,10,10,1
0,10,20,20,20,50,50,50,50,20,10,10,10,10,20,20,10,10,10,10,10,10,10,10,10,20,20,20,20,
20,20,20,20,20,20,40,40,40,40,40,40,40,20,20,20,20,10,20,20,20,20,20,20,20,20,20,20,20
,20,10,10,10,10,10,20,10,10,20,20,20,20,20,20,20,20,20,20,20,20,20,10,20,10,10,20,2
0,20,20,20,10,20,20,10,20,10,20,20,20,10,10,10,20,20,10,10,20,20,20,20,10,10,10,10,10,
10,10,20,20,20,20,20,20,20,20,20,20,20,20,20,20,20,20,20,20,40,40,40,40,40,40,40,20,20
,20,20,10,10,20,20,20,20,20,20,20,20,20,20,20,20,20,20,20,20,20,20,10,20,20,10,20,10,2
0,20,20,20,20,20,20,20,20,10,10,10,20,10,20,20,20,20,20,20,20,20,20,20,20,20,20,10,10,
10,10,20,20,10,20,20,20,20,20,20,20,20,10,10,20,20,20,20,.........
   1.00000     -- Terrain heights - HTFAC - conversion to meters
100,100,100,100,100,100,100,100,100,100,100,100,100,100,125,117,100,100,100,100,100,10
0,100,100,100,100,100,100,100,100,100,100,100,100,100,100,100,100,100,100,100,133,166,
143',119,100,100,100,100,100,100,100,100,100,100,100,100,100,100,100,100,100,109,196,20
0,175,196,202,254,485,542,622,734,855,844,805,814,797,755,706,700,644,613,695,700,700,
702,703,702,703,700,700,600,600,600,601,700,700,700,700,......

 0    - default albedo field
 0    - default Bowen ratio field
 0    - default soil heat flux parameters
 0    - default anthropogenic heat flux field
 0    - default leaf area index field
 0    - default z0 field
 0    - default albedo field
 0    - default Bowen ratio field
 0    - default soil heat flux parameters
 0    - default anthropogenic heat flux field
 0    - default leaf area index field
```

```
UP.DAT          2.0             Header structure with coordinate parameters
   1
Produced by READ62 Version: 5.54  Level: 070627
NONE
  2006  364    0 2008    2   23 500.    2    2
     F    F    F    F
   6201      48455   20061230 0     56                              31
   1013.0,   4.,295.0,  0,  0.0,  1000.0, 115.,295.2, 50,  2.6,   979.0, 300.,295.4, 53,  4.1,   952.0, 542.,294.4, 56,  6.2,
    928.0, 763.,294.0, 60,  8.2,   925.0, 791.,293.8, 60,  8.2,   912.0, 914.,293.4, 65,  6.2,   905.0, 979.,293.2, 64,  5.7,
    880.0,1219.,291.2, 60,  3.1,   850.0,1515.,288.8, 55,  3.6,   819.0,1829.,285.8, 35,  3.1,   795.0,2077.,283.4,355,  2.1,
    790.0,2134.,283.0,345,  2.1,   786.0,2171.,282.8,338,  2.1,   781.0,2224.,283.2,329,  2.1,   775.0,2288.,284.2,317,  2.6,
    770.0,2342.,285.4,307,  2.6,   764.0,2407.,286.4,296,  2.6,   761.0,2438.,286.5,290,  2.6,   756.0,2495.,286.8,291,  3.1,
    748.0,2584.,286.8,292,  3.1,   734.0,2743.,286.1,295,  4.1,   700.0,3138.,284.4,255,  4.1,   671.0,3488.,282.8,248,  3.6,
    657.0,3658.,282.3,245,  3.6,   649.0,3763.,282.0,247,  3.6,   610.0,4267.,279.3,255,  2.6,   601.0,4392.,278.6,266,  3.1,
    566.0,4877.,275.1,310,  5.7,   546.0,5165.,273.1,319,  7.7,   500.0,5860.,268.1,340, 13.4
   6201      48455   2006123012     56                              31
   1013.0,   4.,295.0,  0,  0.0,  1000.0, 115.,295.2, 50,  2.6,   979.0, 300.,295.4, 53,  4.1,   952.0, 542.,294.4, 56,  6.2,
    928.0, 763.,294.0, 60,  8.2,   925.0, 791.,293.8, 60,  8.2,   912.0, 914.,293.4, 65,  6.2,   905.0, 979.,293.2, 64,  5.7,
    880.0,1219.,291.2, 60,  3.1,   850.0,1515.,288.8, 55,  3.6,   819.0,1829.,285.8, 35,  3.1,   795.0,2077.,283.4,355,  2.1,
    790.0,2134.,283.0,345,  2.1,   786.0,2171.,282.8,338,  2.1,   781.0,2224.,283.2,329,  2.1,   775.0,2288.,284.2,317,  2.6,
    770.0,2342.,285.4,307,  2.6,   764.0,2407.,286.4,296,  2.6,   761.0,2438.,286.5,290,  2.6,   756.0,2495.,286.8,291,  3.1,
    748.0,2584.,286.8,292,  3.1,   734.0,2743.,286.1,295,  4.1,   700.0,3138.,284.4,255,  4.1,   671.0,3488.,282.8,248,  3.6,
    657.0,3658.,282.3,245,  3.6,   649.0,3763.,282.0,247,  3.6,   610.0,4267.,279.3,255,  2.6,   601.0,4392.,278.6,266,  3.1,
    566.0,4877.,275.1,310,  5.7,   546.0,5165.,273.1,319,  7.7,   500.0,5860.,268.1,340, 13.4
   6201      48455   20061231 0     31                              16
   1012.0,   4.,295.2,  0,  0.0,  1000.0, 110.,296.0,180,  1.0,   962.0, 448.,297.4,222,  1.5,   925.0, 790.,295.4,265,  2.1,
    866.0,1357.,290.4,222,  0.5,   850.0,1515.,289.0,210,  0.0,   808.0,1942.,285.6,209,  2.1,   788.0,2152.,284.8,208,  3.6,
    767.0,2377.,285.6,207,  4.6,   700.0,3138.,283.2,205,  8.8,   670.0,3500.,282.0,226,  8.8,   646.0,3801.,281.2,243,  8.8,
    555.0,5032.,273.2,315,  9.3,   548.0,5133.,272.7,321,  9.3,   507.0,5750.,270.1,358,  9.8,   500.0,5860.,269.7,  5,  9.8
   6201      48455   2006123112     31                              16
   1012.0,   4.,295.2,  0,  0.0,  1000.0, 110.,296.0,180,  1.0,   962.0, 448.,297.4,222,  1.5,   925.0, 790.,295.4,265,  2.1,
    866.0,1357.,290.4,222,  0.5,   850.0,1515.,289.0,210,  0.0,   808.0,1942.,285.6,209,  2.1,   788.0,2152.,284.8,208,  3.6,
    767.0,2377.,285.6,207,  4.6,   700.0,3138.,283.2,205,  8.8,   670.0,3500.,282.0,226,  8.8,   646.0,3801.,281.2,243,  8.8,
    555.0,5032.,273.2,315,  9.3,   548.0,5133.,272.7,321,  9.3,   507.0,5750.,270.1,358,  9.8,   500.0,5860.,269.7,  5,  9.8
```

The above data are examples of upper air data which are formatted by the CALPUFF PROfessional: READ 62 5.2.0.

```
SURF.DAT        2.0             Header structure with coordinate parameters
   1
Produced by SMERGE Version: 5.3  Level: 030402
NONE
  2007   1   0  2007 365  23   -7    3
   11102
   11101
   31301
  07   1   0
    0.799999  204.000000   66    7  293.550000   78  996.052632 9999
    1.200000   51.000000   66    7  297.850000   67  993.421053 9999
    2.057776  100.000000   66    7  297.350000   52  969.660000 9999
  07   1   1
    0.900000  197.000000   66    7  293.550000   77  996.052632 9999
    0.799999   79.000000   66    7  296.750000   73  993.421053 9999
    2.057776  100.000000   66    7  297.250000   52  969.660000 9999
  07   1   2
    1.100000  198.000000   66    7  292.550000   81  994.736842 9999
    1.000000  104.000000   66    7  296.650000   72  992.105263 9999
    2.057776  100.000000   66    7  297.150000   52  969.660000 9999
  07   1   3
    1.600000  208.000000   66    7  292.950000   77  994.736842 9999
    1.000000   75.000000   66    7  297.050000   69  992.105263 9999
    3.086664  100.000000   66    7  297.050000   51  968.950000 9999
  07   1   4
    1.900000  204.000000   66    7  292.550000   77  994.736842 9999
    1.500000   74.000000   66    7  297.550000   66  992.105263 9999
    3.086664  100.000000   66    7  297.083333   51  968.950000 9999
  07   1   5
    1.500000  202.000000   66    7  292.550000   77  994.736842 9999
    2.100000  101.000000   66    7  297.650000   65  993.421053 9999
    3.086664  100.000000   66    7  297.116667   51  968.950000 9999
  07   1   6
    1.400000  202.000000   66    5  291.950000   80  994.736842 9999
    2.000000   71.000000   66    5  297.450000   66  993.421053 9999
    0.000000    0.000000   66    5  297.150000   48  969.510000 9999
  07   1   7
    1.900000  204.000000   66    5  292.650000   76  997.368421 9999
    2.300000   47.000000   66    5  297.650000   68  994.736842 9999
    0.000000    0.000000   66    5  297.716667   48  969.510000 9999
```

The above data are examples of surface data that are used to prepare the CALMET input meteorological data. The meteorological data are wind speed (m/s), wind direction (degrees), ceiling height (hundreds of feet), opaque sky cover (tenths), air temperature (degree K), relative humidity (percent), station pressure (mbar) and precipitation (mm/h) (9999 is no data). All surface meteorological data are formatted by written C code on the Visual Studio 2005.

```
PRECIP.DAT        2.0            Header structure with coordinate parameters
   1
Produced by SMERGE Version: 5.3  Level: 030528
NONE
  2007   1   0  2008   2  23   -7    2
   11102
   11101
 2007   1  0      0.000  9999.000
 2007   1  1      0.000  9999.000
 2007   1  2      0.000  9999.000
 2007   1  3      0.000  9999.000
 2007   1  4      0.000  9999.000
 2007   1  5      0.000  9999.000
 2007   1  6      0.000  9999.000
 2007   1  7      0.000  9999.000
 2007   1  8      0.000  9999.000
 2007   1  9      0.000  9999.000
 2007   1 10      0.000  9999.000
 2007   1 11      0.000  9999.000
 2007   1 12      0.000  9999.000
 2007   1 13      0.000  9999.000
 2007   1 14      0.000  9999.000
 2007   1 15      0.000  9999.000
 2007   1 16      0.000  9999.000
 2007   1 17      0.000  9999.000
 2007   1 18      0.000  9999.000
 2007   1 19      0.000  9999.000
 2007   1 20      0.000  9999.000
 2007   1 21      0.000  9999.000
 2007   1 22      0.000  9999.000
 2007   1 23      0.000  9999.000
```

The above data are examples of rain precipitation data that are used to prepare the CALMET input data. The unit of rain precipitation data is mm/h.

```
'OZONE', 2, 47, 2007001, 0, 2008002, 0, '5', 'test'
'25T',   707.537,    1606.814
'24T',   701.568,    1624.422
 2007   1  0 9999.0 9999.0
 2007   1  1    7.0 9999.0
 2007   1  2    7.0 9999.0
 2007   1  3    7.0 9999.0
 2007   1  4    0.0 9999.0
 2007   1  5    4.0 9999.0
 2007   1  6    2.0 9999.0
 2007   1  7    7.0 9999.0
 2007   1  8   16.0 9999.0
 2007   1  9   31.0 9999.0
 2007   1 10   43.0 9999.0
 2007   1 11   41.0 9999.0
 2007   1 12   45.0 9999.0
 2007   1 13   52.0 9999.0
 2007   1 14   58.0 9999.0
 2007   1 15   60.0 9999.0
 2007   1 16   59.0 9999.0
 2007   1 17   47.0 9999.0
 2007   1 18   30.0 9999.0
 2007   1 19   29.0 9999.0
 2007   1 20   14.0 9999.0
 2007   1 21   18.0 9999.0
 2007   1 22   10.0 9999.0
 2007   1 23    2.0 9999.0
```

The above data are examples of ozone concentrations (μg/m^3) that are used for the CALPUFF running with chemically reactive modules: RIVAD/ARM3 and MESOPUFF

Appendix E

Wind fields by the CALMET

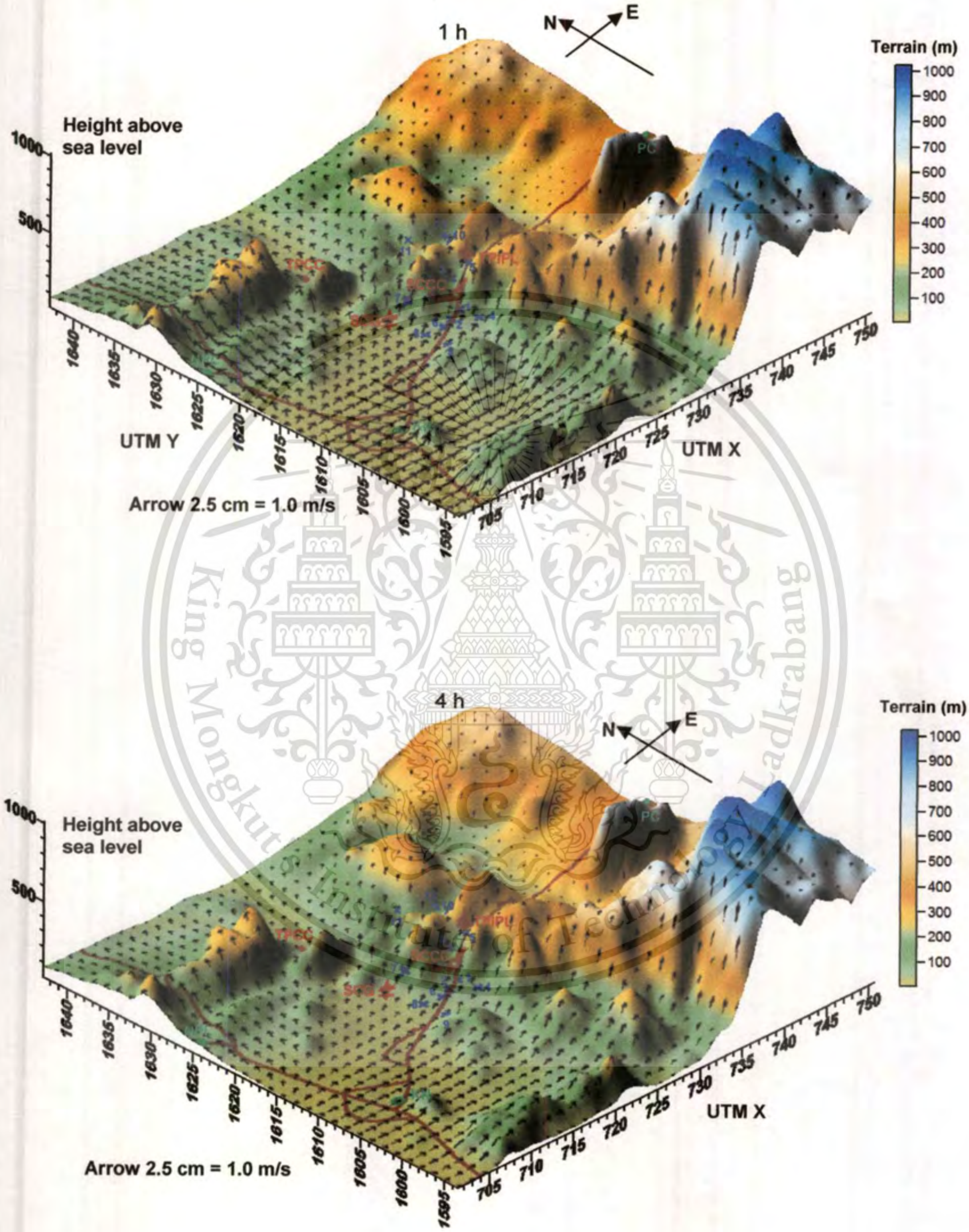

Figure E.1 Surface wind field simulated by the CALMET on March 24, 2007: (●) meteorological stations, (+) receptors and (×) stacks of cement plants.

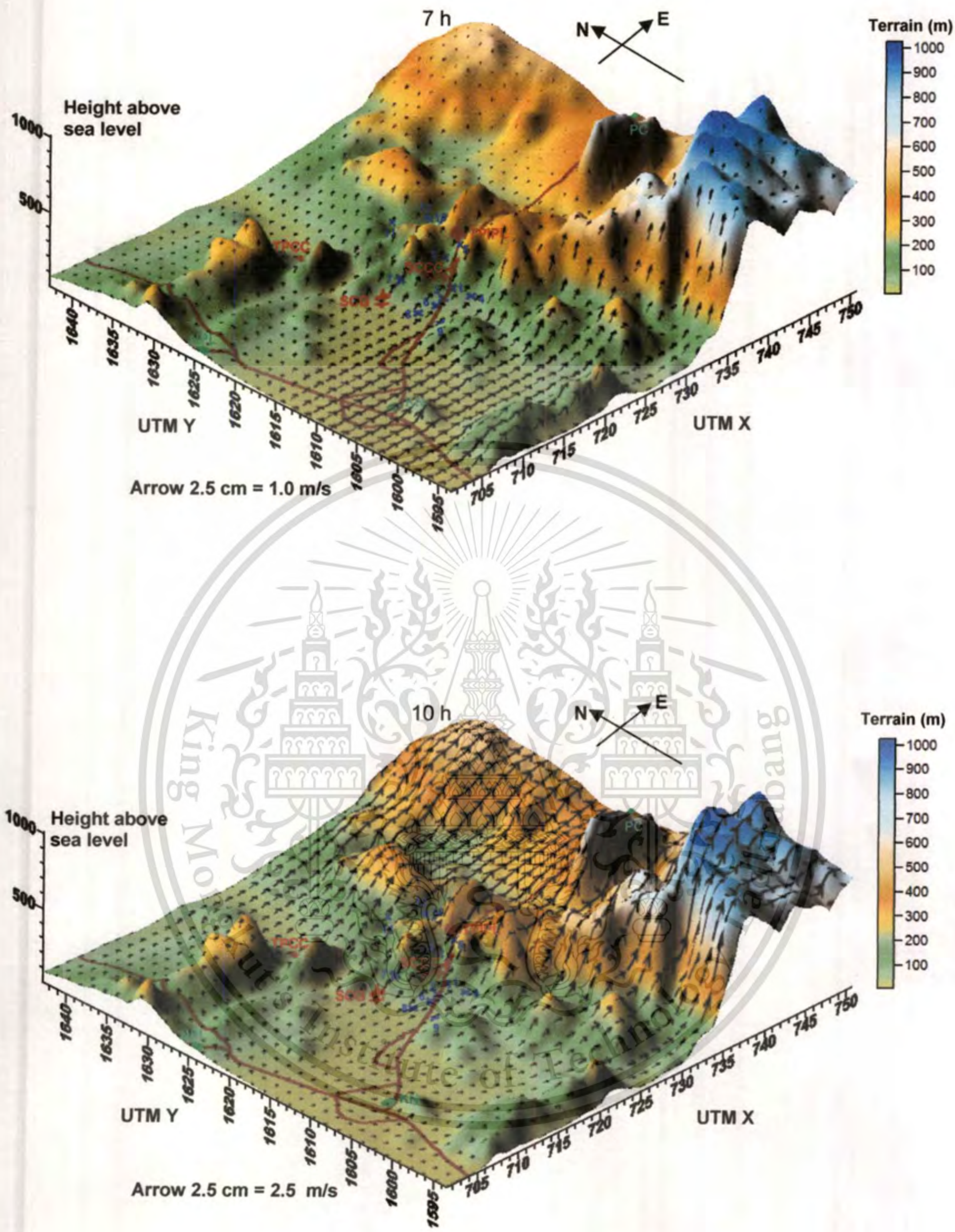

Figure E.1 Surface wind field simulated by the CALMET on March 24, 2007: (●) meteorological stations, (+) receptors and (×) stacks of cement plants (cont.).

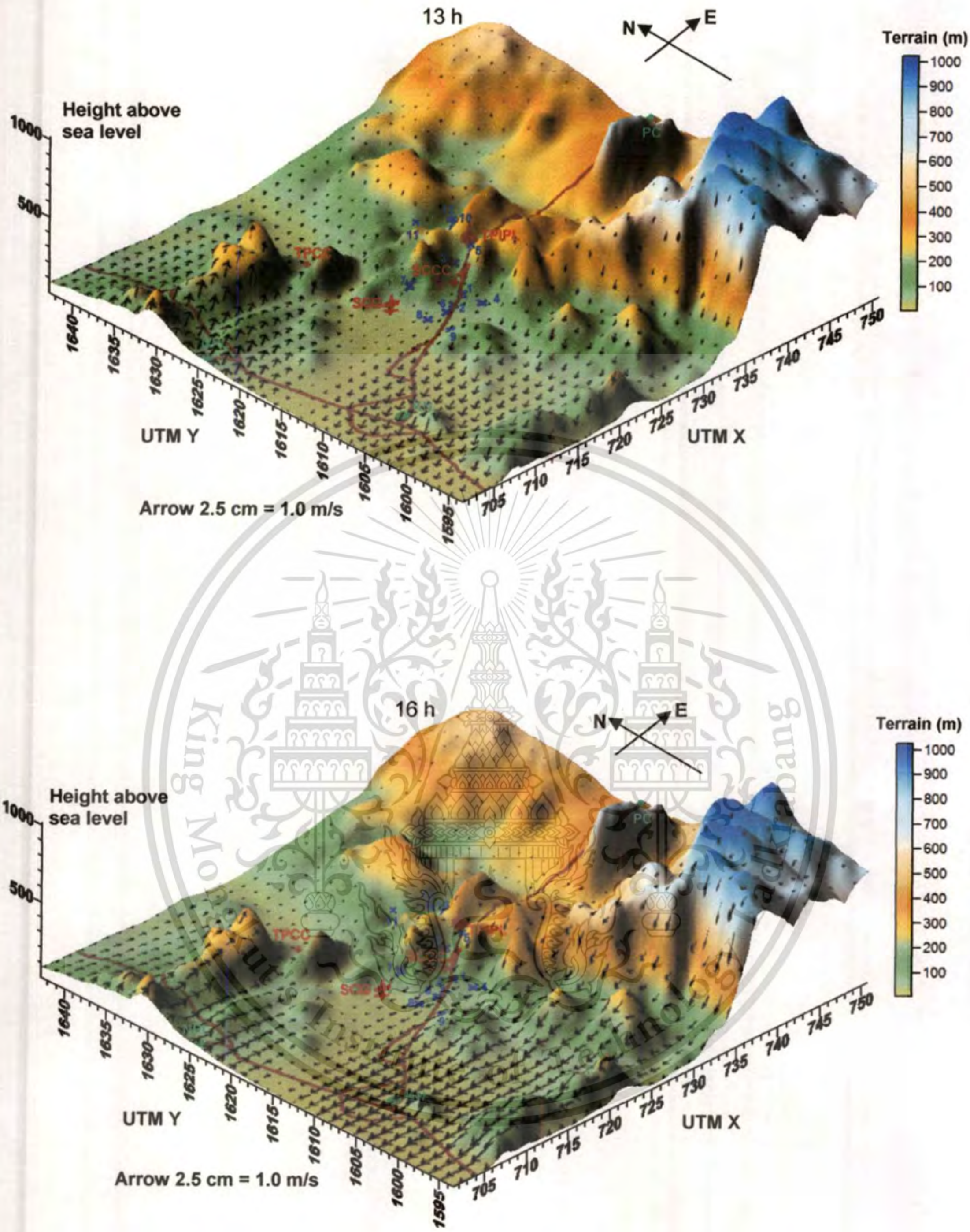

Figure E.1 Surface wind field simulated by the CALMET on March 24, 2007: (●) meteorological stations, (+) receptors and (×) stacks of cement plants (cont.).

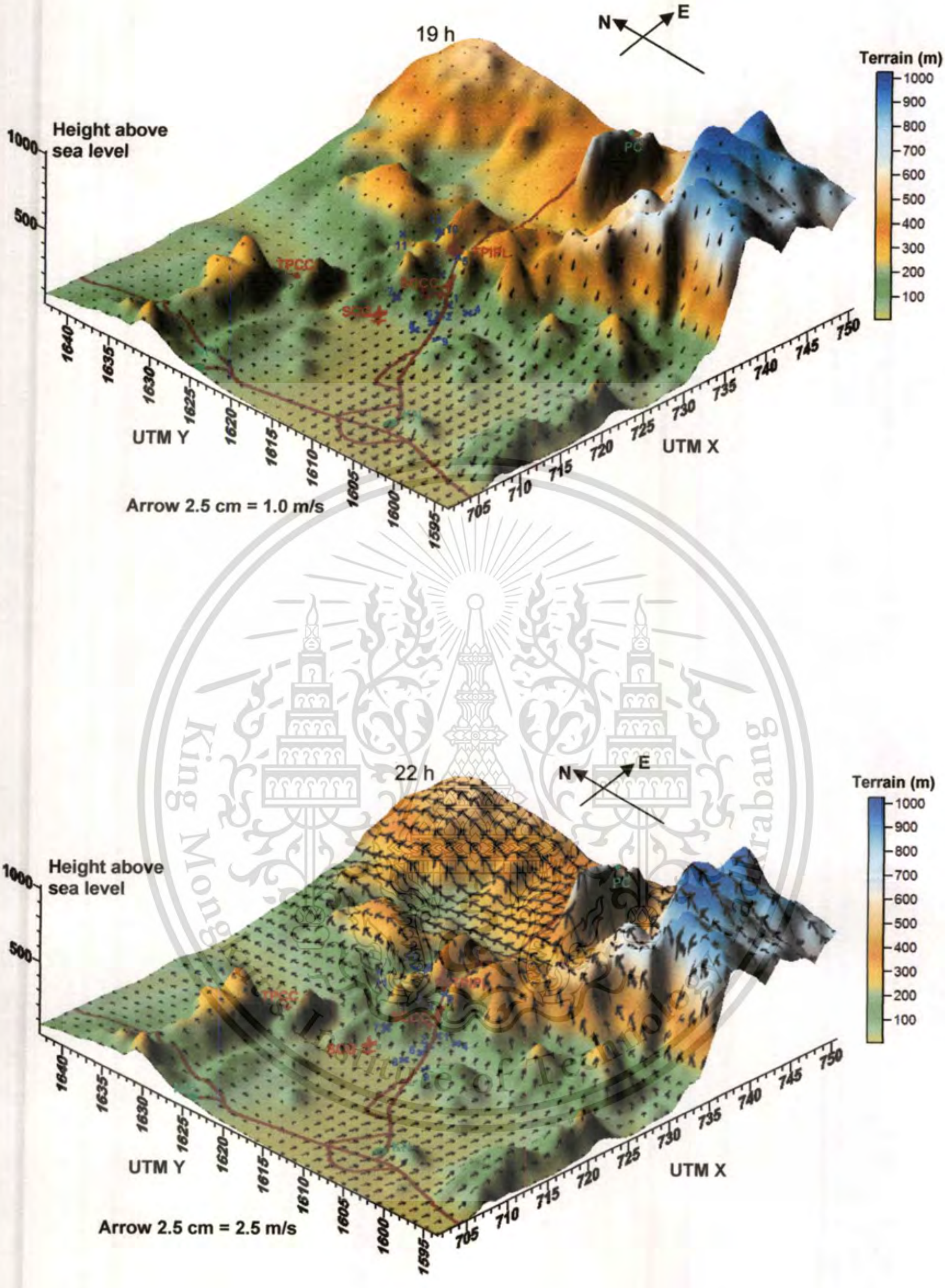

Figure E.1 Surface wind field simulated by the CALMET on March 24, 2007: (●) meteorological stations, (+) receptors and (×) stacks of cement plants (cont.).

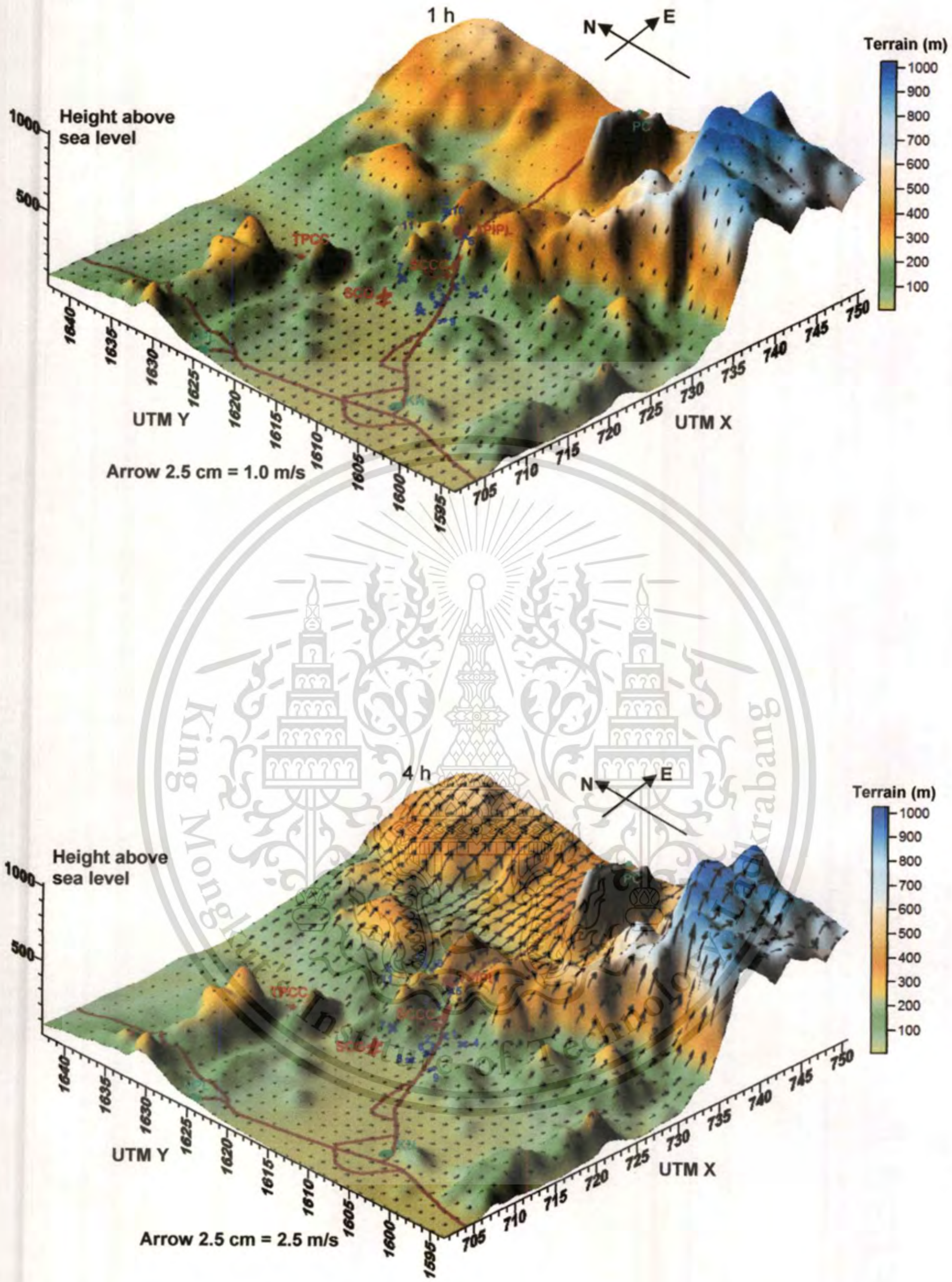

Figure E.2 Surface wind field simulated by the CALMET on October 12, 2007: (●) meteorological stations, (+) receptors and (×) stacks of cement plants.

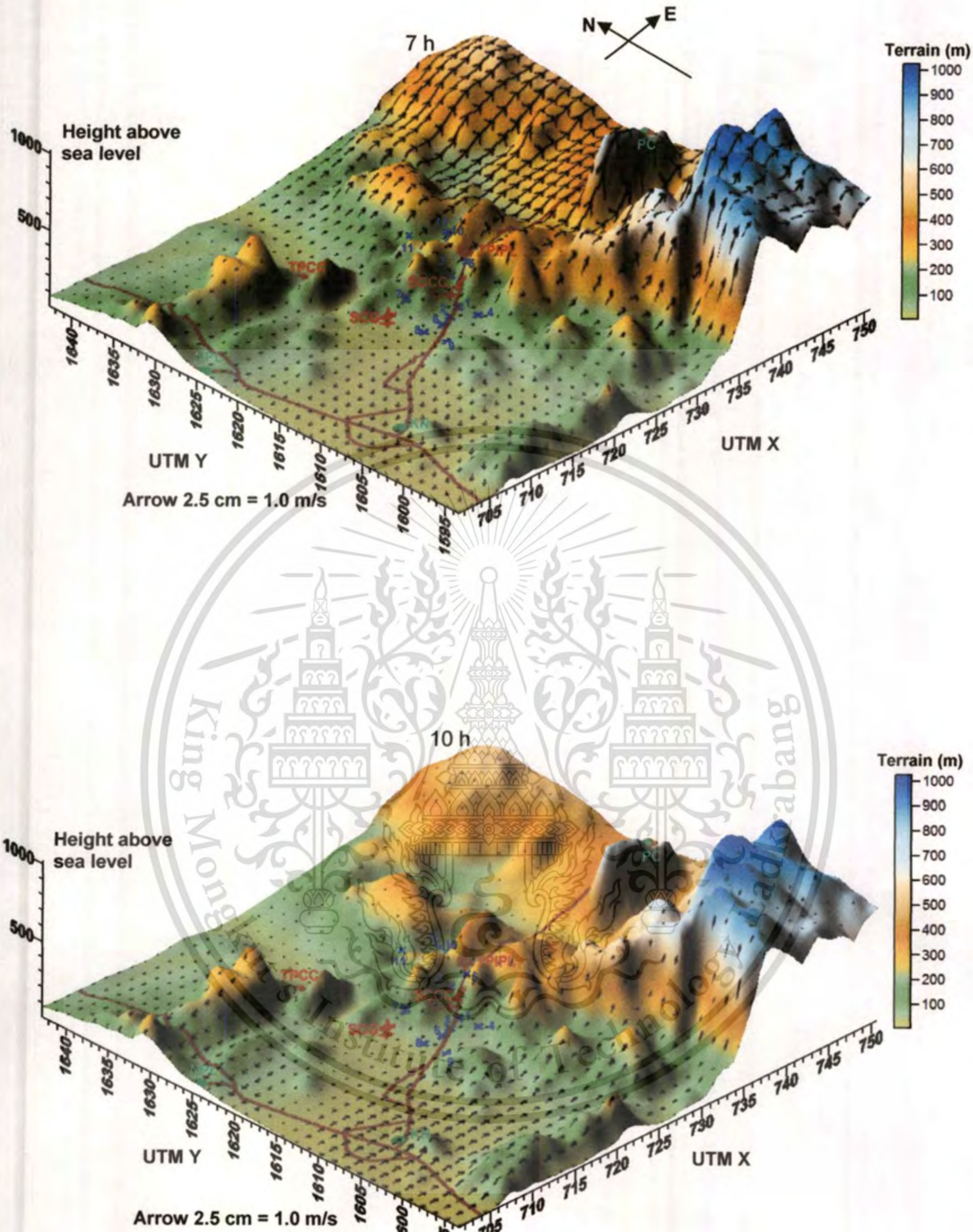

Figure E.2 Surface wind field simulated by the CALMET on October 12, 2007: (●) meteorological stations, (+) receptors and (×) stacks of cement plants (cont.).

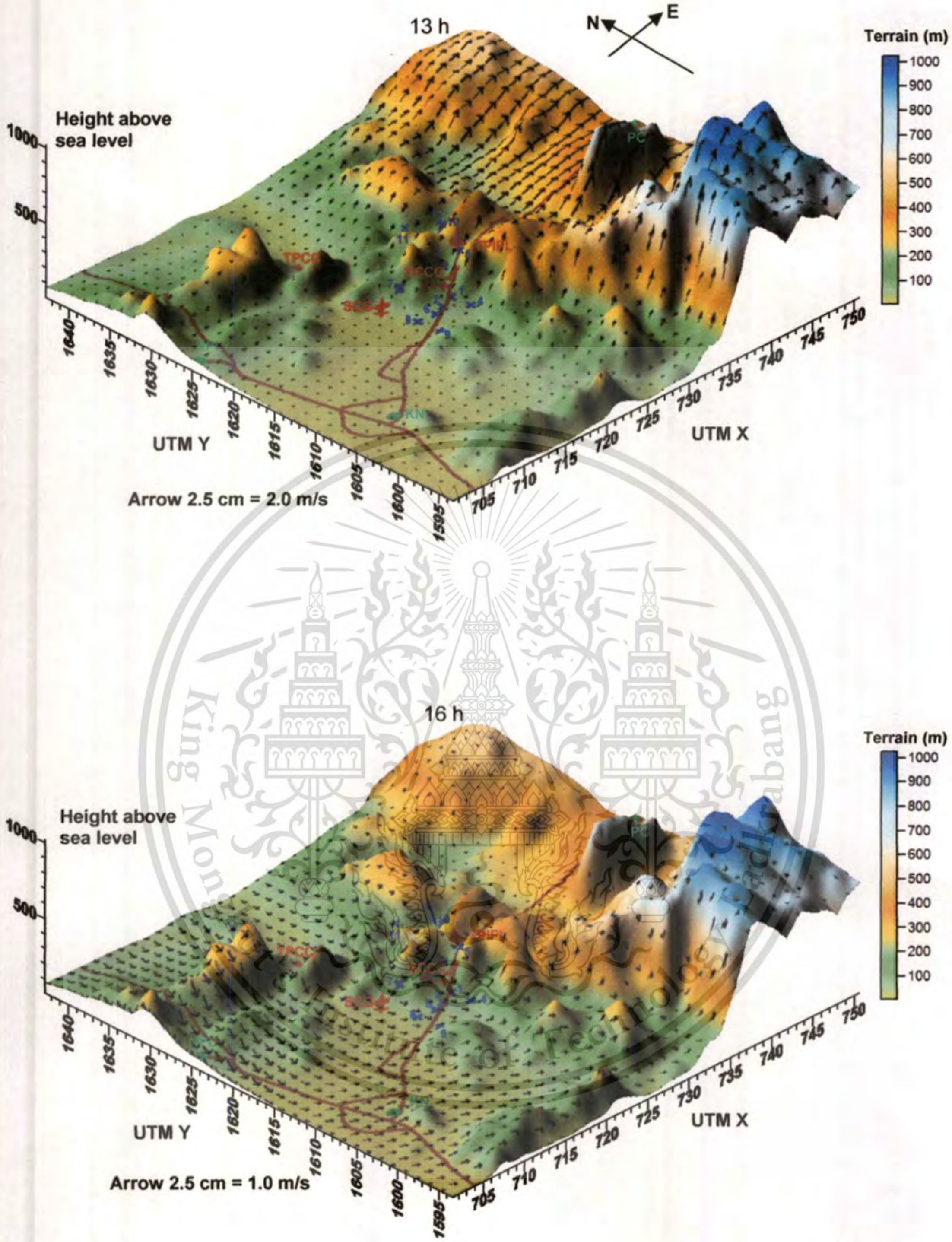

Figure E.2 Surface wind field simulated by the CALMET on October 12, 2007: (●) meteorological stations, (+) receptors and (×) stacks of cement plants (cont.).

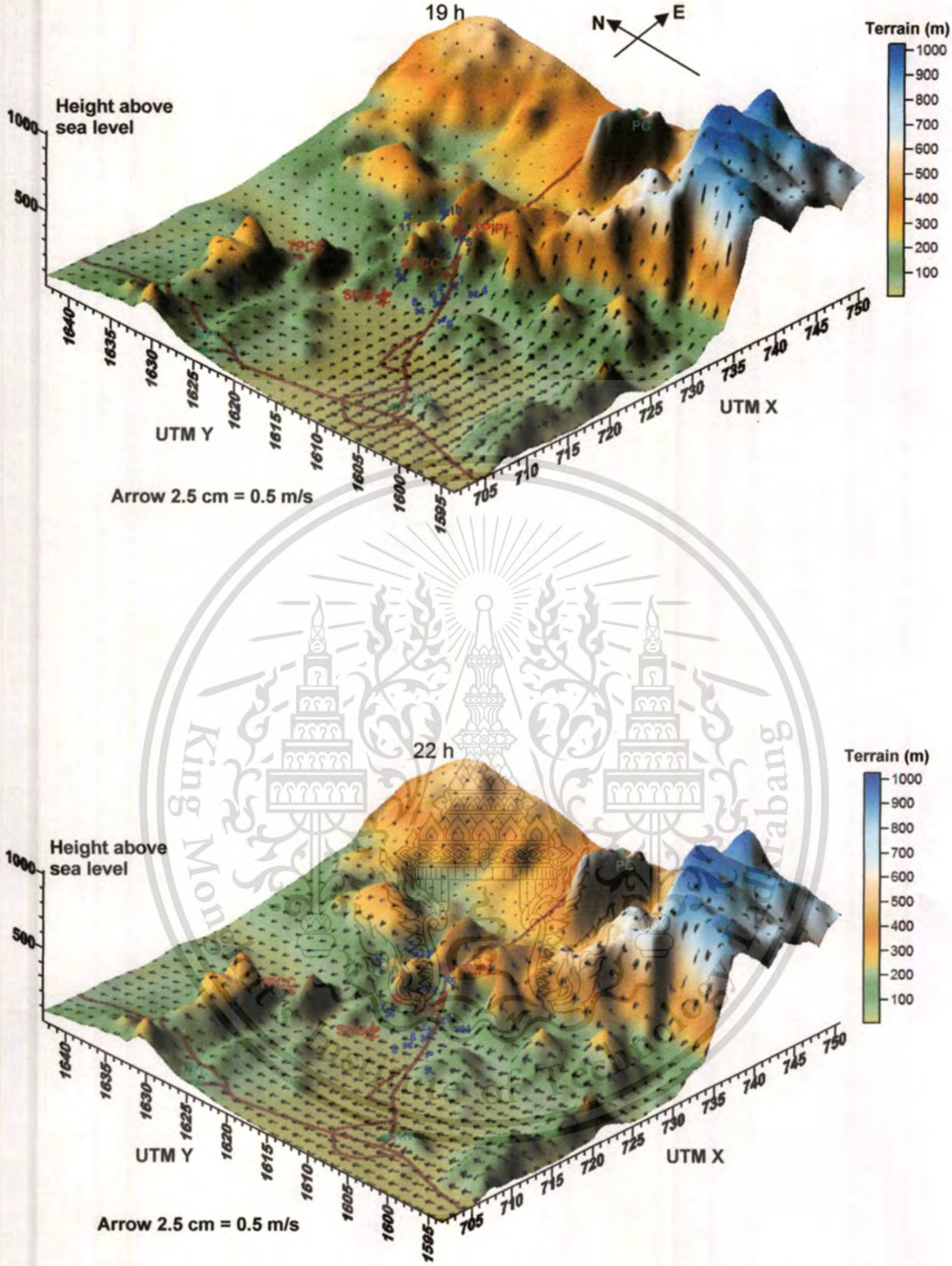

Figure E.2 Surface wind field simulated by the CALMET on October 12, 2007: (●) meteorological stations, (+) receptors and (×) stacks of cement plants (cont.).

Appendix F

Ground concentration of NO_2 by the CALPUFF

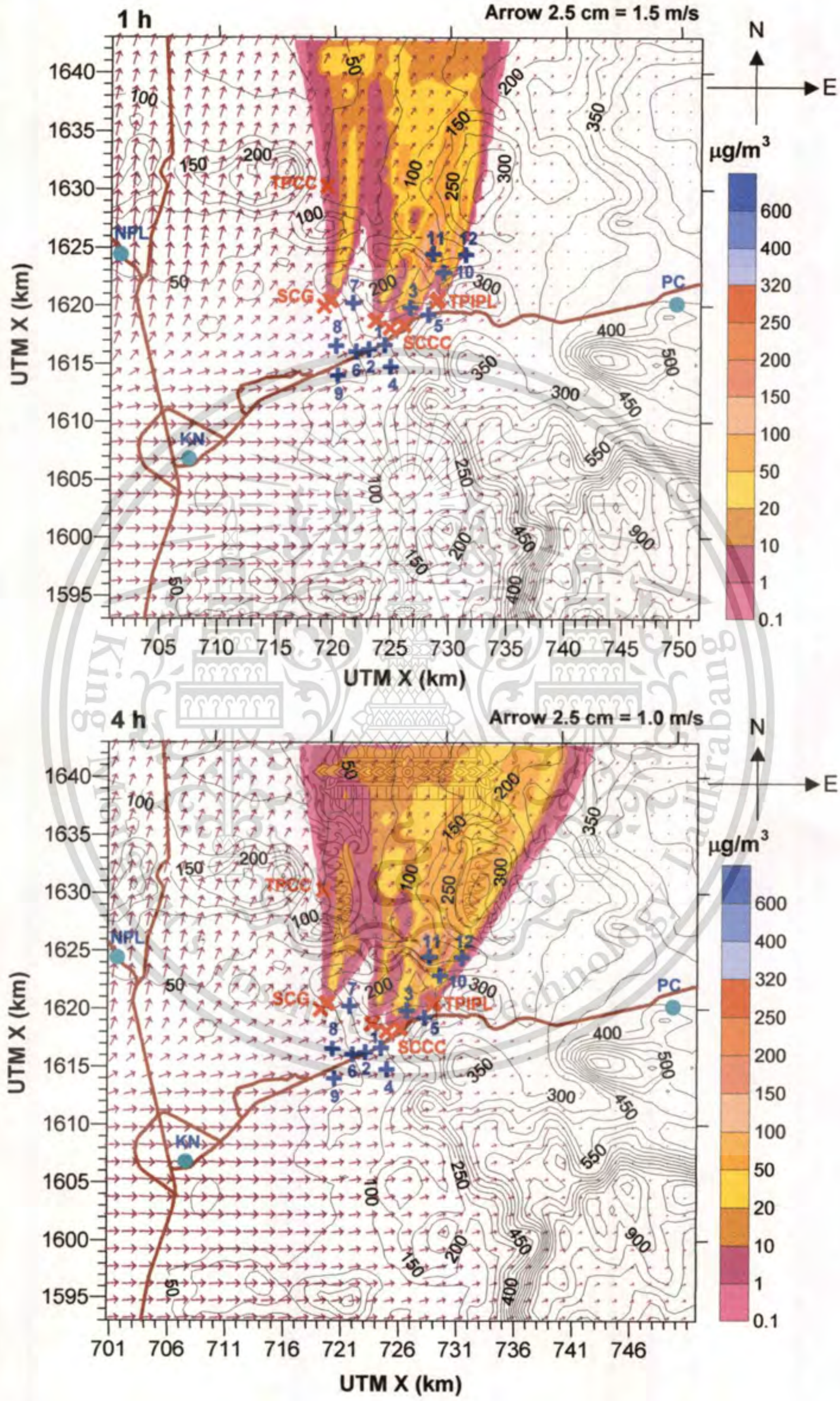

Figure F.1 Plumes of NO_2 simulated by CALPUFF on March 24, 2007 (●) meteorological stations, (+) receptors and (×) stacks of cement plants.

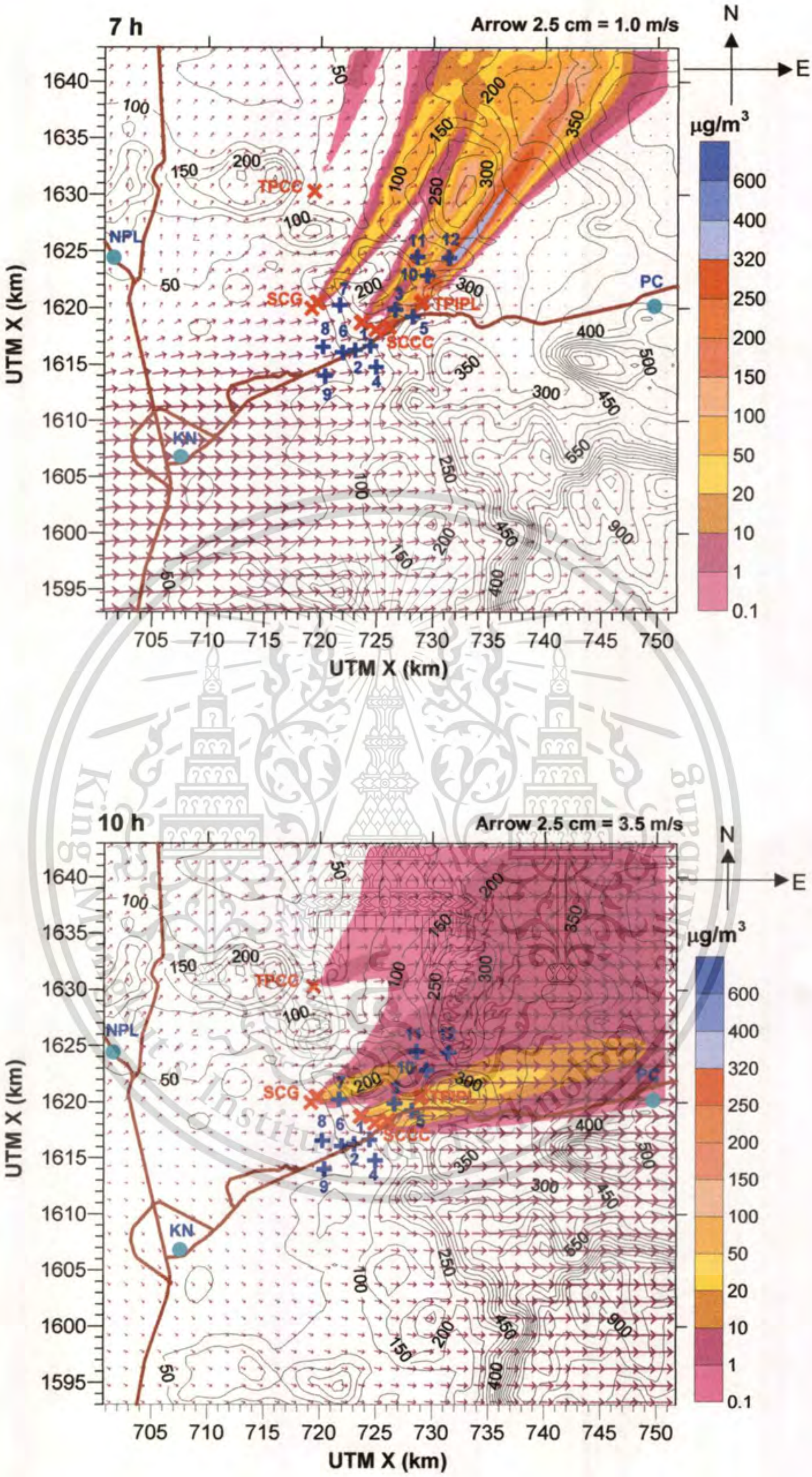

Figure F.1 Plumes of NO_2 simulated by CALPUFF on March 24, 2007 (●) meteorological stations, (+) receptors and (×) stacks of cement plants (cont.).

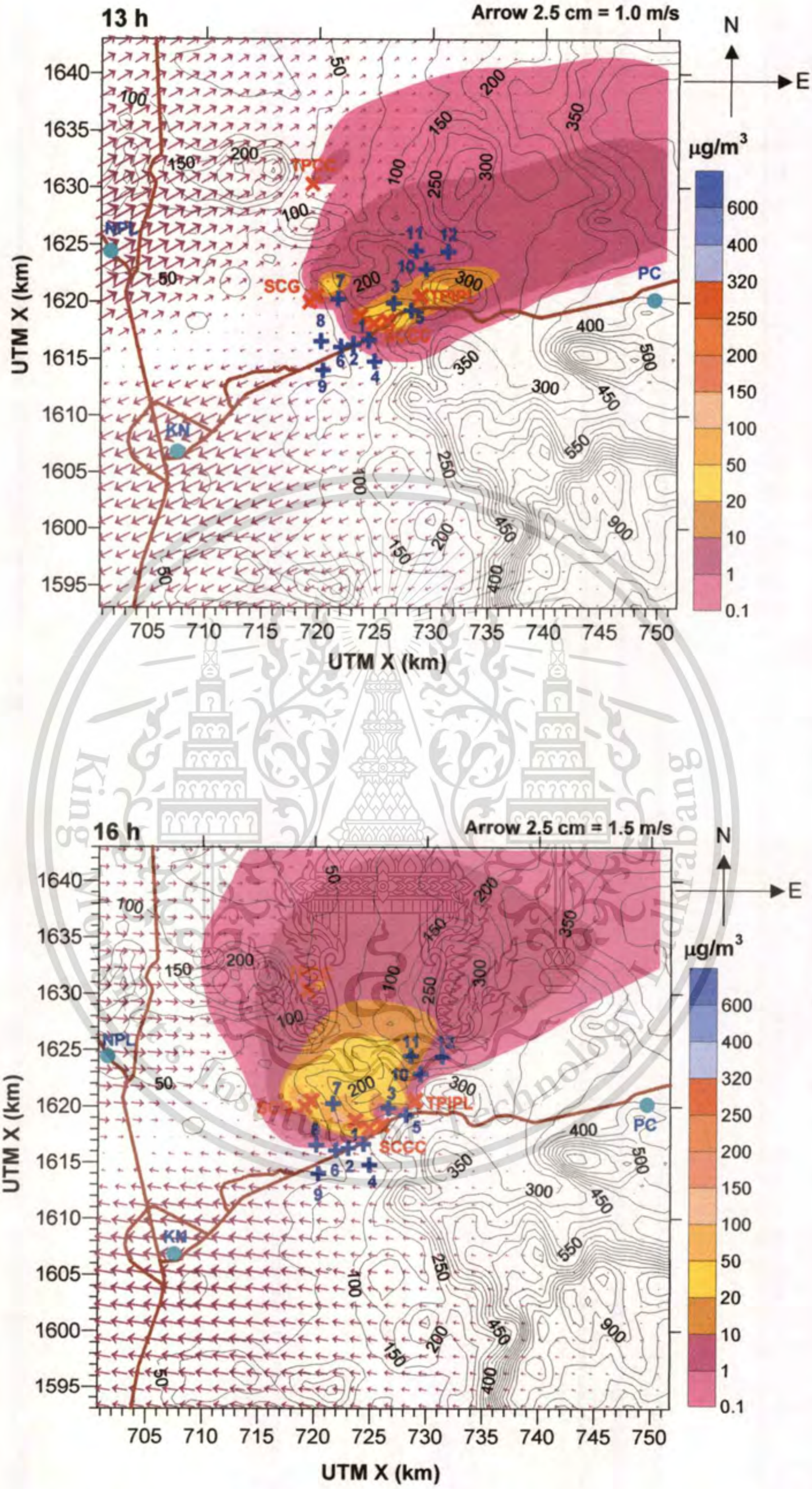

Figure F.1 Plumes of NO_2 simulated by CALPUFF on March 24, 2007 (●) meteorological stations, (+) receptors and (×) stacks of cement plants (cont.).

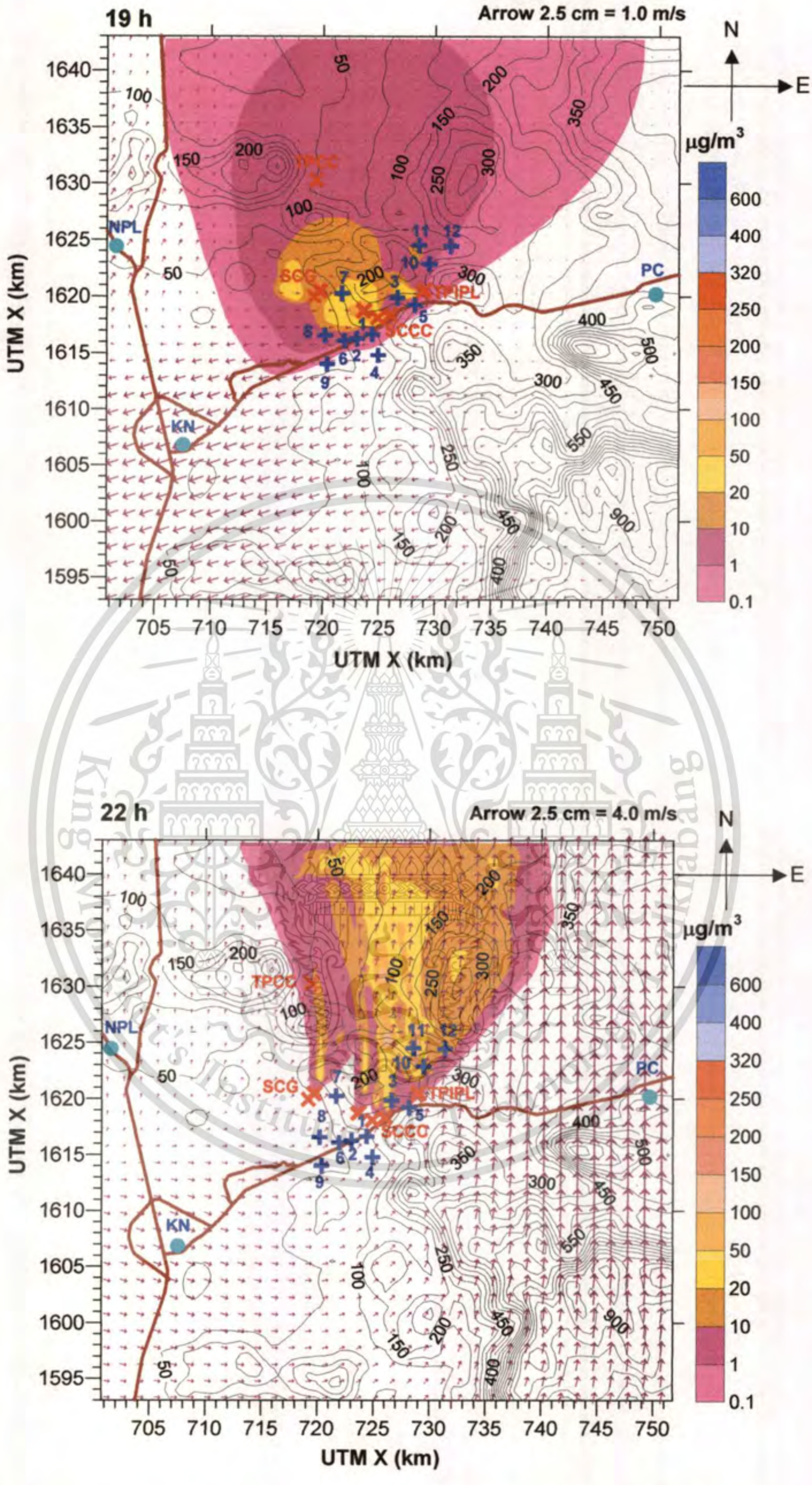

Figure F.1 Plumes of NO_2 simulated by CALPUFF on March 24, 2007 (●) meteorological stations, (+) receptors and (×) stacks of cement plants (cont.).

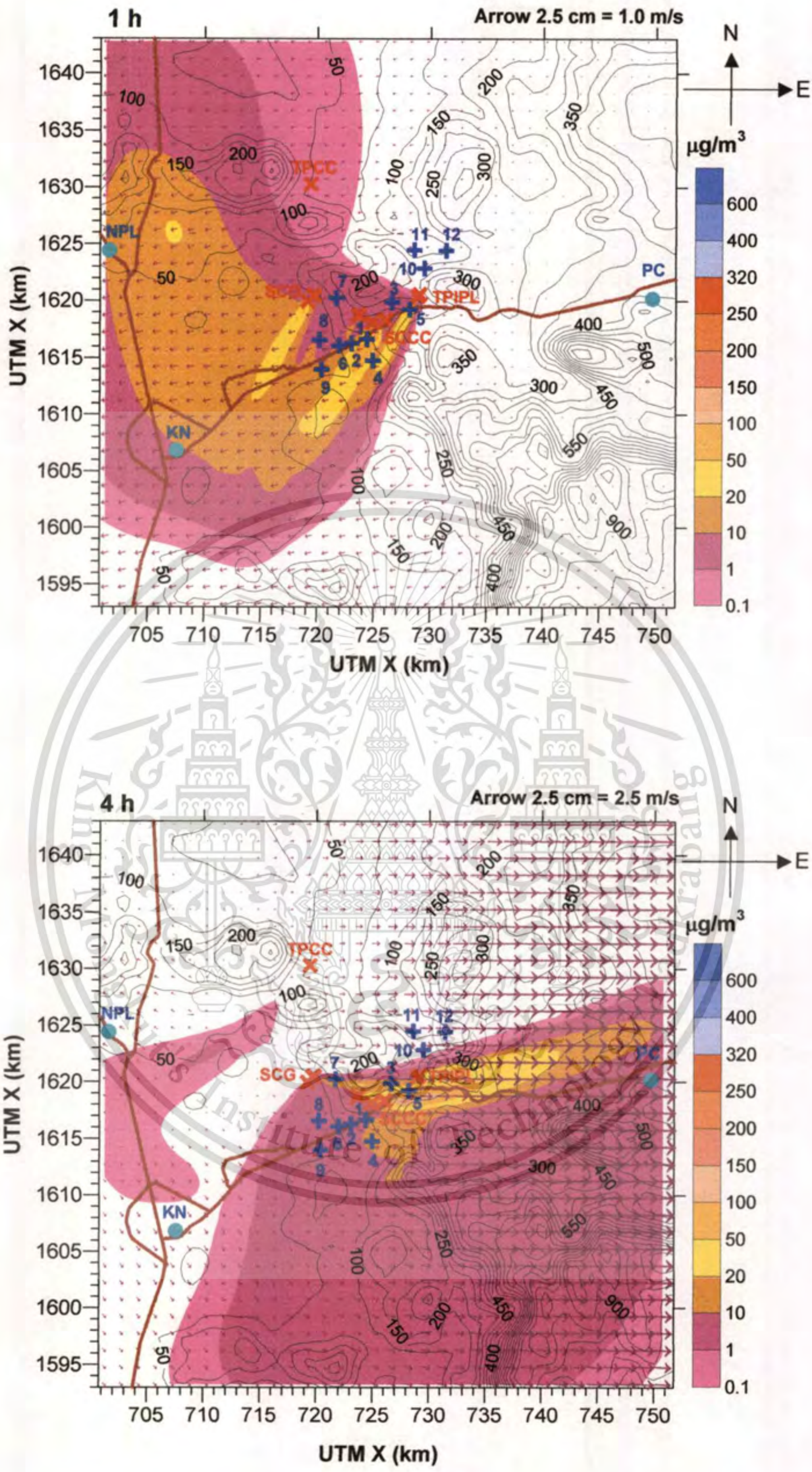

Figure F.2 Plumes of NO_2 simulated by CALPUFF on October 12, 2007: (●) meteorological stations, (+) receptors and (×) stacks of cement plants.

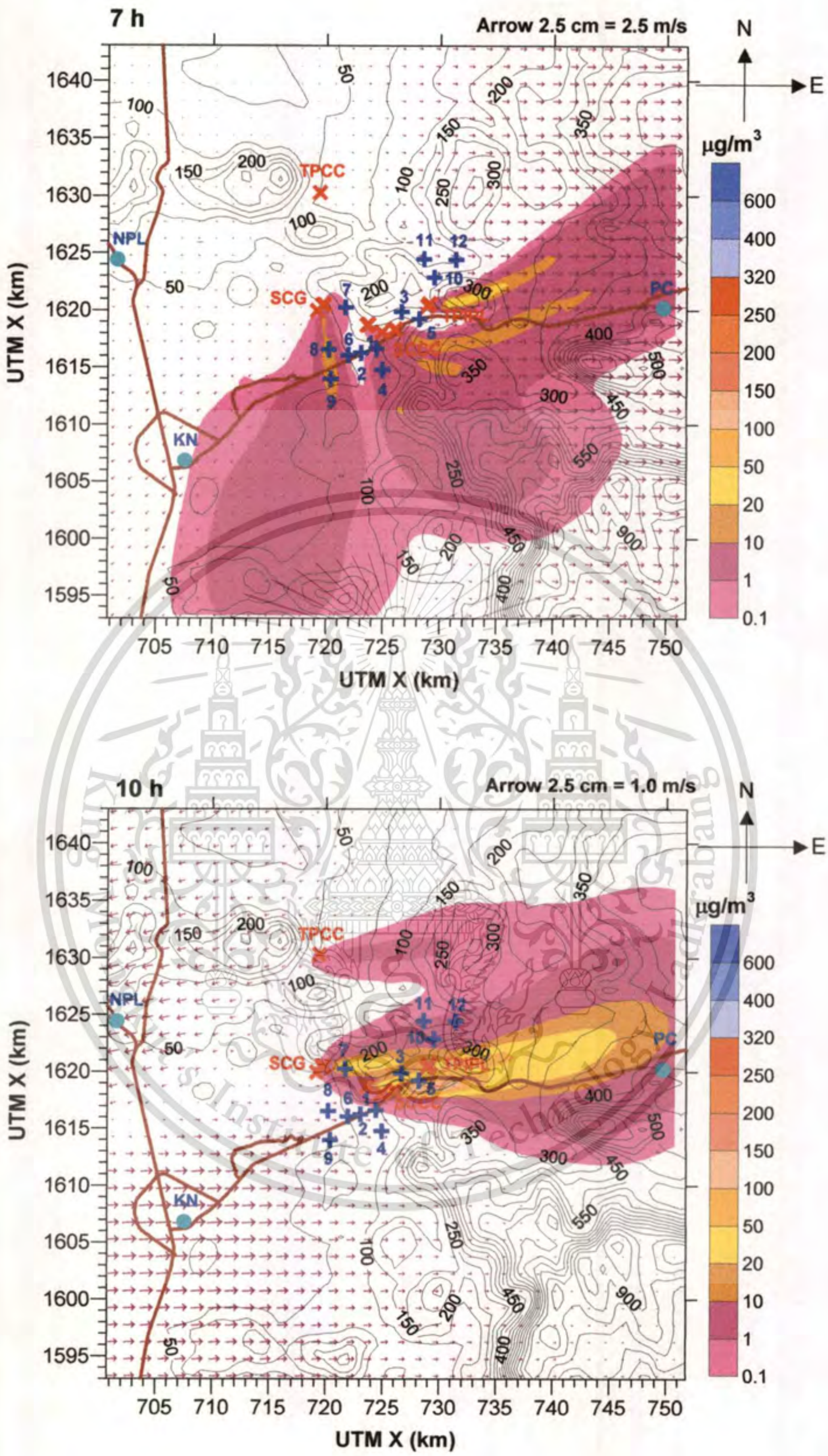

Figure F.2 Plumes of NO_2 simulated by CALPUFF on October 12, 2007: (●) meteorological stations, (+) receptors and (×) stacks of cement plants (cont.).

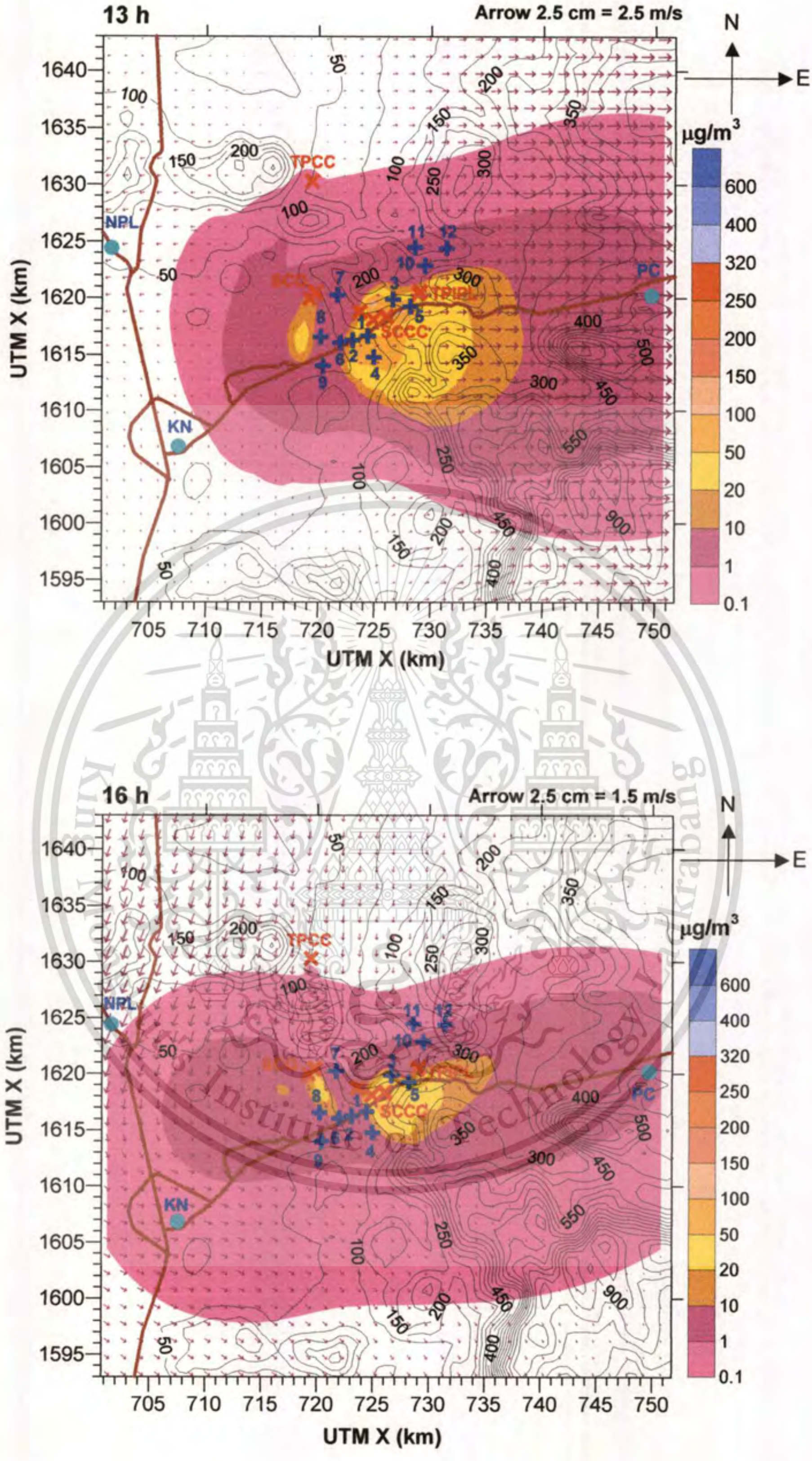

Figure F.2 Plumes of NO_2 simulated by CALPUFF on October 12, 2007: (●) meteorological stations, (+) receptors and (×) stacks of cement plants (cont.).

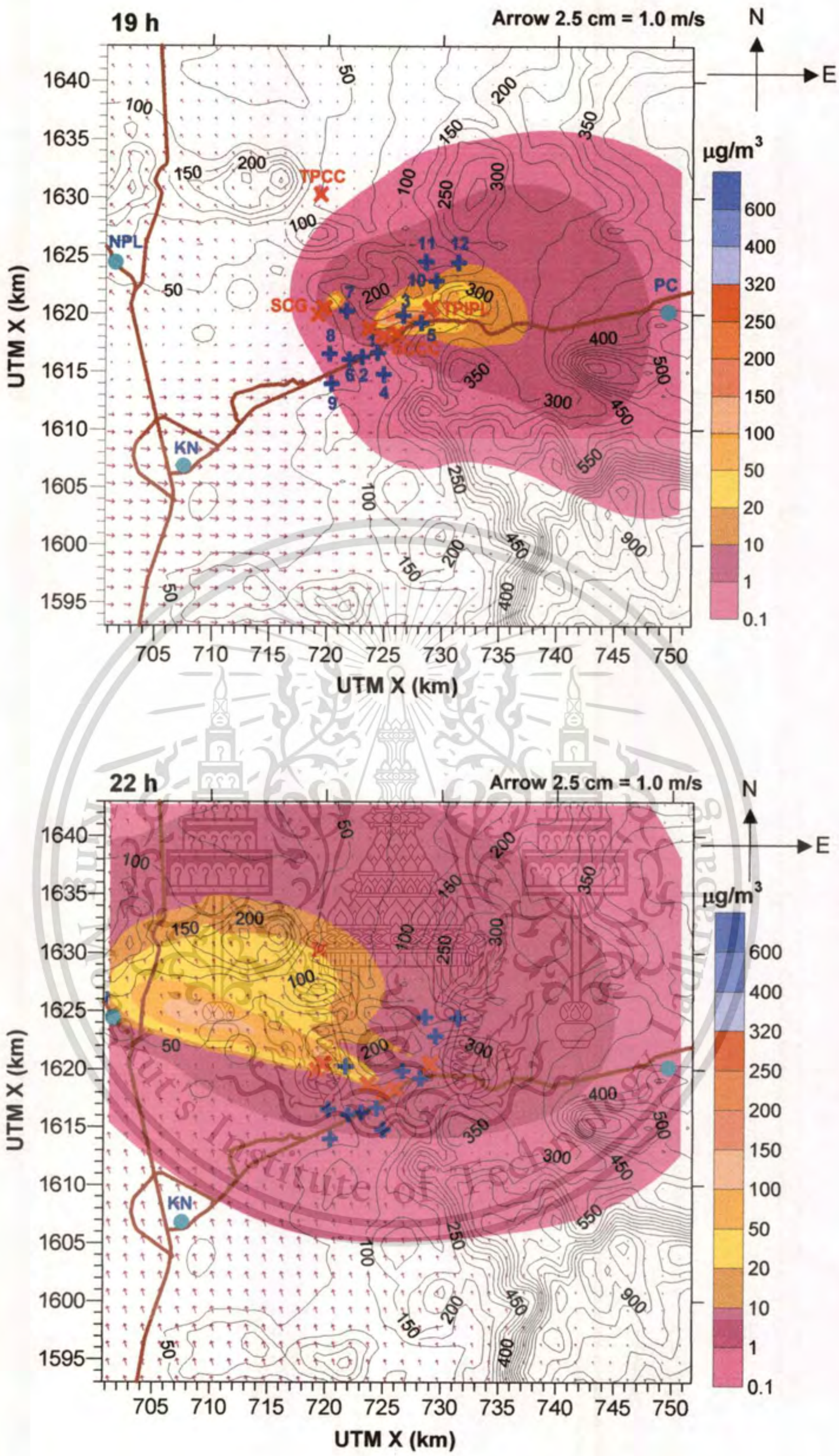

Figure F.2 Plumes of NO_2 simulated by CALPUFF on October 12, 2007: (●) meteorological stations, (+) receptors and (×) stacks of cement plants (cont.).

Appendix G

Gaussian plume

The pollutant concentration at ground level can be predicted by using the Gaussian plume dispersion equation. From Equation G.1, the effective stack height (H_{eff}) is the summation of stack height (H) and plume rise (dH). The plume rise is calculated from Briggs' Plume Rise equation (Equation G.2). In the Pasquill atmospheric stability categories A-F in Table G.1, different equations are selected to calculate plume dispersion coefficients at lateral and vertical distances (σ_y and σ_z). The stability class influenced by atmospheric turbulence can be categorized into 6 stability classes, namely A, B, C, D, E and F. Class A is the most unstable or the most turbulent atmospheric condition and class F is the most stable or the least turbulent condition.

$$C(x,y,z)=\frac{Q}{2\pi u\sigma_y\sigma_z}\left\{\exp\left[-\frac{(z-H_{eff})^2}{2\sigma_z^2}\right]+\exp\left[-\frac{(z+H_{eff})^2}{2\sigma_z^2}\right]\right\}\left\{\exp\left[-\frac{(y)^2}{2\sigma_y^2}\right]\right\} \tag{G.1}$$

where

C (x,y,z)	=	downwind concentration at a point x,y,z (g/m^3)
Q	=	pollutant emission rate (g/s)
σ_y, σ_z	=	plume dispersion coefficients at lateral and vertical distances, respectively (m)
H_{eff}	=	effective stack height (m)
u	=	mean wind speed along the downwind in x direction (m/s)
y	=	lateral distance (m)
z	=	vertical distance (m)

Briggs' Plume Rise equation

$$F_b = \omega_0 R_0{}^2 \frac{g}{T_{p0}}\left(T_{p0}-T_{a0}\right) \tag{G.2}$$

where

F_b	=	initial buoyancy flux (m^4/s^3)
ω_0	=	initial plume speed (m/s)
R_0	=	inside stack radius (m)

T_{p0}	=	initial plume temperature (K)
T_{a0}	=	ambient temperature at stack height (K)
g	=	gravity acceleration (9.8 m/s^2)

Plume rise (dH) = $21F_b^{0.75/u_H}$; $F_b < 55\ m^4/s^3$ (u_H= wind speed at height H (m/s))

= $38.71F_b^{0.6/u_H}$; $F_b \geq 55\ m^4/s^3$

Table G.1 Equations for the variation of σ_y and σ_z with stability class [52].

Stability class	σ_y	σ_z
A: very unstable	$0.22x(1+0.0001x)^{-0.5}$	$0.2x$
B: moderately unstable	$0.16x(1+0.0001x)^{-0.5}$	$0.12x$
C: slightly unstable	$0.11x(1+0.0001x)^{-0.5}$	$0.08x(1+0.0002x)^{-0.5}$
D: neutral	$0.08x(1+0.0001x)^{-0.5}$	$0.06x(1+0.0015x)^{-0.5}$
E: stable	$0.06x(1+0.0001x)^{-0.5}$	$0.03x(1+0.0003x)^{-1}$
F: very stable	$0.04x(1+0.0001x)^{-0.5}$	$0.016x(1+0.0003x)^{-1}$

Note: Equations for the variation of σ_y and σ_z are applicable in the range 100 m < x < 10 km.

Wind speed above the ground level affecting the pollutant dispersion can be calculated in Equation G.3.

$$u(z) = u_0\ (z/z_0)^p \tag{G.3}$$

where

u(z)	=	wind speed at height z (m/s)
u_0	=	wind speed at height z_0 measured by an anemometer
z	=	height above ground level (m)
z_0	=	height of an anemometer above ground level, 10 m
p	=	wind exponent which varies with the stability class in Table G.2.

Table G.2 The wind speed exponent at different stability classes [52].

Stability class	**p**
A: the most unstable	0.07
B: moderately unstable	0.07
C: slightly unstable	0.10
D: neutral	0.15
E: stable	0.35
F: the most stable	0.55

The ground distance where the plume from the stack hit the ground can be calculated according to the basic of Gaussian plume for each stability class. The calculation of the NO_2 plume released from the stack No. 1 of the SCCC under the stability class A is shown below.

Given: emission rate (Q) = 98.28 g/s

stack height (H) = 95 m

inside stack radius (R_0) = 1.8 m

initial plume speed (ω_0) = 16.19 m/s

wind speed at height of an anemometer (u_0) = 2 m/s

initial plume temperature (T_{p0}) = 433 K

ambient temperature at stack height (T_{a0}) = 303 K

1) From Equation G.3 and Table G.2, wind speed at stack height of 95 m is

$u \text{ (at 95 m)} = (2)(95/10)^{0.07}$

$= 2.34$ m/s

2) Calculate F_b and H_{eff}

$$F_b = 16.19(1.8)^2 \frac{9.8}{433}(433-303)$$

$= 154.34$

for $F_b \geq 55$, $dH = 38.71 F_b^{0.6/u_H}$

$= 38.71(154.34)^{0.6/2.34}$

$= 141$ m

then, $H_{eff} = 95 + 141 = 236$ m

3) Find σ_y and σ_z, assume x = 50 m at downwind direction from the stack

From $\sigma_y = 0.22x(1+0.0001x)^{-0.5}$

$= 0.22(50)(1+0.0001(50))^{-0.5}$

$= 10.97$ m

From $\sigma_z = 0.2x$

$= 0.2(50)$

$= 10$ m

4) Find the distance of NO_2 plume from the stack No.1 under the stability class A

From Equation G.1, NO_2 concentration at 50 m from the stack No 1 is

$$C(50,0,0) = \frac{98.28}{2\pi \times 2.34 \times 10.97 \times 10}\left\{\exp\left[-\frac{(0-236)^2}{2\times(10)^2}\right] + \exp\left[-\frac{(0+236)^2}{2\times(10)^2}\right]\right\}\left\{\exp\left[-\frac{(0)^2}{2(10.97)^2}\right]\right\}$$

$= 1.07 \times 10^{120} g/m^3$

From the above calculation, the NO_2 concentrations at ground level under 6 stability classes are observed at the various closest possible distances. The distances that NO_2 concentrations of 6 stability classes hit the ground are plotted in Figure G.1. It can be seen that the longer distance that the plumes of NO_2 concentrations landing on the ground varies with the most unstable class A to the most stable class F. The 1.1-km longest landing distance of NO_2 plume on the ground is in the boundary of the SCCC because the stack No. 1 is away from the residential areas more than 2 km. The basic calculation by Gaussian plume dispersion cannot identify the impact area from NO_2 plume. The more-refined models such as the AERMOD and CALPUFF can predict the effect of NO_2 plume closer to the actual dispersion.

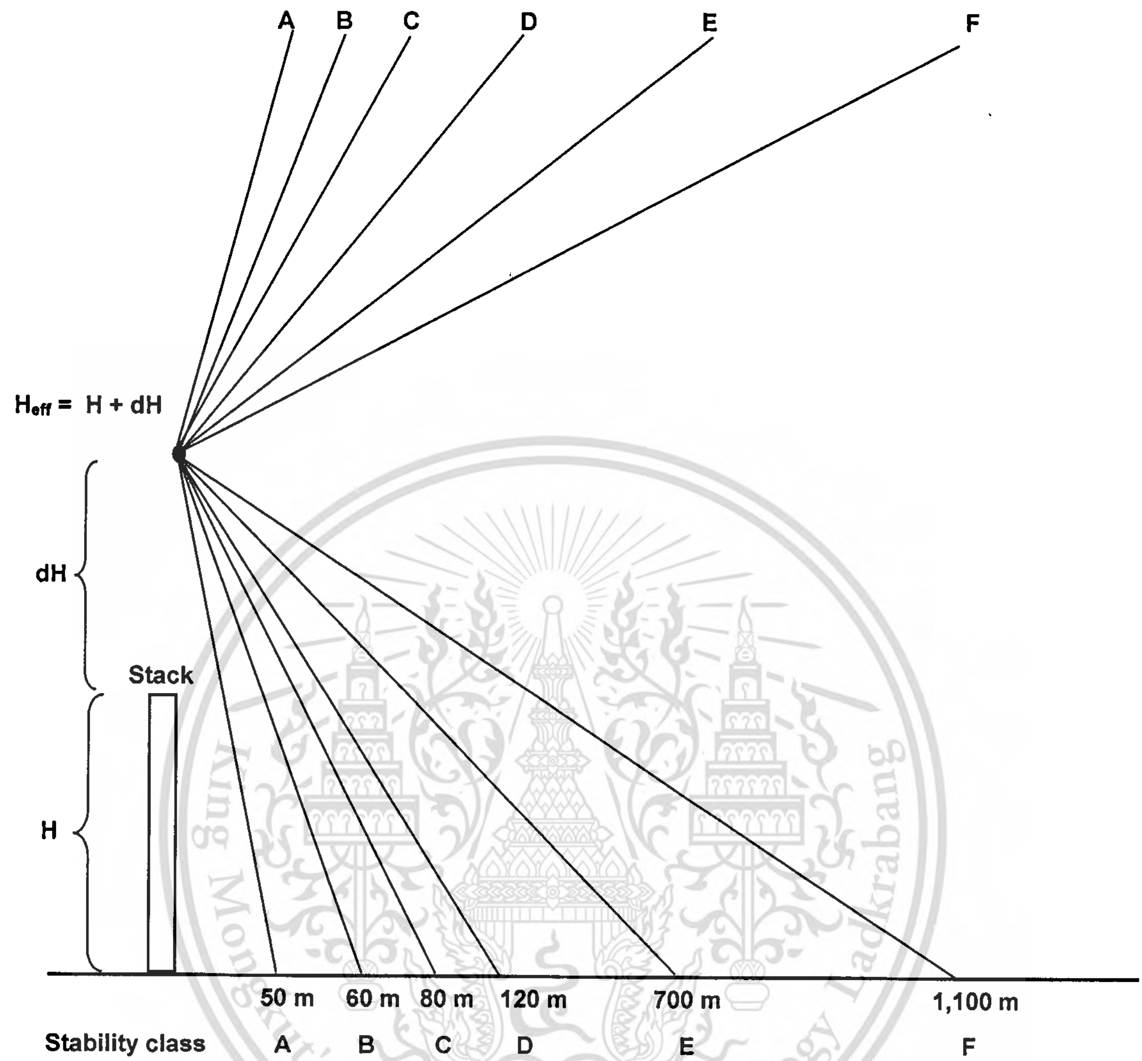

Figure G.1 NO_2 ground concentration of 6 stability classes.

Biography

Name: Ms. Kanyanee Seangkiatiyuth

Date of birth: 25 October 1976

Place of birth: Nan, Thailand

Education:

1995-1999 B.Sc. (Industrial Chemistry)
Department of Industrial Chemistry, Faculty of Science
Chiang Mai University

1999-2002 M.Eng. (Petrochemical Engineering),
Department of Chemical Engineering, Faculty of Engineering,
King Mongkut's Institute of Technology Ladkrabang

National publication

อัญชลีพร วาริทสวัสดิ์ หล่อทองคำ อิทธิพล แจ้งชัด และ**กัญญาณี แสงเกียรติยุทธ** "การศึกษาคุณสมบัติเบื้องต้นของวัสดุผสมระหว่างผงยางรถยนต์ใช้แล้วกับพอลิไวนิลคลอไรด์เพื่อการผลิตท่อน้ำซึม" วิศวกรรมสาร มก., ฉบับที่ 44, สิงหาคม-พฤศจิกายน 2544 หน้า 81-89.

International conferences

1. Anchaleeporn W. Lothongkum, **Kanyanee Seangkiatiyuth** and Vanisa Surapipith, "Measuring and Modeling of Particulate Dispersion from the Cement Plants" The Better Air Quality 2008 (BAQ 2008) - Air Quality and Climate Change : Scaling up Win-Win Solutions for Asia, 12^{th}-14^{th} November 2008 The Imperial Queen's Park Hotel, Bangkok, Thailand.
2. A Anchaleeporn W. Lothongkum, **Kanyanee Seangkiatiyuth** and Vanisa Surapipith, "Estimation of NO_x Impact from the Cement Plant by AERMOD and CALPUFF", Commemorative International Conference of the Occasion of the 4th Cycle Celebration of KMUTT, Sustainable Development to Save the Earth: Technologies and Strategies Vision 2050: (SDSE2008), Paper A-0097 (O), 1031-1038, 7^{th}-9^{th} April 2009, Millennium Hilton Bangkok Hotel, Bangkok, Thailand.
3. Anchaleeporn W. Lothongkum, **Kanyanee Seangkiatiyuth** and Vanisa Surapipith, "Estimation of NO_x Impact from the Cement Plant Located on the Mountain Areas", The 15^{th}

International Interdisciplinary Conference on the Environment, 8th-11th July 2009, Daytona Beach, Florida, USA.

International journals

Kanyanee Seangkiatiyuth, Vanisa Surapipith, Kraichat Tantrakarnapa and Anchaleeporn W. Lothongkum, "The AERMOD Modeling System for Environmental Impact Assessment of NO_2 Emission from the Cement Complex" Journal of Environmental Sciences, Vol. 23, No. 6, June 2011. (Impact factor 1.412).